TECHNISCHE UNIVERSITÄT MÜNCHEN

Wissenschaftszentrum Weihenstephan für Ernährung, Landnutzung und Umwelt

Lehrstuhl für Ernährung und Immunologie

Immunoregulatory role of *Helicobacter pylori* γ-glutamyltransferase during infection

Stefanie Wüstner

Vollständiger Abdruck der von der Fakultät Wissenschaftszentrum Weihenstephan für Ernährung, Landnutzung und Umwelt der Technischen Universität zur Erlangung des akademischen Grades eines

Doktors der Naturwissenschaften

genehmigten Dissertation.

Vorsitzender:	Univ.-Prof. Dr. S. Scherer
Prüfer der Dissertation:	
1.	Univ.-Prof. Dr. D. Haller
2.	Univ.-Prof. Dr. M. Gerhard
3.	Univ.-Prof. Dr. P. A. Knolle

Die Dissertation wurde am 20.07.2015 bei der Technischen Universität München eingereicht und durch die Fakultät Wissenschaftszentrum Weihenstephan für Ernährung, Landnutzung und Umwelt am 12.11.2015 angenommen.

Abstract

Persistent infection with *Helicobacter pylori* (*H. pylori*) affects almost half of the world's population and is the leading cause of gastric cancer. This human specific pathogen is extremely well adapted to the harsh stomach environment. Several strategies, developed to cope with the innate and adaptive immune response, facilitate persistent colonization of *H. pylori* and prevent clearance by immune cells. *H. pylori* γ-glutamyltransferase (gGT) impairs T-lymphocyte proliferation and thus might act as immunoregulatory factor. The aim of this thesis was to elucidate the underlying mechanism of T-cell inhibition and to study the impact of *H. pylori* gGT on the immune response during infection.

To address how the enzymatic activity of gGT might shape the local environment of lymphocytes migrating to the site of infection, stimulated T-lymphocytes were exposed to medium preconditioned with *H. pylori* wild-type, its isogenic gGT-deletion strain (ΔgGT), or recombinant gGT. Thereby it was found that *H. pylori* gGT compromised T-cell activation and effector cytokine expression in a glutamine-dependent manner. Assessment of signaling cascades affected by *H. pylori* gGT revealed that expression of cMyc and IRF4, transcription factors required for activation-induced metabolic adaptation of T-lymphocytes, was highly sensitive to extracellular glutamine levels and down-regulated upon gGT treatment. Remarkably, IRF4 expression was also decreased in T-lymphocytes infiltrating into the gastric mucosa of *H. pylori*-positive patients compared to T-cell infiltrates of *H. pylori*-independent gastritis, which may suggest that *H. pylori* gGT affects T-cells also during infection.

To study the role of *H. pylori* gGT during the establishment of a persistent infection and the induction of gastric inflammation, mice were inoculated with *H. pylori* PMSS1 wt and ΔgGT. *H. pylori* gGT facilitated initial colonization and affected colonization density. Interestingly, the gGT-deficient strain persistently colonized up to 50 % of mice with a trend towards a lower bacterial burden. When comparing those mice infected with *H. pylori* wt or ΔgGT at a similar colonization level, a major contribution of gGT to induction of gastric inflammation was observed. This inflammatory response was characterized by a CD8-dominated T-cell influx and strong increase in expression of proinflammatory chemokines and cytokines, such as IFNγ, whereas regulatory T-cell responses were dependent on colonization level but not on presence of gGT. This indicates that *H. pylori* gGT contributes to inflammation rather than dampening it, probably due to a direct detrimental effect on gastric epithelial cells resulting a proinflammatory environment. Supplementation of glutamine reversed *H. pylori* gGT-induced effects and attenuated the inflammatory response, indicating that glutamine deprivation indeed affects host cells when gGT is present.

Collectively, the results from this thesis demonstrate that *H. pylori* gGT is important to the bacterium contributing to its colonization capacity. Furthermore, it seems to deprive the gastric mucosa from glutamine which results in a proinflammatory environment but may, at the same time, impair T-cell effector function.

Zusammenfassung

Fast die Hälfte der Weltbevölkerung ist von einer persistenten Infektion mit *Helicobacter pylori* (*H. pylori*) betroffen, welche die Hauptursache für Magenkrebs darstellt. Dieser human-spezifische Krankheitserreger ist sehr gut an seinen Wirt angepasst und hat immunevasive Strategien entwickelt die eine dauerhafte Besiedelung ermöglichen. Die *H. pylori* γ-glutamyltransferase (gGT) könnte als immunregulatorischer Faktor fungieren, da sie die Proliferation von T-Lymphozyten beeinträchtigen kann. Das Ziel dieser Arbeit bestand darin, aufzuklären welcher Mechanismus dieser Beobachtung zugrunde liegt und den Einfluss der *H. pylori* gGT auf die Immunantwort während der Infektion zu untersuchen.

Um zu analysieren welchen Einfluss der gGT-abhängige Abbau von Glutamin auf die Lymphozyten am Infektionsherd hat, wurden aktivierte T-Lymphozyten mit Medium behandelt, das entweder mit *H. pylori* wt, mit dem isogenen gGT-defizienten Stamm (ΔgGT) oder mit rekombinanter gGT vorinkubiert wurde. Auf diese Weise konnte gezeigt werden, dass die T-Zell-Aktivierung und die Expression von Effektorzytokinen durch die *H. pylori* gGT in Abhängigkeit vom verfügbaren Glutamin beeinträchtigt wurde. Eine Untersuchung der Signalkaskaden und Transkriptionsfaktoren, die durch *H. pylori* gGT betroffen sein könnten, ergab, dass die Expression von cMyc und IRF4 durch gGT-Behandlung herunter reguliert wurde und stark abhängig war vom extrazellulären Glutaminlevel. Beide Transkriptionsfaktoren werden für die aktivierungsbedingte metabolische Anpassung von T-Zellen benötigt. Bemerkenswerterweise war die IRF4-Expression in T-Lymphozyten, die in die Magenschleimhaut von *H. pylori*-positiven Patienten einwandern, ebenfalls herunterreguliert. Dies deutet darauf hin, dass die *H. pylori* gGT T-Zellen auch während der Infektion beeinträchtigt.

Um die Rolle der *H. pylori* gGT während der Etablierung der Infektion und der Induktion der Entzündung zu untersuchen, wurden Mäuse mit *H. pylori* PMSS1 wt bzw. ΔgGT inokuliert. *H. pylori* gGT begünstigte die initiale Kolonisierung und beeinflusste auch die Besiedelungsdichte. Interessanterweise besiedelte der gGT-defiziente Stamm dauerhaft bis zu 50 % der Mäuse mit einem etwas verringerten Kolonisationslevel. Ein Vergleich zwischen Mäusen mit einer ähnlichen Besiedelungsdichte mit *H. pylori* wt bzw. ΔgGT ergab, dass die gGT stark zur Induktion der Entzündung im Magen beiträgt. Diese war durch eine CD8-dominierte T-Zell-Einwanderung und einen starken Anstieg der Expression von proinflammatorischen Zytokinen und Chemokinen, wie IFNγ, gekennzeichnet, wohingegen die regulatorische T-Zellantwort abhängig von der Besiedelungsdichte war, jedoch nicht von der Anwesenheit der gGT. Die Gesamtauswirkung der *H. pylori* gGT besteht also eher darin die Entzündung zu fördern als sie zu mildern. Die Supplementation von Glutamin konnte die durch *H. pylori* gGT induzierten Effekte umkehren und die Entzündungsantwort abmildern. Diese Beobachtung legt nahe, dass die Wirtszellen in Gegenwart der gGT tatsächlich von einem Glutaminentzug beeinträchtigt werden.

Zusammenfassend zeigen die Ergebnisse dieser Arbeit, dass die gGT *H. pylori* zu einer besseren Besiedelungsfähigkeit verhilft und der Magenschleimhaut das Glutamin zu entziehen scheint, was entzündungsfördernd wirkt, jedoch gleichzeitig auch die T-Zell-Effektorfunktion beeinträchtigen könnte.

Contents

1 Introduction **1**

1.1 *Helicobacter pylori* infection . . . 1

1.1.1 Characterization of *H. pylori* . . . 1

1.1.2 Colonization of the stomach . . . 2

1.1.3 Prevalence and Transmission . . . 3

1.1.4 Pathogenesis and clinical disease outcome . . . 3

1.1.5 Treatment . . . 4

1.1.6 Animal models . . . 5

1.2 Immunological response towards *H. pylori* . . . 5

1.2.1 Innate immune response to *H. pylori* infection . . . 6

1.2.2 Adaptive immune response to *H. pylori* infection . . . 9

1.2.3 Strategies of *H. pylori* to cope with the adaptive immune response . . . 24

1.3 *H. pylori* γ-glutamyltransferase . . . 24

1.3.1 Characterization of *H. pylori* gGT . . . 24

1.3.2 Physiological effects of *H. pylori* gGT . . . 25

1.4 Glutamine-dependent metabolism of activated T-cells . . . 29

1.4.1 T-cell receptor-dependent activation of T-cells . . . 29

1.4.2 Shift of T-cell metabolism upon activation . . . 30

1.4.3 Control of glutamine metabolism in T-lymphocytes . . . 31

1.4.4 Glutamine in immune function . . . 33

1.5 Hypothesis and Aims . . . 33

2 Material and methods **34**

2.1 *Helicobacter* strains and culture . . . 34

2.1.1 *Helicobacter* media, plates, and supplements . . . 34

2.1.2 *H. pylori* strains . . . 34

2.1.3 *H. pylori* culture and stock preparation . . . 34

2.1.4 Genotyping of *H. pylori* strains . . . 35

2.2 Expression of recombinant proteins . . . 36

2.2.1 Cultivation, induction, and harvesting . . . 36

2.2.2 Purification by affinity, ion exchange, and size exclusion chromatography . . . 36

2.2.3 Determination of protein quality and concentration . . . 36

2.3 Assessment of gGT activity . . . 37

2.3.1 gGT activity assay . . . 37

2.3.2 Enzymatic glutamate assay . . . 37

2.3.3 Quantitative liquid chromatography/mass spectrometry . . . 37

2.4 Cell culture based analyses . . . 38

2.4.1 Isolation and cultivation of primary lymphocytes and cell lines . . . 38

2.4.2 Preparation of preconditioned medium . . . 38
2.4.3 Activation and *H. pylori* gGT treatment of lymphocytes . . . 38
2.4.4 [^{3}H]-thymidine incorporation assay . . . 39
2.4.5 Viability assay . . . 39
2.4.6 Caspase-3/-7 activation assay . . . 39
2.5 Murine infections . . . 39
2.5.1 Mouse strains and housing . . . 39
2.5.2 Experimental infection with *H. pylori* . . . 40
2.5.3 Harvesting of organs . . . 41
2.5.4 Quantitative assessment of colonization . . . 43
2.6 Molecular biological techniques . . . 44
2.6.1 Enzyme-linked immunosorbant assay . . . 44
2.6.2 Flow cytometry . . . 44
2.6.3 SDS polyacrylamide gel electrophoresis . . . 45
2.6.4 Western blot . . . 46
2.6.5 Two-dimensional gel electrophoresis/mass spectrometry . . . 47
2.6.6 Real-time PCR . . . 48
2.7 Histological techniques . . . 49
2.7.1 Human and murine stomach tissue . . . 49
2.7.2 Hematoxylin/Eosin and Warthin-Starry silver stain . . . 50
2.7.3 Immunohistochemical staining . . . 50
2.7.4 Histological evaluation . . . 50
2.8 Statistical analysis . . . 50

3 Results **51**
3.1 Effect of *H. pylori* gGT on human T-lymphocytes . . . 51
3.1.1 Enzymatic activity of *H. pylori* gGT induces inhibition of T-cell proliferation without inducing apoptosis . . . 51
3.1.2 Turnover of γ-glutamyl substrates by *H. pylori* gGT . . . 55
3.1.3 *H. pylori* gGT blocks expansion of activated T-lymphocytes via glutamine deprivation . . . 55
3.1.4 *H. pylori* gGT inhibits T-lymphocyte activation in a glutamine-dependent manner . . . 57
3.1.5 Glutathione degradation-dependent effects of *H. pylori* gGT on T-cells . . . 64
3.1.6 Activation-induced signaling pathways in T-cells affected by *H. pylori* gGT . . . 67
3.1.7 Untargeted approach to identify *H. pylori* gGT regulated proteins . . . 68
3.1.8 *H. pylori* gGT-induced glutamine deprivation down-regulates IRF4 expression 69
3.2 Role of *H. pylori* gGT during experimental infection . . . 74
3.2.1 *H. pylori* gGT contributes to initial colonization and determines bacterial burden . . . 74
3.2.2 gGT-dependent differences in the adaptive immune response towards *H. pylori* 80
3.2.3 Infection of lymphocyte-deficient Rag$^{-/-}$ mice with *H. pylori* wt and ΔgGT . . . 89
3.2.4 CD4$^+$ T-cell reconstitution of *H. pylori* wt- or ΔgGT-infected Rag$^{-/-}$ mice . . . 92
3.2.5 Adoptive transfer of CD4$^+$/CD44$^-$ cells in *H. pylori* wt- or ΔgGT-infected Rag$^{-/-}$ mice . . . 93
3.3 Effects of *H. pylori* gGT glutaminase activity during infection . . . 95
3.3.1 Glutamine level and transcriptional regulation during H. pylori infection . . . 96
3.3.2 Supplementation of glutamate and glutamine during *H. pylori* infection . . . 97

4 Discussion **103**
4.1 Effect of *H. pylori* gGT-induced glutamine deprivation on T-cells 103
4.1.1 H. pylori gGT acts on T-cells independently of glutathione degradation products 103
4.1.2 T-cell functionality is affected by gGT-dependent changes in glutamine level . 104
4.1.3 H. pylori gGT manipulates expression of transcription factors required for metabolic reprogramming of activated T-cells 104
4.2 Role of *H. pylori* gGT during infection 105
4.2.1 *H. pylori* gGT activity promotes ability to establish infection 105
4.2.2 Supplementation of glutamate cannot support *H. pylori* ΔgGT 106
4.2.3 *H. pylori* gGT contributes to a higher colonization density 107
4.2.4 *H. pylori* with gGT activity induces stronger gastric inflammation 108
4.2.5 Supplementation of glutamine suppresses gGT-induced gastric inflammation . 111

5 Conclusion **113**

Chapter 1

Introduction

1.1 *Helicobacter pylori* infection

The (re-)discovery of *Helicobacter pylori* (*H. pylori*) infection and the proof of its harmful consequences by Barry Marshall and Robin Warren was a mile stone in medicine. The presence of spiral shaped bacteria in human stomachs was observed long before their studies and clinical relevance had been debated but could not be proven [1, 2]. Marshall and Warren firmly established its pathogenic character when they demonstrated an association between *H. pylori* infection and the development of gastritis and gastric ulcers through the fulfillment of Koch's postulates in a self-experiment drinking a pure *H. pylori* culture [3]. In 2005, they received the Nobel Prize for their achievement. Since then, a great number of studies has been performed to further our understanding on pathogen, host, and environmental factors that contribute to lifelong persistence and pathogenesis of *H. pylori* infection. Bacterial factors that may also be exploited for treatment are of particular interest. One factor that is important for the bacterium but also manipulating host cells, namely *H. pylori* γ-glutamyltransferase, is in the focus of this thesis.

1.1.1 Characterization of *H. pylori*

H. pylori belongs to the *Helicobacter* genus, which is comprised of more than 20 species [4, 5]. *Helicobacter* species can be divided in two major groups according to their organ specificity: gastric and enterohepatic (non-gastric) *Helicobacter* species. Several *Helicobacter* species are associated with human disease or are used to model the human *Helicobacter* infection in animals.

Enterohepatic *Helicobacter* species are more diverse than gastric *Helicobacters*. In humans, they can cause persistent infections of the lower gastrointestinal tract; well known representatives are *H. hepaticus* or *H. bilis*. Co-infection with non-gastric *Helicobacter* species modulates the inflammatory response towards *H. pylori* in the stomach, at least in mice [6].

The gastric *Helicobacter* species include *H. pylori*, *H. felis*, and *H. heilmannii* (*sensu lato*). *H. heilmannii* (*s.l.*) is actually a group of non-pylori *Helicobacters* such as *H. suis*, *H. salomonii*, and *H. heilmannii* (*sensu stricto*) each selectively colonizing the stomach of specific species [7]. Colonization of humans with *H. heilmannii* is generally attributed to close contact with animals carrying the bacteria. The infection is accompanied by a rather mild gastritis and occurs very seldom, with a prevalence below 0.5 % [8]. *H. felis* has been isolated from the stomach of cats, dogs, and mice [9]. *H. felis* is also spiral shaped but larger than *H. pylori* and causes acute gastritis upon zoonotic transmission to humans [10]. The murine infection with *H. felis* resembles *H. pylori* infection of humans in several aspects [11].

H. pylori is the by far most widespread *Helicobacter* among humans. It is a gram-negative spiral shape bacterium that measures 2 - 4 µm in length and 0.5 - 1 µm in width. It is equipped

with 2 - 6 unipolar sheathed flagella that confer motility. The bacterium is characterized by its positivity for catalase, oxidase, and urease. *H. pylori* is a microaerophilic organism that grows best at 37 °C under neutral pH conditions [12]. Initially, *H. pylori* was difficult to cultivate since it is a fastidious microorganism being a cholesterol auxotroph, for example [13]. Therefore, complex supplements such as blood or serum are needed to cultivate the bacterium. Whole genome comparison revealed that *H. pylori* possess only a third of environmental sensors such as two-component systems compared to *E. coli* and a much lower overall number of potential regulatory DNA-binding proteins [14]. This emphasizes that *H. pylori* is very specialized and highly adapted to its natural habitat, the human stomach.

1.1.2 Colonization of the stomach

For a long time the human stomach was considered to be sterile due to its acidic environment (pH 2). Back then, bacteria detected in stomach were thought to be contaminants from ingested food. Yet, *H. pylori* does not only survive the acidic environment of the stomach during transit but is able to truly colonize this hostile niche. Even though the gastric microbiota seems to be more diverse than previously thought, *H. pylori* is the dominant species in the stomach of infected individuals [15]. The narrow host spectrum explains why this bacterium is highly adapted to the conditions encountered in the human stomach. Several bacterial factors facilitate colonization (Figure 1). As *H. pylori* is a neutralophilic organism, it possesses several strategies to tolerate the extremely acidic environment in the gastric lumen. Those are distinct from other pathogens that mainly use decarboxylases; instead, its strategy to resist the acidic environment is characterized by production of ammonia [16]. The most important mechanism relies on the expression of urease, which converts urea to ammonia and carbon dioxide [17]. Urease activity in combination with expression of urea transporters allows the bacterium to keep the cytosolic and also the periplasmic pH at a tolerable level.

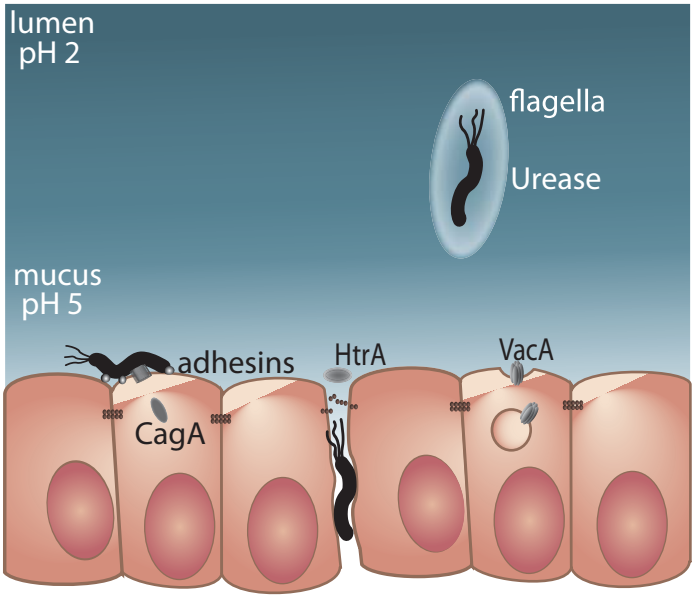

Figure 1: Bacterial factors facilitating the colonization of the gastric mucosa with *H. pylori*.

To escape the acidic lumen, *H. pylori* colonizes the gastric mucus close to the epithelial cell layer. Spiral shape and flagella are morphological attributes that allow the bacterium to move rapidly through the viscous mucus layer on top of the epithelial cells [18, 19]. The pH gradient

in the mucus seems to be the most important stimulus to guide the bacterium [20]. While most bacteria are located inside the gastric mucus, about 20 % of *H. pylori* adhere to the apical surface of gastric epithelial cells [20]. The bacterium possesses a wide variety of adhesion factors that mediate attachment to epithelial cells and are associated with pathology, such as the Hop proteins BabA (HopS), SabA (HopP), AlpA (HopC), AlpB (HopB), and OipA (HopH) [9]. Occasionally, *H. pylori* is found deep inside crypts and in the intercellular space where it directly encounters immune cells of the lamina propria [21]. It is controversial whether *H. pylori* invades into the gastric mucosa since events when *H. pylori* is found in the intracellular space are rare. However, *H. pylori* is thought to disrupt intercellular junctions by several bacterial factors, such as vacuolating toxin A (VacA), Cytotoxin-associated gene A (CagA), Urease, and HtrA [22, 23, 24, 25]. HtrA is a secreted virulence factor that has been recently found to facilitate access of *H. pylori* to the intercellular space. It is a protease that cleaves E-cadherin thereby disrupting cell-cell contact between epithelial cells [25]. Increased mucosal permeability through damaged epithelial cells and disruption of epithelial integrity may provide nutrients for bacterial growth [26]. *H. pylori* needs to exploit external nutrient sources as it lacks biosynthesis pathways of several amino acids [27].

1.1.3 Prevalence and Transmission

H. pylori infection affects about half of the world's population. Notably, the prevalence shows large variations dependent on geographic location, socioeconomic status, and age. Great differences in infection status can be observed comparing developing to industrialized countries. A prevalence of over 80 % in African (e.g. Ethiopia, Nigeria), South American (e.g. Brazil, Chile), and Asian (e.g. Bangladesh, India, Taiwan) countries has been observed; while the prevalence of *H. pylori* in Western countries, such as USA, Canada, Australia, and Germany, is between 20 - 50 % [28]. *H. pylori* infection rates in developing countries are still constantly high, probably due to lack of basic hygiene, poor diets, and overcrowding; yet, they are declining in Western countries, where prevalence is decreasing in particular among children [29].

Generally, *H. pylori* infection is thought to be acquired during early childhood and mainly transmitted within families as strains isolated from parents of affected children mostly display a conserved genotype [30]. It is well established that the human stomach is the main reservoir of *H. pylori* and that the infection is passed on from person-to-person. Nevertheless, the predominant route of transmission is still unknown. Several means of transmission have been suggested since *H. pylori* has been isolated from saliva, dental plaque, vomitus, and feces [31, 32, 33]. Therefore, most likely routes of infection are oral-oral, gastro-oral, and fecal-oral.

1.1.4 Pathogenesis and clinical disease outcome

Similarly to commensals, *H. pylori* is generally not cleared spontaneously but colonizes persistently throughout life. Even though the majority of infected individuals do not develop symptoms, a superficial gastritis is always present. Severe clinical disorders of the upper gastrointestinal tract are less frequent. About 10 - 20 % of *H. pylori*-infected individuals develop peptic ulcers, 1 - 2 % develop gastric cancer, and in less than 1 % MALT lymphoma occurs [9]. Meta-analyses and prospective long-term studies have established a strong association between persistent *H. pylori* infection and gastric cancer [34, 35]. Accumulating evidence has led to the classification of *H. pylori* as a group I (definite) carcinogen [36]. This is particularly remarkable since gastric cancer is the second most common cause of cancer-related deaths [37]. It is assumed that a complex combination of factors determine the clinical outcome. The wide variety of pathology from mild to severe depends on host, bacterial, and environmental factors.

The topography of infection, for example, is an important indicator for clinical disease outcome

that is determined by host and bacterial factors. The topography of *H. pylori* infection is associated with disease development and determines the risk of gastric carcinoma. Antral-predominant gastritis is associated with hyperchlorhydria (a decreased gastric pH). This restricts *H. pylori* colonization to the antrum and typically leads to the development of duodenal ulcers [38]. Corpus-predominant gastritis, also termed pangastritis, extends to the corpus. It is associated with a higher gastric pH and is found in patients that are more likely to develop gastric ulcers, intestinal metaplasia, and gastric cancer [39]. Host factors that influence topography are interleukin 1β (IL-1β) and tumor necrosis factor α (TNFα). Both are potent inhibitors of gastric acid secretion and favor a corpus-predominant gastritis [40]. Thus, polymorphisms that lead to increased expression of IL-1β are associated with a higher intragastric pH, atrophic gastritis, and a greater risk for gastric adenocarcinoma [41].

Not only host factors, but also bacterial factors play an important role in the development of the symptoms and disease outcome. CagA, the most extensively studied virulence factor of *H. pylori*, is postulated to drive carcinogenesis. It is encoded in a pathogenicity island (*cag*PAI) which contains a type-IV secretion system for CagA translocation into host cells. Individuals carrying a CagA-positive *Helicobacter* strain are at higher risk of developing gastric ulcers or cancer than individuals infected with a CagA-negative strain [42]. Thus, gastric carcinomas are more prevalent in areas where a high proportion of *H. pylori* carries the *cag*PAI, as is the case in Asia [43]. CagA facilitates the colonization of the corpus which leads to a corpus-predominant gastritis and an increased rate of gastric carcinomas [44, 45]. Another virulence factor contributing to severity of disease and maintenance of gastritis is VacA [46, 47]. In essence, VacA induces vacuolation in gastric epithelial cell, causing apoptosis and enhancing inflammatory responses [48, 49]. VacA-positive strains are associated with an increased risk for peptic ulcer and gastric cancer [42].

As previously mentioned, environmental factors also contribute to the disease outcome in *H. pylori*-infected individuals. Smoking, for example, increases the risk of *H. pylori*-related gastric precancerous lesions [50]. Consequently, it is important to extend our understanding of these factors. This might help to identify persons at highest risk to develop disease and offer extensive treatment to this subpopulation.

1.1.5 Treatment

There is antibiotic treatment available against *H. pylori* infection. A triple therapy of a proton pump inhibitor, clarithromycin, and either amoxicillin or metronidazole is recommended as first-line treatment [51]. Increasing resistance to the most effective component, clarithromycin, however, requires alternative treatment such as a bismuth-containing quadruple therapy. Concerning costs, the likelihood of asymptomatic disease, and the development of antibiotic resistances; it is not desirable to use antibiotic treatment for mass eradication. It might be preferable to identify persons with genetic polymorphisms and carriers of particularly virulent strains that are exposed to an increased risk for a severe course of disease. Therefore, diagnostic tools are developed to identify patients that have raised an antibody response against particular *H. pylori* antigens (e.g. CagA) that indicate the type of strain they carry [52]. Eradication of patients with a particular high risk concerning their genetic predisposition as well as type of strain could prevent gastric cancer.

Additionally, efforts are undertaken to develop alternative treatments, such as antiinfectives including specific inhibitors, or vaccines. To specifically target the bacterium and to direct the immune response against essential bacterial factors, we require a deeper understanding of processes that induce or dampen an effective immune response against infection. This can be explored in detail by the use of animal models.

1.1.6 Animal models

As *H. pylori* is a human specific pathogen, there is no model available that perfectly mirrors all aspects of the human disease. Some studies have used non-human primates, gnotobiotic piglets, or guinea pigs to study pathogenicity of *Helicobacter* [53, 54, 55, 56]. *H. pylori* infection of Mongolian gerbil is commonly used for long-term infection as well as immunization studies [57]. This model is suitable to characterize cancer development as pathology progresses from gastritis to gastric ulcers, intestinal metaplasia, and adenocarcinoma [58]. Like in humans, development of gastric cancer is associated with CagA-positivity in Mongolian gerbils [59]. Yet, due to a limited number of tools, this model is not well suited to analyze immunological responses.

Consequently, the most widely used animal model to study pathogenicity of *Helicobacter* is the mouse. Experimental infection of mice is an extremely valuable tool to study immunity since the immune response is well characterized and knockout strains for all kind of immune cells and factors are available. However, only a limited number of primary *H. pylori* isolates are colonizing the murine stomach. *H. pylori* Sydney strain 1 (SS1) is the best characterized mouse-adapted strain [60, 61, 62]. Yet, *H. pylori* SS1 is unable to translocate CagA, colonizes almost exclusively the antral-fundic junction, and causes only mild inflammation [63, 64]. In mice, *H. pylori*-induced gastritis qualitatively resembles the human situation with infiltration of neutrophils, macrophages, and lymphocytes; however, no progression to peptic ulcers, metaplasia and gastric cancers can be observed. To study cancer development and more severe inflammation, *H. felis* infection is used. This bacterium colonizes throughout the murine antrum and fundus, and induces an inflammatory response dominated by mononuclear cells [11]. More recently, stable infection of mice and CagA translocation has been described for the parental strain of SS1, termed "pre-mouse SS1" (PMSS1), a clinical isolate which has been described to be more virulent than SS1 [65]. Therefore, *H. pylori* PMSS1 was used in this thesis.

1.2 Immunological response towards *H. pylori*

Infection with *H. pylori* is associated with active and chronic gastritis which is characterized by infiltration of polymorphonuclear cells (PMNs, mainly neutrophils) and lymphocytes, respectively [38]. Thus, innate and adaptive immune responses are initiated by the infection. Other immune cells migrating to the site of infection are macrophages (Mϕs), monocytes, dendritic cells (DCs), eosinophils, mast cells, and plasma cells [66, 67, 68]. Considering this complex mixture of inflammatory cells, the most interesting question is which cell types play the most prominent role in controlling the bacterial load and driving pathological changes? Figure 2 gives an overview of innate and adaptive inflammatory responses during *H. pylori* infection.

In humans, *H. pylori* is co-localized with inflammatory cells. An increased density of *H. pylori* is directly correlated with increased numbers of neutrophils and lymphocytes, and with epithelial damage [38]. In immunocompetent mice the level of gastritis is inversely correlated to bacterial load. Thus, in mice that control bacterial load better than others, infiltration of inflammatory cells into the gastric mucosa is increased during the natural progression of *H. pylori* colonization [69, 70]. Yet, is still obscure why the immune response fails to clear the infection. It has to be considered that the immune response found in adult humans represents a more or less stable equilibrium that has been established over decades of persistent infection and is the result of pro-inflammatory and regulatory mechanisms. The ineffectiveness of the immune response towards *H. pylori* is not surprising in light of more than 60 000 years of co-evolution [71]. The pathogen has evolved strategies to overcome, evade, and dampen the host defense system that allow persistent colonization.

Data of early or acute *H. pylori* infection are limited and either derived from studies with

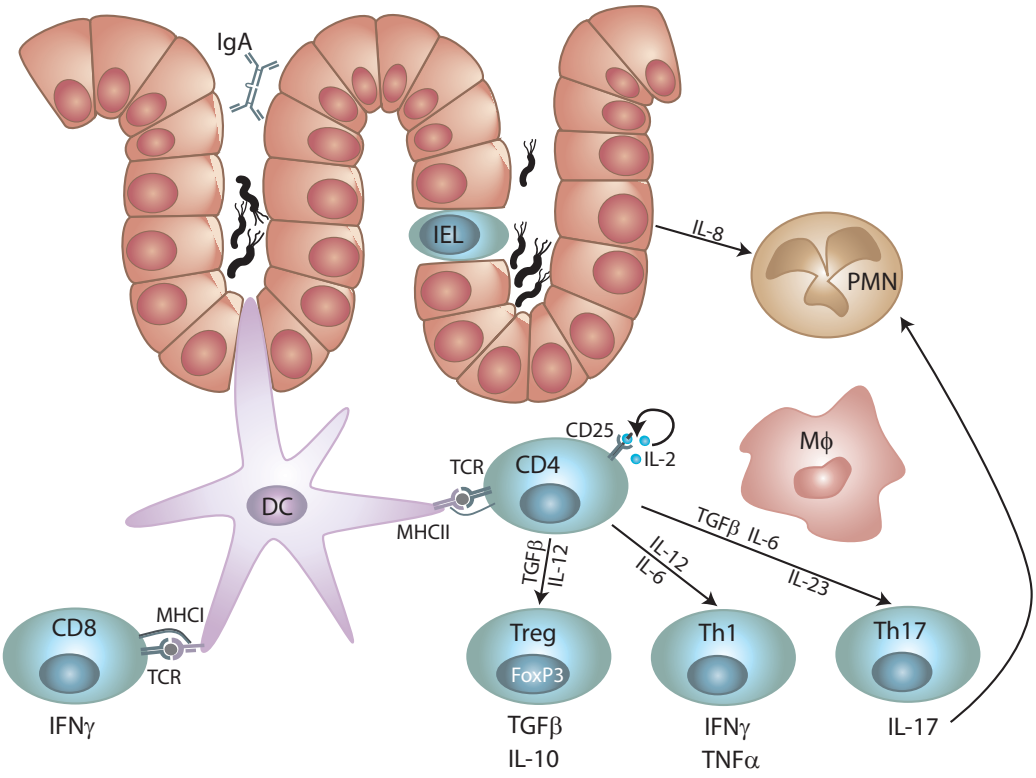

Figure 2: Immune response towards *H. pylori*.

naturally infected children or experimentally infected volunteers. Therefore, animal models of infection offer the opportunity to analyze different phases of infection and to set up experimental conditions where different immune cell subsets or mediators are absent or induced. The natural immune response in mice does not clear *H. pylori* infection either. However, protective immunity can be induced by immunization with *H. pylori* antigens in mice [72]. Immunization with *H. pylori* lysate confers protection and is associated with increased immunopathology [73]. The most common immunization strategy for functional studies of immune responses in mice is prophylactic administration of a *Helicobacter* lysate with cholera toxin as adjuvant [74, 75, 76, 77].

1.2.1 Innate immune response to *H. pylori* infection

As the gut-associated lymphoid tissue is the largest immune organ of the body, it is important to understand the lines of priming and defense in the context of *H. pylori* infection. Immune cells patrolling the mucosa home to several lymphoid compartments that are directly or more distantly associated with the stomach (Figure 3).

The gastric epithelial monolayer represents a physical barrier that is covered by a highly glycosylated mucus layer. Generally, the gastric mucus layer is inaccessible to immune cells which reside in the lamina propria and is thus a rather safe habitat for *H. pylori*. Cells that experience direct contact with *H. pylori* and its antigens in the stomach are mainly gastric epithelial cells, intraepithelial lymphocytes (IEL), and also dendritic(-like) cells that traverse the epithelial cell layer and reach into the mucus [78].

To alert the immune system, microorganisms that pose a threat have to be recognized and classified. Initially, rather unspecific pattern recognition receptors (PRR) such as toll-like receptors (TLRs) and NOD-like receptors detect bacteria by common characteristics, so called pathogen-

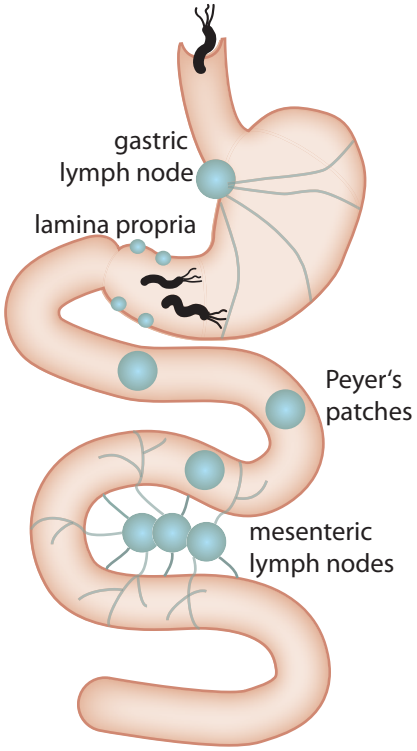

Figure 3: Lymphoid structures associated with the gastrointestinal tract.

associated molecular patterns, such as lipopolysaccharides (LPS) of the bacterial cell wall [79]. These receptors are expressed on dendritic cells, monocytes, macrophages, and also gastric and intestinal epithelial cells. *H. pylori* LPS and flagellin are modified in ways that mask them from TLR recognition. In contrast to other gram-negative bacteria, where LPS activates TLR4, *H. pylori* LPS has a low endotoxic activity. This is due to the fact that the O-antigen, the outer part of LPS, is structurally related to the Lewis antigens and the lipid A chain has a different acylation pattern [80]. *H. pylori* gains double benefits from this molecular mimicry since it also actively reduces inflammatory responses in dendritic cells [81]. Flagella are generally recognized by TLR5. *H. pylori* flagellin, however, is a poor TLR5 ligand due to modifications at the N-terminal recognition site [82]. Besides TLR4 and TLR5 also TLR2 has been extensively studied in the context of *H. pylori* infection [83]. However, TLR2 seems to rather induce a regulatory response instead of alerting the immune system [84]. Thus, TLRs mediate a proinflammatory as well as an anti-inflammatory signal during *H. pylori* infection. Besides TLRs, NOD1 seems to be an important PRR particularly in CagA-positive strains. NOD1 responds to peptidoglycan from *H. pylori* cell wall which is translocated into epithelial cells via a type IV secretion system [85, 86].

To differentiate a pathogen from commensal bacteria that share structural features, additional danger signals are needed to induce an inflammatory response. These signals are generally up-regulated in response to tissue damage. Attachment of *H. pylori*, translocation of CagA and secretion of VacA and other virulence factors contribute to disruption of epithelial integrity, to induction of apoptosis, and to stress responses. Upon *Helicobacter* infection, NFκB expression in epithelial cells is up-regulated, which results in the production of proinflammatory cytokines such as IL-1β, IL-6, TNFα, and IL-8 [87, 88]. IL-8 released by gastric epithelial cells in response of *H. pylori* infection is a strong chemoattractant for neutrophils which accumulate in the gastric mucosa [89]. In response to experimental *H. pylori* challenge, IL-8 levels increased more than 20-fold in the gastric mucosa of human volunteers within two weeks [90]. IL-8 expression is further

up-regulated by IL-1β and TNFα, early pro-inflammatory cytokines produced by macrophages and monocytes reinforcing *H. pylori*-associated mucosal injury [91].

Digested bacterial antigens are presented on antigen presenting cells (APCs). This allows a specific response to individual bacterial species in the context of the surrounding cytokine milieu. During *Helicobacter* infection, gastric epithelial cells actively participate in the mucosal defense. They act as antigen presenting cells as they up-regulate major histocompatibility complex molecule class II (MHCII) and also costimulatory molecules, such as CD80 and CD86 [92]. Up-regulation of MHCII in gastric/intestinal epithelial cells is driven by IFNγ [93, 94]. In this way, antigen presenting gastric epithelial cells are also important for the activation of CD4 T-lymphocytes. Furthermore, professional APCs such as macrophages and dendritic cells are activated by *H. pylori* [67]. In fact, dendritic cells are the most effective APCs that have been shown to have a pivotal role orchestrating humoral and cellular responses during *H. pylori* infection [95]. Studies with bone marrow-derived dendritic cells incubated with *H. pylori* have demonstrated that these cells have proinflammatory capacity inducing IL-12 and IL-23 cytokine expression [96, 97]. Yet, more recently it has emerged that dendritic cells exposed to *H. pylori* remain immature and acquire a rather tolerogenic phenotype supporting oral tolerance [86, 98].

APCs take up bacteria and bacterial factors and process them before they migrate to draining lymphoid organs, such as the paragastric lymph node for the stomach and the mesenteric lymph nodes for the small intestine. There they encounter naïve T-cells and present the bacterial antigens. Then, primed lymphocytes home to the site of infection attracted by cytokine and chemokine gradients. Additionally, Peyer's patches (PPs) are important for induction of mucosal immunity in the gut. Evidence derived from studies in mice indicates that priming of CD4 T-cells during *H. pylori* infection also takes place in PPs and that these cells are subsequently directed to migrate to the stomach mucosa [99]. Specific T-cell responses amplify effector functions of polymorphonuclear cells and macrophages by production of proinflammatory cytokines. In the human gastric mucosa, ongoing antigen presentation takes place in lymphoid follicles comprised of B-cells, CD4-positive T-cells, and dendritic cells that can be found during persistent infection [100]. Electron microscopy images revealed that *H. pylori* can reach the lamina propria, which allows direct contact of the bacterium as well as bacterial factors with cells of the innate and adaptive immune system [21]. Although macrophages generally do not traverse epithelial barriers, large numbers are recruited to the site of infection that take up bacteria after progressive damage of epithelial integrity. Even though phagocytes such as monocytes, macrophages, and neutrophils ingest *H. pylori*, they fail to clear the infection. On the one hand, *H. pylori* products such as urease attract inflammatory cells and activate macrophages [101, 102]. On the other hand, *H. pylori* interferes with uptake by phagocytes and also evades phagocytic killing [103]. Nevertheless, activation of these innate immune cells leads to recruitment of lymphocytes and development of a characteristic T helper cell response.

H. pylori secreted neutrophil-activating protein, for example, stimulates IL-12 and IL-23 secretion from neutrophils and monocytes thus promoting a Th1 response [104]. Further bacterial factors interfere directly with effector molecules, such as reactive nitrogen and oxygen molecules. *H. pylori* catalase and superoxide dismutase are thought to neutralize reactive oxygen species, whereas arginase competes with macrophages for arginine, the substrate for the inducible NO synthase (iNOS), thus contributing to the survival of the bacterium [105, 106].

Intraepithelial lymphocytes (IELs) are also good candidates for *H. pylori* immune recognition as they are localized within the stomach epithelium. The majority of IELs in the gastrointestinal tract is CD3/CD8$\alpha\alpha$-positive, expresses a $\gamma\delta$ T-cell receptor and has cytotoxic and IFNγ-producing capacity [107]. IELs were not found to be increased in *H. pylori*-associated gastritis in adults, but in *H. pylori*-associated lymphocytic gastritis ($>$ 25 lymphocytes/100 epithelial cells). Moreover, IEL count was negatively correlated with *H. pylori* density in both cases [108, 109]. The role of

IELs during *H. pylori* infection is not yet well explored.

1.2.2 Adaptive immune response to *H. pylori* infection

The adaptive immune response to *H. pylori* infection is characterized by a specific cytokine profile. In *H. pylori*-infected patients, expression of IFNγ, IL-17, IL-1β, TNFα, IL-6, IL-8, IL-10, and IL-12 is increased compared to uninfected individuals but functional contribution to immunity cannot be easily dissected [110, 111, 112, 113, 114]. Therefore, studies in mice that include functional analysis of adaptive immune responses to *Helicobacter* help to understand the role of different components (Tables 1 - 7). Since many conclusions on the role of adaptive immune cells and components of the adaptive immune response during *H. pylori* infection have been derived from immunization experiments, results from natural infection and immunization are compared in the following paragraphs.

In mice that are unable to mount an adaptive immune response; such as $Rag^{-/-}$ (lacking mature B- and T-cells), SCID (severe combined immunodeficient), and nu/nu (athymic nude) mice; *Helicobacter* colonization is persistently higher than in wild-type mice [69, 115, 116, 117, 118] (Table 1). At the same time, these *Helicobacter*-infected mice, defective in B- and T-lymphocyte responses, display no signs of gastritis in contrast to wild-type mice. Mice reconstituted with adaptive immune cells display an even stronger gastritis than in immunocompetent mice. Adoptive transfer of whole splenocytes or lymph node cells into these mice results in increased gastritis which is correlated with reduced colonization [116, 117, 119]. Remarkably, Eaton *et al.* (2001) demonstrated that inflammation of the gastric mucosa resolves when the infection is cleared this way [119]. These results demonstrate that the adaptive immune response is crucial for induction of pathology as well as for the control of bacterial load, and can even be sterilizing under some conditions.

1.2.2.1 Humoral response against *H. pylori* antigens

Generally, mucosal infections induce secretory IgA antibodies to exclude bacteria from mucosal surfaces. Specific IgA antibodies are also raised against commensals in the intestine to control bacterial density in the lumen without causing detrimental inflammation of the mucosa [120]. In *H. pylori*-infected humans, increased infiltration of B-cells and systemic IgM, IgA, and IgG responses have been detected; additionally, IgA levels were locally increased in the gastric juice [121]. However, unstable non-secretory monomeric IgA predominates in the stomachs of *H. pylori*-infected individuals, suggesting that it is unable to efficiently coat and exclude the pathogen [122]. In line with this, studies in B-cell-deficient (µMT; unable to produce antibodies) mice as well as in IgA-deficient mice suggest that antibodies are dispensable for protective immunity, as they display similar bacterial burdens compared to wild-type mice upon infection and immunization [69, 123, 124] (Table 2). When IL-4 was lacking or neutralized in these mice, they were still protected by immunization to the same extent [125].

Table 1: *Helicobacter* infection of mice deficient in B- and T-cell responses.

Setting		Infection							
Mouse strain	**Transfer**	***Helicobacter* strain**		**Results**				**Conclusion**	**Reference**
				Colonization		**Pathology**			
C57Bl/6 SCID	none	*H. pylori* SPM326	5, 10 wk		Yes	↓	mild	T-cells mediate mucosal inflammation	[115]
C57Bl/6 SCID	none	*H. felis*	8 wk	↑		↓	mild	Low level of inflammation in absence of adaptive immunity	[126]
Balb/c SCID	none	*H. felis*	8 wk	↑		↑	mild	Lymphocytes are required for inflammation	[117]
C57Bl/6 nu/nu	none	*H. pylori* SS1	2, 6, 12 wk		stable		none		
C57Bl/6 Rag1$^{-/-}$	none	*H. felis* 49179	4 to 22 wk	↑	stable	↓	none	Adoptive immune response is required for gastric pathology and bacterial clearance	[69]
C57Bl/6 Rag1$^{-/-}$	none	*H. felis*	8 wk	↗		↓	mild	Lack of inflammation without lymphocytes	[126]
C57Bl/6 Rag2$^{-/-}$	none	*H. pylori* SS1	12, 16 wk		Yes		none	B- and T-cells are required to control bacterial load and induction of gastritis	[118]
C57Bl/6 SCID	Splenocytes	*H. pylori* SS1	4 wk	↓		↑	severe	Adoptive transfer of splenocytes induces gastritis and reduces bacterial burden	[116]
C57Bl/6 nu/nu	Lymphocytes	*H. pylori* SS1	2, 6, 12 wk	↘		↑	severe	Lymphocytes are required for inflammation	[117]

Arrows refer to level compared to wild-type or untransferred mice. Wk, indicates weeks of infection

Table 2: *Helicobacter* infection and immunization of mice deficient in humoral and Th2 cell responses.

Infection

Setting Mouse strain	*Helicobacter* strain		Results Colonization	Pathology	Conclusion	Reference
C57Bl/6 µMT	*H. felis* ATCC 49179	4 to 22 wk	↔ transient	↔ severe	Gastric pathology develops also in absence of B-cells	[69]
C57Bl/6 µMT	*H. felis*		↔	↔ severe	Antibody-dependent immune responses are not important for pathogenesis and protection	[124]
C57Bl/6 µMT	*H. pylori* SS1	4 wk	↔	↔ moderate	B-cells and IL-4 do not play a role in severity of gastritis nor influence bacterial load	[125]
C57Bl/6 µMT IL-4$^{-/-}$	*H. pylori* SS1	4 wk	↔	↔ moderate		
C57Bl/6 IL-4$^{-/-}$	*H. pylori* SS1	4 wk	↔	↔ moderate		
C57Bl/6 IL-4$^{-/-}$	*H. pylori* SPM326 (VacA/CagA)	5, 10 wk	yes	↗ mild	Slight increase of gastritis and IFNγ production by restimulated splenocytes may suggest that IL-4 suppresses inflammation	[115]
C57Bl/6 IL-4$^{-/-}$	*H. pylori* SS1	2 wk, 2 mo	↔	↔ mild	*H. pylori* infection of IL-4$^{-/-}$ mice displays same phenotype as in wt mice regarding colonization and histopathology	[76]
C57Bl/6 pIgR$^{-/-}$	*H. pylori* SS1	3 mo 6 mo	↔ ↓	↔ moderate	Secretory antibodies modulate the progress of *H. pylori* infection	[70]
(C57Bl/6) IgA$^{-/-}$	*H. felis*	n.a.	↔	↔ severe	n.a.	[124]

Arrows refer to level compared to wild-type (wt) mice. n.a. not available. Wk or mo, indicates weeks or months of infection

Immunization followed by *Helicobacter* challenge

Setting Mouse strain	Immunization	*Helicobacter strain*		Results Protection	Pathology	Conclusion	Reference
C57Bl/6 µMT IL-4$^{-/-}$	Lysate + CT	*H. pylori* SS1	4 wk	↔	↔ moderate	Th2 and B-cell responses are not necessary for protection. Protection in IL-4$^{-/-}$ mice is not dependent on antibodies and vice versa	[125]
C57Bl/6 µMT	Lysate + CT	*H. pylori* SS1	4 wk	↔	↔ moderate		
C57Bl/6 IL-4$^{-/-}$	Lysate + CT	*H. pylori* SS1	4 wk	↔	↔ moderate		
C57Bl/6 µMT	Lysate + CT, αIL-4 antibody	*H. pylori* SS1	4 wk	↔	n.a.	Depletion of IL-4 during immunization or challenge does not block protective immunity	[125]
C57Bl/6 µMT	Urease +LT	*H. pylori* X47-2AL	2wk	↔	n.a	Clearance of *H. pylori* after immunization independent from antibodies	[123]
C57Bl/6 IL-4$^{-/-}$	Lysate + CT	*H. pylori* SS1	2wk	↔	↓	IL-4 plays a role in post immunization gastritis but not in bacterial clearance	[76]
C57Bl/6 µMT	Lysate + CT	*H. felis*	n.a.	↔	↔ severe	Antibody-dependent immune responses are not important for protection	[124]
(C57Bl/6) IgA$^{-/-}$	Lysate + CT	*H. felis*		↔	n.a.		

Arrows refer to level compared to immunized/challenged wild-type mice or mice without antibody treatment. n.a., not available. Wk, indicates weeks of infection

Other reports suggest that the humoral response partially contributes to mucosal immunity. Gorrell *et al.* (2013) demonstrate that the stomach of mice lacking the polymeric immunoglobulin receptor (pIgR$^{-/-}$), that is required to transfer polymeric antibodies like secretory IgA across the mucosal surface, was colonized at levels similar to that of wild-type mice for up to three month post-infection [70]. Yet, during that period, the *H. pylori* load in the duodenum of pIgR$^{-/-}$ mice was higher than in wild-type mice and after six month in the stomach as well [70]. This suggests that secretory antibodies can control bacterial numbers to some extent. Yet, this observation was most prominent in the duodenum where only a minority of bacteria resided.

Collectively, these studies indicate that systemic and local antibody responses play only a minor role during *H. pylori* infection and in vaccine-induced immunity. As gastric pathology still develops in absence of B-cells and antibodies, antibody-independent cellular immune mechanisms must be responsible for pathogenesis and protection during *Helicobacter* infections.

1.2.2.2 T-cell responses to *H. pylori* infection

H. pylori-induced immunopathology is clearly T-cell driven, even though the infection is not cleared. In most functional studies performed in mice, T-cell responses are analyzed regarding two different aspects: 1) What causes gastric histopathology? 2) What are immune correlates that limit bacterial number during infection or confer protective immunity upon immunization?

During natural and experimental *H. pylori* infection in humans**,** gastric **T-lymphocytes** are increased [127, 128] and increased numbers of T-cell activation marker (CD25 and CD69)-positive cells are present compared to uninfected individuals [129]. T-lymphocyte-deficient (TCR$\beta^{-/-}$, lacking $\alpha\beta$ T-cell subset) mice are colonized with *Helicobacter* at higher levels concomitant with very low levels of inflammation [73, 130] (Table 3). Thus, $\alpha\beta$ T-cells are absolutely required to induce pathological changes and suppress bacterial expansion.

The T-lymphocyte population is comprised of CD8$^+$ cytotoxic T-cells and CD4$^+$ T-helper (Th) cells that are activated by antigens presented on MHCI and MHCII, respectively. In human stomach tissue, CD8 and CD4 cells are increased upon *H. pylori* infection [128, 131, 132]. Furthermore, *H. pylori*-specific CD4 and CD8 T-cells are found in humans [133]. In experimental *H. pylori* infection of mice, CD8 as well as CD4 T-cells contribute to control colonization since absence of either T-cell subtype, due to MHCI- or MHCII-deficiency, leads to a similar increase in bacterial burden compared to wild-type mice [134]. Mice deficient in CD4 T-cells developed a strong CD8-dominated gastritis in response to *H. pylori* infection with a trend towards a lower colonization level compared to wild-type mice [135]. After immunization of wild-type as well as MHCI-deficient mice, CD4 T-cells dominated in the stomach mucosa and colonization level was reduced. On the contrary, a strong infiltration of CD8 T-cells in MHCII$^{-/-}$ mice did not confer protection, which suggests a predominant role for CD4 T-cells in vaccine-induced immunity [123, 134]. A protective role for CD4 cells has also been inferred from inverse correlation of CD4 and inflammatory cytokines expression with bacterial load [136]. Unfortunately, the level of CD8 expression was not reported in this study. The role of CD4 cells was confirmed by transfer of splenocytes into *H. pylori*-infected SCID mice, which resulted in increased gastritis and reduction of bacterial load, only when CD4$^+$ T-cells were included [116]. Based on these results, many immunologic studies on *Helicobacter* infection *in vitro* and *in vivo* focus on the CD4 T-cells subset only.

CD4 T-cells can be subdivided into several T helper cell subpopulations that are characterized by secretion of specific cytokine profiles. The contribution of each subset to the natural and vaccine-induced immune response to *H. pylori* infection has been in the scope of several studies. Functional *in vivo* studies that have tried to elucidate the role of the individual subpopulations to protection and inflammation have been performed mostly in mice.

Table 3: *Helicobacter* infection and immunization of mice deficient in T-cell responses.

Infection

Setting Mouse strain	Transfer	*Helicobacter strain*		Results Colonization	Pathology	Conclusion	Reference
C57Bl/6 TCR$\beta/\delta^{-/-}$	none	*H. felis* ATCC 49179	4 to 22 wk	↑ stable	n.a.	T-cells required to control bacterial load	[69]
C57Bl/6 TCR$\beta^{-/-}$	none	*H. felis*	3 mo	↑	↓ none	Lack of α/β T-cells impairs control of infection and protects against pathology	[130]
C57Bl/6.BM1.GK1.5 (CD4 deficient)	none	*H. pylori* SS1	1 to 13 wk	↔	↑ severe	A CD8 cell-dominated gastritis develops in absence of CD4 cells.	[135]
C57Bl/6.BM1.GK2.43 (CD8/CD4 deficient)	none	*H. pylori* SS1	13 wk	↔	↔ mild		
C57Bl/6 β_2m$^{-/-}$ (MHCI-deficient)	none	*H. pylori* SS1	2 wk	↑	n.a.	$CD4^+$ as well as $CD8^+$ T-cells regulate the bacterial load to the same extent	[134]
C57Bl/6 I-A$^{b-/-}$ (MHCII-deficient)	none	*H. pylori* SS1	2 wk	↑	n.a.		
C57Bl/6 SCID	$CD4^+$ splenocytes	*H. pylori* SS1	4 wk	↓	↑	$CD4^+$ T-cells are both necessary and sufficient for gastritis due to *H. pylori* infection in mice	[116]
C57Bl/6 SCID	CD4-depleted splenocytes	*H. pylori* SS1	4 wk	↔	↔ none		
C57Bl/6 Rag2$^{-/-}$	$CD4^+$ effector T-cells	*H. pylori* SS1	12, 16 wk	↓	↑ severe	$CD4^+$ effector T-cells mediate *H. pylori*-dependent gastritis	[118]
C57Bl/6 Rag1$^{-/-}$	$CD4^+/CD25^-$ cells (infected donor)	*H. felis*	4 wk	↓	↑ severe	$CD4^+$ effector T-cells clear infection and induce strong histopathology	[73]
C57Bl/6	Low-dose CD4 (Treg low)	*H. pylori* SS1	n.a.	n.a.	↑ severe	A critical number of Tregs is required for engraftment which results in reduced T-cell infiltration and gastritis in infected mucosa	[137]
C57Bl/6	High-dose CD4 (Treg high)	*H. pylori* SS1	n.a.	n.a.	↗ moderate		

Arrows refer to level compared to wild-type or untransferred mice. n.a. not available. Wk or mo, indicates weeks or months of infection

Immunization followed by *Helicobacter* challenge

Setting Mouse strain	Immunization	*Helicobacter strain*		Results Protection	Pathology	Conclusion	Reference
C57Bl/6 β_2m$^{-/-}$ (MHCI-deficient)	Lysate + CT	*H. pylori* SS1	2 wk	↔	n.a	Induction of $CD4^+$ after mucosal immunization is protective against *H. pylori*.	[134]
C57Bl/6 I-A$^{b-/-}$ (MHCII-deficient)	Lysate + CT	*H. pylori* SS1	2 wk	none	n.a	$CD8^+$ cells are only induced in absence of $CD4^+$ cells and are not protective	
C57Bl/6 β_2m$^{-/-}$ (MHCI-deficient)	Urease + LT	*H. pylori* X47-2AL	2 wk	↔	↔ moderate	$CD8^+$ cells do not play an important role in vaccine-induced immunity	[123]
C57Bl/6 I-A$^{b-/-}$ (MHCII-deficient)	Urease + LT	*H. pylori* X47-2AL	2 wk	none	↓ mild		

Arrows refer to level compared to immunized/challenged wild-type mice. n.a. not available. Wk, indicates weeks of infection

T-helper type 2 (Th2) cells are characterized by secretion of IL-4, IL-5, and IL-13 and induce a B-cell response to generate antibodies that combat extracellular bacteria. Since *H. pylori* is a non-invasive pathogen, dominance of a Th2 response would be expected, which is paradoxically not the case. In *H. pylori*-infected stomachs of humans and mice, hardly any IL-4 expression can be detected [138, 139, 140]. Indeed, IL-4 does not play a major role during *H. pylori* infection, as *H. pylori*-infected IL-4-deficient mice display the same colonization level and histopathology as wild-type mice [76, 115] (Table 2). Immunization of IL-4$^{-/-}$ mice with *H. pylori* lysate confers the same protection as immunization of wild-type mice [76]. This stresses that humoral immunity does not play a major role in the immune response against *H. pylori*.

A **Th1 response** is naturally elicited against *H. pylori* infection. Th1 cells are required for cellular immunity, which is generally directed against intracellular pathogens. Therefore, it was not clear whether this response could contribute to protection from extracellular *H. pylori*. This T-cell subtype mainly produces TNFα, IFNγ, and IL-2 and is induced by IL-12 released by monocytes, dendritic cells, and macrophages. Therefore, TNFα and IFNγ have been used as surrogate markers to study Th1 responses. Nevertheless, one has to keep in mind that substantial amounts of these cytokines might be produced by other cell types such as macrophages, natural killer (NK) cells, and CD8 T-cells.

TNFα expression in the stomach is increased during *H. pylori* infection in humans [110]. However, *Helicobacter* infection of TNFα-deficient mice did not change severity of gastritis yet resulted in higher colonization compared to wild-type mice [141] (Table 4). Thus, TNFα released during infection does not seem to be a major effector molecule in driving the immunopathology even though it contributes to control of bacterial load.

Many studies focused on IFNγ, when a Th1-dominant response was proposed. Indeed, IFNγ production is greatly increased in the inflamed gastric mucosa of *H. pylori*-infected individuals and mice [115, 138]. Furthermore, IFNγ expression was inversely correlated with bacterial load and positively correlated with histopathology in mice, suggesting a protective role for IFNγ due to increased inflammation [73].

Since it is generally accepted that Th1 effects are mediated by IFNγ, IFNγ-deficient (IFN$\gamma^{-/-}$) mice have been widely used to study the contribution of Th1 cells. In *Helicobacter*-infected mice lacking IFNγ, histopathology was absent and a similar or higher bacterial load compared to wild-type mice was observed [73, 75, 76, 77, 115, 137, 141] (Table 4). Thus, studies with IFNγ-deficient mice agree on the fact that IFNγ is absolutely required for induction of gastritis and controls the bacterial load to some extent. Neutralization of IFNγ confirmed these findings. After treatment with an anti-IFNγ antibody, no signs of gastritis were elicited in response to *H. pylori* infection [137]. Unfortunately, the effect of IFNγ depletion on colonization density was not reported in this study.

Studies on immunization of IFN$\gamma^{-/-}$ mice are contradictory, although IFNγ expression in the stomach of immunized mice is inversely correlated to bacterial load [136]. While Sawai *et al.* (1999) and Garhart *et al.* (2003) reported that immunized IFN$\gamma^{-/-}$ mice were as protected as wild-type mice [75, 77], Akhiani *et al.* (2002) and Sayi *et al.* (2009) observed less or no protection in IFN$\gamma^{-/-}$ mice in contrast to wild-type mice [73, 76]. In the work of Garhart *et al.* (2003), absence of IFNγ led to similar inflammation in stomachs of *H. pylori*-challenged mice compared to wild-type mice but only upon immunization [77]. This suggests that another cell type takes the predominant role mediating immunity in this study. Conversely, Akhiani *et al.* (2002) reported less severe gastritis in IFN$\gamma^{-/-}$ mice that were not protected after immunization [76]. Nevertheless, the level of IFNγ-induced gastritis correlated inversely with the number of bacteria; thus, it seems to be a very important factor to control bacterial load in response to immunization as well.

Table 4: Functional studies on Th1-cell responses in mice upon *H. pylori* infection and immunization.

Setting		Infection							
Mouse strain	**Transfer/treatment**	***Helicobacter* strain**		**Results**				**Conclusion**	**Reference**
				Colonization		**Pathology**			
C57BL/6 IFNγ$^{-/-}$	none	*H. pylori* CPY2052	4, 8 wk, 15 mo	↗ ↔			none	IFNγ is required for gastric inflammation	[75]
C57BL/6 IFNγ$^{-/-}$	none	*H. pylori* SPM326 (VacA/CagA)	5, 10 wk		yes	↓	mild	IFNγ has an important role for induction of gastric inflammation	[115]
C57BL/6 IFNγ$^{-/-}$	none	*H. pylori* SS1	2, 8 wk	↔		↓	none	IFNγ is involved in development of gastritis	[76]
C57BL/6 IFNγ$^{-/-}$	none	*H. pylori* SS1	16 wk	↔			n.a.	IFNγ induces MIP-2 as inflammatory mediator	[142]
C57BL/6 IFNγ$^{-/-}$	none	*H. pylori* SS1	4 wk	↗		↘	mild	IFNγ plays a role in controlling the level of colonization and inflammation	[77]
C57BL/6 IFNγ$^{-/-}$	none	*H. felis*	2 wk 3, 6 mo	↓ ↑		 ↓	n.a. mild	IFNγ is critical for control of bacterial load during adaptive immune response	[73]
C57BL/6 IFNγ$^{-/-}$	none	*H. pylori* SS1	n.a.		n.a.		none	IFNγ strongly contributes to gastritis	[137]
C57BL/6 IFNγ$^{-/-}$		*H. pylori* CPY2052	6 mo	↑		↓	none	IFNγ plays a protective role in infection and contributes to pathogenicity	[141]
C57BL/6 SCID	IFNγ$^{-/-}$ splenocytes	*H. pylori* SS1	4 wk. 8 wk	↑		↔ ↓	mild mild	IFNγ secretion from splenocytes contributes to gastric inflammation, but is not sufficient	[116]
C57BL/6 Rag2$^{-/-}$	IFNγ$^{-/-}$ CD4^{+}	*H. pylori* SS1	n.a.		n.a.	↓	mild	IFNγ produced by CD4^{+}cells contributes to gastritis in Rag mice	[137]
C57BL/6 Rag1$^{-/-}$	IFNγ$^{-/-}$ CD4^{+}/CD25^{-}	*H. felis*	4 wk	↑		↓	mild	IFNγ production by CD4 effector T-cells is essential for efficient clearance of *Helicobacter*	[73]
C57BL/6	αIFNγ antibody	*H. pylori* SS1	n.a.		n.a.	↓	none	IFNγ is required for gastritis	[137]
C57BL/6 TNFα$^{-/-}$	none	*H. felis*	6 mo		n.a.	↔	moderate	TNFα does not appear to play a role in gastric inflammation induced by *H. felis* infection	[141]
C57BL/6 TNFα$^{-/-}$	none	*H. pylori* CPY2052/KP142	6 mo	↑		↔	moderate	TNFα plays a protective role in infection independently from grade of gastritis	[141]
C57BL/6 IL-12 p35$^{-/-}$	none	*H. felis*	3 mo	↔		↔	moderate	IL-12 deficiency does not impact gastric colonization and histopathology	[130]
C57BL/6 IL-12 p35$^{-/-}$	none	*H. pylori* PMSS1	3 mo	↔		↔	severe		
C57BL/6 IL-12 p35$^{-/-}$		*H. felis*	1 mo	↗			n.a.	Role of IL-12 in control of bacterial load during *Helicobacter* infection not clear	[64]
C57BL/6 IL-12 p35$^{-/-}$		*H. pylori* SS1	1 mo	↘			n.a.		
BALB/c	rIL-12 i.p.	*H. felis*	3 mo	↓	cleared	↑	severe	IL-12 treatment is protective	[64]

Arrows refer to level compared to wild-type (wt), untreated, or mice transferred with wt cells. n.a. not available, i.p. intraperitoneal. Wk or mo, indicates weeks or months of infection

Immunization followed by *Helicobacter* challenge

Setting				**Results**		**Conclusion**	**Reference**
Mouse strain	**Immunization/ Treatment**	***Helicobacter strain***		**Protection**	**Pathology**		
C57BL/6 IFN$\gamma^{-/-}$	Lysate + CT	*H. pylori* CPY2052	3 wk	$\leftrightarrow$	n.a.	IFNγ plays important role in inflammation rather than protection from *H. pylori*	[75]
C57BL/6 IFN$\gamma^{-/-}$	Lysate + CT	*H. pylori* SS1	2 wk	none	$\downarrow$ moderate	IFNγ is very important for development of gastritis and protective immunization	[76]
C57BL/6 IFN$\gamma^{-/-}$	Lysate + CT	*H. pylori* SS1	2, 7 wk	less	n.a.	IFNγ is induced upon and required for vaccination induced protection	[73]
C57BL/6 IFN$\gamma^{-/-}$	Lysate + CT	*H. pylori* SS1	4 wk	$\leftrightarrow$	$\nearrow$ severe	IFNγ is not required for protection or gastric inflammation in immunized mice	[77]
C57BL/6	Lysate + CT, αIFNγ antibody	*H. pylori* SS1	2 wk	$\leftrightarrow$	n.a.	No role for IFNγ in vaccine-induced immunity	[136]
C57BL/6 IL-12 p35 $^{-/-}$	Lysate + CT	*H. felis*	1 mo	less	n.a.	Immunization is protective in mice lacking IL-12, most likely compensation by IL-17	[64]
C57BL/6 IL-12 p35 $^{-/-}$	Lysate + CT	*H. pylori* SS1	1 mo	$\leftrightarrow$	n.a.		
C57BL/6	Lysate + CT + rIL-12	*H. pylori* SS1	2 wk	more	n.a.	IL-12 drives Th1 response and IFNγ production	[76]

Arrows refer to level compared to immunized/challenged wild-type or untreated mice. n.a. not available. Wk or mo, indicates weeks or months of infection

Although $CD4^+$ cells producing IFNγ are of Th1 type, not all IFNγ is produced by CD4 T-cells. In fact it has been shown that a substantial amount of IFNγ is produced by CD8 cells in the infected stomachs of patients [132, 139]. Nevertheless, primarily, the role of IFNγ production by CD4 cells has been investigated. Upon mitogenic and antigen restimulation, a substantial percentage of CD4 T-cells from the gastric mucosa of infected individuals produce IFNγ and thus display a Th1 phenotype [139, 140].

Adoptive transfer of IFNγ-deficient splenocytes or $CD4^+$ cells into *H. pylori*-infected immunodeficient SCID or $Rag^{-/-}$ mice induced less severe gastritis than wild-type cells and failed to control colonization as efficiently [116, 137]. Thus, IFNγ produced by CD4 T-lymphocytes seems functionally relevant in the *H. pylori*-driven immune response. IFNγ from CD4 cells contributed to immunopathology but was not sufficient, as some gastritis was also induced in its absence. Another report demonstrated that CD4 cells promote inflammation, in part, independently from IFNγ production. This was shown by adoptive transfer of Tbet-deficient CD4 cells (unable to differentiate into Th1 phenotype or produce IFNγ) into SCID mice [143]. $Tbet^{-/-}$ CD4 cells induced gastric lesions but to a lesser extent than control cells (CD4 cells able to produce IFNγ).

The Th1 response is induced by IL-12 (p40/p35) which leads to differentiation and activation of CD4 T-cells to produce Th1 cytokines. IL-12p35-deficient mice were infected with *Helicobacter*. Surprisingly, IL-12p35-deficient mice infected with *Helicobacter* had similar pathology and bacterial load compared to wild-type mice [64, 130]. The T-cell profile was not analyzed in these studies, but IFNγ expression did not differ, which suggests that IFNγ from other sources might induce gastritis in these mice. Still, a contribution of IL-12 to gastric inflammation was established by induction of IL-12 expression during immunization or administration of recombinant IL-12. IL-12 has been shown to increase inflammation and to be protective against *H. felis* infection supposedly by induction of a Th1 response [64, 76].

In summary, IFNγ and *H. pylori*-specific CD4 T-cells strongly contribute to induction of gastritis, but not necessarily IFNγ-producing CD4 T-cells. *H. pylori*-specific CD4 cells might act independently from IFNγ production through production of other cytokines, such as IL-17, for example. During immunization, *H. pylori*-specific IFNγ-producing CD4 T-cells seem to be induced and confer protection.

More recently, another T-helper cell subtype producing the lineage-defining cytokine IL-17 (**Th17 cells**) was described. Th17 cells are involved in fighting extracellular bacteria and fungi. Th17 differentiation is induced by TGFβ and IL-6 produced by dendritic cells and macrophages [144]. For expansion and maintenance of Th17 cells, IL-23 (p40/p19) is required which shares the p40 subunit with IL-12, while the p19 subunit is specific for IL-23 [145]. IL-17 commonly refers to IL-17A, although the IL-17 family is comprised of six members. This cytokine promotes the release of proinflammatory cytokines and chemokines (such as TNFα, IL-6, and IL-8) that recruit neutrophils, macrophages, and lymphocytes. CD4 T-cells are the major source of IL-17.

During *H. pylori* infection, IL-17 expression is increased in the gastric mucosa of *H. pylori*-infected individuals and it acts on epithelial cells to induce IL-8 [112, 113]. In this way, IL-17 is a potent mediator of neutrophil recruitment that promotes inflammation [113]. In *H. pylori*-infected children, reduced levels of IL-17 were observed in the gastric mucosa compared to adults that were accompanied by less infiltration of neutrophils and lower gastric inflammation [146, 147].

Surprisingly, the level of gastritis and the colonization density are not inversely but directly correlated when IL-17 is absent during *Helicobacter* infection in mice (Table 5). IL-17-deficient mice have lower bacterial colonization accompanied by less infiltration of neutrophils and a lower inflammatory score [148, 149]. These findings were confirmed by neutralization of IL-17 during *H. pylori* infection with an anti-IL-17 antibody, which resulted in reduced colonization [149]. On the contrary, adenoviral overexpression of IL-17 increased gastritis and bacterial burden. This contradicts earlier work by Velin *et al.* (2009), who observed reduced colonization in *H. felis*-infected

mice upon treatment with recombinant IL-17 [150]. This reduction might be attributed to increased inflammation induced by IL-17. These controversies may arise due to different *Helicobacter* strains, infection periods, and mouse strains used. Indeed, comparing IL-17-deficient mice infected with *H. felis* to those infected with *H. pylori*, DeLyria *et al.* (2011) found that *H. felis* induced more severe inflammation even though higher colonization was observed [74]. Collectively, most studies agree that IL-17 contributes to gastritis but seems to support the bacterium at the same time during natural infection of immunocompetent wild-type mice [74, 137, 148, 149].

The role of the Th17 response during infection was further examined in a study where IL-17-deficient $CD4^+$ splenocytes were transferred into *H. pylori*-infected immunodeficient recipient mice [137]. Mice receiving IL-$17^{-/-}$ $CD4^+$ cells did display a similar degree of gastritis, infiltration of $CD4^+$ cells, and infiltration of Tregs into the gastric lamina propria compared to mice that received wild-type $CD4^+$ cells. Hence, IL-17 did not contribute strongly to gastritis in this setting.

It is equally debated whether IL-17 is required for vaccine-induced immunity. The Th17 response is greatly induced upon immunization and inversely correlated to bacterial load [136]. In immunized mice, IL-17 release from antigen re-stimulated $CD4^+$ T-cells is much higher compared to cells from mice that were only infected [151]. This was associated with a strong increase in neutrophil infiltration. Protective immunity was lost when neutrophils were depleted by an antibody, indicating that protective immunity is conferred through IL-17-mediated recruitment of neutrophils to the site of infection [151]. In a later study, the same group showed that immunized IL-17-deficient mice were protected to the same extent as wild-type mice, which again questions the role of IL-17 in protective immunity [74]. However, when mice were first immunized and then IL-17 was neutralized during challenge phase, protection against *Helicobacter* infection was lost [136, 150]. This implies that IL-17-producing CD4 T-cells, induced upon immunization, confer protection. When IL-17 is absent during immunization another kind of immune response might be induced that is as effective during challenge phase as if IL-17 was present. This may explain why IL-$17^{-/-}$ mice were as protected as wild-type mice.

This issue is further complicated by the fact that IL-23p19 seems to be dispensable for immunity upon *Helicobacter* infection as well as upon immunization followed by *Helicobacter* challenge [64, 130]. In IL-23-deficient mice, a decrease of IL-17A expression in favor of increased IFNγ expression was observed only upon vaccination and not during chronic *Helicobacter* infection [64]. This suggests that IFNγ-producing cells that compensate for a lack of IL-17-producing cells are induced upon immunization and confer protective immunity.

Table 5: Functional studies on Th17-cell responses in mice upon *H. pylori* infection and immunization.

Infection

Setting				**Results**			**Conclusion**	**Reference**
Mouse strain	**Transfer/ treatment**	***Helicobacter strain***		**Colonization**	**Pathology**			
C57Bl/6 IL-17$^{-/-}$	none	*H. pylori* CPY2052	1 to 12 mo	↓	↓	mild	IL-17 is not protective, but required for inflammatory response (neutrophils)	[148]
C57Bl/6 IL-17$^{-/-}$	none	*H.pylori* SS1	n.a.	n.a.	↓	moderate	IL-17A contributes to gastritis	[137]
C57Bl/6 IL-17$^{-/-}$		*H. pylori* CCS9803	4 wk	↓	↓	mild	Absence of IL-17 contributes to bacterial clearance and prevents inflammation, while overexpression has the opposite effect	[149]
C57Bl/6	αIL-17 antibody	*H. pylori* CCS9803	4 wk	↓	↓	mild		
C57Bl/6	AdIL-17	*H. pylori* CCS9803	4 wk	↑	↑	moderate		
Balb/c IL-17$^{-/-}$	none	*H. pylori* SS1	2 wk	↓	↔	mild	(no conclusion on unchallenged mice)	[74]
Balb/c IL-17$^{-/-}$	none	*H. felis*	2 wk	↑	↑	mild		
Balb/c IL-17R$^{-/-}$	none	*H. pylori* SS1	2 wk	↔	↑	moderate		
C57Bl/6	rIL-17	*H. felis*	2 wk	↓		n.a.	IL-17 therapy decreases *H. felis* burden	[150]
C57Bl/6 Rag2$^{-/-}$	IL17$^{-/-}$ CD4^{+}	*H. pylori* SS1	n.a.	n.a.	↔	moderate	Not clear whether IL-17A from CD4^{+} cells contribute to gastritis	[137]
C57Bl/6 IL-23 p19 $^{-/-}$	none	*H. pylori* SS1	1 mo	↔		n.a.	IL-17 does not contribute to bacterial clearance during natural infection	[64]
C57Bl/6 IL-23 p19 $^{-/-}$	none	*H. felis*	3 mo	↔	↔	moderate	Gastric histopathology in IL-23$^{-/-}$ mice is not different from wt mice	[130]
C57Bl/6 IL-23 p19 $^{-/-}$	none	*H. pylori* PMSS1	3 mo	↔	↓	moderate	Gastric histopathology is less severe that of wt	[130]

Arrows refer to level compared to wild-type (wt), untreated, or mice transferred with wt-cells. n.a. not available. Wk or mo, indicates weeks or months of infection.

r, recombinant. Ad, adenoviral overexpression

Immunization followed by *Helicobacter* challenge

Setting				**Results**			**Conclusion**	**Reference**
Mouse strain	**Immunization/ treatment**	***Helicobacter strain***		**Protection**	**Pathology**			
Balb/c IL-17$^{-/-}$	Lysate + CT	*H. pylori* SS1	2 wk	↔	↔	moderate	Also in absence of IL-17A or its corresponding receptor effective immunity is induced. No compensatory mechanism found.	[74]
Balb/c IL-17$^{-/-}$	Lysate + CT	*H. felis*	2 wk	↔	↔	moderate		
Balb/c IL-17R$^{-/-}$	Lysate + CT	*H. pylori* SS1	2 wk	more	↑	severe		
C57Bl/6	Urease + CT , αIL-17 antibody	*H. felis*	10 d	none	↓	moderate	IL-17 is important in immunization-induced reduction of bacterial load.	[150]
C57Bl/6	lysate + CT, αIL-17 antibody	*H. pylori* SS1	2 wk	less		n.a.	Important role for IL-17 in vaccine-induced immunity	[136]
C57Bl/6 IL-23 p19 $^{-/-}$	Lysate + CT	*H. pylori* SS1	1 mo	↔		n.a.	Immunization is protective in mice lacking IL-23, compensation by Th1	[64]

Arrows refer to level compared to immunized/challenged wild-type or untreated mice. n.a. not available. D, wk or mo, indicates days, weeks, or months of infection

As indicated, **Th1 and Th17 responses might interact** during *H. pylori* infection and immunization. Th1 and Th17 responses might compensate for each other during infection in mice with a congenital defect in either T-cell subtype. As IL-12 and IL-23 share the p40 subunit, mice lacking this molecule are considered to be defective in Th1 and Th17 responses. Surprisingly, *H. pylori*-infected IL-12/23p40-deficient mice were equally colonized as wild-type mice and levels of gastritis were similar or not significantly reduced compared to wild-type mice [76, 77] (Table 6). Concerning infection, IL-12/23p40-deficient mice display not only a similar phenotype to wild-type, but also to IL-12p35- and IL-23p19-deficient mice, which refutes a compensatory mechanism on the level of IL-12/IL-23 induction.

Upon immunization, an inverse correlation of IL-12/IL23p40 and bacterial load has been observed in mice [136]. Interestingly, vaccine-induced immunity failed to protect IL-12/IL-23p40-deficient mice although mice lacking either IL-12p35 or IL-23p19 were protected to the same extent as wild-type mice [76, 77, 137]. Only when both Th subtype responses were compromised, mice were not protected. This suggests that induction of either pathway during immunization is sufficient for protective immunity upon challenge. This hypothesis is supported by the fact that neutralization of IL-12/IL23p40 during the immunization phase abrogated immunity in wild-type mice challenged with *H. pylori* [64].

Further studies were trying to dissect the role of Th1 and Th17 response by depleting mice from the effector cytokines IFNγ and IL-17. Mice deficient in both IFNγ and IL-17A did not show any signs of gastritis, similar to those lacking IFNγ only [64]. Likewise, transfer of IFN$\gamma^{-/-}$/IL-17A$^{-/-}$ CD4^{+} cells into *H. pylori*-infected Rag$^{-/-}$ mice induced less gastritis than transfer of wild-type cells but similar gastritis compared to transfer of IFN$\gamma^{-/-}$ CD4^{+} cells [64]. Unfortunately, data about the effect of IFNγ produced by CD4 cells on bacterial burden were not reported this study. Collectively, these data stress that IFNγ is more important than IL-17 for the induction of gastric inflammation during infection.

The opposite was observed in immunization studies. Neutralization of IL-17 and/or IFNγ during effector phase suggested that IL-17 was more important for protection than IFNγ, indicating that vaccine-induced IL-17-producing cells are of critical importance for bacterial clearance after immunization [136].

In summary, studies directly comparing Th1 and Th17 responses reveal that IFNγ, in general, and IFNγ produced by CD4 cells, in particular, strongly contributes to gastritis and to control of bacterial load during chronic *H. pylori* infection, whereas preventive immunization induces a particularly efficient Th17 response that is associated with strong infiltration of IL-17-producing CD4 cells that control bacterial load.

Table 6: Functional studies on Th1/Th17-cell responses in mice upon *H. pylori* infection and immunization.

Infection

Setting Mouse strain	Transfer	*Helicobacter strain*		Results Colonization	Pathology	Conclusion	Reference
C57Bl/6 IL-12/23 p40 $^{-/-}$		*H. pylori* SS1	2, 8 wk	↔	↔ mild	IL-12/23 is not important for development of gastritis	[76]
C57Bl/6 IL-12/23 p40 $^{-/-}$		*H. pylori* SS1	4 wk	↗	↘ mild	IL-12/23 might be involved in development of gastritis	[77]
C57Bl/6 IFNy$^{-/-}$/IL17A$^{-/-}$		*H.pylori* SS1	5 to 8 mo	n.a.	↓ none	IFNγ contributes more strongly to gastritis than IL-17A	[137]
C57Bl/6 Rag$^{-/-}$	IFNy$^{-/-}$/IL-17$^{-/-}$ CD4^{+}	*H. pylori* SS1	5 to 8 mo	n.a.	↓ mild	IFNγ produced by CD4^{+} cells contribute more than IL-17 to gastritis in Rag mice	[137]

Arrows refer to level compared to wild-type (wt), or mice transferred with wt-cells. n.a. not available. Wk or mo, indicates weeks or months of infection

Immunization followed by *Helicobacter* challenge

Setting Mouse strain	Immunization/ treatment	*Helicobacter strain*		Results Protection	Pathology	Conclusion	Reference
C57Bl/6	Lysate + CT, αIL-17/αIFNγ	*H. pylori* SS1	2 wk	less	n.a.	Important role for IL-17 in vaccine-induced immunity in contrast to IFNγ	[136]
C57Bl/6 IL-12/23 p40 $^{-/-}$	Lysate + CT	*H. pylori* SS1	2 wk	none	↓ moderate	Th1/Th17 response is important for protective immunity and is also involved in post-immunization gastritis	[76]
C57Bl/6 IL-12/23 p40 $^{-/-}$	Lysate + CT	*H. pylori* SS1	4 wk	none	↔ moderate	IL-12p40 plays an important role in the development of protection but not in gastric inflammation	[77]
C57Bl/6	Lysate + CT αIL-12 p40	*H. pylori* SS1	1 mo	none	n.a.	Neutralization of IL-12/IL-23 reduced immunity in immunized mice	[64]

Arrows refer to level compared to immunized/challenged wild-type or untreated mice. n.a. not available. Wk or mo, indicates weeks or months of infection

The role of **regulatory T-cells** (Tregs) in *H. pylori* persistence is emerging. FoxP3 is a lineage determining transcription factor that is specifically expressed in naturally occurring $CD4^+/CD25^{high}$ Tregs. Regulatory T-cells counteract T-helper cell-mediated immunity. They secrete IL-10 and TGFβ to suppress inflammatory processes. Commensal bacteria in the intestine induce a specific regulatory response to suppress inflammatory responses and allow persistent colonization. Likewise, *H. pylori* may profit from induction of a Treg response. In children, the immune response against *H. pylori* is primarily regulatory with low levels of Th1 and Th17 cytokines in contrast to adults [146, 147, 152]. This tolerogenic response is associated with less gastritis. Thus, the regulatory component of the immune response might be lost over time during adulthood and lead to progression of pathogenesis as Th1 and Th17 responses take over. Nevertheless, chronic *H. pylori* infection is associated with the presence of regulatory T-cells and up-regulation of FoxP3, IL-10, and TGFβ in the gastric mucosa in adults as well [83, 114, 153, 154]. In the gastric mucosa of patients, total Tregs and the proportion of Tregs within $CD4^+$ cells correlate positively with bacterial density, which indicates that these cells are specifically recruited to the site of infection [154, 155].

The mouse model mirrors human infection in inducing a regulatory T-cell response, as Tregs are induced during *H. pylori* infection in immunocompetent mice [83, 117, 156]. This might partially explain why a rather mild inflammation is observed during chronic infection in mice. Indeed, it has been clearly demonstrated that IL-10 contributes to persistence of *H. pylori* infection. IL-10-deficient mice display a much lower colonization level with concomitant more severe gastritis than wild-type mice [116, 157, 158] (Table 7). In a long term infection study, complete clearance of *Helicobacter* with resolution of a transient IFNγ-dominated gastritis has been reported in $IL\text{-}10^{-/-}$ mice [159]. Remarkably, this demonstrates again that the natural immune response is capable to fight *Helicobacter* infections in absence of a regulatory response and suggests that overcoming tolerogenic mechanisms might lead to protective immunity. In absence of IL-10, neutrophils seem to effectively kill bacteria, as neutrophil depletion delays clearance of *H. pylori* in $IL\text{-}10^{-/-}$ mice [158]. Furthermore, adoptive transfer of IL-10-deficient splenocytes into immunodeficient mice resulted in augmented levels of gastritis compared to transfer of wild-type cells [116]. This suggests that T-cells are the major source of IL-10. This was confirmed with $IL\text{-}10^{-/-}$ $Rag^{-/-}$ mice, where IL-10-deficiency had no additional effect on the development of gastritis or colonization density [126]. Similar to the IL-10 driven phenotype, adoptive transfer of Tregs ($CD4^+CD25^{high}$) into $Rag^{-/-}$ mice was associated with less severe gastritis and higher bacterial load in these mice than when whole $CD4^+$ cells or effector $CD4^+$ cells were transferred [117, 118, 137]. In line with this, Tregs lacking IL-10 co-transferred with wild-type effector T-cells were unable to control inflammation and resulted in inflammation similar to transfer of effector cells only [118]. Tregs unable to produce IL-10 seem to lose their regulatory function and thus colonization was reduced to a similar extent as with effector CD4 cells alone. Conversely, reconstitution of immunodeficient mice with lymphocytes depleted from $CD25^+$ cells resulted in increased gastritis score and reduction of bacterial colonization [117]. The same phenotype of augmented gastritis and decreased bacterial burden was observed when Tregs were depleted by an anti-CD25 antibody [83]. Thus, Tregs seem to establish an equilibrium, preventing pathology but also allowing the bacterium to persistently colonize.

Table 7: Functional studies on regulatory T-cell responses in mice upon *H. pylori* infection

Setting		Infection		Results					
Mouse strain	**Transfer/treatment**	***Helicobacter* strain**		**Colonization**		**Pathology**		**Conclusion**	**Reference**
C57Bl/6 IL-10$^{-/-}$	none	*H. pylori* SS1	4 wk	↓		↑	severe	IL-10 is required to control gastritis	[116]
129/Sv/Ev C57Bl/6 IL-10$^{-/-}$	none	*H. pylori* SS1	6 wk	↓		↑	severe	IL-10 is an inhibitor of the protective immune response to *H. pylori*	[157]
129/EvSv IL-10$^{-/-}$	none	*H. felis*	1, 2 wk	↓	cleared	↑	severe	Neutrophils clear *H. pylori* in absence of IL-10	[158]
C57Bl/6 IL-10$^{-/-}$	none	*H. pylori* SS1	4, 16 wk	↓	cleared	↑	moderate transient	Natural immunity in absence of IL-10	[159]
C57Bl/6 IL-10$^{-/-}$	none	*H. felis*	8 wk	↓		↑	severe	IL-10 limits gastric inflammation and hinders *H. pylori* clearance	[126]
C57Bl/6 Rag1$^{-/-}$ IL-10$^{-/-}$	none	*H. felis*	8 wk	↑	as Rag	↓	mild, as Rag	In absence of T-cells, inflammation is limited independently of IL-10	[126]
C57Bl/6 SCID	IL-10$^{-/-}$ splenocytes	*H. pylori* SS1	4 wk	↓		↑	severe	IL-10 from splenocytes suppresses gastritis	[116]
C57Bl/6 nu/nu	CD25^{-} lymphocytes	*H. pylori* SS1	2, 6, 12 wk	↓		↑	severe	More severe immunopathology and lower bacterial load in absence of Treg	[117]
C57Bl/6 Rag2$^{-/-}$	CD4^{+}eff T-cells (wt) CD4^{+}reg T-cells (wt)	*H. pylori* SS1	12, 16 wk	↑		↓	moderate	Tregs from wt suppressed effector T-cell mediated gastritis more effectively than Tregs from IL-10$^{-/-}$ mice	{[118]
C57Bl/6 Rag2$^{-/-}$	CD4^{+} eff T-cells (wt) CD4^{+} Treg cells (IL-10$^{-/-}$)	*H. pylori* SS1	12, 16 wk	↔		↔	moderate		
C57Bl/6 Rag2$^{-/-}$	CD4^{+}CD25^{+} enriched cells	*H. pylori* SS1			n.a.	↓	moderate	Tregs ameliorate gastritis	[137]
C57Bl/6	αCD25 antibody	*H. pylori* SS1	4 wk	↓		↑	severe	Tregs dampen gastric inflammation and allow higher colonization	[83]

Arrows refer to level compared to wild-type (wt), untreated or mice transferred with wt cells. n.a. not available. Wk, indicates weeks of infection

Collectively, these studies demonstrate that the degree of gastritis and the colonization levels are generally inversely correlated in mouse models defective in cells or cytokines of the adaptive immune response. Furthermore, a complex T-helper cell response emerges during *H. pylori* infection that changes over time and is distinct from the vaccine-induced immunity. During infection, IFNγ and T-cells are required to induce gastritis and also limit bacterial numbers but are inhibited by IL-10-producing Tregs. Thus, the immune response elicited against *H. pylori* is effective but not vigorous enough which may, in part, be attributable to the regulatory responses. The cellular immune compartment seems to be able to control the infection at the cost of severe pathology, yet effector mechanisms ultimately killing the bacterium are poorly understood. Still, bacterial factors that inhibit effector T-cells and enhance regulatory T-cell responses may contribute to immune evasion and favor persistence of *H. pylori* in the stomach.

1.2.3 Strategies of *H. pylori* to cope with the adaptive immune response

In addition to immune evasion mechanisms that interfere with innate immunity, such as TLR recognition, *H. pylori* possesses factors to counteract adaptive immune responses. Two secreted virulence factors have been implicated in inhibition of T-cell responses, namely VacA and γ-glutamyl transferase (gGT). VacA and gGT have been shown to inhibit T-cell activation and proliferation by inducing a G1 arrest [160, 161, 162, 163].

The mode of action on T-lymphocytes has been described for VacA: Binding to LFA1 facilitates internalization of VacA into lymphocytes, where it interferes with T-cell receptor signaling by inhibiting nuclear factor of activated T-cells (NFAT) translocation to the nucleus which blocks IL-2 expression and subsequent T-cell proliferation [161].

The T-cell inhibitory capacity of *H. pylori* gGT was reported by our group [163, 164]. However, the mechanism and signaling pathways by which this effect is mediated as well as the *in vivo* relevance were still to be explored.

1.3 *H. pylori* γ-glutamyltransferase

1.3.1 Characterization of *H. pylori* gGT

In contrast to VacA and CagA, *H. pylori* gGT is highly conserved and present in all clinical isolates described so far. Hence, gGT activity is a common trait of gastric *Helicobacter*s [62, 165]. The strong gGT activity of *H. pylori* has long been recognized, as the enzyme is constitutively expressed at high levels [166, 167]. It is among the 50 most abundant proteins in *H. pylori* and is mainly found in the soluble fraction [168].

H. pylori gGT encoded by the *hp1118* gene was first cloned by Chevalier *et al.* (1999), who described several structural characteristics [62]. The enzyme is expressed as a pre-proform of about 60 kDa that contains a signal sequence for export into the periplasm. There it is autocatalytically cleaved into a 40 kDa and a 20 kDa subunit, which form the enzymatically active heterodimer [169]. Serines at position 451 and 452 are important residues for coordinating the α-carboxylate group of the substrate [170]. Substitution of these serines for alanins renders the enzyme inactive [163]. Therefore, the S451/S452A *H. pylori* gGT has been used as an enzymatically inactive control in this thesis.

γ-Glutamyltransferases (Enzyme Comission number 2.3.2.2.) are N-terminal nucleophile hydrolases, that transfer γ-glutamyl moieties to an amino acid or short peptide (transpeptidation) or to a water molecule (hydrolysis). This enzyme is widely distributed among eukaryotes as well as prokaryotes and was found to be structurally-related. In particular, the γ-glutamyl binding site is highly conserved among gGTs [170]. Great homologies were found within gGTs from *Helicobacter*

species while *H. pylori* gGT shares about 50 % amino acid identity with other bacterial species and 22 % with the human gGT [62, 171, 172]. From a structural perspective, it has been suggested that *H. pylori* gGT rather acts as hydrolase than transpeptidase since it possesses a less defined acceptor binding site compared to human gGT [170]. This supports the observation that *H. pylori* gGT activity is induced upon presence of the acceptor substrate diglycyl, but to a lesser extent compared to human gGT [170]. In mammals gGT is the key enzyme of glutathione metabolism breaking down extracellular glutathione to release substrates to refill the intracellular stores for *de novo* glutathione synthesis [173].

The most abundant γ-glutamyls of the stomach are glutamine and glutathione, which are most likely the physiological substrates of *H. pylori* gGT. Glutamine is hydrolyzed to glutamate and ammonium while glutathione is converted to glutamate and cysteinylglycine. Strong glutaminase activity of *H. pylori* has been recognized even before gGT was described [174]. Subsequently, very efficient conversion of glutamine and glutathione by *H. pylori* gGT has been demonstrated [175]. Furthermore, the production of ammonia by *H. pylori* in presence of 5 mM glutamine was mainly gGT dependent [165].

1.3.2 Physiological effects of *H. pylori* gGT

The primary effects of *H. pylori* gGT activity, such as depletion of γ-glutamyl compounds and production of ammonia or pro-oxidant factors, may affect the bacterium and the host during infection in different ways (Figure 4). On the one hand, the bacterium seems to profit from gGT activity by making important carbon and nitrogen sources accessible. On the other hand, gGT activity may injure host cells by production of toxic ammonia, depletion of essential nutrients, and interference with host metabolism.

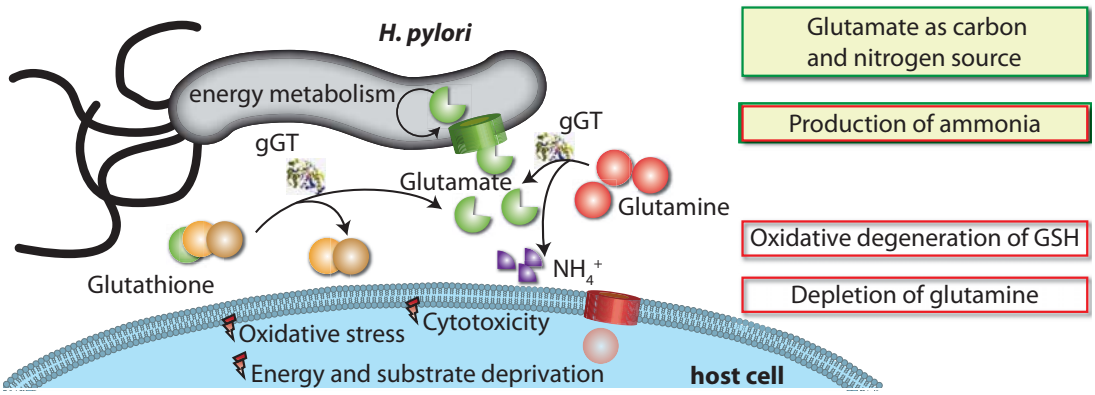

Figure 4: Possible effects of *H. pylori* gGT during infection.

1.3.2.1 Role of *H. pylori* gGT in bacterial metabolism

Even though isogenic *H. pylori* gGT-deletion mutants show no growth defect *in vitro*, it has been proposed that the bacterial metabolism profits from gGT activity [62, 175]. Initially, a γ-glutamyl cycle has been considered to be involved in uptake of amino acids and glutathione turnover as observed in yeast. However, only very low concentrations of glutathione have been found in *H. pylori* compared to other bacteria irrespective of gGT activity [62].

Three important ways in which *H. pylori* gGT supports the bacterium have been proposed: it facilitates access to glutamine as a carbon source, it is indirectly involved in nitrogen metabolism, and it contributes to adjust the periplasmic pH (Figure 5).

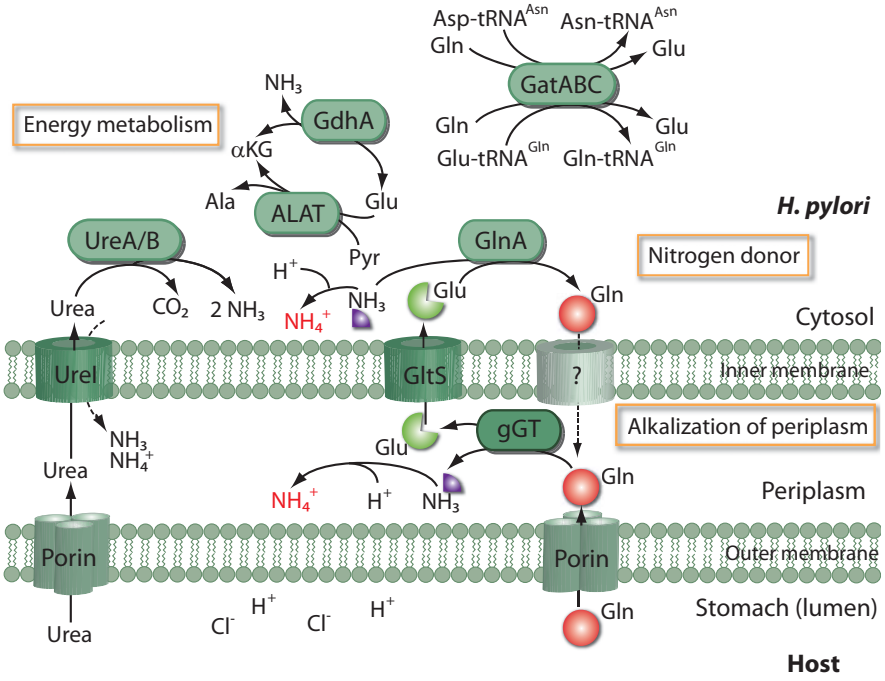

Figure 5: Contribution of *H. pylori* to energy metabolism, nitrogen assimilation, and acid stress resistance.

Glutamine and glutamate are very important for meeting the **metabolic requirements** of *H. pylori*. Under microaerophilic conditions, *H. pylori* preferably uses non-essential amino acids such a glutamine, glutamate, asparagine, aspartate, serine, and proline as energy source that are metabolized to acetate, formate, succinate, and lactate [174, 176]; while glucose is metabolized rather slowly and to a lesser extent [177]. Glutamine/glutamate is consumed at a more than 3-fold higher rate (0.483 mM/h) than other amino acids in defined medium comprised of an amino acid mixture and essential compounds, such as nucleotide precursors and vitamins [176]. Following ^{1}H-NMR spectra over time revealed that deamination is the first step of amino acid catabolism and that the highest deaminase activity was due to deamination of glutamine [176]. The glutaminase activity has been shown to be almost exclusively attributable to *H. pylori* gGT activity [174]. This highlights the importance of *H. pylori* gGT in bacterial metabolism.

Glutamine cannot be internalized unless deaminated to glutamate by *H. pylori* gGT in the periplasm even though genetic annotation indicated that *H. pylori* possesses an ATP-dependent glutamine transport system (GlnH and GlnQ) [175]. It has been demonstrated that glutamate is taken up by *H. pylori* through the glutamate permase (GltS) [175]. Once internalized, glutamate is converted into intermediates of the energy metabolism such as succinyl-CoA, α-ketoglutarate/succinate and glutamine [165, 175].

By making extracellular glutamine available, *H. pylori* gGT indirectly contributes to intracellular **nitrogen metabolism**. *H. pylori* encodes for a glutamate dehydrogenase (GdhA/HP0380), which catalyzes the reversible conversion of glutamate to α-ketoglutarate and ammonium [14]. α-Ketoglutarate can be fermented or transformed into other amino acids. Furthermore, *H. pylori* encodes for a glutamine synthetase (GlnA/HP0512) that catalyzes ATP-dependent formation of glutamine from glutamate and ammonia [178]. This pair of glutamine synthetase and glutamine dehydrogenase is found in all living organisms. Glutamine synthetase seems to play a particular important role for *H. pylori*, as *glnA* deletion mutants could not be generated [178, 179]. *H. pylori* wild-type could internalize and utilize ^{14}C-glutamate as well as ^{14}C-glutamine, while in

gGT-deficient *H. pylori* intracellular radiolabeled glutamine was only detected when ^{14}C-labeled glutamate was added to the bacteria [175]. In this way the intracellular glutamine level of *H. pylori* depends on periplasmic gGT activity.

Like in mammalian cells, glutamine is an important nitrogen donor and precursor for proteins and for nucleotide biosynthesis in *H. pylori*. Glutamine is required for the amidation of mischarged tRNAs, for instance. Thus, a sufficient intracellular supply of glutamate and ammonia are likely to be critical for *H. pylori* viability. The main nitrogen sources in the gastric mucosa available to *H. pylori* are urea and amino acids. Like in many bacteria, ammonia plays a central role in nitrogen assimilation in *H. pylori* [180]. Nitrogen is required for synthesis of nucleotides and other key biosynthetic pathways of cellular metabolism. Intracellular conversion of urea to ammonia and carbon dioxide by urease activity is a major source of nitrogen. Urease is a highly abundant protein that makes up to 10 % of the total protein content [181]. It has been demonstrated that glutamine and glutamate are major compounds produced by nitrogen assimilation from urea-dependent ammonia production by *H. pylori* [180]. Thus, nitrogen assimilation depends on glutamate dehydrogenase and glutamine synthetase activity. Surprisingly, an increase in ammonia assimilation by enhancing glutamine synthetase and glutamate dehydrogenase activity is correlated with increased acid resistance together with an increase of extracellular pH and urea-dependent ammonia production [179]. This indicates that ammonia may be shuttled out of the cell in an assimilated form, as glutamine, for example, and may be liberated by *H. pylori* gGT in the periplasm.

It has been demonstrated that *H. pylori* gGT is part of the compartmentalized **acid resistance** network that is comprised of intracellular urease, glutamine synthetase, and glutamate dehydrogenase and of periplasmic amidases (glutaminase/gGT, asparaginase/AsnB). As production of ammonia results in alkalization, nitrogen metabolism and acid resistance of *H. pylori* are intimately linked. *H. pylori* is highly adapted to the acidic environment of the stomach. The pH in the lumen of murine stomachs is around pH 3 (fed) and pH 4 (fasted) [182]. In humans, even lower pH values of pH 2 are observed in the gastric juice under fasting conditions. Therefore, bacteria are almost exclusively found in the mucus close to the epithelial cell layer where the pH is near neutral [20].

Acid resistance of *H. pylori* is mainly mediated by urease-dependent conversion of urea to CO_2 and ammonia . Intracellular urease activity has been demonstrated to maintain periplasmic pH at 6.2 [183]. However, at a neutral intracellular pH almost all of this ammonia is protonated (NH_4^+, pKa=9.24) which cannot diffuse freely and, therefore, not directly contribute to lowering the periplasmic/extracellular pH. Yet, it is still unclear how alkalization of the cytosol and toxic effects of NH_4^+ to the bacterium are avoided. It has been suggested that the urea transporter, UreI, may act as antiporter that exports NH_4^+ in exchange for urea [184]. However, urease-independent intracellular ammonium produced by overexpressed amidase AmiE was exported independently of UreI [185]. Another suggestion was that export of glutamine would be a way of a net efflux of ammonia [179]. Shibayama *et al.* (2007) described that when bacteria were incubated with ^{14}C-glutamate, radiolabeled glutamine accumulated only in the cytosol of *H. pylori* ΔgGT, not *H. pylori* wild-type [175]. From this observation it could be speculated that export of glutamine may be dependent on gGT activity.

Urease is not necessarily the major producer of ammonia. It has been demonstrated that several nitrogen sources can contribute to production of ammonia and alkalization of the surrounding environment. In a *H. pylori* culture supplied with amino acids, but a limited amount of urea, a considerable amount of up to 18 mM ammonia was produced mainly by deamination of glutamine and asparagine by periplasmic glutaminase/gGT and asparaginase/AsnB, respectively [174]. Addition of glutamine at a low urea concentration (0.1 mM) has been shown to protect *H. pylori* at pH 3, while no additional effect of glutamine could be observed at a high urea concentration (2.5 mM) [183]. Therefore, availability of these nitrogen sources in the habitat of *H. pylori* may be critical.

Urea concentration in the stomach is about 1 - 5 mM, but this might be strongly reduced in the environment surrounding the bacteria [186].

Periplasmic gGT activity has been linked to urease-dependent ammonia assimilation. Lack of gGT led to an almost complete loss of urease-mediated acid resistance when *H. pylori* was exposed to citric acid buffer containing 20 mM urea pH 3 [179]. Furthermore, *H. pylori*-deficient in gGT was unable to raise the pH of the urea-containing buffer starting from pH 4.5 or pH 7.2 in contrast to wild-type bacteria [179]. As no glutamine was provided in the buffer, it has been suggested that glutamine might be exported to the periplasm where it could be hydrolyzed by gGT to release ammonia [179]. This indicates that gGT-dependent hydrolysis of glutamine resulting in glutamate and ammonium raises the periplasmic pH as ammonium (NH_3) is immediately protonated to NH_4^+.

Collectively, these reports indicate that contribution of *H. pylori* gGT to energy metabolism, nitrogen assimilation, and acid resistance are intimately linked in an interdependent network. However, the importance of gGT for *H. pylori* metabolism during infection has not been studied *in vivo*.

1.3.2.2 Role of *H. pylori* gGT during infection

Unlike other virulence factors such as CagA or VacA, *H. pylori* gGT is important for **colonization** of the stomach. The fact that gGT-deficient *H. pylori* strains are viable and expand *in vitro* but that gGT activity is nonetheless present in all clinical isolates indicates that it is providing a major advantage during infection. There are conflicting reports from animal studies on whether gGT activity is required for initial infection and/or persistence. The first report on experimental infection of outbred Swiss mice with a gGT-deficient *H. pylori* SS1 strain concluded that gGT is essential for colonization also in mice, since bacteria failed to establish infection from the first day on [62]. In a consecutive study gnotobiotic-piglet and C57Bl/6 mice were infected with gGT-deficient *H. pylori* M5 and got colonized, albeit at a lower rate [187]. Remarkably, a threefold lower colonization was detected in mice that got infected with the gGT-deficient strain compared to those colonized with the wild-type bacterium. A third study proposed the requirement of gGT for persistence [98].

Furthermore, *H. pylori* gGT activity is associated with **severity of disease**. The gGT activity of *H. pylori* isolated from patients has been correlated to the histopathology in these individuals. Bacterial isolates from patients with duodenal and gastric ulcers had more active gGT than isolates from individuals with non-ulcer dyspepsia [171]. Another study found that gGT activity was greater in gastric cancer patients compared to those with chronic gastritis [188], supporting the hypothesis that *H. pylori* gGT is indeed clinically relevant.

To answer the question how *H. pylori* gGT contributes to gastric inflammation and even cancer development, several studies have been performed on **human gastric epithelial cells**. Mostly, the gastric adenocarcinoma cell line AGS was used. Induction of inflammation and cell death by production of toxic ammonia, depletion of glutamine and induction of oxidative stress have been attributed to *H. pylori* gGT activity [171, 188, 189, 190, 191, 192]. Initially, fractionation of *H. pylori* supernatants led to identification of *H. pylori* gGT as an apoptosis inducing factor in AGS cells [189]. Native purified enzyme as well as recombinant *H. pylori* gGT induced cell death in gastric epithelial cells, which was strictly dependent on enzymatic activity [189, 190, 191]. A major CagA/VacA-independent contribution of gGT in *H. pylori*-induced cell death was confirmed by the use of gGT-deletion mutants. *H. pylori* lacking gGT was no longer able to cause death of epithelial cells [189, 190, 191, 192]. *H. pylori*-associated cell death has been reported to be apoptotic and necrotic. *H. pylori* gGT-induced apoptosis was shown to be dependent on mitochondria-mediated pathways through caspase-3 and -9 activation and Bcl-2 family members and to be a consequence of a cell cycle arrest at G1-S phase transition [190]. In contrast to apoptosis, necrosis

of gastric epithelial cells induced by *H. pylori* gGT might favor release of nutrients but also of proinflammatory proteins [189].

Moreover, inflammatory pathways altered in response to *H. pylori* gGT activity were studied in gastric epithelial cells. In contrast to gGT-deficient strains, wild-type *H. pylori* induced oxidative stress in gastric epithelial cells which affected the expression of stress responsive genes, such as NFκB, Cox-2, and survivin, and promoted oxidation of DNA [171, 192, 193]. *H. pylori* gGT was shown to induce Cox-2 and EGF-related peptides though PI3K and p38 pathways [193]. Furthermore, gGT reduced survivin level and interfered with host cell viability [192]. *H. pylori* gGT-derived H_2O_2 activated NFκB and led to increased IL-8 secretion [194]. Thus, *H. pylori* gGT may induce oxidative stress and promote inflammatory responses in gastric epithelial cells through the NFκB-IL-8 pathway. Supplementation of glutamine and glutathione could counteract the effects of *H. pylori* gGT on IL-8 induction in gastric epithelial cells, whereas release of ammonia was shown to be insufficient to cause damage [188]. In another study, supplementation of glutathione protected from *H. suis* gGT-induced apoptosis but resulted in increased non-apoptotic cell death due to lipid peroxidation by glutathione-derived H_2O_2 [191]. Collectively, these results suggest that *H. pylori*-induced apoptosis of epithelial cells and increase of IL-8 secretion may, in part, be attributed to gGT activity.

Additionally, *H. pylori* gGT directly affects **immune cells**. gGT may contribute to persistence of *H. pylori* infection through manipulation of immune cells. Immunoregulatory effects of *H. pylori* gGT have been suggested for T-lymphocytes and dendritic cells [98, 163]. Bone marrow-derived dendritic cells pulsed with gGT-deficient *H. pylori* or dendritic cells isolated from mice infected with gGT-deficient *H. pylori* failed to direct naïve T-cells towards a regulatory phenotype in contrast cells exposed to *H. pylori* wild-type [98]. Thus, *H. pylori* gGT may contribute to induce tolerogenic dendritic cells that suppress effector T-cell responses. Moreover, a direct inhibitory effect of *H. pylori* gGT on effector T-cells has been proposed. Supernatant from wild-type *H. pylori* blocked proliferation of T-cells, whereas the supernatant from the isogenic gGT-deletion mutant did not [163]. Inhibition of proliferation was due to the enzymatic activity of gGT as the recombinant protein was able to confer the effect, but the enzymatically inactive mutant was inefficient. Impairment of proliferation was attributed to cell cycle block and to changes in the Raf-signaling pathway; yet, a more detailed mechanism remained to be explored.

As previous results from our group show that gGT affects T-cell proliferation and since T-cells are very important for immune responses against *H. pylori* infection, gGT-dependent effects on T-cells were analyzed in this thesis.

1.4 Glutamine-dependent metabolism of activated T-cells

H. pylori gGT has glutaminase activity and glutamine supply is critical for activated T-cells. Thus, the glutamine level might link gGT activity to functional defects of immune cells.

1.4.1 T-cell receptor-dependent activation of T-cells

Activation of T-cells requires two stimulatory signals: T-cell receptor (TCR) ligation and co-stimulatory signal induction. First, T-cells need to recognize a cognate peptide antigen bound to MHC molecules through ligation of a surface bound TCR with an adequate affinity. A TCR is comprised of two out of four highly polymorphic protein chains linked via disulfide bonds to form heterodimers. $\alpha\beta$ T-cells are most common and account for up to 95 - 98 % of T-cells in lymphatic organs or the blood stream, while $\gamma\delta$ T-cells are mainly found in epithelial cell layers, as intraepithelial lymphocytes. $\alpha\beta$ T-cells display highly diverse TCRs that recognize specific peptide-MHC complexes, whereas antigen recognition of $\gamma\delta$ T-cells is more generic and does not require

classical MHC presentation. The T-cell receptor complex is formed by TCR with accessory CD3- and ζ-chains. Second, co-stimulatory factors are required since otherwise anergy is induced [195]. CD28 is a very potent co-stimulatory molecule that binds to APC-associated accessory B7 molecules (CD80 and CD86) and enhances TCR-mediated signaling via the PI3K pathway [196]. Another factor that augments TCR-dependent signaling is CD2. When a peptide engages with the TCR in the context of an MHC molecule together with co-stimulatory factors, an activation signal is transduced inside the cells to activate the T-lymphocyte. CD4 molecules support the interaction with MHCII in T helper cells and CD8 molecules are required for interaction with MHCI in cytotoxic lymphocytes. Activation of T-cells induces multiple signaling pathways involving calcium flux, MAPK, and PI3K signaling that ultimately result in up-regulation of activation markers (e.g. CD69), IL-2 signaling, induction of proliferation, and differentiation into cytokine secreting effector cells. Cytokines act in a autocrine and paracrine manner resulting in a positive feedback loop to fully activate T-cells.

1.4.2 Shift of T-cell metabolism upon activation

Activation of naïve T-cells requires metabolic reprogramming to meet the energetic and biosynthetic demand of the following phase the clonal expansion [197]. Only recently, our understanding was extended on how TCR-dependent activation and adaptation of the metabolic machinery are linked to allow proper induction of immune responses. Upon stimulation, T-cells undergo a phase of cell growth for about 24 hours, which is characterized by an increase in biomass and cell size [197]. During this period, protein and fatty acid biosynthesis as well as ATP synthesis is strongly increased in activated T-cells [197]. These adaptations are necessary to prepare lymphocytes for rapid cell divisions during clonal expansion.

Activated lymphocytes consume large amounts of glucose and glutamine for energy and biosynthetic metabolism. While resting T-cells derive most of their energy from oxidative phosphorylation, proliferating lymphocytes switch to aerobic glycolysis and glutaminolysis, even though oxygen is not limiting [197] (Figure 6).

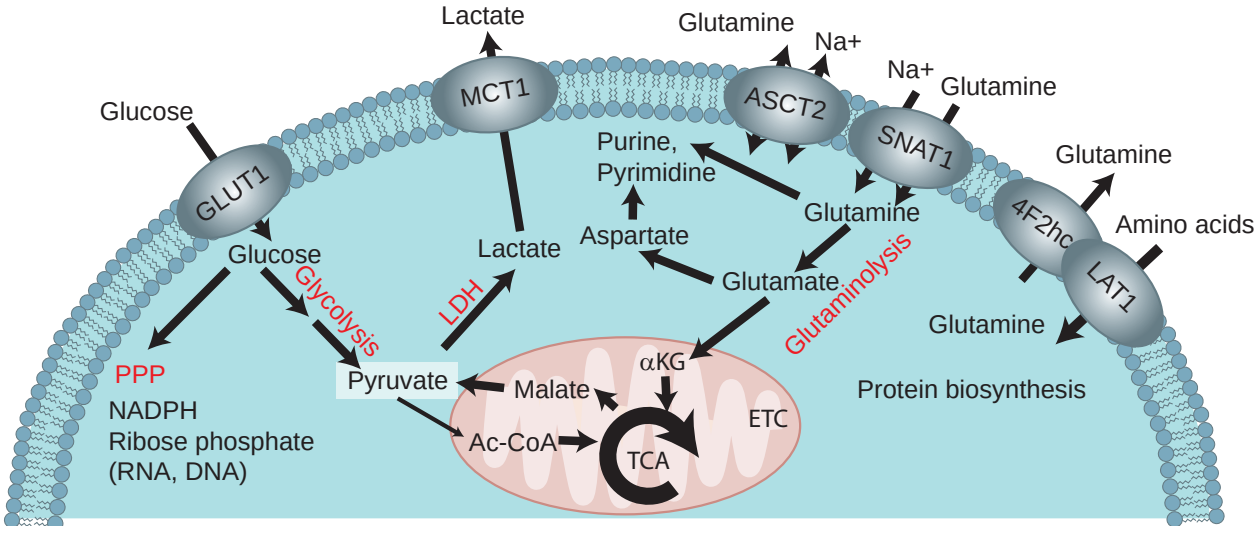

Figure 6: Metabolism of activated T-cells is shifted towards glutaminolysis and glycolysis.

Upon stimulation, glucose uptake is massively increased (up to 50-fold) [198]. In resting T-cells, pyruvate derived from glucose is converted to acetyl-CoA that enters the tricarboxylic acid (TCA) cycle, whereas pyruvate is mostly used for formation of lactate by lactate dehydrogenase in activated

T-cells [197]. Although this activation-induced metabolic mode is less efficient concerning the yield of ATP production, it provides intermediates for metabolic pathways. Another advantage is that ATP can be generated at a higher speed [199].

Glutamine uptake and rate of utilization is induced to a similar or even greater extent than that of glucose upon lymphocyte activation [200, 201]. Following uptake into lymphocytes, glutamine is rapidly converted to glutamate [201, 202]. This reaction is performed by a highly active glutaminase and represents the first and most important step of glutamine utilization. Glutamine has an important role as precursor of glutamate, the most abundant amino acid intracellularly. Most glutamine taken up by activated lymphocytes ends up as glutamate, aspartate, lactate, ammonia, and a low percentage as CO_2 [203]. Hence, glutamine is only partially oxidized (glutaminolysis). Glutaminolysis is the main pathway of glutamine utilization in T-cells with a high flux to meet the requirements of biosynthetic pathways that branch from it at lower rates when demanded [204]. Thus, glutamine is not solely used as an energy source but also as an important precursor of nucleotides, proteins, and glutathione biosynthesis [205, 206]. Although T-cells are capable of *de novo* glutamine synthesis in principle, glutamine is conditionally essential for rapidly dividing cells such as activated lymphocytes [200, 207].

1.4.3 Control of glutamine metabolism in T-lymphocytes

Metabolic reprogramming induced upon T-cell activation is tightly regulated by coordinated expression of different transcription factors. One of the best studied is cMyc, which activates genes involved in mitochondrial biogenesis, glycolysis, glutamine metabolism, and transport in activated T-lymphocytes [197]. Additionally, cMyc expression depends on glutamine levels and is directly linked to proliferation of activated lymphocytes [197, 208]. Furthermore, mammalian/mechanistic target of rapamycin (mTOR), extracellular signal kinase (ERK), and AKT pathway are involved in cMyc induction upon stimulation [197].

More recently, interferon regulatory factor 4 (IRF4) has been pointed out as another important transcription factor involved in activation-induced metabolic reprogramming of T-cells that regulates the expression of essential enzymes required for aerobic glycolysis of effector T-cells [209].

1.4.3.1 Glutamine sensing in T-lymphocytes

Even though it is clear that T-lymphocytes are extremely sensitive to extracellular glutamine levels, it is still not well known how T-lymphocytes sense glutamine and deal with glutamine-limiting conditions. Direct and indirect modes of glutamine sensing have been suggested (Figure 7).

A particularly well-characterized nutrient-sensing signaling pathway driving anabolic metabolism involves mTOR that surveys amino acid availability and integrates a wide array of environmental cues- To control cell growth, it promotes protein biosynthesis and ribosomal biogenesis. The best characterized mTOR targets are ribosomal S6 kinase (S6K) and eukaryotic translation initiation factor 4E binding proteins (4E-BPs) [210]. In T-cells, mTOR is a key regulator that integrates immune signals and metabolic state to allow proper activation and differentiation [211]. Glutamine indirectly activates mTOR by facilitating uptake of essential amino acids, such as leucine, via the SLC7A5/SLC3A2 (LAT1/4Fhc) antiporter [212]. These, in turn, modulate mTOR activity by a yet unknown mechanism. Besides amino acid availability, energy balance and costimulatory factors modulate mTOR activity. AMP-activated protein kinase (AMPK) senses the ratio of AMP to ATP as an indicator for the intrinsic energy level. AMPK activation leads to conservation of ATP through inhibition of mTOR activation and subsequent biosynthetic pathways. In T-cells, AMPK is activated by TCR-induced calcium flux activation [213]. CD28 costimulation on T-cells promotes PI3K/AKT pathway which can also activate mTOR. AKT is known to be a key regulator

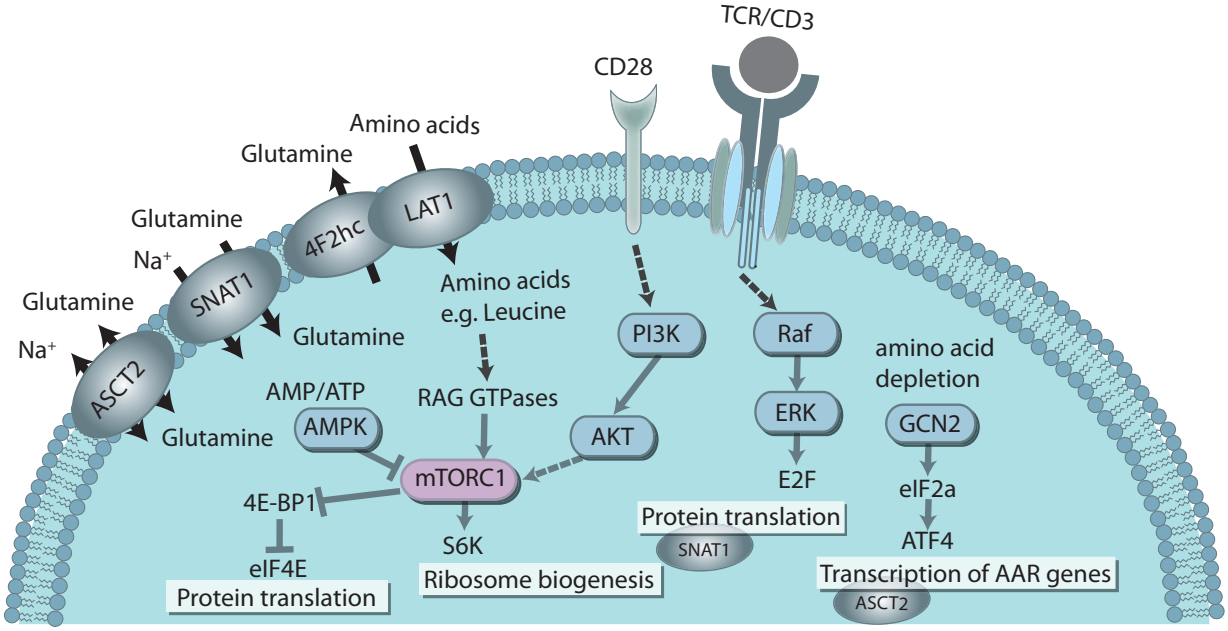

Figure 7: Amino acid sensing pathways in T-lymphocytes.

of glucose metabolism in T-cells [214, 215].

Another pathway known to be involved in nutrient sensing is the MAP-kinase pathway. Three groups of MAP-kinases (ERK, p38, and JNK) are activated by different stimuli. The Raf/ERK pathway is induced upon TCR-dependent, growth factor, and mitogen mediated stimulation. It induces cellular growth, proliferation, and differentiation; while p38 and JNK are activated by cellular stress and are associated with apoptotic pathways.

Amino acid deprivation, mainly of arginine and tryptophan, trigger the amino acid response pathway [216]. The effector kinase of this pathway is general control nonderepressible 2 (GCN2) kinase that senses free tRNA, stops protein biosynthesis by phosphorylation of eukaryotic initiation factor 2a (eIF2a), and increases activating transcription factor 4 (ATF4) that binds to amino acid response elements (AARE) of target genes [217].

1.4.3.2 Glutamine transport in activated T-lymphocytes

The great demand for external glucose and glutamine of activated T-cells is associated with enhanced uptake. Yet, T-cells require external signals to up-regulate transporters for import of nutrients. For glucose, ligation of TCR together with CD28 induces import of glucose via Glut1 in a PI3K/AKT-dependent manner [198, 214]. Likewise, the expression level of transporters limits glutamine import. Besides their transport activity, they may act as nutrient sensors [218]. TCR activation strongly induces glutamine but not glutamate import into T-cells [219]. A lack of transport mechanisms explains why glutamate plus ammonia, aspartate, or asparagine cannot replace glutamine [200]. As glutamate is negatively charged at neutral pH, it cannot use the same transporter as glutamine. Only nucleotides and nucleosides can partially substitute for the glutamine required for proliferation, in particular in combination with α-ketoglutarate [197, 220].

Glutamine transporters that have been shown to be required to import glutamine in activated lymphocytes are sodium-coupled neutral amino acid transporter 1 (SNAT1/SLC38A1) and ASC-like sodium-dependent neutral amino acid transporter 2 (ASCT2/SLC1A5) that cotransport glutamine along an inward sodium gradient [219, 221]. SNAT2 expression is induced upon T-cell

activation and is controlled by ERK in response to amino acid deprivation [219, 222]. Besides SNAT2, ASCT2 is also required for activation-induced uptake of glutamine in T-cells [221]. Moreover, ASCT2 is the only glutamine-responsive gene with a putative AARE in its promoter [223].

1.4.4 Glutamine in immune function

Despite the fact that glutamine is the most abundant amino acid in plasma (300 - 700 µM), it becomes limiting to immune cells under conditions of metabolic stress. Glutamine-deprivation results in inhibition of lymphocyte activation and proliferation [219]. Not only lymphocytes, but also cells of the innate immune system, such as macrophages and neutrophils, depend on sufficient glutamine supply to exert their phagocytic and secretory ability [204]. Interestingly, decreased glutamine levels in response to severe injury and trauma are associated with increased susceptibility to infections. Moreover, glutamine supplementation for critically ill patients is general practice in intensive care units to support immune function [224]. Therefore, it has been proposed that glutamine depletion results in immunosuppression. Indeed, oral glutamine supplementation has beneficial effects regarding inflammation and pathology during *H. pylori* infection in rodents [225, 226]. Yet, it is not clear whether this is only beneficial for epithelial cells or whether immune cells also profit from additional glutamine.

1.5 Hypothesis and Aims

Our understanding of how *H. pylori* gGT interacts with the host's immune system is still rudimentary; even though its great importance in pathogenicity and for colonization has been clearly demonstrated. The underlying mechanisms remain obscure, particularly in the *in vivo* situation. Although effects on various cell types have been described, the role of *H. pylori* gGT during infection is still unknown. On the one hand, the bacteria may profit from production of ammonia and glutamate. On the other hand, *H. pylori* gGT may harm the host through depletion of glutamine and production of ammonia. Induction of inflammation due to damaged epithelial cells and immunomodulatory effects due to dampening of efficient T-cell responses may be the consequences. Thus, *H. pylori* gGT may, in part, account for the lack of an adequate immune response towards the bacterium.

The main aim of this thesis was to explore how *H. pylori* gGT modifies T-cell responses and interferes with T-cell functionality *in vitro* and *in vivo*.

The specific aims were:

- To identify the molecular mechanisms by which *H. pylori* gGT inhibits T-cell proliferation.
- To investigate how *H. pylori* gGT affects T-cell activation and effector cytokine production.
- To identify signaling pathways in T-lymphocytes that were altered by *H. pylori* gGT.
- To analyze contribution of gGT activity to immune modulation *in vivo*.
- To assess whether inhibition of gGT activity or supplementation of glutamine enhance the host's protective immune response against *H. pylori*.

Chapter 2

Material and methods

2.1 *Helicobacter* strains and culture

2.1.1 *Helicobacter* media, plates, and supplements

For plating of *H. pylori*, Wilkins Chalgren (WC) blood agar plates were used. 43 g/l WC-agar (Oxoid) and 0.8 g/l potassium nitrate (Merck) were dissolved in deionized water. WC-agar was autoclaved and cooled down below 60 °C before 1 vial Dent supplement (Oxoid) and 10 % defibrinated horse blood (Oxoid) were added. Dent's supplement is an antibiotic mixture comprised of vancomycin, trimethoprim, cefsoludin and amphotericin B [227]. To prepare plates for plating of stomach homogenates, 1 % (v/v) "Extra" supplement including further antibiotics (200 µg/ml bacitracin, 10 µg/ml nalidixic acid, 3 µg/ml polymycin B) to select for *H. pylori* was added. Plates were stored at 4 °C.

Brucella broth (BB) dent medium was used as liquid medium for *H. pylori*. 45 g/l Brucella broth (Oxoid) was dissolved in deionized water and autoclaved. After medium cooled down, 1 vial Dent supplement and 10 % fetal calf serum (FCS, Sigma-Aldrich) were added. Medium was stored at 4 °C.

2.1.2 *H. pylori* strains

H. pylori "pre-mouse" Sydney strain 1 (PMSS1) was used in this thesis (kindly provided by Prof. Anne Müller, Institute of Molecular Cancer Research, University of Zurich). In contrast to the commonly used mouse adapted SS1 strain, it is capable to translocate CagA into host cells [65]. Thus, PMSS1 possesses a higher virulent potential leading to more severe pathology. Additionally, *H. pylori* PMSS1 ΔgGT, a gGT-deficient isogenic strain, was used (kindly provided by Raphaela Semper [98]). The deletion mutant was created by insertion of a kanamycin resistance gene into the gGT gene of the sequenced *H. pylori* strain G27 [163]. The competence of *H. pylori* to undergo natural transformation was exploited to transfer the insertion into the PMSS1 background. 2 µg DNA from G27 harboring the interrupted gene was mixed with *H. pylori* PMSS1. The mixture was incubated for 30 min at 37 °C and plated on WC-dent plates that contained 50 µg/ml kanamycin to select transformed bacteria. Several colonies were picked and expanded. Deletion of gGT was confirmed by genotyping (Chapter 2.1.4) and a gGT activity assay (Chapter 2.3.1).

2.1.3 *H. pylori* culture and stock preparation

H. pylori were plated on WC-dent agar and kept in a microaerophilic (5 % O_2, 10 % CO_2) humidified atmosphere at 37 °C. gGT-deficient *H. pylori* was cultivated on plates containing 50 µg/ml

kanamycin as selective antibiotic. To minimize genetic variations, aliquots were prepared and freshly thawed for each experiment. Bacteria (100 µl aliquots) were stored in freezing medium (BB-dent, 20 % FCS, 20 % glycerol) at -80 °C. To obtain highly viable bacteria, *H. pylori* stocks were plated on WC-dent blood agar plates, incubated overnight and then spread on further plates to expand bacteria for two to three days. Viability and high proportion of spiral-shaped bacteria was confirmed by microscopy.

2.1.4 Genotyping of *H. pylori* strains

2.1.4.1 Isolation of bacterial DNA

Genomic DNA of *H. pylori* was isolated with the DNeasy Blood & Tissue Kit (Qiagen) following manufacturer's instruction. DNA concentration was determined by absorbance at 260 nm measured with a spectrophotometer (NanoDrop ND-1000, Thermo Scientific). Absorption of 1 at 260 nm corresponds to 50 µg/ml DNA.

2.1.4.2 Polymerase chain reaction

To amplify and determine the length of a desired DNA fragment, polymerase chain reaction (PCR) was performed. PCR allows exponential amplification of DNA segments using specific complementary oligonucleotide primers.

A PCR mix was prepared and a PCR program was run in a T3000 Thermocycler (Biometra).

PCR Mix		**PCR Program**	
2x GoTaq Green Mastermix	10 µl	Initial denaturation	95 °C, 2 min
forward primer 10 µM	1 µl	Cycle (30x)	
reverse primer 10 µM	1 µl	Annealing	55 °C, 30 sec
DNA (20 - 100 ng)	1 µl	Elongation	72 °C, 1 min
nuclease free water	7 µl	Denaturation	95 °C, 30 sec
Σ	20 µl	Final extension	72 °C, 5 min

The 2x GoTaq Green Master Mix (Promega) contained Tag DNA polymerase, 3 mM MgCl, 400 µM dNTPs and a blue and yellow dye to monitor progress during gel electrophoresis. Following primers were used to screen for insertion of the kanamycin resistance cassette in the *H. pylori* gGT gene: forward 5'- AAACGATTGGCTTGGGTGTGATAG -3' and reverse 5'- GACCGGCTTAG-TAACGATTTGATAG -3'.

2.1.4.3 Agarose gel electrophoresis

The size of amplified DNA fragments was determined by agarose gel electrophoresis. When DNA is placed into agarose gel matrix, it can be separated by size in an electric field. This method is based on the property of negatively charged DNA to migrate towards the positively charged anode. To prepare agarose gels, 1 % agarose (w/v) were solved in TAE-buffer (40 mM Tris, 20 mM acetic acid, 1 mM EDTA, pH 8.4) by heating and cooled below 60 °C before 5 µl Roti-GelStain (Roth) were added to 100 ml agarose solution. Gel was cast in a gel tray before it was submerged in a horizontal electrophoresis tank (Bio-Rad) containing TAE buffer. PCR samples (5 µl) were directly loaded into gel pockets. A 1 kb GeneRuler DNA Ladder (Thermo Scientific) was loaded into the first lane to estimate fragment size. Electrophoresis was performed at 100 V for about 30 min. Gels were imaged under UV light using the ChemiDoc Imager (Bio-Rad).

2.2 Expression of recombinant proteins

gGT from *H. pylori*, *Campylobacter jejuni* (*C. jejuni*) and horse (*Equus caballus*) were used in this thesis. *H. pylori* gGTs were obtained as described below. Expression strains and *C. jejuni* gGT were kindly provided by Dr. Christian Bolz. Equine gGT was purchased from Sigma-Aldrich.

2.2.1 Cultivation, induction, and harvesting

Recombinant *H. pylori* gGT (rgGT) and inactive S451/452A gGT mutant were recombinantly expressed as previously described [163]. In short, 500 ml TBex medium (12 g/l trypton (Oxoid), 24 g/l yeast extract (BD), 0.4 % glycerol, 89 mM K-Pi, 2 mM $MgSO_4$, 100 µg/ml ampicillin, 0.2 g/l polypropylene glycol 2000) per 2 l shaking flasks were inoculated with *E. coli* expression strain and incubated overnight in an orbital shaker (275 rpm, 30 °C). For recombinant protein expression, bacteria were induced with 1 mM Isopropyl-β-D-Thiogalaktopyranosid (IPTG) for 6 h at 25 °C. Bacteria were harvested by centrifugation (5 000 g, 10 min, 4 °C). The pellet was resuspended in 10 volumes (w/v) cell disruption buffer (100 mM Tris pH 8.0, 500 mM NaCl, 150 U/g DNaseI, 5 mM $MgCl_2$, 0.1 mM 4-(2-Aminoethyl)-benzolsulfonylfluorid) with an Ultra-Turrax T25 (IKA) and disrupted by a high pressure homogenizer (GEA Niro Soavi) at 800 - 1 200 bar. The supernatant was cleared by centrifugation (20 000 g, 30 min, 4 °C).

2.2.2 Purification by affinity, ion exchange, and size exclusion chromatography

Proteins were purified by a sequence of different chromatography steps performed using an Äkta avant 25 system (GE Healthcare). First, polyhistidine-tagged proteins were purified by immobilized metal affinity chromatography (IMAC). Recombinant proteins were held back by Ni-ions immobilized on a HisTrap FF crude 5 ml column (GE Healthcare). After contaminations were washed out, the protein was eluted by an imidazole gradient. Therefore, the binding buffer (100 mM Tris, 500 mM NaCl, pH 8) was replaced by increasing amounts of the elution buffer (100 mM Tris, 500 mM NaCl, 500 mM Imidazole, pH 8.0). To remove salt from protein fractions, buffer was changed by cross flow filtration or dialysis. Secondly, cation exchange (CEX) chromatography was performed using a HiScreen SP FF column (GE Healthcare). Finally, polishing was achieved by size exclusion chromatography (SEC) with HiLoad Superdex 200 column (GE Healthcare). Protein was concentrated with 10 kDa Amicon Ultra 15 ml centrifugal filter devices (Merck Millipore) to about 1 mg/ml, aliquoted, and stored at -80 °C.

2.2.3 Determination of protein quality and concentration

Sodium dodecyl sulfate poly acrylamide gel electrophoresis (SDS PAGE) (Chapter 2.6.3) was performed with protein fractions from SEC and gels were stained with Coomassie brilliant blue to confirm purity and auto processing of the enzymes. Furthermore, *H. pylori* gGT activity was checked in the gGT activity assay (Chapter 2.3.1). After protein fractions were pooled, protein concentration was determined either by Pierce BCA Protein Assay Kit (Thermo scientific) according to the manufacturer's instructions using a bovine serum albumin (BSA) standard or by spectrophotometry at 280 nm using the NanoDrop ND-1000. The NanoDrop Software calculated protein concentration (c) from absorption at 280 nm (A280), the molecular weight (MW), and molar extinction coefficient (ε280) of the protein of interest by the following equation:

$$c = \frac{A280 * MW}{\varepsilon 280}$$

For *H. pylori* gGT MW is 59.64 kDa and ε280 49 280 M^{-1} cm^{-1}.

2.3 Assessment of gGT activity

2.3.1 gGT activity assay

To determine gGT activity in presence of various substrates or in preconditioned medium, a colorimetric gGT activity assay was used. This assay is based on the transfer of a γ-glutamyl group from the donor substrate L-γ-glutamyl-p-nitroanilide (gGpNA, Sigma-Aldrich) to glycyl-glycine (GlyGly, Sigma-Aldrich) as acceptor dipeptide which results in the liberation of p-nitroaniline (yellow). The assay was performed in a 96-well format in 200 µl reaction volume. 0.1 M Tris-HCl pH 8 was used as reaction buffer and the reaction was started by addition of gGpNA (final concentration 0.5 mM, if not stated differently) and GlyGly (final concentration 20 mM). Release of p-nitroaniline was measured at 405 nm by spectrophotometry (Mithras LB940 Multimode Microplate Reader, Berthold) over 15 min at 37 °C.

2.3.2 Enzymatic glutamate assay

An enzymatic assay to determine the glutamate concentration in cell culture medium treated with *H. pylori* gGT was conducted as described by Wickham *et al.* (2011) [228]. In principle, glutamate is oxidized by glutamate dehydrogenase (GDH) while nicotinamide-adenine dinucleotide (NAD^+) is reduced to NADH. NADH, in turn, is oxidized by diaphorase, reducing iodonitrotetrazolium (INT) to the colored product INT-formazan that can be detected at 490 nm. The amount of INT-formazan formed is stoichiometric to the amount of L-glutamate. The assay was performed in a 96-well format. A glutamate standard curve and sample medium was diluted in assay buffer (100 mM Na_2HPO_4, 3.2 mM KCl, 1.8 mM KH_2PO_4, 27.5 mM NaCl, pH 7.4) to a final volume of 100 µl. Then, 40 µl of reaction solution (238 mM triethanolamine, 30.1 mM K_2HPO_4, 1.5 % Triton X-100, 0.013 % sodium azide, 3.85 mM NAD^+, 275.1 mM INT, 25 mU diaphorase, 500 mU GDH, pH 7.4) was added to initiate the reaction. The reaction was monitored continuously at 490 nm in a Mithras Microplate Reader (Berthold) for 30 min at 37 °C. The glutamate concentration was calculated from the absorption differences ($\Delta A = A_{max} - A_{min}$) using a glutamate standard curve.

2.3.3 Quantitative liquid chromatography/mass spectrometry

Quantitative analysis of glutamine and glutamate was established by Max Koch (Chair of organic chemistry, Prof. Sieber, TUM) using liquid chromatography followed by mass spectrometry (LC-MS). To measure glutamine and glutamate levels, preconditioned medium was shock frozen at indicated times and filtered through 3 kDa centrifugal filter tubes at 4 °C. Stomach tissue was homogenized in 500 µl 0.1 M Tris pH 8 and cleared by centrifugation (10 000 g, 15 min, 4 °C). Then, supernatant was filtered through a 3 kDa centrifugal filter at 4 °C. Samples were stored at -80 °C.

The samples were analyzed by LC-ESI-MS on a Thermo Finnigan LTQ FT-ICR and were eluted by a Dionex UltiMate 3000 with a flow of 0.2 ml/min over a Phenomenex Luna aminopropyl column (150 x 2.0 mM, 5.0 µm particle size) at 30 °C. Eluting buffers were 0.1 % formic acid in H_2O (pH 2.7) and 0.1 % formic acid in H_2O/acetonitrile 10/90 (pH 2.9). The chromatographic eluent was directly introduced into the ion source. All data acquisition and processing were controlled by LTQ software (Xcalibur 2.1). Mass calibration curves of L-glutamine and L-glutamate were obtained at six different concentration ratios. For absolute quantification the internal standards were added to the samples and the areas of deuterated and undeuterated amino acid were determined. The absolute concentrations were calculated from the obtained ratios and the linear equations of the calibration curves.

2.4 Cell culture based analyses

2.4.1 Isolation and cultivation of primary lymphocytes and cell lines

2.4.1.1 Jurkat T cell line

The non-adherent leukemic T-cell line Jurkat [229] was obtained from the American Type Culture Collection (Number TIB-152). Cells were cultured in RPMI-1640 (Gibco, Life Technologies) medium containing 2 mM L-glutamine supplemented with 1 % penicillin/streptomycin (Gibco, Life Technologies) and 10 % FCS. Cell concentration was maintained between 5 x 10^4 to 1 x 10^6 cells/ml at 37 °C in a 5 % CO_2 atmosphere. Cells were split every three to four days. For the experiments, Jurkat cells were diluted to 5 x 10^4 cells/ml. Prior to treatment with preconditioned medium, cells were washed with phosphate buffered saline (PBS, Gibco, Life Technologies).

2.4.1.2 Isolation of PBMCs and T cells

Human peripheral blood mononuclear cells (PBMCs) were isolated from whole blood by density centrifugation using Biocoll (1.077 g/ml; Biochrom) after informed consent. In brief, heparinized blood was diluted 1:1 with PBS, layered over an equal volume of Biocoll in 50 ml conical tubes and centrifuged without brake at 400 g for 30 min. The mononuclear cell layer, found at the interface between plasma and Biocoll, was carefully transferred into a new tube and washed twice with PBS (300 g, 10 min). T-cells were purified from PBMCs using Pan T-cell Isolation Kit (Miltenyi Biotec) with LS separation columns by negative selection with antibodies against CD14, CD15, CD16, CD19, CD34, CD36, CD56, CD123, and CD235a according to manufacturer's instructions. Cells were incubated overnight at 1.25 to 2.5 x 10^6 cells/ml in glutamine-free RPMI-1640 (Gibco, Life Technologies) medium supplemented with 1 % penicillin/streptomycin and 10 % FCS at 37 °C and used for experiments the next day.

2.4.2 Preparation of preconditioned medium

Preconditioned media were prepared as follows: glutamine-free RPMI-1640 medium containing 10 % FCS was used. 2 mM glutamine was added before preconditioning when indicated. Subsequently medium was either treated with recombinant *H. pylori* gGT or live *H. pylori* at a multiplicity of infection (MOI) of 5. As a suspension with an optical density of 1 at 600 nm corresponded to an inoculum of about 2 x 10^8 colony-forming units (CFU), the OD600 was adjusted to 0.03. Then, the medium was incubated at 37 °C to allow enzymatic turnover of substrates for 24 h or 72 h. To abrogate enzymatic activity before cells were placed into preconditioned medium, the medium was subjected to heat-treatment (65 °C, 30 min). To confirm inactivation, 50 µl aliquots of each preparation were subjected to the gGT activity assay (Chapter 2.3.1). Corresponding control media leaving out glutamine and/or rgGT and/or *H. pylori* wt/ΔgGT and/or heat-treatment were prepared in parallel. The experiment started when PBMCs were placed into preconditioned medium and supplemented with glutamine or other factors.

2.4.3 Activation and *H. pylori* gGT treatment of lymphocytes

Primary lymphocytes were either activated with mitogens, 20 ng/ml Phorbol-12-myristate-13-acetate (PMA) and 500 ng/ml Ionomycin (Iono) obtained from Sigma-Aldrich, or TCR-dependently stimulated with αCD3-, αCD2-, and αCD28-coated T-cell expansion beads (2:1 cell:bead ratio, Miltenyi Biotec). For supplementation, substances such as L-glutamine (Applichem), D-glutamine (Sigma-Aldrich), reduced glutathione (Applichem), dithiothreitol (Applichem), β-mercaptoethanol (Sigma-Aldrich) and recombinant human IL-2 (eBioscience) were added at the time of stimulation.

H. pylori gGT was either directly added to the cells or medium preconditioned with gGT was used to expose cells to gGT effects. Cells were incubated at 37 °C in a 5 % CO_2 atmosphere for different times.

2.4.4 [^{3}H]-thymidine incorporation assay

A thymidine incorporation assay was employed to analyze proliferation of lymphocytes. This assay monitors DNA synthesis as the radiolabeled [^{3}H]-thymidine is incorporated into new strands of DNA. Thus, the amount of radioactivity measured as counts per minute (cpm) is proportional to number of proliferating cells. Stimulated PBMCs (1.25 x 10^5 cells/well) or Jurkat cells (5 x 10^3 cells/well) were seeded in 96-well plates (100 µl/well) and treated for 72 hours. [^{3}H]-thymidine (1 µCi/well) (Hartman Analytic) diluted in PBS was added (10 µl) 24 hours before termination of cultivation using a multipette with sterile 0.5 ml Combitips (Eppendorf). After cultivation, cells were quantitatively transferred onto glass fiber filters by a cell harvester (Molecular Devices). Filters were air dried and radioactivity was measured by a β scintillation counter (Packard Direct Beta Counter Matrix TM 9600, Packard Instruments).

2.4.5 Viability assay

The CellTiter-Glo Luminescent Cell Viability Assay (Promega) was used to assess proliferation and cytotoxicity. This assay generates a luminescent signal that is proportional to ATP released from lysed cells. ATP, in turn, is proportional to number of metabolically active cells. Stimulated PBMCs (1.25 x 10^5 cells/well) or Jurkat (5 x 10^3 cells/well) were seeded in 96-well plates (100 µl/well) and treated for 72 hours. Then, an equal volume of CellTiter-Glo reagent was added to plates that were equilibrated at room temperature for 30 min. Plates were shaken to promote cell lysis for 1 min. Finally, 150 µl were transferred into white assay plates and incubated for 10 min at room temperature before luminescence was recorded using a Mithras LB940 Multimode Microplate Reader (Berthold).

2.4.6 Caspase-3/-7 activation assay

Induction of cell apoptosis was assessed using Caspase-Glo 3/7 assay (Promega) which measures caspase-3 and -7 activities. These caspases play a central role during apoptosis of mammalian cells. For this assay, PBMCs (2 x 10^4 cells/well) were seeded in a 96-well plate and treated with 1 µg/ml of rgGT for different times. 5 µM staurosporine was added 1 h prior to analysis as a positive control. After cultivation, 1 volume of Caspase-Glo reagent was added and plates were incubated at room temperature for 30 min before luminescence was measured in a Mithras LB940 microplate reader.

2.5 Murine infections

2.5.1 Mouse strains and housing

Six to eight-week old in-bred wild-type C57BL/6 mice (purchased from Harlan) or C57BL/6 Rag$^{-/-}$ mice (derived from in-house breeding) were housed in microisolator cages under specific pathogen free conditions. If not stated differently, mice were fed standard mouse chow (Teklad, Harlan) and water was provided *ad libitum*.

2.5.2 Experimental infection with *H. pylori*

Mice were fasted for four to six hours and then orogastrically inoculated with 10^9 CFU of *H. pylori* wt, ΔgGT, or a combination of both in 200 µl BB/10 %FCS. In most experiments, mice were infected only once. When indicated, the infection was repeated twice in two day intervals. After infection, bacterial suspensions used for inoculation were plated in serial dilutions to confirm administration of equal numbers of viable bacteria cells and an equal proportion of wt and gGT-deficient *H. pylori*. Groups of four to eight mice were used and sacrificed by isoflourane or CO_2 inhalation after different time points post infection.

2.5.2.1 Treatment with gGT inhibitor or recombinant protein

Mice infected with *H. pylori* wt were treated with gGT inhibitor Acivicin (α-amino-3-chloro-4,5-dihydro-5-isoxazoleacetic acid, Sigma-Aldrich) (Figure 8). 40 µg Acivicin per mouse was *intraperitoneally* (i.p.) administered two days prior to infection, at infection day and the two consecutive days. Infection status was determined after three days.

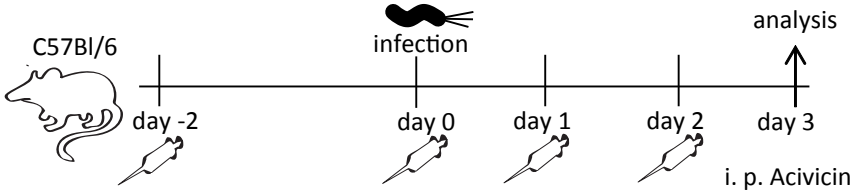

Figure 8: Treatment of mice with acivicin during a short term *H. pylori* infection experiment.

Mice infected with *H. pylori* ΔgGT were treated with recombinant gGT to complement for lack of gGT activity. Recombinant gGT was diluted in PBS and 200 µl were administered by oral gavage at infection day and the two consecutive days (Figure 9). Infection status was determined after three days of infection.

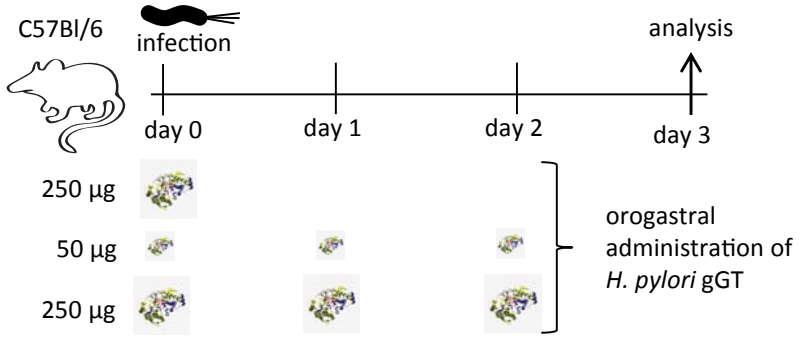

Figure 9: Oral complementation of gGT-deficient *H. pylori* with recombinant gGT during experimental infection in mice.

2.5.2.2 CD4 cell transfer

To analyze the effect of the CD4 T-cell response on *H. pylori* gGT-proficient and -deficient bacteria, $Rag^{-/-}$ mice (lacking mature B- and T-cells) were infected with *H. pylori* and CD4 T-cells were adoptively transferred after the infection had been established (Figure 10A). $Rag^{-/-}$ mice were infected with *H. pylori* wt or ΔgGT three times within five days. In order to facilitate initial infection of the *H. pylori* ΔgGT strain, 250 µg *H. pylori* gGT was added to the inoculum. One

month after infection CD4 cells from C57/Bl6 donor mice were transferred. Therefore, spleens and lymphnodes of donor mice were removed under sterile conditions and grinded through a 100 µm filter to disintegrate tissue and obtain a single cell suspension. Erythrocytes were lysed with ammonium chloride tris (ACT) solution (153 mM NH_4Cl, 17 mM Tris-HCl, pH 7.2) for three minutes at room temperature. Then, lymphocytes were washed and were resuspended in FACS buffer (0.5 % BSA in PBS) at 10^8 cells/ml. Cells were stained with 0.5 µg/ml propidium iodide (PI, BD Pharmingen) and a murine anti-CD4 antibody coupled to eF450 (1:100, eBioscience) for 20 min at 4 °C in the dark. After staining, cells were washed twice with FACS buffer (300 g, 5 min) before CD4 cells were sorted on a FACSAria cell sorter (BD Biosciences). Sorted $CD4^+$ cells were resuspended in sterile PBS and 100 µl cell suspension corresponding to 300 000 cells were transferred into $Rag^{-/-}$ recipient mice by i.p. injection. After another month, the experiment was terminated. Blood and stomach were obtained for further analysis. In a separate experiment $Rag^{-/-}$ mice were infected with *H. pylori* wt or ΔgGT for 1.5 month before 300 000 $CD4^+/CD44^-$ cells/mouse were transferred (Figure 10B). This experiment was performed as described above with the exceptions that no rgGT was given at the time of infection and that cells were stained with an additional anti-CD44 antibody coupled to FITC (1:100, eBioscience) before sorting. Analysis was performed three months post infection.

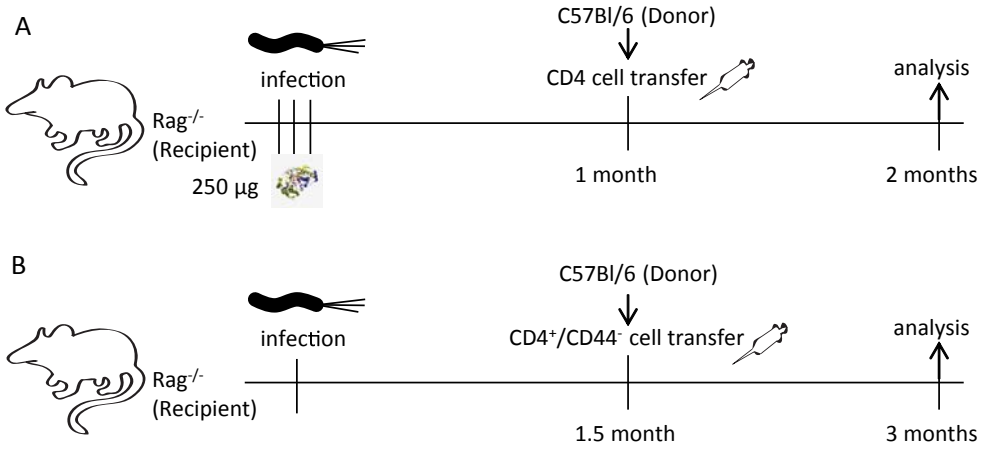

Figure 10: Adoptive transfer of CD4 cells into Rag-/- mice infected with *H. pylori*.

2.5.2.3 Oral supplementation of glutamine and glutamate

Excessive amounts of glutamine and glutamate were orally administered to mice infected with *H. pylori* wt and ΔgGT to analyze their effect on infection status and immune response.

Monosodium glutamate (MSG, Sigma-Aldrich) was supplemented in drinking water prior (for 4 days) and/or during (for 3 days) a short term infection experiment (Figure 11A). Furthermore, 10 % (w/v) glutamate was administered in drinking water for three to four days in the beginning or by the end of a one month infection period (Figure 11B).

Additionally, mice infected with *H. pylori* were fed a diet containing 10 % glutamate, 20 % glutamine, or an isonitrogenous control diet (ssniff Spezialdiäten) for one month starting four days prior to infection (Figure 12A) or when mice were already infected for one month (Figure 12B).

2.5.3 Harvesting of organs

After mice were sacrificed, blood, lymphoid organs, and stomach were removed.

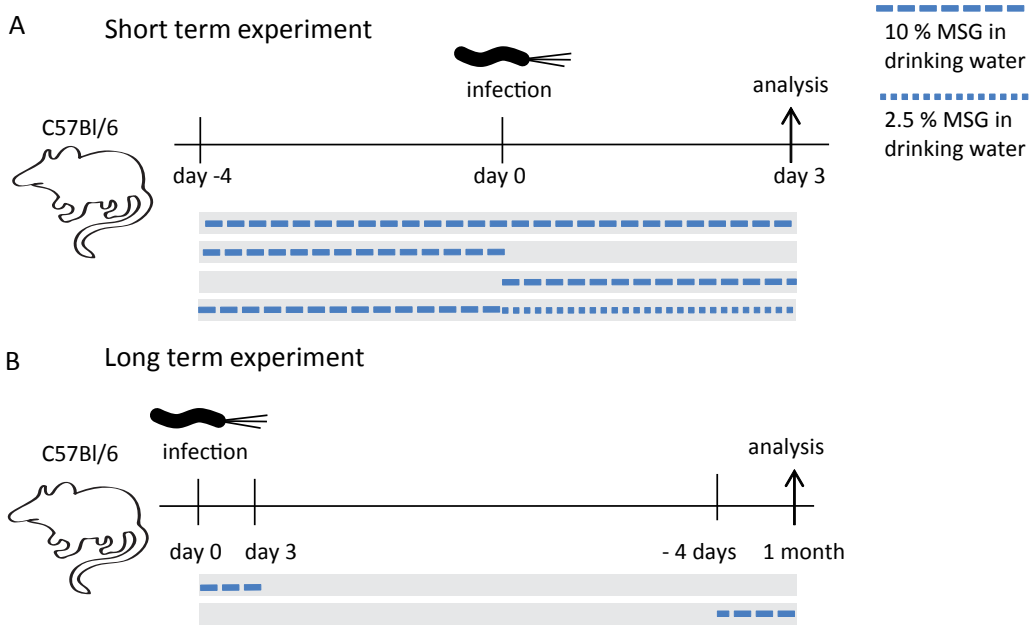

Figure 11: Administration of glutamate (MSG) in drinking water during infection with *H. pylori* wt and ΔgGT.

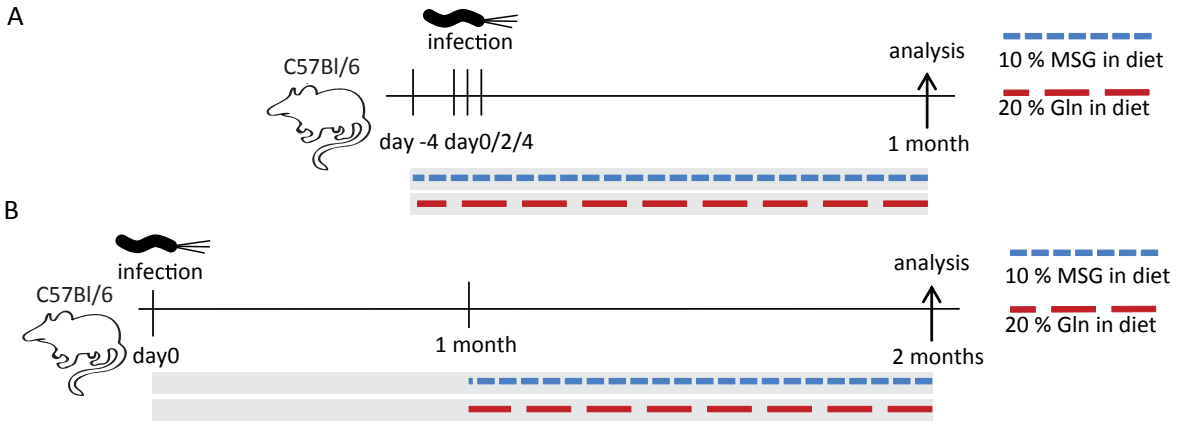

Figure 12: Glutamine- and glutamate-enriched diet during *H. pylori* infection.

2.5.3.1 Collection of plasma and lymphocytes from blood

Blood was drawn from the heart with a heparinized syringe. For the collection of plasma, blood was centrifuged at 2 000 g for 10 min. The plasma was placed in a fresh tube and stored at -20 °C. For flow cytometry, 100 µl of blood were placed in 10 ml prewarmed ammonium chloride tris (ACT) solution (153 mM NH_4Cl, 17 mM Tris-HCl, pH 7.2). Erythrocytes were lysed at 37 °C for 10 min before cells were harvested (300 g, 5 min) and washed with FACS buffer.

2.5.3.2 Preparation of single cell suspensions from lymphoid organs

Mesenteric lymphnodes, paragastric lymphnodes, spleen and peyer's patches were quickly removed and single cell suspensions were prepared by grinding and filtering through a 70 µm nylon mesh. Erythrocytes from spleen were lysed with ACT solution for 10 min at room temperature. Cells were washed twice with cell culture medium (300 g, 5 min). Viable cells were counted with a hemocytometer after trypan blue exclusion stain. The isolated lymphocytes were analyzed by flow cytometry (Chapter 2.6.2). Therefore, 10^6 cells/100 µl were either directly stained or cytokine production was induced by 100 ng/ml PMA and 500 ng/ml ionomycin stimulation for 4 hours before cells were stained.

2.5.3.3 Processing of stomach tissue

For evaluation of colonization and inflammation, glandular stomachs were retrieved, opened on the longer curvature and washed in cold PBS. Longitudinal sections of gastric tissue were prepared for analysis of bacterial load, histology, cytokine expression, infiltration of immune cells and glutamine/glutamate content. Stomach pieces for quantitative LC-MS analysis (Chapter 2.3.3) were shock frozen in liquid nitrogen and stored at -80 °C. For mRNA expression analysis (Chapter 2.6.6), stomach strips were either immediately shock frozen and processed the next day or treated with RNAlater (Qiagen) overnight at 4 °C and stored at -80 °C. For determination of infection status (Chapter 2.5.4), one piece was placed into 1 ml BB-dent and kept at room temperature. For histological evaluations (Chapter 2.7), a 2 mm wide stripe from the greater curvature was fixed in 3.5 - 3.7 % buffered formaldehyde solution (Fischar) on a piece of balsa wood. For flow cytometry (Chapter 2.6.2), stomach stripes were enzymatically processed using 1 mg/ml Collagenase IV (Sigma-Aldrich) and 200 µg/ml DNase I (Roche Diagnostics) in 2 ml cell culture medium for 30 min at 37 °C shaking at 200 rpm. Following digestion, gastric mucosa was carefully separated from the muscular layer between two glass slides. The mucosal cells were passed through a 70 µm filter and washed with FACS buffer.

2.5.4 Quantitative assessment of colonization

One stomach section of about 20 mg was used for quantitative bacterial colony count. Therefore, gastric tissue samples were homogenized with an Ultra Turrax in 1 ml of BB containing 10 % FCS and serial dilutions were plated on WC-dent extra plates: 1:10, 1:100, 1:500 (1:5 000 for $Rag^{-/-}$ mice). Stomachs of mice infected with *H. pylori* ΔgGT were additionally plated on WC-dent extra plates containing kanamycin (50 µg/ml). Plates were kept under microaerobic conditions for four to six days before number of CFU per gram of stomach tissue was determined by colony count.

2.6 Molecular biological techniques

2.6.1 Enzyme-linked immunosorbant assay

2.6.1.1 Cytokine secretion

Cytokine secretion by lymphocytes was determined in culture supernatants by enzyme-linked immunosorbant assay (ELISA). Ready-Set-Go! ELISA Kits to detect human TNFα, IFNγ, IL-17A, and IL-2 were purchased from eBioscience and conducted as recommended by the supplier. In brief, 96-well flat-bottom plates (Corning) were coated overnight at 4 °C with capture antibodies. Plates were washed (0.05 % Tween 20 in PBS) and blocked for 1 h at room temperature. Diluted samples and standards were added and incubated overnight at 4 °C. After washing, plates were incubated with biotin-conjugated detection antibody for 1 h. Then, avidin-coupled horse radish peroxidase (HRP) was added for 30 min. Plates were extensively washed (7 - 10 times) prior to addition of tetrametylbenzidine (TMB) substrate. The reaction was stopped by 1 M H_3PO_4 and absorbance was measured at 450 nm using a microplate reader (Sunrise, Tecan). Cytokine levels were determined by a standard curve comprised of a serial dilution of known concentrations for each cytokine.

2.6.1.2 HpaA antibody response

A non-commercial ELISA was used to detect antibodies against the *H. pylori* surface antigen *H. pylori* adhesin A (HpaA) that were induced upon infection. 96-well plates were coated with 100 µl recombinant HpaA (2 µg/ml in PBS) at 37 °C for 2 h. Plates were washed with 0.5 % Tween 20 in PBS. Then, plates were blocked with 200 µl blocking buffer (1 % BSA in PBS) at 4 °C overnight. Murine plasma was diluted in blocking buffer. Plasma samples were applied and incubated at 37 °C for 60 min. Plates were washed before 100 µl goat-anti-mouse IgG coupled to HRP (STAR120P, AbD serotec) was added in a 1:10 000 dilution. Samples were incubated with the detection antibody for 60 min at 37 °C before excessive antibody was washed away. Then, 100 µl of TMB substrate reagent (BD OptEIA) was added. Plates were kept for 15 min at room temperature before reaction was stopped by adding 50 µl of 1 M H_3PO_4. Absorbance was measured at 450 nm using a Sunrise microplate reader (Tecan).

2.6.2 Flow cytometry

Flow cytometry was used to analyze cell division, expression of activation markers and of intracellular cytokines and distribution of T-cell subsets. This technique allows characterization of multiple properties on a single cell level. If not stated otherwise, antibodies and reagents for flow cytometry were purchased from eBioscience. Staining protocols were conducted in 96-well plates as described by the manufacturer. Sample materials for flow cytometry were single cell suspensions derived from murine blood, lymphoid organs, stomach tissue or primary human lymphocyte cultures.

2.6.2.1 Labeling with proliferation dye 670

To analyze proliferation on a single cell level, cells were loaded with a proliferation dye that is equally distributed between daughter cells when cells divide. Thus, a defined reduction in fluorescence intensity indicates number of cell divisions. Cells were washed twice with PBS (300 g, 5 min) to remove serum. To stain, cells were incubated in 5 µM Cell Proliferation Dye 670 (PD670) in PBS for 10 min at 37 °C. Labeling was stopped by 4 volumes of cold cell culture medium. Excessive dye was removed by washing with cell culture medium. Then, cells were seeded in 96-well plates, stimulated, treated, and cultivated for the time indicated.

2.6.2.2 Live/dead cell discrimination

For live/dead discrimination, cells were either stained with propidium iodide (PI) when cells were analyzed directly or with ethidium monoazide bromide (EMA, MoBiTec) when cells were fixed prior to analysis. PI selectively permeates into dead cells and interacts with DNA. PI (1:400) was added shortly prior to flow cytometry when surface antigens were already stained. Cells were stained with 0.2 µg/ml EMA in FACS buffer (0.5 % BSA in PBS) for 30 min on ice before surface and intracellular antigens were stained. Like PI, EMA is generally excluded from viable cells. Under light exposure, photolysed EMA is covalently bound to DNA thereby selectively labeling the DNA of dead cells. Murine cells were simultaneously treated with anti-mouse CD16/CD32 (1:500, eBioscience) to block any unspecific Fc receptor-mediated reactions.

2.6.2.3 Surface staining

After washing with FACS buffer (300 g, 5 min), fluorochrome-conjugated antibodies raised against human CD3, CD4 (Invitrogen), CD25, CD137 or murine CD45, CD3, CD4, CD8α, CD25, CD44 were added to the cells in a 1:100 dilution (with exception of CD4; 1:50) as recommended by the manufacturer. Cells were incubated with antibodies for 30 min on ice protected from light. Excessive antibody was washed away and cells were resuspended in FACS buffer. After staining of surface antigens, cells were either directly analyzed, fixed with an equal volume of 1 % paraformaledhyde (PFA, Roth) in PBS or intracellular/intranuclear antigens were stained.

2.6.2.4 Intracellular cytokine staining

Prior to intracellular cytokine staining, cells were treated with Golgi Plug containing Brefeldin A (1:500, Bekton Dickinson) to block cytokine secretion during PMA/Iono stimulation. After surface staining, cells were fixed and permeabilized using Cytofix/Cytoperm Kit (Bekton Dickinson). Then, cells were stained with fluorescent-coupled antibodies against human or murine IFNγ and IL-17A (1:100) according to the recommendations of the supplier for 30 min on ice in the dark. Finally, cells were fixed with 0.5 % PFA and analyzed the next day.

2.6.2.5 Intranuclear FoxP3 staining

Intranuclear expression of FoxP3 in $CD4^+$ T cells was detected using an anti-murine flourochrome-coupled FoxP3 antibody with the FoxP3/Transcription Factor Staining Buffer Set (eBioscience). After surface antigen staining, cells were fixed and permeabilized according to the manufacturer's instructions for 30 min on ice in the dark. Then, cells were washed and stained in permeabilisation buffer with FoxP3 antibody (1:100) for 30 min. Cells were washed and resuspended in 0.5 % PFA in FACS buffer before they were analyzed by flow cytometry.

2.6.2.6 Data acquisition and analysis

Flow cytometry data was acquired by a CyAN ADP 9 color analyzer (Beckman Coulter). Unstained and single color controls were used for compensation purposes. Data were evaluated using FlowJo Software (Treestar). In all flow cytometry analyses, cells were gated on lymphocytes (forward/sideward scatter) and a live/dead discrimination was performed prior to downstream gating.

2.6.3 SDS polyacrylamide gel electrophoresis

SDS polyacrylamide gel electrophoresis (SDS PAGE) leads separation of proteins by size through a polyacrylamide mesh. Therefore, proteins are denatured and linear structure maintained by the

anionic detergent SDS that supports migration of proteins in an electric field.

First, a separating gel was prepared using 40 % (w/v) acrylamide/bis 19:1 solution from Ambion (Life technologies). Ammonium persulfate (APS) and tetramethylethylenediamine (TEMED) were added directly prior to gel cast as they initiate polymerization reaction. After the separating gel had polymerized, the stacking gel was poured on top. Then, gels were placed into electrophoresis chambers filled with running buffer (25 mM Tris, 200 mM glycin, 0.1 % SDS). Electrophoresis was performed in the XCell SureLock mini-Cell Electrophoresis System (Life Technologies).

SDS gel	**Separating gel**	**Stacking gel**
Acrylamide	10 to 15 %	5 %
Tris-HCl	375 mM pH 8.8	125 mM pH 6.8
SDS	0.1 %	0.1 %
APS	0.1 %	0.1 %
TEMED	0.1 %	0.1 %

To prepare samples for SDS-PAGE, cells were washed with PBS (300 g, 5 min), lysed in 100 µl SDS lysis buffer (62.5 mM Tris pH 6.8, 2 % SDS, 10 % Glycerol, 50 mM DTT, 0.05 % Bromophenol blue) and disrupted by sonication. Then, proteins were denatured at 95 °C for 5 min and 5 to 10 µl sample were loaded into gel pockets. A prestained molecular weight marker (Peqlab) was used to estimate protein size. SDS gels were either directly stained with filtered Coomassie Brilliant Blue solution (50 % ethanol, 10 % acetic acid, 0.1 % Coomassie Brilliant Blue G250) or used for Western blot analysis.

2.6.4 Western blot

Western blot analysis allows detection of individual proteins by a specific antibody. Therefore, proteins separated by SDS-PAGE were transferred onto a Protan 0.45 µm nitrocellulose membrane (Whatman). Before transfer, gels were equilibrated in transfer buffer (25 mM Tris, 200 mM glycin, 20 % ethanol). The blot was performed in a Western Blot X cell blot module (Invitrogen, Life Technologies) at 230 mM for 2 h. After transfer of proteins, membranes were checked by reversible stain with Ponceau S solution (0.5 % Ponceau S (Sigma-Aldrich), 1 % acetic acid). After destaining with water, membranes were blocked in 5 % skimmed milk in TBS-T (50 mM Tris-HCl pH 7.5, 150 mM NaCl, 0.1 % Tween 20) for 1 h at room temperature. Then, primary antibodies against human proteins diluted in 5 % BSA in TBS-T were applied overnight at 4 °C. Following antibodies were obtained from Cell Signaling Technology and diluted as recommended by the supplier: AMPKα, p-AMPKα (Thr308), 4E-BP1, p-4E-BP1(Thr37/46), cyclin D3, ERK1/2, p-ERK1/2 (Thr202/Tyr204), IRF4, cMyc. p-p70S6Kα (Ser411), and p70S6Kα were purchased from Santa Cruz. β-actin (Sigma-Aldrich) was used as loading control. After washing with TBS-T, horseradish peroxidase-conjugated secondary anti-IgG antibodies (Promega) raised against the appropriate species (mouse or rabbit) were diluted 1:3 000 in 5 % skimmed milk in TBS-T and membranes were incubated for 1 h at room temperature. After extensive washing (6 times 10 min), protein bands were detected using Pierce ECL Western Blotting substrate (Thermo scientific). Quantification of bands was performed using ImageJ 1.48 (NIH) or LabImage 1D (INTAS) software.

2.6.5 Two-dimensional gel electrophoresis/mass spectrometry

Two-dimensional gel electrophoresis (2DGE), an untargeted approach, was utilized to identify proteins with altered expression level upon *H. pylori* gGT treatment. Whole protein extracts were separated through isoelectric focusing in the first dimension and then by size in the second dimension utilizing SDS-PAGE. Each gel represented one sample and proteins with altered expression were identified by mass spectrometry.

2.6.5.1 Sample preparation and gel run

3 x 10^7 TCR stimulated PBMCs from six donors were cultivated in presence of 1 µg/ml active (wild-type) or inactive (S451/452A) *H. pylori* gGT in 10 cm cell culture dishes (2.5 x 10^6 cells/ml) at 37 °C for 24 hours. Cells were washed with PBS and lysed in 200 µl buffer comprised of 7 M urea, 2 M thiourea, 4 % protease inhibitor (Roche Diagnostics), 2 % CHAPS, 2 % Pharmalyte (Amersham Biosciences), and 1 % DTT. Protein concentration was determined using the Bio-Rad Protein assay and a BSA standard curve.

For isoelectric focusing, immobilized pH-gradient strips (IPG, pH 3 - 10, 18 cm, GE Healthcare) were rehydrated in rehydration buffer (8 M urea, 15 mM DTT 0.5 % CHAPS and, 0.5 % IPG). Then, 250 µg protein was applied on strips and protein extracts were separated according to their isoelectric point in the first dimension in an Ettan IPGphor 3 unit (GE Heathcare). Thereafter, stripes were equilibrated for 15 min in an equilibration buffer (6 M urea, 1.5 M Tris-HCl pH 8.8, 2 % SDS, 1 % DTT) and another 15 min in another equilibration buffer containing 4 % iodoacetamide instead of 1 % DTT. Stripes were used to load proteins on 12.5 % SDS-Gels. SDS-PAGE was performed in a PROTEAN plus Dodeca Cell (Bio-Rad) with 5 mA/gel for 2 h followed by 15 mA/gel overnight. 2D-Gels were fixed in 40 % ethanol and 10 % acetic acid. Proteins were detected by Coomassie staining in a solution containing 10 % ammonium sulphate, 1 % phosphoric acid, 25 % methanol and 0.625 % Coomassie Brilliant blue G250. Gels were destained with until background was clear (Figure 13).

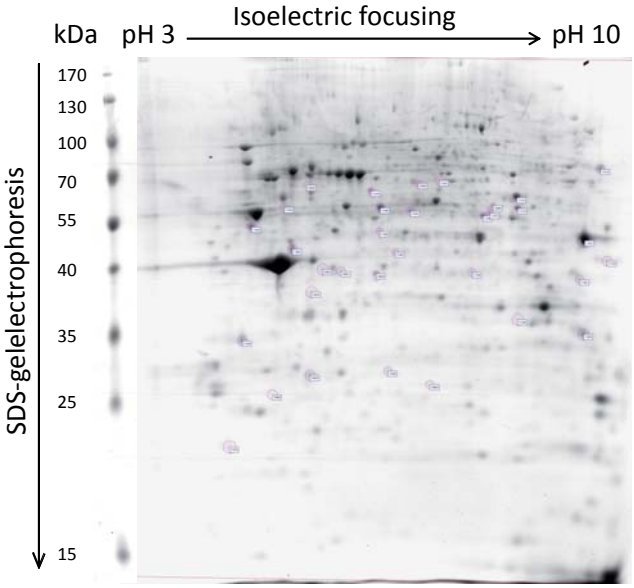

Figure 13: Protein profile in a 2D gel derived from PBMC cell lysates. 250 µg protein was loaded onto IPG strips and separated by isoelectric focusing and in the second dimension by SDS electrophoresis. Circled spots were marked for mass spectrometry. One representative gel of 12 samples (six in each group) is depicted.

2.6.5.2 Identification of altered protein spots

Gels were scanned and analyzed using ProteomWeaver software (Definiens). Protein spots were identified and matched. Furthermore, background subtraction and normalization was performed. Then, relative protein abundance was determined. Spots representing proteins with altered expression with active gGT compared to inactive gGT were selected, picked and destained by alternating wash steps with acetonitrile and 50 mM NH_4HCO_3. Then, spots were digested overnight at 37 °C by 0.1 µg Trypsin (Promega) in 50 mM NH_4HCO_3. An equal volume of 1 % trifluoroacetic acid (TFA, Sigma-Aldrich) was added and ultrasound was used to extract digested peptides for 15 min at room temperature. Tryptic digests were subjected to MALDI-TOF/TOF-MS analysis (UltrafleXtreme, Bruker Daltonics) that was performed as suggested by the provider. Extracted peptides (2 µl) mixed with an equal volume of 0.1 % TFA were spotted onto the thin-layer affinity HCCA AnchorChip preparation (Bruker Daltonics). Proteins were identified from mass spectrum finger prints using ProteinScape 2.1 (Bruker Daltonics).

2.6.6 Real-time PCR

Quantitative real-time PCR (RT-PCR) was employed to analyze cytokine expression in the stomach mucosa upon *H. pylori* infection. In this way, information on relative quantity and quality of inflammatory response was obtained.

2.6.6.1 RNA-extraction

Prior to RNA extraction, all surfaces were decontaminated with RNase away (Molecular BioProducts). 350 µl Qiagen Lysis Buffer RLT containing 1 % β-mercaptoethanol was added to frozen stomach tissue and preparation was homogenized using an Ultra-Turrax (IKA). Total RNA was purified with the RNeasy mini Kit (Qiagen) according to manufacturer's instructions. On-column DNase digestion with DNase I (Qiagen) was performed for 15 min at room temperature. RNA was eluted in 35 µl nuclease-free water and stored at -80 °C. A 5 µl aliquot was used to assess RNA quantity and quality. RNA was quantified using a spectrophotometer, NanoDrop ND-1000. Absorption (A) of 1 at 260 nm corresponds to 40 µg/ml RNA. RNA was considered to be pure when the A260/280 was between 1.8 and 2.1. Furthermore, RNA integrity was confirmed by 2 % agarose gel electrophoresis (Chapter 2.1.4.3).

2.6.6.2 Reverse Transcription

RNA concentration was adjusted to 100 ng/ml before RNA was reversely transcribed into cDNA. 150 ng random hexamer primer (Promega) were added to 1 µg RNA and incubated for 5 min at 70 °C to dissolve secondary structure before mixture was cooled down on ice. cDNA was synthesized by M-MLV reverse transcriptase (Promega). Reverse transcription mix (14 µl) was added to template RNA with annealed primers (11 µl) and incubated for 10 min at room temperature followed by an extension period for 50 min at 42 °C and an inactivation step for 15 min at 70 °C. A reverse transcriptase negative control was prepared in parallel for each sample . Finally, cDNA was diluted (1:5) by addition of 100 µl of nuclease-free H_2O and stored at -20 °C.

Reverse transcription mix (per sample)	
5x reaction buffer	5 µl
10 mM dNTPs	1.25 µl
M-MLV	1 µl
nuclease-free H_2O	6.75 µl

2.6.6.3 RT-PCR run and evaluation

Quantitative real-time PCR analyses were performed using a two-step program in a CFX384 Touch real-time PCR cycler (Bio-Rad). The reactions were run in 384-well plates with a reaction volume of 10 µl. 2x KAPA SYBR FAST qPCR Master Mix (Kapa Biosystems) was used containing DNA Polymerase, dNTPs, SYBR Green I dye, $MgCl_2$ and reaction buffer. RT-PCR Primers used are listed in Table 1. None template controls (water) were included for each primer pair.

Real-time PCR Mix		**RT-PCR Program**	
2x qPCR Master Mix	5 µl	Initial denaturation	95 °C, 3 min
forward primer 10 µM	0.5 µl	Cycle (40x)	
reverse primer 10 µM	0.5 µl	Annealing and elongation	60 °C, 45 sec
sample (32 ng cDNA)	4 µl	Denaturation	95 °C, 15 sec
Σ	10 µl	Melt curve	65 to 95 °C

GAPDH was used as housekeeping gene for normalization and uninfected stomachs were set as base line. The relative gene expression level was calculated by the comparative cycle threshold ($\Delta\Delta$Ct) method [230].

Table 8: Oligonucleotides for RT-PCR

Target	**Species**	**Forward primer 5'→3'**	**Reverse primer 5'→3'**	**Size**
UreA	*H. pylori*	CGTGGCAAGCATGATCCAT	GGGTATGCACGGTTACGAGTTT	77 bp
MIP-2 (CXCL2)	mouse	AGTGAACTGCGCTGTCAATGC	AGGCAAACTTTTTGACCGCC	143 bp
IL-1β	mouse	CAACCAACAAGTGATATTCTCCATG	GATCCACACTCTCCAGCTGCA	152 bp
IL-12 p40	mouse	TGCCAGGAGGATGTCACCT	GGCGGGTCTGGTTTGATGAT	137 bp
IL-6	mouse	AGTTGCCTTCTTGGGACTGA	CAGAATTGCCATTGCACAAC	191 bp
IL-23 p19	mouse	ATGCTGGATTGCAGAGCAGTA	ACGGGGCACATTATTTTTAGTCT	213 bp
IFNγ	mouse	TCAAGTGGCATAGATGTGGAAGAA	TGGCTCTGCAGGATTTTCATG	92 bp
TNFα	mouse	CGATGGGTTGTACCTTGTC	CGGACTCCGCAAAGTCTAAG	284 bp
IL-17A	mouse	GCTCCAGAAGGCCCTCAGA	AGCTTTCCCTCCGCATTGA	141 bp
FoxP3	mouse	AGGAGCCGCAAGCTAAAAGC	TGCCTTCGTGCCCACTGT	80 bp
IL-10	mouse	CTAGAGCTGCGGACTGCCTTC	CCTGCTCCACTGCCTTGCTCTTAT	301 bp
TGFβ	mouse	ATCCTGTCCAAACTAAGGCTCG	ACCTCTTTAGCATAGTAGTCCGC	167 bp
IRF4	mouse	GGAAACTCCTCACCAAAGCA	GGCCCAACAAGCTAGAAAGA	139 bp
cMyc	mouse	TTCTCTTCCTCGTCGCAGAT	TGAAGGCTGGATTTCCTTTG	127 bp
LIX (CXCL5)	mouse	GGTCCACAGTGCCCTACG	GCGAGTGCATTCCGCTTA	131 bp
RANTES (CCL5)	mouse	CACCACTCCCTGCTGCTT	ACACTTGGCGGTTCCTTC	131 bp
GAPDH	mouse	GCCTTCTCCATGGTGGTGAA	GCACAGTCAAGGCCGAGAAT	151 bp

2.7 Histological techniques

2.7.1 Human and murine stomach tissue

Human and murine gastric biopsies were evaluated regarding pathological changes. Tissue samples from *H. pylori*-induced and non-*H. pylori*-related gastritis were obtained from the paraffin-embedded tissue bank of the Institut für Pathologie, Klinikum Bayreuth (Bayreuth, Germany) after approval of the local ethics committee. Formalin-fixed murine stomach samples from infection experiments were dehydrated and embedded into paraffin. Then, 4 µm sections were prepared for staining.

To allow penetration of aqueous solution, paraffin sections were dewaxed by treatment with xylene (2 times 10 min) before staining. Xylene was removed by a descending alcohol series and

slides washed with deionized water.

2.7.2 Hematoxylin/Eosin and Warthin-Starry silver stain

Sections were stained with hematoxylin and eosin to assess histopathological changes. Hematoxylin stains negatively charged cellular compounds, in particular the phosphate backbone of DNA, while eosin forms salts with positively charged compounds such as several amino acids and is used to counterstain the cytosol. Slides were treated with Mayer's hematoxilin for 6 min and washed with tap water. Then, the sections were counterstained by 1 % eosin for another 6 min and slides rinsed with tap water.

For microscopic detection of *H. pylori*, Warthin Starry silver staining was employed. Sections were covered with a prewarmed (57 °C) acidic staining solution (pH 4) that is comprised of 0.4 % silver nitrate, 2.6 % gelatin and 0.4 % hydroquinone. Slides were washed with water. To reduce background staining, sections were treated with 5 % sodium thiosulfate.

Finally, HE and WS-stained slides were dehydrated by a graded series of alcohol with increasing percentage before they were mounted.

2.7.3 Immunohistochemical staining

Heat-induced antigen retrieval was performed in 0.01 M sodium citrate pH 6 and slides were blocked in TBS containing 1 % Tween 20 and 5 % goat serum for 1 h at room temperature. Then, sections were incubated with anti-IRF4 (Cell Signaling) or anti-CD3 (Neomarkers LabVision Corperation) antibodies overnight at 4 °C according to manufacturer's instructions. Sections were developed using SignalStain DAB substrate (Cell Signaling). Finally, samples were counterstained with hematoxylin (Morphisto).

2.7.4 Histological evaluation

Histological evaluation was performed by Prof. Dr. Michael Vieth (Bayreuth) according to the Updated Sydney System for the classification of gastritis [68]. Hematoxylin/Eosin stained sections were scored for chronicity (defined by density of lymphocyte and plasma cell infiltration) and activity (characterized by density of neutrophil granulocytes). A semiquantitative score of 0 (none), 1 (mild), 2 (moderate), and 3 (marked/severe) was given for chronicity and activity in the antrum and corpus. Therefore, the overall gastritis score could range from 0-12. For automated image acquisition, an Olympus Virtual Slide System VS120 (Olympus) was used.

2.8 Statistical analysis

Statistical analysis was performed using GraphPad Prism 5 software. Effects of gGT treatment on PBMCs and T-cells were assessed by Students t-test. A paired t-test was used to account for donor dependent levels of cytokine release. More than two groups were compared by ANOVA with post hoc Bonferroni test.

Colonization status of mice was compared using the non-parametric Mann-Whitney U test. Kruskal-Wallis test with Dunn's multiple comparison was used to establish differences in histological and mRNA expression analyses. Other comparisons among mouse groups were done using one-way ANOVA followed by a Bonferroni post hoc test, as indicated in the figure legends. Significantly different results from uninfected control group are indicated by asterisks on top of the treatment groups. Differences among other groups are indicated by a connecting bar with asterisks showing the level of significance on top.

Chapter 3

Results

3.1 Effect of *H. pylori* gGT on human T-lymphocytes

In a previous study from our group, *H. pylori* gGT was identified as a virulence factor inhibiting T-cell activation and proliferation [163]. However, the mechanisms behind this observation was not clear. Therefore, one of the main objectives of this thesis was to elucidate how this effect is mediated and how T-cell functionality was affected.

3.1.1 Enzymatic activity of *H. pylori* gGT induces inhibition of T-cell proliferation without inducing apoptosis

H. pylori gGT was expressed in *E. coli* and purified using affinity and size exclusion chromatography in its wild-type and its enzymatically inactive S451/452A form. Correctly processed highly pure proteins comprised of two subunits were obtained (Figure 14A/B). Enzymatic activity was confirmed for the wild-type form with a gGT activity assay and shown to be absent for the mutant gGT (Figure 14C).

When recombinant *H. pylori* gGT (rgGT) was added to TCR-activated PBMCs, it a dose-dependently inhibited T-cell proliferation (Figure 15A). Enzymatic activity of this virulence factor was absolutely required to block proliferation, since increasing gGT concentration resulted in decreasing proliferation while enzymatically inactive S451/452A rgGT had no effect. Studies with intestinal cell lines suggested that *H. pylori* gGT may induce apoptosis [190]. Yet, neither were unstimulated T-cells affected by *H. pylori* gGT indicated by live/dead staining after 72 h incubation, nor did activated cells incubated with *H. pylori* gGT display any signs of cell death (Figure 15B). Additionally, activated PBMCs treated with gGT were not apoptotic as shown by monitoring of caspase-3/7 activation for up to 48 h (Figure 15C). Upon T-cell stimulation, early activation markers, such as CD69 and 41BB/CD137, were up-regulated also in presence of gGT, albeit cells did not proliferate in contrast to cells that were untreated or incubated with inactive gGT (Figure 15B). After 48 h, stimulated cells had expanded in cell size and undergone one cell division when active *H. pylori* gGT was absent (Figure 15B). Effects of *H. pylori* gGT on proliferation could only be monitored after 48 h, since then the first cell division had taken place. Changes of activation markers or cytokines expression were expected to precede cell division. Indeed, secretion of pro-proliferative and pro-inflammatory cytokines IL-2, IFNγ, and IL-17, measured after 24 h, was suppressed by *H. pylori* gGT activity (Figure 15D). Effects on proliferation and cytokine secretion were clearly dependent on enzymatic activity, which might either act directly on the cells or on the composition of the cell culture medium.

H. pylori gGT exerted a stronger effect on proliferation when it was already added to the medium overnight prior to activation (Figure 16A). Moreover, when gGT was added to cells

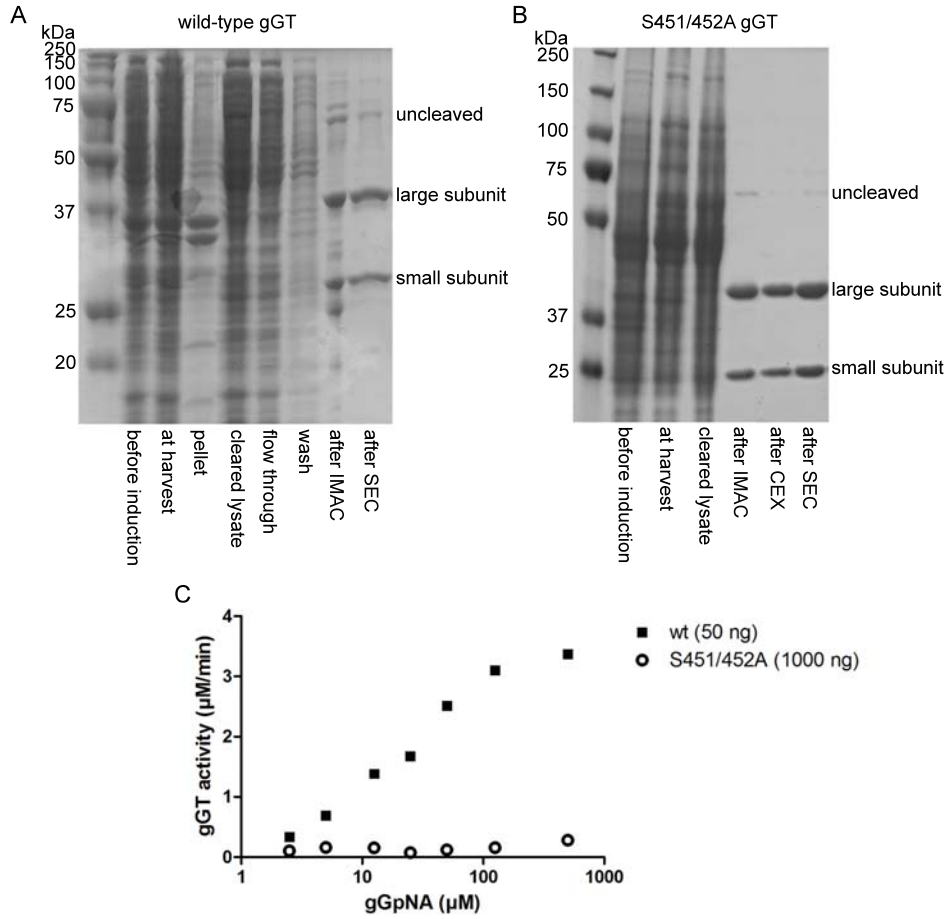

Figure 14: Purification of recombinant *H. pylori* gGT. Expression of recombinant *H. pylori* gGT from *E. coli* was induced by IPTG. Several steps of purification of *H. pylori* gGT wt (A) and S451/452A (B) are shown on a Coomassie-stained poly acrylamide gel. (C) Enzymatic gGT activity of recombinant proteins measured in 0.1 M Tris pH 8 at 37 ℃ with 0.5 mM gGpNA as substrate in the presence of 20 mM glycyl-glycine as acceptor. Data from one run performed in duplicate is shown.

overnight and medium was replaced before the cells were stimulated, cells proliferated to the same extent as untreated cells (Figure 16B), excluding that gGT irreversibly modifies the cells or has direct toxic effects. When gGT was added to cells that were already activated and proliferating one or two days after stimulation, it still exerted an anti-proliferative effect which was only delayed (Figure 16C/D). These results strongly suggested that gGT modifies the cell culture medium in a way that it cannot support proper lymphocyte function anymore.

To gain some insight in the sequence of events, expression of cell cycle related proteins such as cyclin D3 and p27 was monitored over time (Figure 16E). In the course of stimulation, expression of cell cycle inhibiting factor p27 was reduced independently of *H. pylori* gGT. On the contrary, cyclin D3 required for cell cycle G1/S transition was induced upon stimulation and much more strongly expressed in absence of gGT. However, this was only observed after 24 h and 48 h. Additionally, protein expression of activation-induced factors such as cRaf and cMyc initially followed the pattern of activated cells in presence of *H. pylori* gGT while changes in response to gGT treatment could only be observed after 24 h and 48 h (Figure 16E). Therefore, it remained unclear at which time point gGT activity came into play and what signaling pathways were mediating the gGT-dependent effect. Thus, enzymatic activity of *H. pylori* gGT was analyzed in more detail.

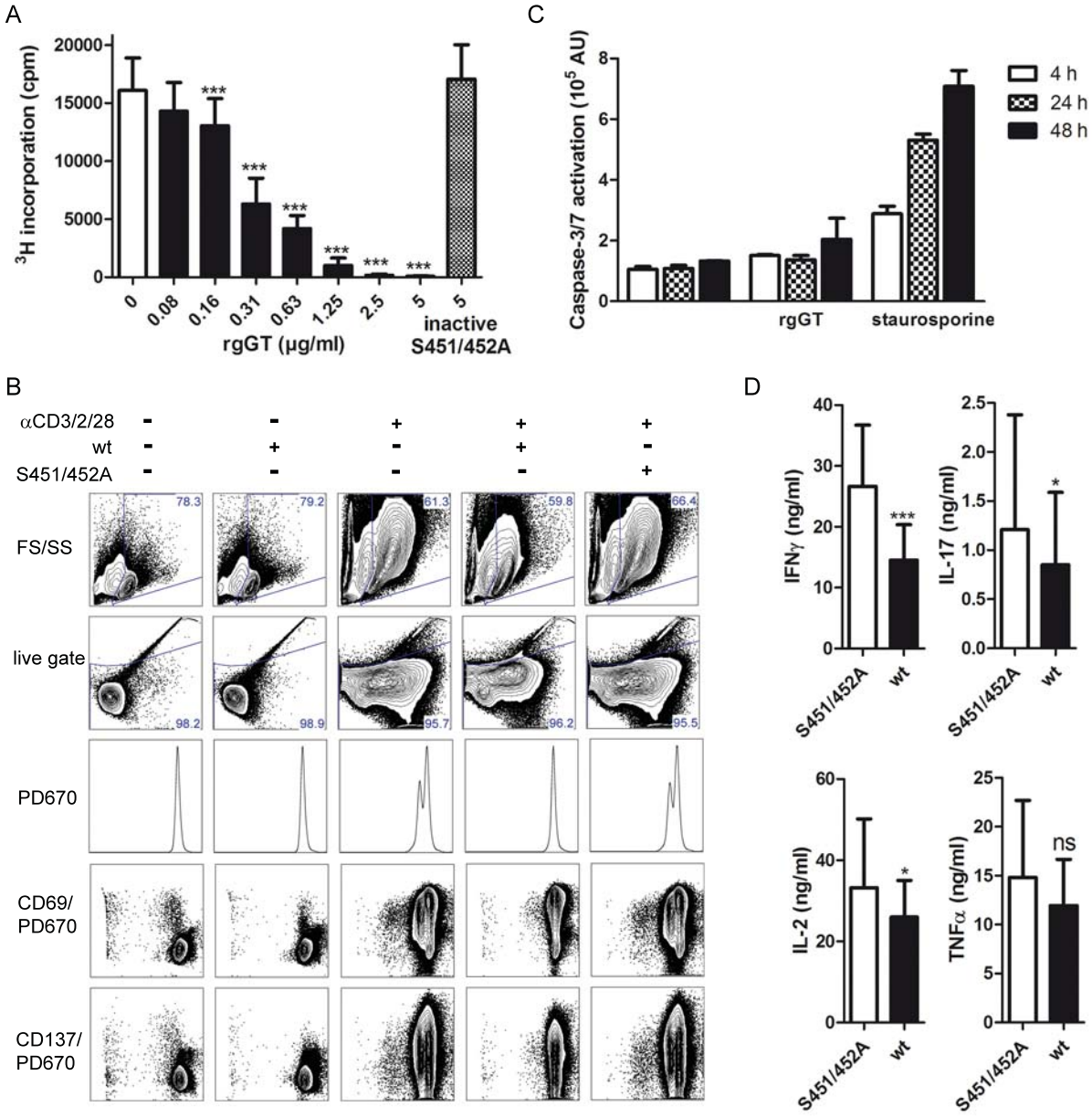

Figure 15: *H. pylori* gGT-induced effects on activated human lymphocytes. (A) TCR-dependent stimulation of human PBMCs treated with different amounts of recombinant gGT (rgGT) or the inactive S451/452A mutant gGT for 72 h. Cell proliferation was measured in triplicates as increase in radioactively labeled [^{3}H]-thymidine incorporation during the last 24 h of a 72 h incubation period. Cpm, counts per minute. Results are presented as mean ± SD from three independent donors (*** $p < 0.001$). (B) T-cells isolated from PBMCs were stimulated with αCD3/αCD2/αCD28-coated beads, treated with 1 µg/ml of active (wt) or inactive (S451/452A) rgGT. Cells were preloaded with proliferation dye 670 and incubated for 48 h hours. At the time of analysis cells were stained for CD69, CD137 and with PI for live/dead discrimination. (C) PBMCs stimulated with PMA/Ionomycin were incubated with rgGT (1 µg/ml). Induction of apoptosis was measured by Caspase-3/-7 activation at times indicated. 10 µM staurosporine were added as positive control. AU, arbitrary units. Results are presented as mean ± SD from a triplicate measurement. (D) T-cells isolated from PBMCs were stimulated with αCD3/αCD2/αCD28-coated beads and treated with 1 µg/ml of active (wt) or inactive (S451/452A) rgGT. Cytokine secretion into medium was measured by ELISA after 24 h. Results are presented as mean ± SD from twelve donor preparations (* $p < 0.05$;*** $p < 0.001$).

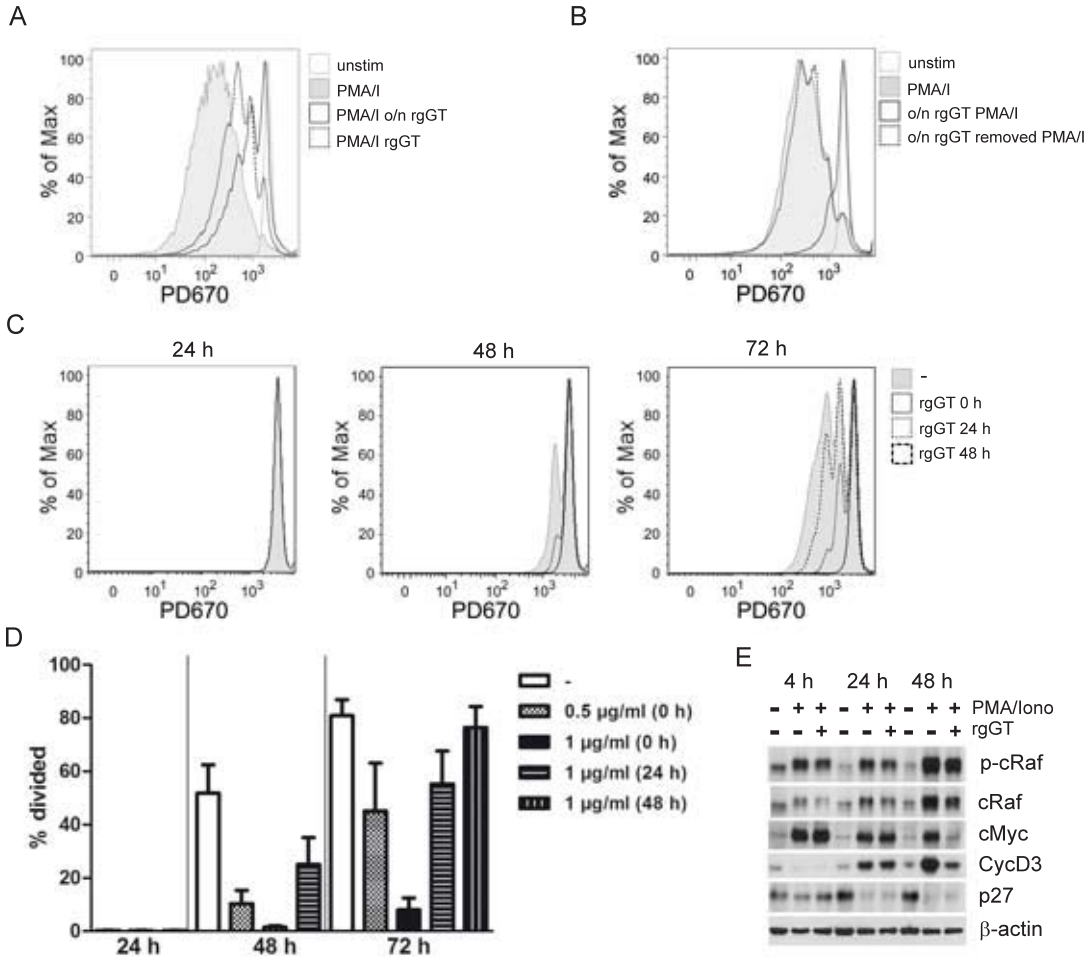

Figure 16: Time dependency of *H. pylori* gGT-mediated effects on proliferation. (A-D) PBMCs were loaded with proliferation dye prior to cultivations and cell divisions were analyzed by flow cytometry. (A+B) PBMCs incubated with rgGT (1 µg/ml) prior and/or after stimulation with PMA/Ionomycin analyzed on day five (A) or four (B). (C+D) PBMCs activated with αCD3/CD2/CD28-coated beads were incubated with rgGT (1 µg/ml) added at the time of stimulation or at times indicated. Cells were analyzed by flow cytometry after 24 h, 48 h, and 72 h. (C) Proliferation of live $CD3^+$ T-cells of one representative experiment is shown. (D) Proportion T-cells that had undergone cell division from three donors are summarized in this graph. Results are presented as mean ± SD. (E) PBMCs stimulated with PMA/Ionomycin and treated with 1 µg/ml rgGT for the times indicated were subjected to Western blot analysis. β-actin was used as loading control.

3.1.2 Turnover of γ-glutamyl substrates by *H. pylori* gGT

As glutamine and reduced glutathione are proposed physiological substrates of *H. pylori* gGT [175], these substances were introduced into a competition assay with gGpNA, an artificial gGT substrate. Increasing glutamine and glutathione concentrations were able to displace gGpNA from *H. pylori* gGT resulting in slower p-nitroaniline release (Figure 17A). Interestingly, L-glutamine interacted with the enzyme more efficiently than glutathione, since lower concentrations were needed to compete with gGpNA. Half maximal inhibitory concentration value (IC50) for L-glutamine was 14.4 µM, for glutathione 36.5 µM, for L-glutamate 59.7 µM, and for D-glutamine 1043 µM. These results suggest that L-glutamine (hereafter referred to as glutamine) is the preferred substrate of *H. pylori* gGT and therefore might be the most relevant substrate under physiological conditions, whereas D-glutamine hardly interacted with gGT. Conversely, L-glutamate might show inhibitory effects due to product inhibition. When IC50 values for glutamine were compared between gGTs of different species, *Campylobacter* gGT, which is very similar to *H. pylori* gGT, showed a comparable IC50 value of 28.1 µM, while equine gGT, a commercially available representative of mammalian gGTs, had a much higher IC50 value above 4 mM (Figure 17B). As the gGpNA assay monitors transpeptidation reaction in a Tris-buffered system, an enzymatic glutamate assay was established to analyze hydrolysis of glutamine and glutathione in cell culture medium. Therefore, glutamine and glutathione were titrated into glutamine-free RPMI cell culture medium containing *H. pylori* gGT and incubated at 37 ℃. Release of glutamate correlated to the amount of substrate introduced into the medium, which demonstrated that glutamine as well as glutathione were hydrolyzed by *H. pylori* gGT (Figure 17C). A time course experiment revealed that an equimolar amount of glutamate was produced with different concentrations of *H. pylori* gGT by the end of a 48 h incubation period when 2 mM of glutamine were initially present in the medium (Figure 17D). To confirm that glutamine is quantitatively hydrolyzed to glutamate by *H. pylori* gGT, glutamine and glutamate levels in cell culture medium were monitored by quantitative LC-MS. Indeed, glutamine was almost completely hydrolyzed to glutamate within 24 h and completely depleted after 48 h (Figure 17E).

3.1.3 *H. pylori* gGT blocks expansion of activated T-lymphocytes via glutamine deprivation

Considering the facts that *H. pylori* gGT has strong glutaminase activity and that T-cells absolutely require glutamine for proliferation, glutamine deprivation due to glutamine hydrolysis by gGT could be responsible for inhibition of T-cell proliferation. Thus, glutamine was supplemented to cells treated with *H. pylori* gGT to overcome gGT induced effects. As glutamine is not stable in aqueous solutions for long term, glutamine-free RPMI cell culture medium supplemented with 10 % FCS was used and glutamine was added prior to experiments when required. To study the effect of glutamine supplementation, human PBMCs were stimulated in a TCR-dependent manner, treated with gGT, and incubated in cell culture medium containing increasing concentrations of glutamine. It has to be noted that glutamine is present in serum at high levels. Thus, cell culture medium contained 0.07 mM glutamine from FCS even without addition of glutamine. Proliferation was either measured by tritium incorporation, determined as percentage of dye-loaded cells that had undergone cell division, or assessed by a viability assay. Indeed, addition of glutamine to *H. pylori* gGT-treated cells restored proliferation of T-lymphocytes in a dose-dependent manner (Figure 18A/B). Conversely, increasing gGT concentration lowered proliferation rate presumably through hydrolysis of supplemented glutamine. Not only proliferation of primary lymphocytes was affected by *H. pylori* gGT, but also proliferation of the transformed Jurkat T-cell line (Figure 18C). Although Jurkat cells divide independently of TCR stimulation, glutamine supplementation could

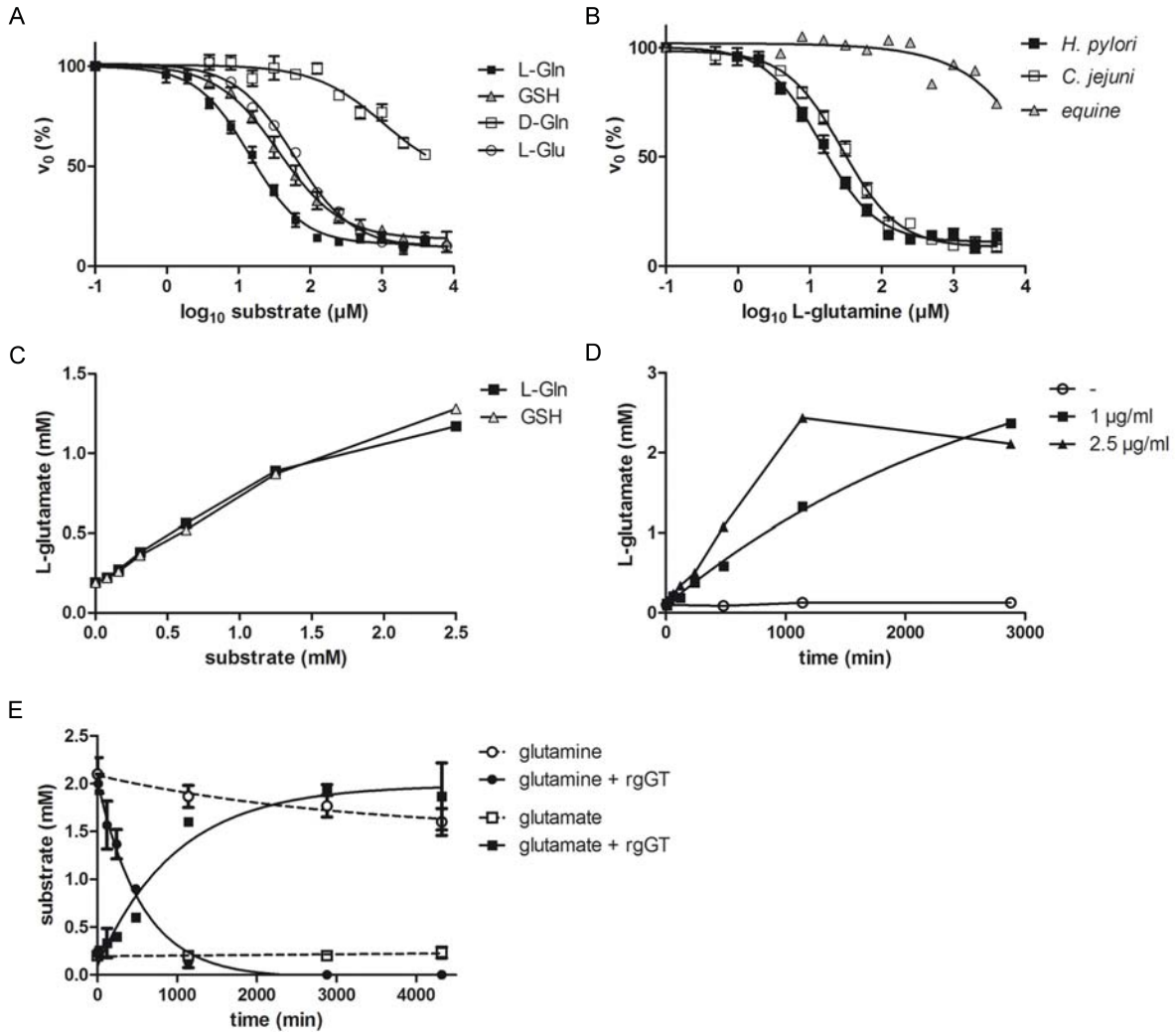

Figure 17: Enzymatic activity of *H. pylori* gGT metabolizes glutamine and glutathione.
(A) *H. pylori* gGT substrates were titrated in a gGT activity assay to compete for an artificial substrate. Increasing concentration of L-glutamine (L-Gln), glutathione (GSH), D-glutamine (D-Gln), and L-glutamate (L-Glu) were introduced. Enzyme kinetics were measured in 0.1 M Tris pH 8 at 37 ℃ with 48 µM gGpNA as colorimetric substrate in presence of 20 mM glycyl-glycine as acceptor. Data ± SD from four runs performed in duplicates are shown. V_0, initial velocity. (B) Competition between glutamine and the artificial gGT substrate gGpNA for gGTs from different species was analyzed. For direct comparison, the amount of gGT introduced was adjusted to comparable V_{max} and concentration of gGpNA was adjusted to the K_m value of each gGT species. Thus, 50 ng *H. pylori* gGT, 100 ng *C. jejuni* gGT, and 250 ng *equine* gGT were used with 48 µM, 34 µM, and 768 µM gGpNA, respectively. Enzyme kinetics were measured in 0.1 M Tris pH 8 at 37 ℃ in the presence of 20 mM glycyl-glycine as acceptor. V_0, initial velocity; V_{max}, maximal velocity. (C+D) Production of glutamate in cell culture medium due to *H. pylori* gGT enzymatic activity was measured using an enzymatic glutamate assay. (C) Different amounts of glutamine or glutathione were added to Gln-free RPMI/10%FCS and incubated with *H. pylori* gGT (2.5 µg/ml) for 20 h at 37 ℃. (D) Cell culture medium (RPMI/10%FCS) containing 2 mM glutamine was incubated with different amounts of *H. pylori* gGT for various times as indicated. (E) *H. pylori* gGT glutaminase activity analyzed by LC-MS. Cell culture medium (RPMI/10% FCS/2 mM Gln) was incubated with or without rgGT (2.5 µg/ml) at 37 ℃. The amount of glutamine and glutamate was determined by quantitative LC-MS analysis at times indicated. Data ± SD from three independent experiments are shown.

restore proliferation of these cells.

To further substantiate that glutamine deprivation is responsible for inhibition of T-cell proliferation induced by gGT, cell culture medium was preconditioned with recombinant *H. pylori* gGT and proliferation of $CD3^+$ T-cells was studied by flow cytometry after 72 h incubation. In glutamine-free medium containing only low amounts of glutamine from FCS, few $CD3^+$ T-cells were able to divide once, while medium containing 2 mM glutamine was optimal for T-cell proliferation (Figure 19A/B). *H. pylori* gGT-treated medium inhibited cell division, even when glutamine was supplemented, since the enzyme was still active, thus, consuming the additional glutamine during the 72 hour cultivation period. In order to clearly discriminate between the effects of enzymatic activity of gGT during pretreatment of the medium and after supplementation of glutamine, the enzymatic activity was abolished by heat-inactivation of the preconditioned medium (Figure 20). In this way, the cells did not encounter active gGT but only modified cell culture medium. After inactivation of *H. pylori* gGT, glutamine supplementation completely restored cell division rate irrespectively of glutamine level during the preconditioning phase (Figure 19A/B). The presence of glutamine as a γ-glutamyl donor during conditioning phase excluded the possibility of a dominant toxic effect by a γ-glutamyl compound formed due to gGT activity, as reconstitution of medium with glutamine completely restored proliferation. The same results regarding proliferation were obtained with Jurkat cells incubated in preconditioned medium and supplementation of glutamine, with the exception that no TCR-dependent stimulation was required (Figure 19C).

Further parameters that were related to proliferation such as cyclin D3 expression and size of activation-induced lymphocyte aggregates were analyzed. These parameters were also clearly inhibited by *H. pylori* gGT in a glutamine-dependent manner in TCR-activated PBMCs analyzed after 24 h and 48 h, respectively (Figure 21A/B and Figure 22).

Whole bacteria were used to study the effects of *H. pylori* gGT in a more physiological context. To show that gGT expression by whole bacteria is sufficient to block T-cells proliferation, medium was preconditioned with *H. pylori* PMSS1 (MOI 5), which was sufficient (wt) or deficient (ΔgGT) in gGT. Recombinant gGT was taken along as a control. Proliferation of TCR-stimulated human PBMCs was significantly inhibited when cells were incubated in medium pretreated with *H. pylori* wt or with rgGT alone, while cells incorporated thymidine in absence of active gGT (Figure 23). Glutamine could also overcome the inhibitory effect of gGT on proliferation under these conditions.

These data indicate that inhibition of proliferation of T-lymphocytes by *H. pylori* gGT is due to glutamine deprivation, which is dependent on the level of glutamine, gGT concentration, and incubation time.

3.1.4 *H. pylori* gGT inhibits T-lymphocyte activation in a glutamine-dependent manner

Promotion of T-cell proliferation requires paracrine and autocrine IL-2 signaling. Therefore, the effect of gGT on the expression of the α-chain of IL-2R, CD25, was analyzed. This early activation marker was up-regulated upon TCR-dependent stimulation in presence of glutamine (Figure 24A/B and Figure 19C). Only complete glutamine depletion in medium preconditioned with gGT abolished the expression of CD25. As only CD25-positive T-cells were capable to divide, no cell proliferation occurred with active gGT (Figure 24A and Figure 25). Glutamine supplementation induced CD25 expression, but still did not allow proliferation when gGT was active. CD25 up-regulation and consecutive proliferation in gGT-conditioned medium was only observed when gGT enzymatic activity was abrogated. Under these conditions, glutamine was available during the complete cultivation period. To demonstrate that CD25 up-regulation precedes proliferation, CD25 expression of $CD4^+$ T-cells was analyzed after 24 h. Up-regulation of CD25 was inhibited in presence of active gGT in preconditioned medium and expression could be restored by addition of glutamine

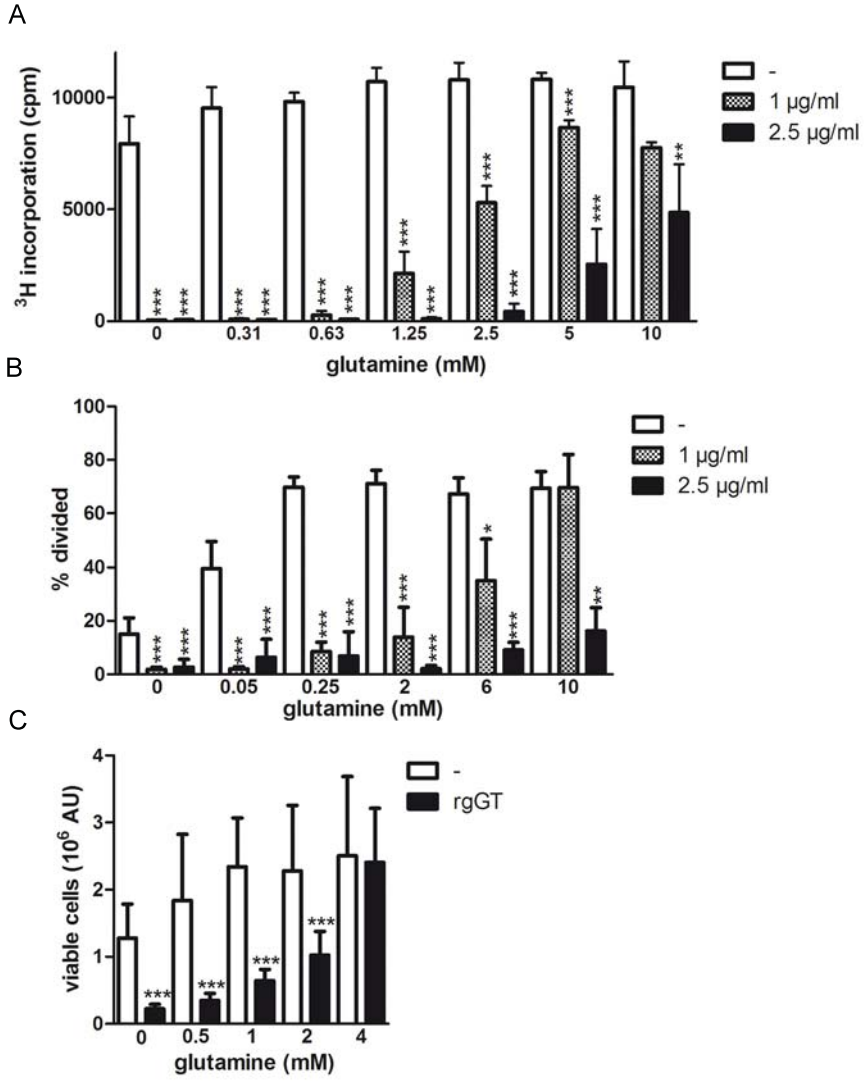

Figure 18: Glutamine supplementation restores proliferation of gGT-treated lymphocytes. Cells were incubated in glutamine-free RPMI medium containing 10 % FCS which was supplemented with glutamine as indicated. (A/B) Human PMBCs were stimulated with αCD3/CD2/CD28-coated beads and treated with rgGT. (A) Proliferation of cells treated with 0, 1 or 2.5 µg/ml rgGT was measured in triplicates as increase in radioactively labeled [^{3}H]-thymidine incorporation during the last 24 h of a 72 h incubation period. Cpm, counts per minute. Results are presented as mean ± SD from three independent donors. (B) To determine percentage of cells that had undergone cell division, PBMCs were loaded with a proliferation dye prior to the 72 h incubation period. Proliferation was assessed by flow cytometry. Results are presented as mean ± SD from six donors. (C) Jurkat cells were incubated with rgGT (1 µg/ml) for 48 h. Proliferation was measured by a viability assay. Values are represented as mean ± SD from four experiments measured in triplicates (* $p < 0.05$; ** $p < 0.01$; *** $p < 0.001$).

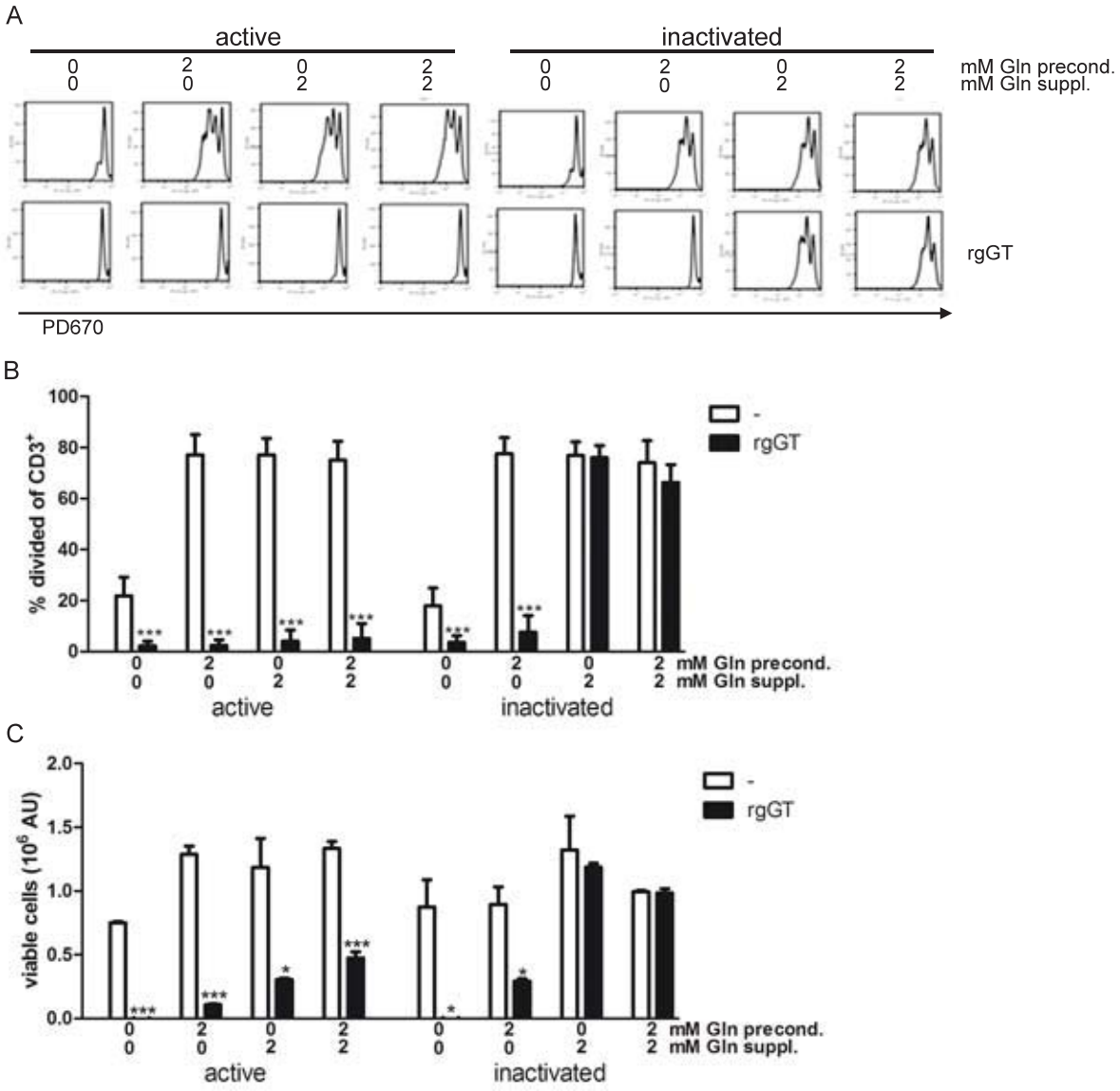

Figure 19: Glutamine supplementation restores proliferation impaired by *H. pylori* gGT only when enzymatic activity is abrogated.
(A+B) αCD3/CD2/CD28-stimulated human PBMCs were loaded with a proliferation dye and incubated with glutamine-free or glutamine sufficient (2 mM) medium preconditioned with 2.5 µg/ml *H. pylori* rgGT for 24 h. Inactivation of preconditioned medium was performed by heat treatment (65 ℃, 30 min). Glutamine was supplemented as indicated when the cells were stimulated. FACS analysis for proliferation dye in $CD3^+$ cells was performed after a 72 h cultivation period. (A) Proliferation of one representative donor is shown. (B) Bars represent mean ± SD of divided $CD3^+$ cells from eleven donors. (C) Jurkat cells were cultivated for 48 h in medium preconditioned as described above. To assess proliferation a viability assay was performed in triplicate. Results are represented as mean ± SD (* $p < 0.05$; *** $p < 0.001$).

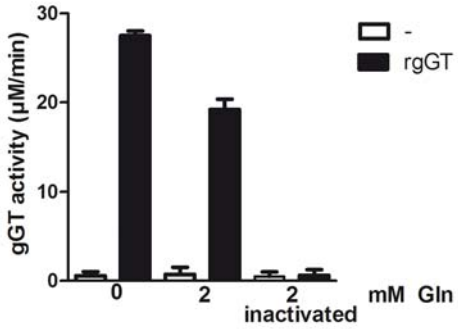

Figure 20: Enzymatic activity of gGT in preconditioned cell culture medium. *H. pylori* gGT activity was measured in cell culture medium preincubated with 2.5 µg/ml rgGT before and after heat-inactivation at 65 ℃ for 30 min. Results (mean ± SD) of three independent experiments are shown.

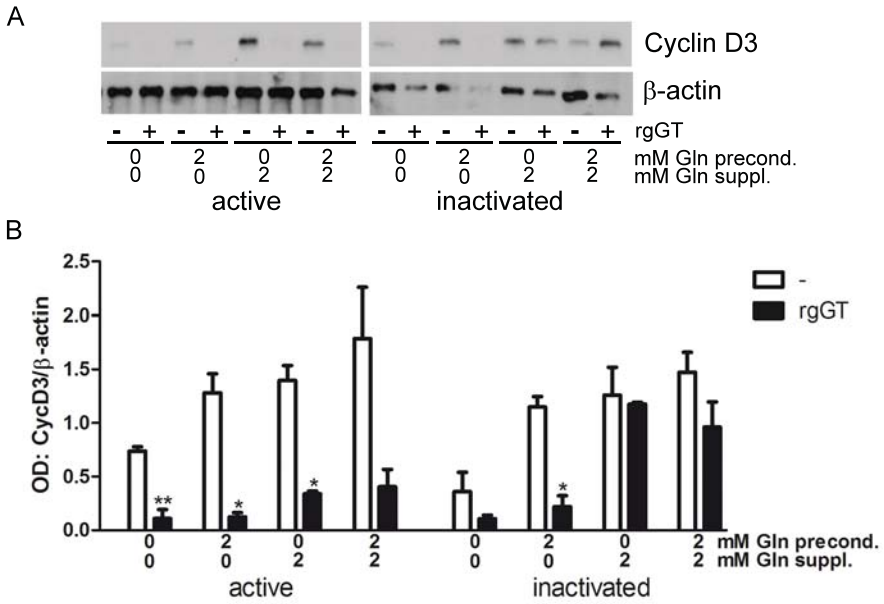

Figure 21: Cyclin D3 expression restored by glutamine when gGT is inactivated. PBMCs were TCR-stimulated and cultivated in cell culture medium (-/+ glutamine) that was preconditioned with 2.5 µg/ml rgGT for 24 h. *H. pylori* gGT in preconditioned medium was inactivated by heat-treatment when indicated. Glutamine was supplemented at the beginning of the cultivation period. For determination of cyclin D3 expression, cells were lysed after 24 hours and subjected to Western blot analysis. (A) Representative cyclin D3 blot with β-actin as loading control. (B) Band densities from three different donors were combined in relation to β-actin expression. Results are represented as mean ± SD (* $p < 0.05$; ** $p < 0.01$).

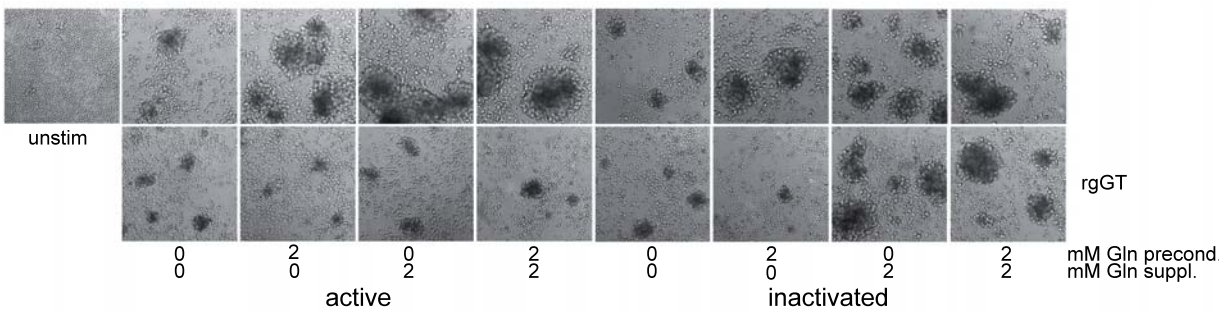

Figure 22: Aggregate size of activated PBMCs is decreased by *H. pylori* gGT activity. αCD3/CD2/CD28-stimulated PBMCs were cultivated in glutamine-free cell culture medium that was supplemented with glutamine before or after preconditioning with 2.5 µg/ml *H. pylori* gGT for 24 h, as indicated. Thus, glutamine was present during preconditioning (precond.) phase and/or supplemented (suppl.) to the cells at the time of stimulation. *H. pylori* gGT was inactivated in preconditioned medium by heat-treatment. Light microscopy images of cell aggregate formation of PBMCs cultivated for 48 h are shown. unstim, unstimulated control

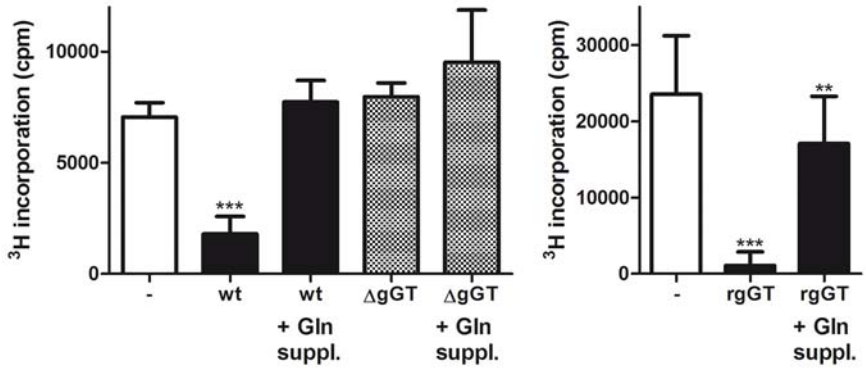

Figure 23: *H. pylori* wt impairs proliferation of T-cells by gGT-dependent glutamine deprivation. TCR-stimulated PBMCs were incubated in cell culture medium (RPMI/2 mM glutamine) that had been preconditioned by adding *H. pylori* PMSS1 (MOI 5) or rgGT (1 µg/ml) for 72 h. 2 mM glutamine was supplemented when cells were stimulated as indicated. Cell proliferation was measured in triplicates as increase in radioactively labeled [3H]-thymidine incorporation during the last 24 h of a 72 h incubation period. Cpm, counts per minute. Results are presented as mean ± SD from three independent donors (*** $p < 0.001$, ** $p < 0.01$)

.

(Figure 24A). This effect was also seen when medium was preconditioned with *H. pylori* wt, while the gGT-deficient mutant impaired CD25 expression only when complemented with rgGT (Figure 24B).

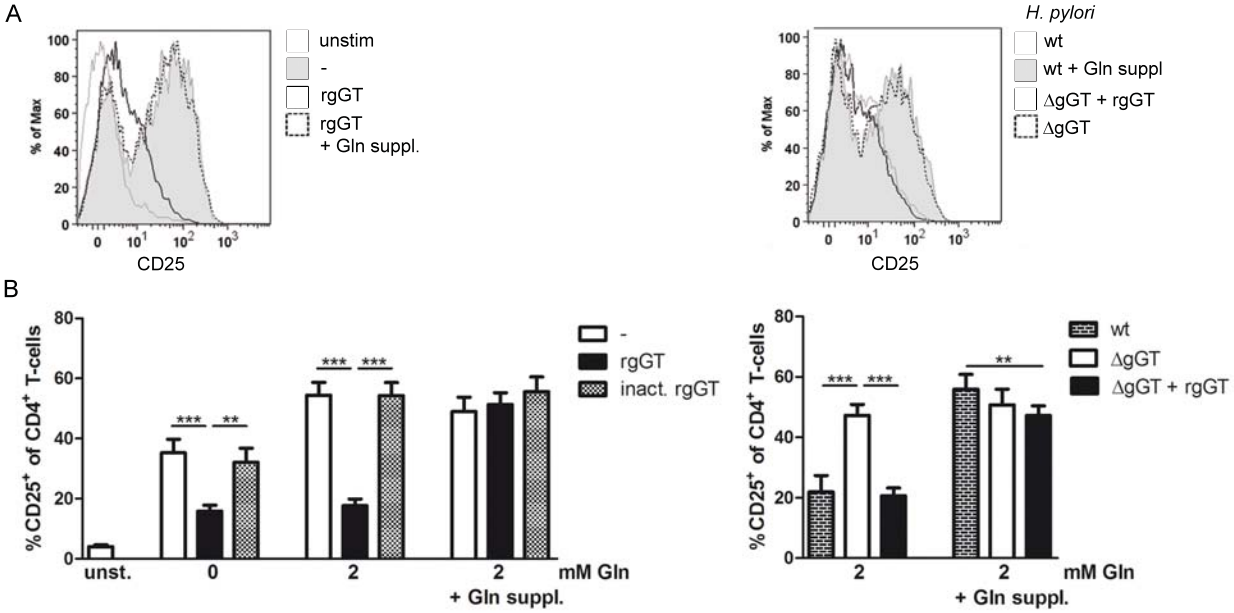

Figure 24: *H. pylori* gGT-induced glutamine deprivation impairs activation of CD4$^+$ T-cells. αCD3/CD2/CD28-stimulated PBMCs were incubated with cell culture medium which had been preconditioned with 1 µg/ml rgGT (left) or *H. pylori* PMSS1 (MOI 5) (right) for 72 h. Inactivated (inact) gGT and gGT-deficient *H. pylori* (ΔgGT) were used as controls. Glutamine was supplemented at the time of stimulation when indicated. FACS analysis was performed after 24 h of cultivation. Cells were stained with fluorophore-coupled antibodies for the surface markers CD3, CD4 and CD25. (A) Histogram of CD25 expression is shown from one representative donor. (B) CD4$^+$/CD3$^+$ cells expressing CD25 from ten donors are displayed as mean ± SEM (*** $p < 0.001$; ** $p < 0.01$). Unst, unstimulated cells.

Furthermore, it was analyzed whether *H. pylori* gGT affects IL-2 secretion. Indeed, gGT treatment resulted in decreased levels of IL-2 released from activated T-lymphocytes after 24 hours (Figure 26A). Interestingly, supplementation of glutamine could rescue IL-2 secretion even in the presence of active gGT (24 hours) while proliferation (72 hours) was still inhibited. As CD25 is also up-regulated under these conditions (24 hours), this indicates that impaired IL-2 signaling is not responsible for the inhibitory effect of *H. pylori* gGT on T-cell proliferation. To confirm this, cells were supplemented with recombinant IL-2. As expected, addition of recombinant IL-2 did not promote proliferation in the presence of gGT (Figure 27). Taken together, these results demonstrate that CD25 expression and IL-2 release are early events promoting proliferation that are suppressed by *H. pylori* gGT in a glutamine-dependent manner. Nevertheless, they are not the central limiting factors for the inhibition of cell division in activated T-lymphocytes observed in the presence of the enzyme.

As the adaptive immune response towards *H. pylori* is dominated by a Th1/Th17 phenotype, the effect of glutamine deprivation induced by *H. pylori* gGT on IFNγ and IL-17 cytokine expression was analyzed by ELISA and flow cytometry. IFNγ secretion as well as percentage of IFNγ-expressing CD4$^+$ T-cells were significantly reduced in the presence of active gGT in stimulated PBMCs, while inactivation or depletion of gGT as well as glutamine supplementation allowed increased cytokine production (Figure 28A and Figure 29A). IFNγ secretion, like IL-2 release, could be induced by glutamine supplementation when active gGT was present, indicating that it is a rather early event (Figure 28A). In contrast to IL-2 and IFNγ release, secretion of TNFα was not

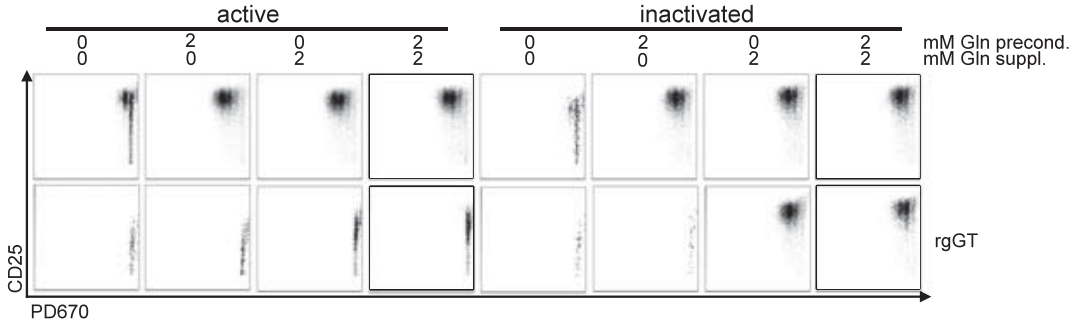

Figure 25: *H. pylori* gGT impairs upregulation of CD25, a prerequisite for proliferation. αCD3/CD2/CD28-stimulated human PBMCs were loaded with a proliferation dye and incubated with glutamine-free or glutamine sufficient (2 mM) medium preconditioned with 2.5 µg/ml *H. pylori* rgGT for 24 h. Inactivation of preconditioned medium was performed by heat treatment (65 ℃, 30 min). Glutamine was supplemented as indicated when the cells were stimulated. FACS analysis for CD25 and proliferation dye in $CD3^+$ cells was performed after a 72 h cultivation period. CD25 expression together with cell proliferation is displayed for one representative donor.

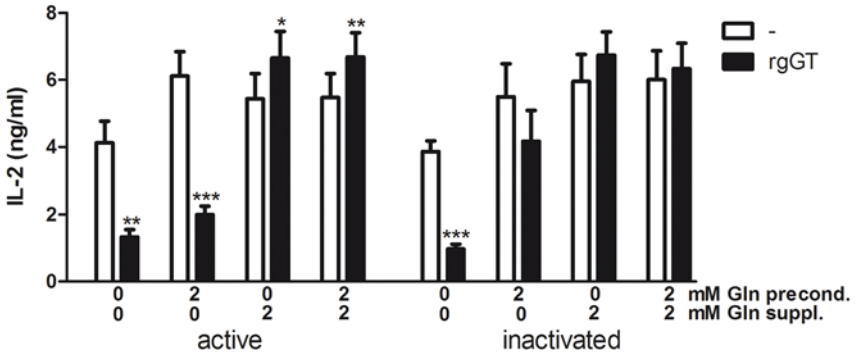

Figure 26: Supplementation of glutamine restores IL-2 secretion from PBMCs treated with *H. pylori* gGT preconditioned medium. αCD3/CD2/CD28-stimulated human PBMCs were incubated with cell culture medium (Gln-free/10 % FCS) which was preconditioned with 2.5 µg/ml *H. pylori* rgGT for 24 h. Glutamine was added during the preconditioning and/or cultivation period, as indicated. Inactivation of *H. pylori* gGT was performed prior to incubation period by heat-inactivation of preconditioned medium (65 ℃, 30 min). IL-2 secretion was measured by ELISA in supernatants that were collected after 24 h of cultivation. Bars represent mean ± SD from nine/three donors/independent experiments (* $p < 0.05$; ** $p < 0.01$; *** $p < 0.001$).

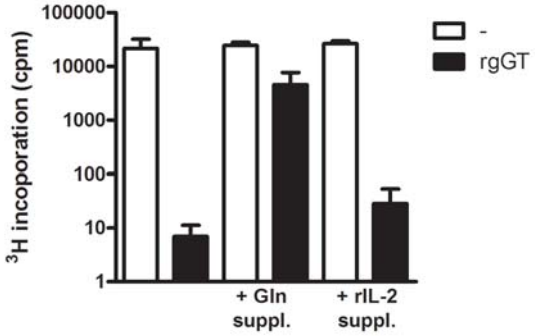

Figure 27: rIL-2 cannot restore proliferation of *H. pylori* gGT-treated PBMCs. αCD3/CD2/CD28-stimulated human PBMCs cultivated in medium preconditioned with 1 µg/ml *H. pylori* gGT for 72 h and supplemented with 10 mM glutamine (Gln) or 50 U/ml rIL-2 at the time of stimulation. Cell proliferation was measured as radioactively labeled [3H]-thymidine incorporation during the last 24 h of a 72 h incubation period. Results (mean ± SD) from two independent experiments conducted in duplicates are shown. Cpm, counts per minute.

reduced by *H. pylori* gGT but rather induced (Figure 28B), which shows that cytokine secretion was not affected in general. Increased TNFα secretion from activated PBMCs in presence of rgGT was most likely due to residual *E. coli* LPS from the protein purification process. IL-17 expression was also down-regulated by gGT-dependent glutamine deprivation (Figure 29B), albeit to a lesser extent than IFNγ. This might be due to the fact that αCD3/CD28-stimulation induced IL-17A expression in only a small percentage of $CD4^+$ T-cells since no TGFβ was added in this experiment.

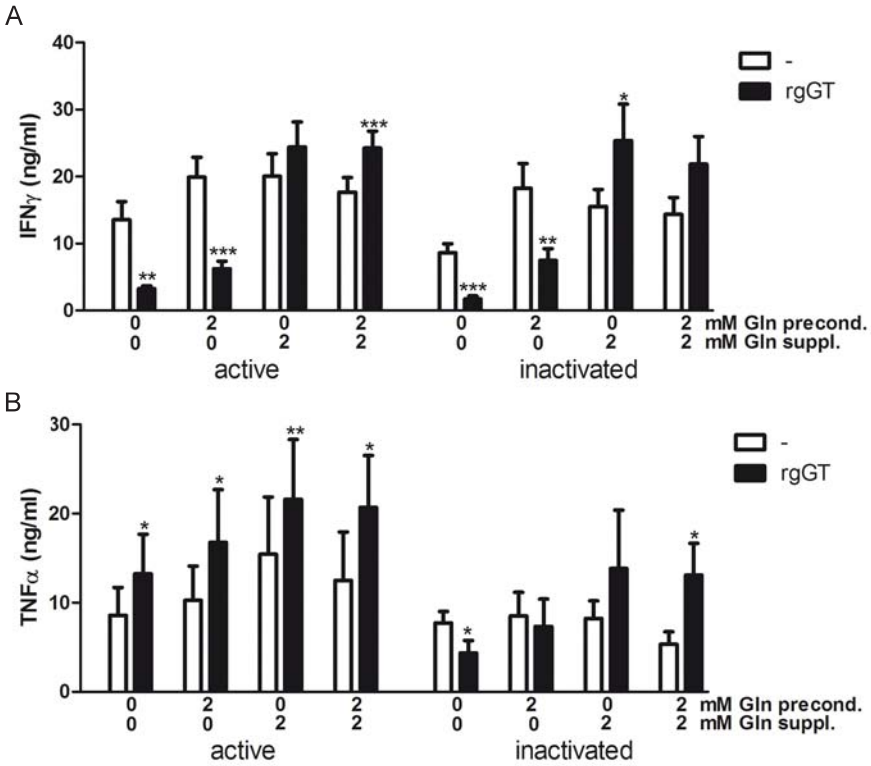

Figure 28: Supplementation of glutamine restores effector cytokine secretion from PBMCs treated with *H. pylori* gGT preconditioned medium. αCD3/CD2/CD28-stimulated human PBMCs were incubated with cell culture medium (Gln-free/10 % FCS) which was preconditioned with 2.5 µg/ml *H. pylori* rgGT for 24 h. Glutamine was added during the preconditioning and/or cultivation period, as indicated. Inactivation of *H. pylori* gGT was performed prior to incubation period by heat-inactivation of preconditioned medium (65 ℃, 30 min). IFNγ (A) and TNFα (B) secretion was measured by ELISA in supernatants that were collected after 24 h of cultivation. Bars represent mean ± SD from nine/three (A) or six/two (B) donors/independent experiments (* $p < 0.05$; ** $p < 0.01$; *** $p < 0.001$).

Collectively, these results show that *H. pylori* gGT inhibits activation and expression of effector cytokines by depriving T-lymphocytes of glutamine.

3.1.5 Glutathione degradation-dependent effects of *H. pylori* gGT on T-cells

As demonstrated before, glutathione seems to be a substrate that is degraded by gGT to a similar extent as glutamine. It has been suggested that hydrolysis of glutathione by gGT might harm lymphocytes through production of pro-oxidant products [231]. Therefore, a viability assay was performed with stimulated lymphocytes in presence of glutathione. In presence of glutathione, similar number of viable cells were detected after gGT treatment as without glutathione (Figure 30A). Thus, no harmful effect of glutathione degradation was observed. In contrast to glutamine supplementation, increasing concentration of glutathione or other reducing agents such as dithiothreitol and β-mercaptoethanol could not restore proliferation in the presence of gGT (Figure 30A-C).

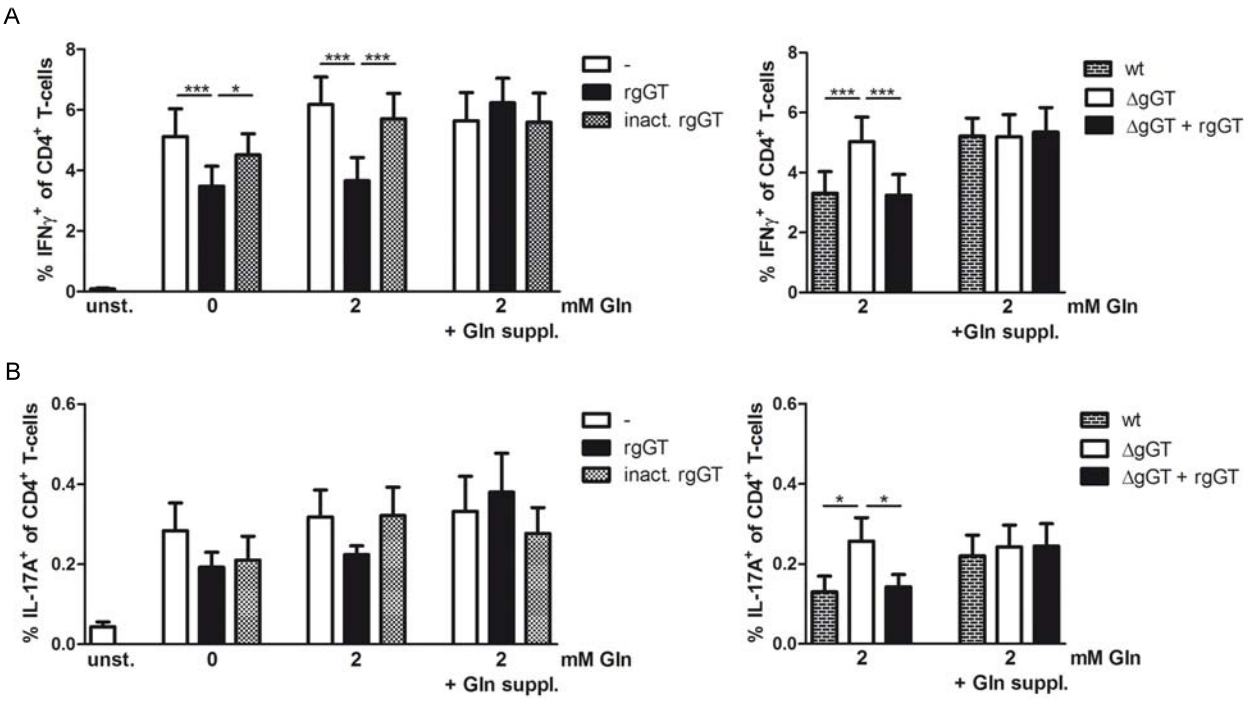

Figure 29: *H. pylori* gGT-induced glutamine deprivation impairs activation and effector cytokine secretion of CD4$^+$ T-cells. αCD3/CD2/CD28-stimulated PBMCs were incubated with cell culture medium which had been preconditioned with 1 µg/ml rgGT (left) or *H. pylori* PMSS1 (MOI 5) (right) for 72 h. Inactivated (inact) gGT and gGT-deficient *H. pylori* (ΔgGT) were used as controls. Glutamine was supplemented at the time of stimulation when indicated. FACS analysis was performed after 24 h of cultivation. Cells were stained with fluorophore-coupled antibodies for the surface markers CD3 and CD4. Intracellular cytokine stain of (A) INFγ (n=8) and (B) IL-17A (n=6) in CD4$^+$ cells is shown as mean ± SEM (*** $p < 0.001$; * $p < 0.05$). Unst, unstimulated cells.

When gGT was absent, an optimal level of reducing agents was observed, which slightly promoted proliferation. Administration of glutathione did not rescue gGT induced inhibition of proliferation in presence of rgGT or *H. pylori* wt (Figure 31A). Interestingly, a synergistic effect of glutathione on promotion of proliferation was observed when glutamine was supplemented but limited due to presence of active gGT (Figure 31A). Thus, glutathione-dependent effects of *H. pylori* gGT on T-lymphocyte proliferation were only minor but beneficial. CD25 expression on CD4 T-cells was not further induced by glutathione supplementation since cells were already fully activated through addition of glutamine (Figure 31B).

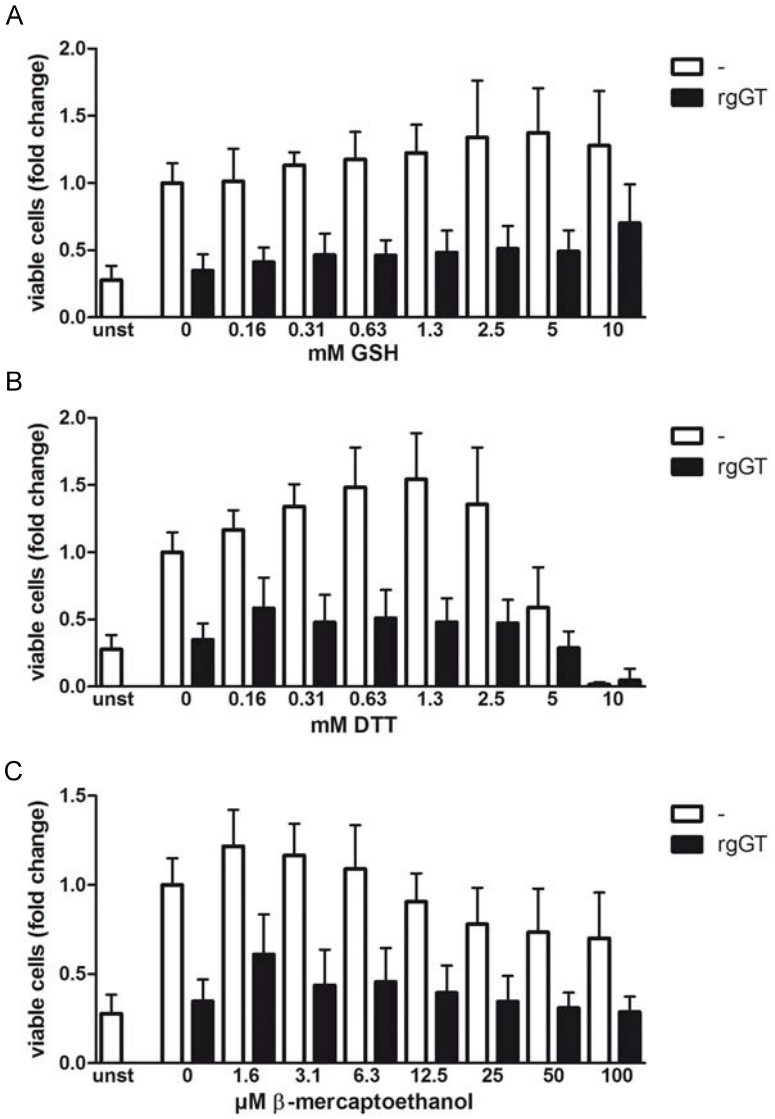

Figure 30: Supplementation of reducing agents to αCD3/CD2/CD28-stimulated PBMCs that were treated with *H. pylori* gGT. Increasing concentration of glutathione (GSH) (A), dithiothreitol (DTT) (B) and β-mercaptoethanol (C) were added to activated PBMCs treated with 1 µg/ml rgGT and incubated in cell culture medium (2 mM Gln) for 72 h. Relative cell numbers were assessed by a viability assay normalized to stimulated but otherwise untreated cells. Results represent mean ± SD from six donors of two independent experiments measured in duplicates.

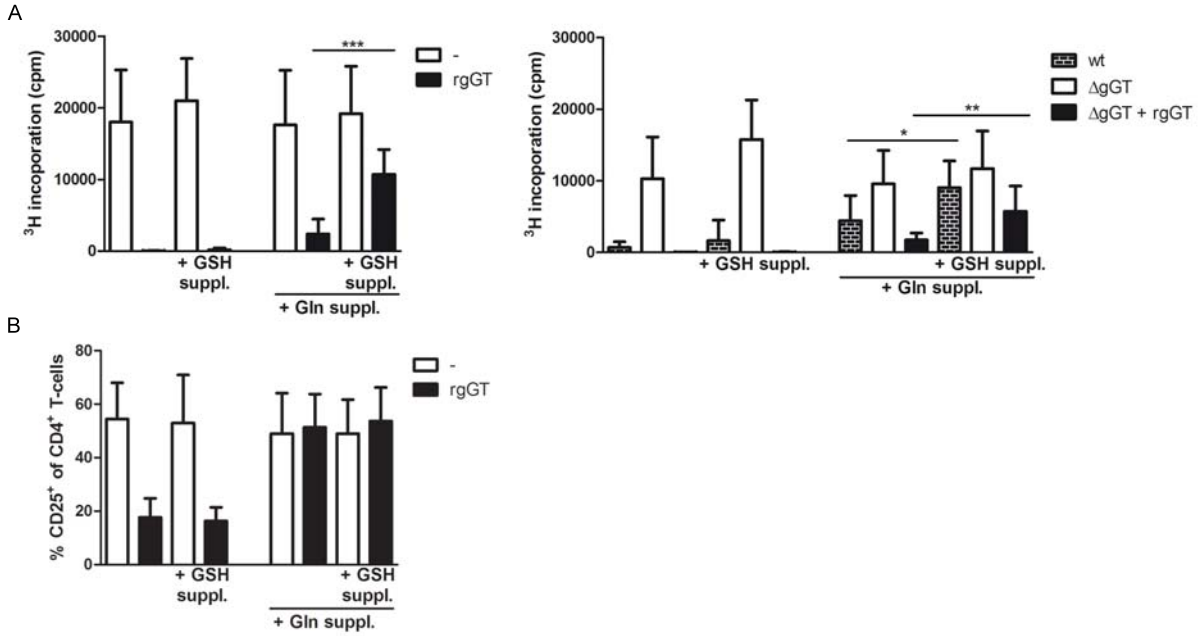

Figure 31: Supportive effect of glutathione only on *H. pylori* gGT-treated PBMCs supplemented with glutamine. PBMCs stimulated with αCD3/CD2/CD28-coated beads were incubated with cell culture medium (2 mM Gln) preconditioned with 1 µg/ml rgGT and/or *H. pylori* (MOI 5) sufficient (wt) or deficient (ΔgGT) in gGT for 72 h. Glutamine (Gln) and/or glutathione (GSH) were supplemented when cells were stimulated and incubated in preconditioned medium. (A) Proliferation of lymphocytes was measured by tritium incorporation within 24 h of a 72 h cultivation period. (B) Cells surface-stained with αCD4 and αCD25 were analyzed after 24 hours. Results are shown as mean ± SD from ten donors. (* $p < 0.05$; ** $p < 0.01$; *** $p < 0.001$).

3.1.6 Activation-induced signaling pathways in T-cells affected by *H. pylori* gGT

The results presented above demonstrate that *H. pylori* gGT compromises T-lymphocyte function in a glutamine-dependent manner. To further assess how glutamine deprivation is sensed and mediates *H. pylori* gGT effects on T-lymphocytes, pathways that have been associated with sensing and adaptation to nutrient availability in lymphocytes, such as mTOR, were analyzed. Active mTOR signaling translates into phosphorylation of eukaryotic initiation factor 4E-binding protein 1 (4E-BP1) and ribosomal protein S6 kinase (p70S6K). Glutamine limiting conditions, caused by *H. pylori* gGT, decreased the levels of phosphorylated and total 4E-BP1 as well as decreased phosphorylation of p70S6K in TCR-stimulated PBMCs after 24 hours (Figure 32).

Upstream pathways that control mTOR activity, such as PI3K/AKT pathway or AMP-activated protein kinase (AMPK), might be modified by glutamine limiting conditions. AKT is strongly activated in T lymphocytes by co-ligation of TCR and CD28 and is thought to regulate glucose but not glutamine metabolism [232]. As glutamine is the preferred energy substrate of activated lymphocytes, energy sensing AMPK protein and phosphorylation level were analyzed upon *H. pylori* gGT treatment and low glutamine levels. Yet, AMPK was not activated by glutamine deprivation (Figure 32). On the contrary, increased overall AMPK and phosphorylation levels were observed under glutamine sufficient conditions after 24 h, stressing the great energy demand when cells are fully activated.

Furthermore, expression of the mTOR downstream targets cyclin D3 and cMyc were analyzed. Up-regulation of cyclin D3 was observed upon TCR-dependent stimulation of PBMCs after 8 hours that peaked at 24 hours (Figure 33). gGT treatment compromised cyclin D3 expression, as pre-

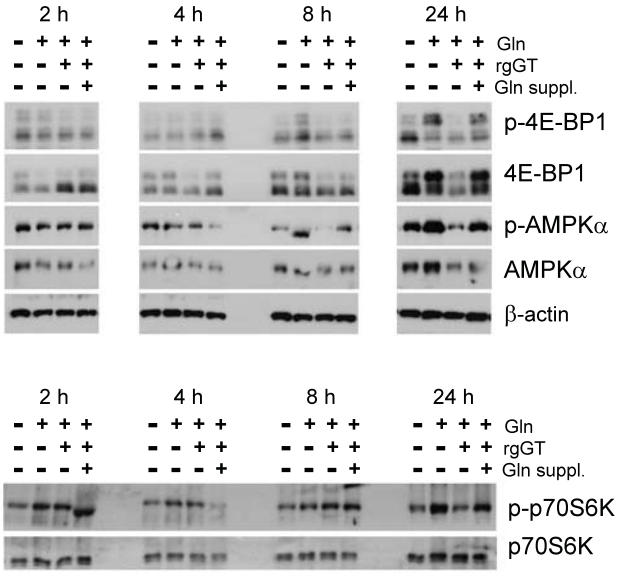

Figure 32: Expression of mTOR up- and downstream targets in *H. pylori* gGT-treated PMBCs. TCR-stimulated PBMCs were cultivated in medium preconditioned with or without rgGT (2.5 µg/ml). 2 mM glutamine was present during the incubation period when indicated. Additionally, 2 mM glutamine was supplemented at the time of stimulation to complement medium after exposure to gGT activity. Cells were lysed at several time points. Phosphorylation and total level of mTOR upstream target AMPKα and downstream targets 4E-BP1 and p70S6K were analyzed by Western blot. One representative experiment of three is shown. β-actin was used as loading control.

viously reported by our group [163], while glutamine supplementation rescued the protein levels. This observation directly links *H. pylori* gGT-induced glutamine deprivation to the inhibition of cell cycle progression. Protein level of cMyc was repressed in TCR-stimulated PBMCs cultivated in glutamine-free or *H. pylori* gGT-treated medium as early as after 2 hours (Figure 33). Since inhibition of the mTOR pathway was observed at a later time point (Figure 32), these results indicate that cyclin D3 and cMyc expression is down-regulated by *H. pylori* gGT prior to changes in mTOR signaling.

cMyc expression has been recently reported to be down-regulated by inhibition of MAPK/ERK signaling in T lymphocytes [197], which regulates proliferation and cell survival. Therefore, it was analyzed whether *H. pylori* gGT influenced the expression and activation levels of ERK and p38. Phosphorylation of ERK was rapidly induced upon TCR stimulation and decreased over time; however, it decreased faster in the absence of gGT or when glutamine was supplemented (Figure 34). Notably, no changes in p38 were observed after incubation of cells with recombinant gGT. These results indicate that MAPK/ERK signaling inhibition is not an upstream event to cMyc down-regulation induced by *H. pylori* gGT.

3.1.7 Untargeted approach to identify *H. pylori* gGT regulated proteins

To identify further pathways or transcription factors altered by *H. pylori* gGT in activated lymphocytes, expression patterns of proteins from TCR-stimulated PBMCs treated either with enzymatically inactive or active gGT for 24 hours were compared. By two-dimensional gel electrophoresis, a number of proteins were found to be differentially expressed (Table 9). However, only few had a functional relevance that could be linked to T-cell activation and proliferation; of those eukaryotic elongation factor 2 (eEF2), Chaperonin containing TCP1 gamma subunit (CCT3), F506-binding protein 4 (FKBP4) and interferon regulatory factor 4 (IRF4) were reduced in presence of active gGT (Figure 35 and Figure 36A).

Table 9: *H. pylori* gGT regulates protein expression in activated PBMCs Differentially expressed proteins identified by 2DGE with lysates from αCD3/CD2/CD28-stimulated PBMCs from six donors cultured either with 1 µg/ml wt or S451/452A rgGT for 24 h. The table includes assigned proteins with a regulation factor (RF) below 0.7 or above 1.3 and a p-value < 0.1 when wt was compared to inactive rgGT.

	Protein	RF	p
MX1	Highly similar to Homo sapiens myxovirus (influenza virus) resistance 1	0.42	0.03
	Serine/threonine-protein phosphatase	0.63	0.00
IDH3A	Isocitrate dehydrogenase 3 (NAD+) alpha, isoform CRA_a	0.64	0.04
VDAC1	Voltage-dependent anion-selective channel protein 1	0.64	0.03
eEF2	Highly similar to Elongation factor 2	0.64	0.06
FKBP4	Peptidyl-prolyl cis-trans isomerase FKBP4	0.65	0.01
	Proteasome 26S non-ATPase subunit 11 variant (fragment)	0.65	0.03
eIF3H	Eukaryotic translation initiation factor 3 subunit H	0.67	0.00
CCT3	T-complex protein 1 subunit gamma	0.68	0.02
	Highly similar to tubulin alpha-ubiquitous chain	0.69	0.08
IRF4	Isoform 2 of Interferon regulatory factor 4	0.69	0.05
DLST	DLST protein	1.42	0.03
SOD	Superoxide dismutase	1.42	0.08
GDH1	Highly similar to Glutamate dehydrogenase 1, mitochondrial	1.44	0.06
SAMHD1	SAM domain and HD domain-containing protein 1	1.48	0.01
ALDH9A1	Highly similar to 4-trimethylaminobutyraldehyde dehydrogenase	1.49	0.01
CAPG	Capping protein (actin filament), gelsolin-like, isoform CRA_a	1.76	0.02

eEF2 is a downstream target of mTOR and promotes protein biosynthesis when de-phosphorylated. CCT is an ATP-dependent chaperon highly expressed in proliferating cells, facilitating correct folding of newly synthetized proteins. RNAi-silencing of CCT results in cell cycle arrest and apoptosis in mammalian cells [233]. In addition to actin and tubulin, cyclin E, cRaf and cMyc were found to interact with this protein [234, 235, 236]. FKBP4 contains a peptidyl-prolyl isomerase domain that converts cis-bonds to their energy favorable trans-form. Collectively these proteins are involved in translation and correct folding of proteins. As protein biosynthesis is strongly induced upon activation of T-cells, this indicates that *H. pylori* gGT interferes with this important anabolic process although the results did not point to a common upstream pathway that would explain these alterations.

3.1.8 *H. pylori* gGT-induced glutamine deprivation down-regulates IRF4 expression

Interestingly, the protein level of the transcription factor IRF4, which has been recently reported to mediate metabolic reprograming upon TCR stimulation in $CD8^+$ T-cells [209], was found to be reduced by a factor of 0.67 ($p = 0.05$) in the presence of the active enzyme (Figure 36B and Table 9). This result was corroborated by Western blot analysis (Figure 36C). IRF4 expression was strongly down-regulated by active *H. pylori* gGT like other factors that had been shown before to be regulated by *H. pylori* gGT, such as cRaf and cyclin D3, while the cell cycle inhibitor p27 was down regulated also in presence of gGT. In a time course experiment, it was shown that IRF4 expression was induced within 8 hours after TCR stimulation under normal conditions, and that the lack of induction in presence of *H. pylori* gGT was glutamine-dependent (Figure 37). To determine whether IRF4 expression in T-cells is altered during *H. pylori* infection *in vivo,* human stomach samples showing *H. pylori*-dependent or -independent gastritis were analyzed. Indeed, $CD3^+$ infiltrates at the site of infection displayed much lower IRF4 expression than infiltrating lymphocytes of *H. pylori*-negative patients (Figure 37), indicating that the presence of the bacterium in the stomach mucosa down-regulates IRF4 expression possibly in a gGT-dependent manner.

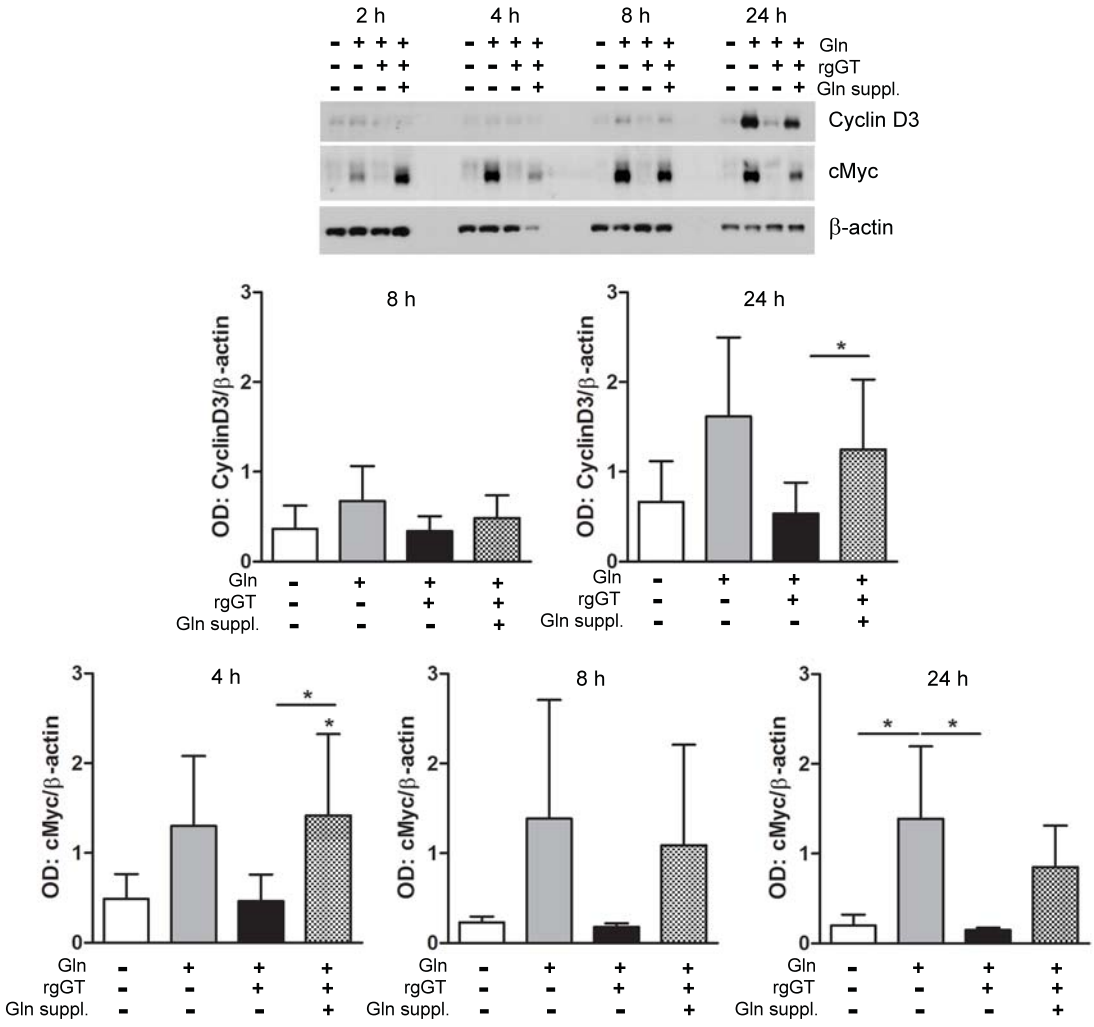

Figure 33: Protein level of Cyclin D3 and cMyc in *H. pylori* gGT-treated PMBCs. TCR-stimulated PBMCs were cultivated in medium preconditioned with or without rgGT (2.5 µg/ml). 2 mM glutamine was present during the incubation period when indicated. Additionally, 2 mM glutamine was supplemented at the time of stimulation to complement medium after exposure to gGT activity. Cells were lysed at several time points and protein expression level of Cyclin D3 and cMyc were analyzed by Western blot. β-actin was used as protein loading control. One representative experiment of three is shown. Expression levels were quantified and subjected to statistical analysis (* $p < 0.05$).

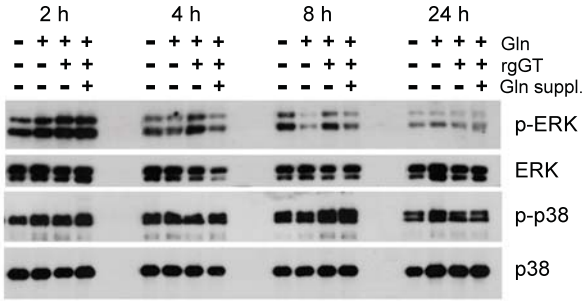

Figure 34: Phosphorylation and expression of MAP kinases ERK and p38. TCR-stimulated PBMCs were cultivated in medium preconditioned with or without rgGT (2.5 µg/ml). 2 mM glutamine was present during the incubation period when indicated. Additionally, 2 mM glutamine was supplemented at the time of stimulation to complement medium after exposure to gGT activity. Cells were lysed at several time points. Phosphorylation and protein expression level of ERK and p38 were analyzed by Western blot. One representative experiment of three is shown.

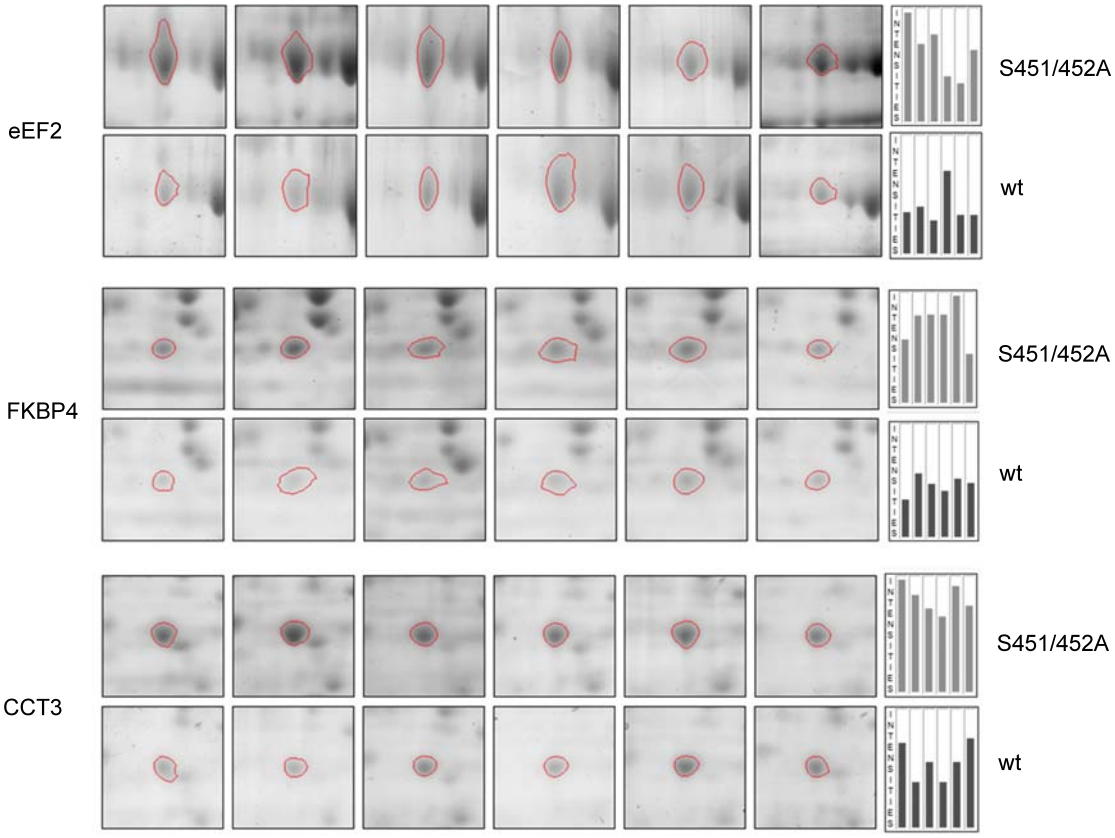

Figure 35: Exemplary protein spots that were differentially regulated by active *H. pylori* gGT. αCD3/CD2/CD28-stimulated PBMCs from six donors were cultured in the presence of 1 µg/ml wt or S451/452 mutant rgGT and lysed after 24 h. Representative spots in Coomassie-stained 2DGE gels assigned and evaluated by ProteomWeaver are shown.

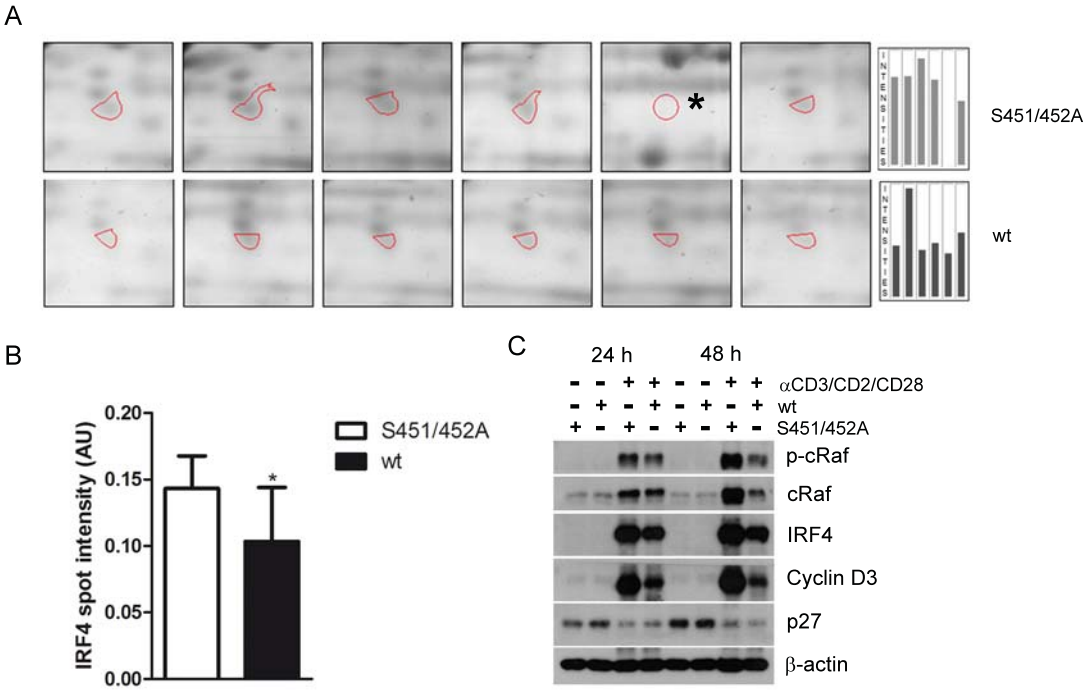

Figure 36: IRF4 expression in stimulated PBMCs is altered by *H. pylori* gGT activity. (A+B) αCD3/CD2/CD28 stimulated PBMCs from six donors were cultured in the presence of 1 µg/ml wt or S451/452 mutant rgGT and lysed after 24 h. (A) IRF4 spots in Coomassie-stained 2DGE gels loaded with samples from six donors. * spot not identified. (B) Statistical evaluation of IRF4 expression level. Data is shown as mean ± SD (* $p < 0.05$). (C) Representative blots of one out of three donors are shown.

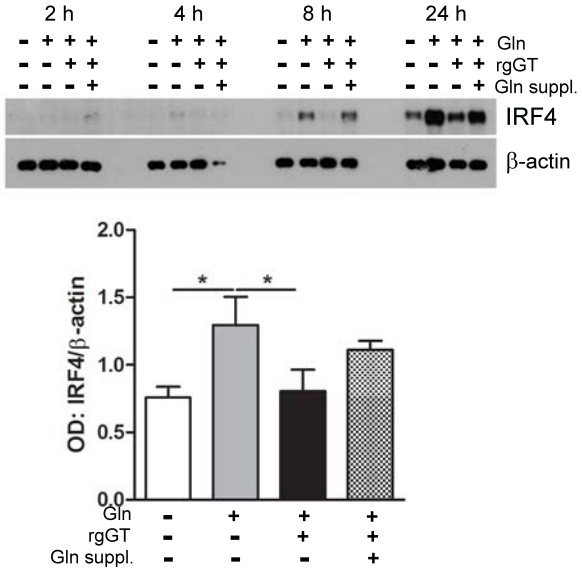

Figure 37: Down-regulation of IRF4 by *H. pylori* gGT is reversed by glutamine supplementation. TCR-stimulated PBMCs were cultivated in medium preconditioned with or without rgGT (2.5 µg/ml). 2 mM glutamine was present during the incubation period when indicated. Additionally, 2 mM glutamine was supplemented at the time of stimulation to complement medium after exposure to gGT activity. Cells were lysed at several time points. Relative IRF4 expression was quantified from three donors at 24 h (* $p < 0.05$).

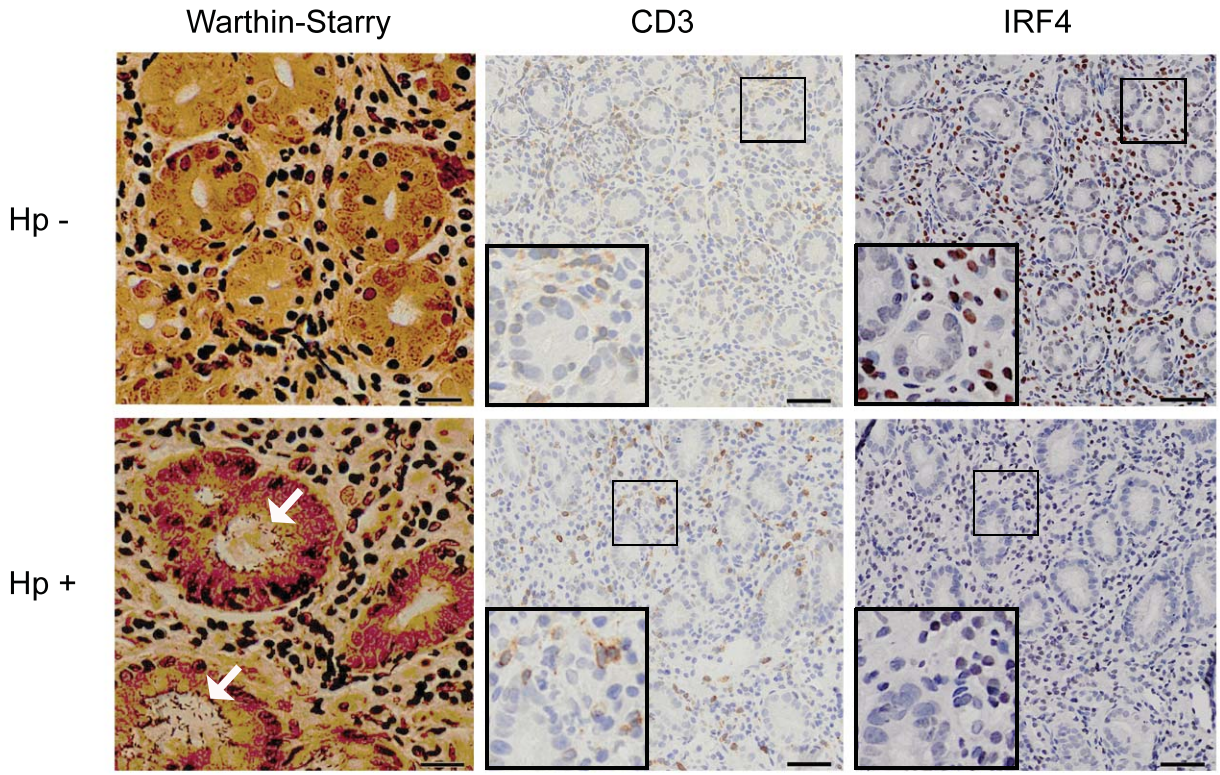

Figure 38: IRF4 and CD3 expression in the gastric mucosa of *H. pylori*-infected individuals. Stomach sections from *H. pylori*-positive (Hp+) and -negative (Hp-) patients with gastritis were subjected to immunohistochemistry. IRF4 expression in $CD3^+$ lymphocytes in the gastric mucosa was compared. Samples were stained with Warthin-Starry stain to identify *H. pylori* and confirm infection status. Arrows indicate location of *H. pylori*. One representative staining from five individuals for each condition is shown (Scale bars, 50 µm in the overview pictures and 20 µm in insets as well as in the Warthin-Starry pictures).

3.2 Role of *H. pylori* gGT during experimental infection

The glutaminase activity of *H. pylori* gGT is well characterized and results from *in vitro* experiments suggest that gGT is able to manipulate T-cell responses. Yet, very little is known about the physiological role of *H. pylori* gGT during infection. Although it has been demonstrated that *H. pylori* gGT is required for effective colonization in mice, the effect on the infection rate and level of bacterial burden was controversial [62, 187, 98]. In previous reports, it remained unclear whether gGT-deficient *H. pylori* has a general defect that does not allow colonization or whether it is cleared by the immune response of the host. Therefore, the contribution of *H. pylori* gGT to initial colonization, to persistence of infection, and to induction of gastric inflammation was investigated using a murine model of infection.

3.2.1 *H. pylori* gGT contributes to initial colonization and determines bacterial burden

To establish the role of *H. pylori* gGT in terms of colonization and immunogenicity C57Bl/6 mice were orogastrically inoculated with 10^9 CFU *H. pylori* PMSS1 wt or an isogenic gGT-deficient strain (ΔgGT) and analyzed at different time points post infection. At the time of analysis, bacterial load was assessed by plating serial dilutions of stomach homogenates.

H. pylori PMSS1 wt did efficiently and highly reproducibly infect mice after one inoculation of bacterial suspension (Figure 39A/B). The colonization was stable and persistent as the bacterial burden remained constant over a six months period. Bacterial load of *H. pylori* PMSS1 was comparable to published data [98].

Conversely, *H. pylori* PMSS1 ΔgGT colonized at a much lower rate than the wt strain (Figure 39A). Notably, bacteria could no longer be recovered in about half of the mice that had been inoculated with *H. pylori* ΔgGT as early as on day three. The high percentage of mice that were not colonized after 3 days showed that *H. pylori* ΔgGT had a defective colonization capacity that was independent from the adaptive immune response. In those mice that were colonized with the gGT-deficient *H. pylori* strain, colonization level was decreased compared to *H. pylori* wt infection, indicating that gGT activity was advantageous to the bacteria in establishing a persistent infection. The bacterial load in mice colonized with gGT-deficient *H. pylori* was 169-fold (day 3), 3-fold (one month, not significant) and 47-fold (three months) lower than in mice colonized with *H. pylori* wt for the same time period (Figure 39A). Besides displaying an overall lower bacterial burden, mice colonized with *H. pylori* ΔgGT showed a greater variability of bacterial load than mice colonized with *H. pylori* wt. Remarkably, *H. pylori* ΔgGT was able to infect at wt levels in some mice. Not only the level of infection but also the colonization rate was more variable in mice colonized with gGT-deficient *H. pylori* compared to mice colonized with *H. pylori* wt (Figure 39B). Independent inoculations with *H. pylori* ΔgGT showed varying colonization rates in contrast to *H. pylori* wt. At six months post infection, bacterial burden in presence and absence of gGT was similar and a higher percentage of mice was colonized with the ΔgGT strain than at earlier time points (Figure 39A). However, in contrast to data from earlier time points that had been derived from at least three independent experiments, six months data were derived from only one experiment. Considering the great variability of colonization rates for *H. pylori* ΔgGT, the overall colonization rates may assimilate to the same level by additional experiments. Nevertheless, the observation that mice were still infected with the gGT-deficient strain after six months demonstrates that *H. pylori* ΔgGT was able to colonize persistently once it had established an infection.

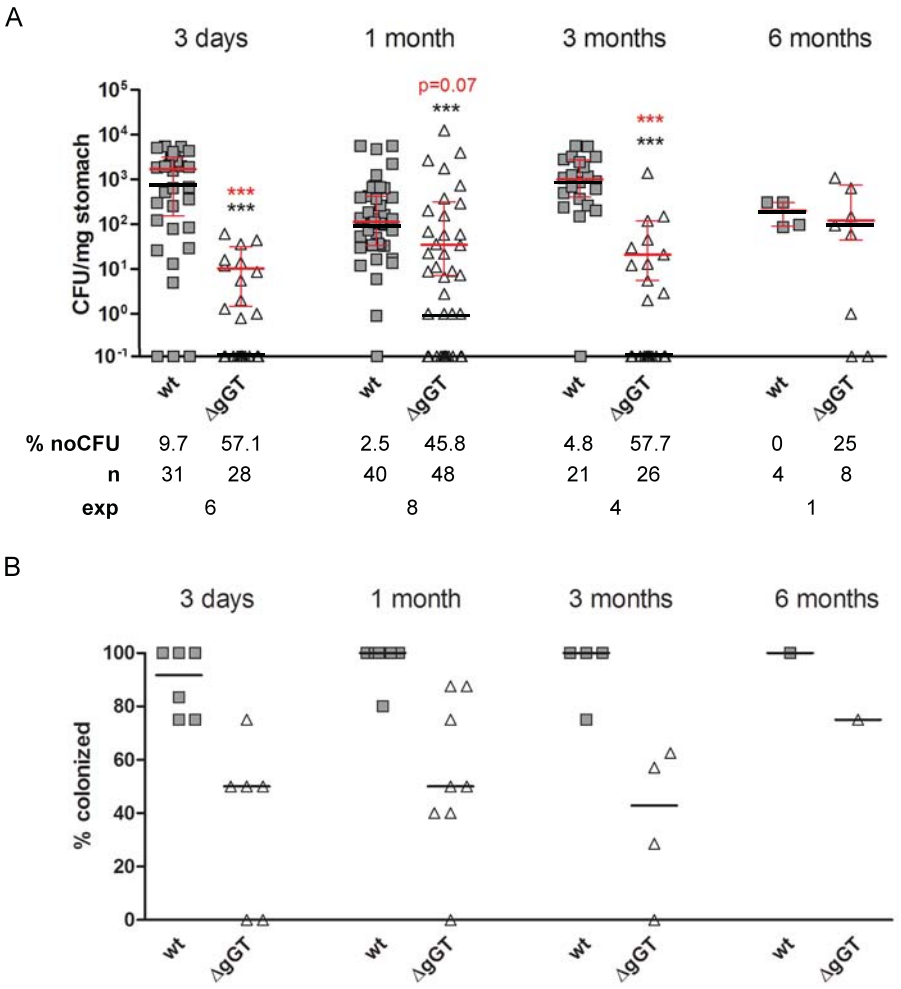

Figure 39: Influence of *H. pylori* gGT on gastric colonization during the course of infection. Adult C57Bl/6 mice were orogastrically infected with 10^9 *H. pylori* PMSS1 wt or ΔgGT for the time indicated. (A) Colonization levels were determined by plating serial dilutions of stomach homogenates. Colony forming units (CFU)/mg stomach are shown. Each symbol represents one mouse. Horizontal lines indicate the median for each group. Black medians include all mice, while medians in red only include those that were colonized at the time of analysis. For those mice also the interquartile range is depicted. Values on the base line are below the detection limit. The table below summarizes percentage of non-colonized mice (% noCFU), number of mice (n), and number of experiments (exp). *** $p < 0.001$ (Mann-Whitney) (B) Colonization rates of independent inoculations are shown. Each symbol represents the colonization rate of one experiment. Horizontal lines indicate the median.

3.2.1.1 Enzymatic activity of *H. pylori* gGT supports initial colonization

To further elucidate in what way gGT supported initial colonization, immune cell infiltration was monitored and availability of gGT activity was modified by administration of rgGT together with the gGT-deficient *H. pylori* strain or co-infection of *H. pylori* wt and ΔgGT.

It had been reported that high numbers of neutrophils and macrophages enter the site of infection within 2 days in FVB/N mice receiving orogastric infection with *H. pylori* SS1 [237]. Concerning colonization data, this might suggest that *H. pylori* ΔgGT copes less well with innate immunity during this early phase of infection compared to *H. pylori* wt. However, no infiltration of immune cells in the gastric mucosa of either *H. pylori* wt- or ΔgGT-infected mice could be detected at day three (Figure 40A). In particular, presence of macrophages or neutrophil granulocytes was not increased in mice infected with either *H. pylori* strain as hardly any chloroacetate esterase (CAE) positive cells were present in the gastric mucosa (Figure 40A). As expected, T-lymphocyte infiltration was not observed at this early time point. To analyze lymphocyte migration in draining lymph nodes of the stomach and intestinal tract, absolute cell counts from gastric lymph node (gLN), peyer's patches (PP), mesenteric lymph nodes (MLN) as well as spleen (SPL) were determined. There was a slight trend towards lower cell numbers in gLN and higher cell numbers in PP and MLN in mice infected with either *H. pylori* wt or ΔgGT compared to uninfected mice (Figure 40B). This might indicate recognition of *H. pylori* by the immune system with migration towards priming organs. Yet, these effects were only minor and independent of gGT. Thus, no evidence was found that could support the hypothesis that *H. pylori* ΔgGT was cleared by the immune system within the first three days.

The incapability of *H. pylori* ΔgGT strain to colonize might be due to the lack of enzymatic activity acting on the environment encountered in the stomach. *H. pylori* gGT may modify availability of amino acids, produce ammonia, or exert oxidative stress; thereby profiting itself or harming the host. To assess the importance of gGT activity for initial colonization, recombinant *H. pylori* gGT was externally complemented by oral administration together with the gGT-deficient *H. pylori* strain. Indeed, rgGT was able to complement the gGT-deficient strain to some extent and allowed infection of a higher percentage of mice (Figure 41A). Increasing the dose (50 or 250 µg) and frequency of application (1 or 3 doses) of the recombinant enzyme increased infection rate with *H. pylori* ΔgGT. Conversely, inhibition of gGT-activity in mice infected with *H. pylori* wt by i.p. administration of acivicin reduced infection rate (Figure 41B). As rgGT was able to complement *H. pylori* ΔgGT to some extent, it was investigated whether co-infection with gGT-sufficient *H. pylori* wt strain would be able to support colonization with *H. pylori* ΔgGT. Mice were infected with either *H. pylori* wt, ΔgGT, or a combination of both and analyzed after one month. Interestingly, gGT-expressed by *H. pylori* wt did not compensate for gGT-deficiency of *H. pylori* ΔgGT as no kanamycin resistant bacteria could be detected in mice that were inoculated with a mixture of *H. pylori* wt and ΔgGT at one month post infection (Figure 41C). On the contrary, *H. pylori* wt outcompeted the ΔgGT strain which was unable to colonize at all when the wt strain was present in the stomach. When *H. pylori* ΔgGT was inoculated alone, 42.9 % of mice were colonized. This indicates that those ΔgGT bacteria that would have been able to colonize were displaced by wild-type bacteria.

These observations demonstrate that *H. pylori* gGT is an important bacterial colonization factor. Taking into account the data presented above, it seems likely that mice inoculated with *H. pylori* ΔgGT that displayed no CFU after three days had not been able to colonize at all. However, adaptations by the host or the bacteria seem to facilitate colonization in mice even in absence of gGT activity once an initial hurdle has been overcome. Thus, gGT-activity provides an advantage to the bacterium but is not an absolutely essential prerequisite for colonization in mice.

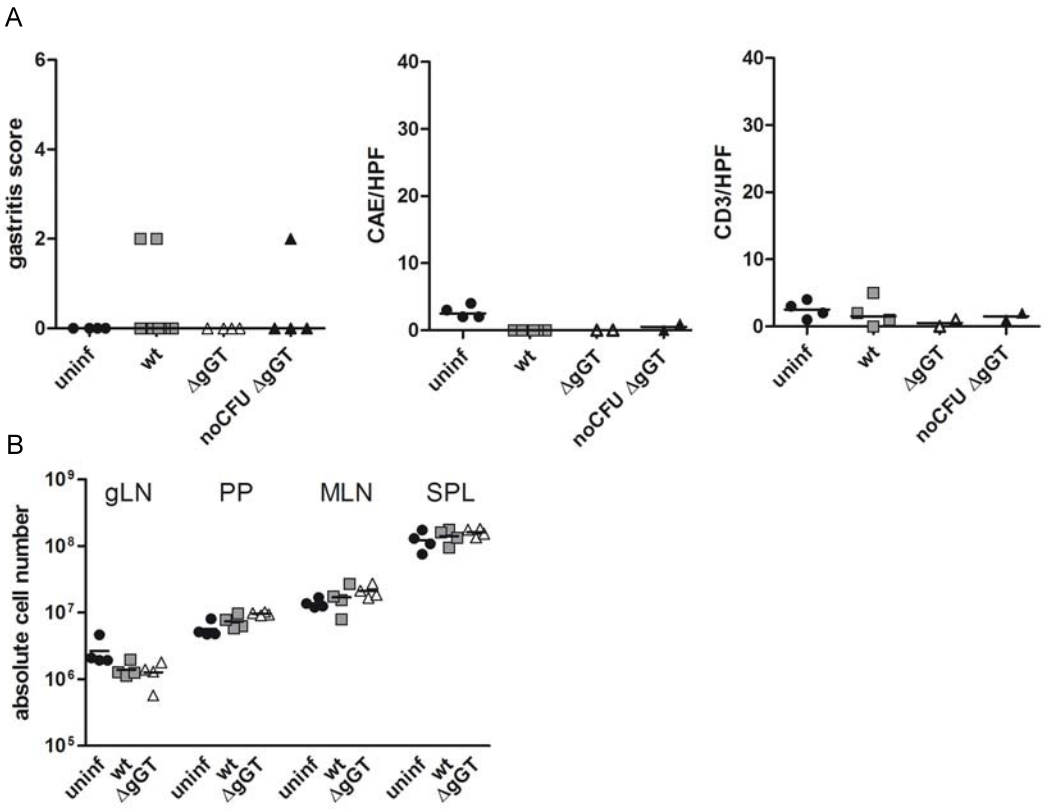

Figure 40: Gastric inflammation and infiltration of immune cells in stomach mucosa or related lymphoid tissue after three days of *H. pylori* infection. C57Bl/6 mice were orogastrically infected with 10^9 *H. pylori* PMSS1 wt or ΔgGT for 3 days. (A) Tissue sections from stomachs were stained with H&E for gastritis score (data from two independent experiments), for chloroacetate esterase (CAE, data from one experiment) and for T-cells (CD3, data from one experiment). Horizontal lines represent median. Number of cells per high power field (HPF). (B) Leucocyte cell count from immune organs three days post infection. Single cell suspensions were prepared and leucocytes counted with a hemocytometer after trypan blue exclusion stain. Horizontal lines represent mean (data from one experiment).

3.2.1.2 Alternative methods for assessing colonization status

To make sure that data derived from plating were truly representing colonization levels in mice, other means of determining colonization were employed.

Besides plating on selective agar and colony counting, there are other parameters that correlate with colonization, such as UreA expression. UreA is particularly suitable for infection analysis, since it is stably expressed during the course of infection [238]. The colonization level assessed by colony counting of serial dilutions from mice infected for one month correlated well with the expression levels of UreA, in particular for the *H. pylori* wt infection (Figure 42A). Furthermore, all mice that were colonized with *H. pylori* wt according to CFU determination were also tested positive for UreA expression. However, two gastric homogenates of *H. pylori* wt- and two ΔgGT-infected mice where bacteria could be reisolated from the stomach were negative for UreA expression analysis. For *H. pylori* ΔgGT, four outliers displayed high UreA expression but low CFU had been observed in these mice. This suggests an up-regulation of UreA mRNA expression, possibly to compensate for a lack of gGT activity. Additionally, three mice inoculated with the gGT-deficient strain showed UreA expression but no bacterial load.

The antigen response against highly abundant *H. pylori* surface proteins is another parameter linked to the colonization status that is determined by the host's immune system. The IgG serum

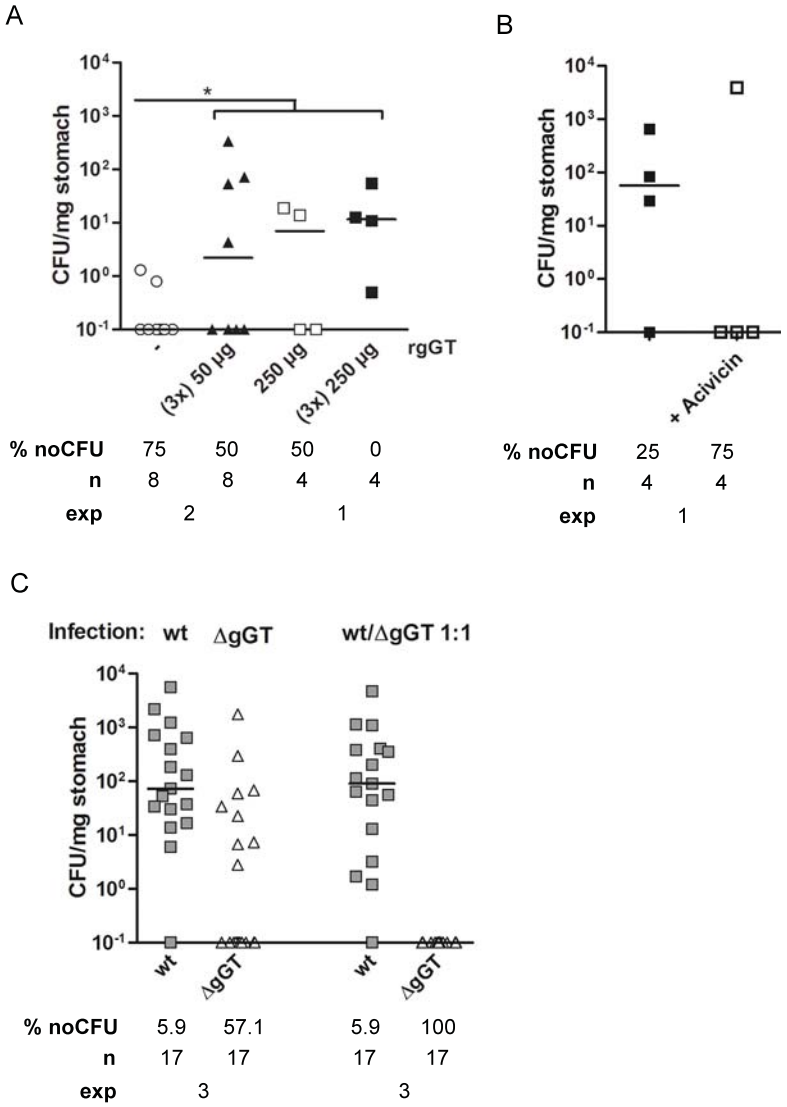

Figure 41: Colonization of mice upon manipulation of *H. pylori* gGT by inhibition and complementation. C57Bl/6 mice were orogastrically infected with 10^9 *H. pylori* PMSS1 wt or PMSS1 ΔgGT for 3 days (A+B) or one month (C). (A) Colonization of C57Bl/6 mice that were orally infected once with 10^9 *H. pylori* PMSS1 ΔgGT. 50 or 250 µg rgGT were given orally at the time of infection and at day one and two after infection (3x) as indicated. Horizontal lines represent median. * $p < 0.05$ (Mann-Whitney) (B) Colonization of C57Bl/6 mice that were orally infected once with 10^9 *H. pylori* PMSS1 wt. 40 µg Acivicin was administered intraperitoneally (i.p.) four times d-2/d0/d1/d2). (C) C57Bl/6 mice were infected with 10^9 *H. pylori* PMSS1 wt, ΔgGT, or a 1:1-mixture. Horizontal lines represent median. Tables below figures summarize percentage of non-colonized mice (% noCFU), number of mice (n), and number of experiments (exp).

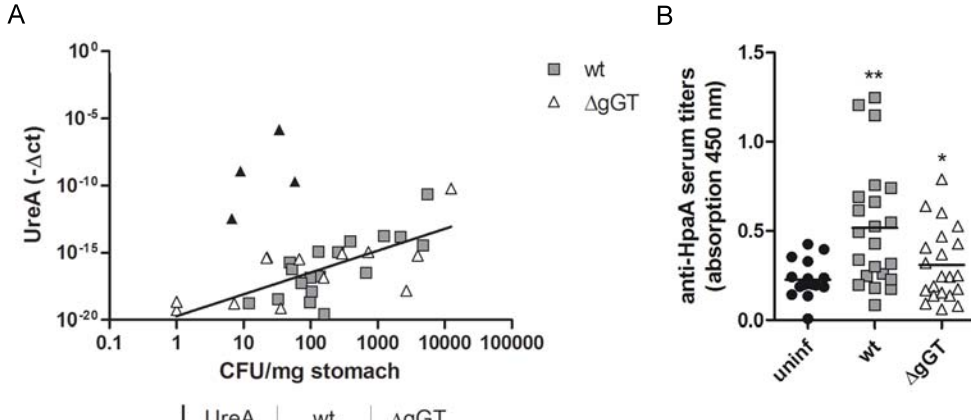

	UreA	wt	ΔgGT
R^2	0.5017	0.5981	0.4869

CFU/UreA	-/-	+/-	-/+	+/+	Σ
uninf	16	0	0	0	16
wt	0	2	0	18	20
ΔgGT	2	2	3	17	24
Σ	18	4	3	35	60

Figure 42: Determination and confirmation of gastric colonization status. (A) Real-time PCR for UreA from stomachs of mice infected with *H. pylori* PMSS1 wt or ΔgGT for one month. Data was normalized to GAPDH. Nonlinear regression analysis was performed and the coefficient of determination (R^2) was determined (wt (n=18) ΔgGT (n=13, 4 outliers (▲) were excluded from the analysis)). Table below shows correlation of positive and negative results from CFU determination and UreA expression for individual mice from four independent experiments. (B) IgG levels towards *H. pylori* HpaA from serum of mice infected for one month were determined by ELISA. Means are indicated by horizontal lines; each symbol represents one mouse. Data in this figure are pooled from three experiments. ** $p < 0.01$, * $p < 0.05$ (ANOVA).

antibody response of infected mice against the highly abundant surface-expressed lipoprotein HpaA was analyzed by ELISA. One month post infection, mice infected with *H. pylori* wt or ΔgGT showed a significantly enhanced IgG response against HpaA (Figure 42B). However, the HpaA-specific response did not correlate with bacterial burden and was only pronounced in half of the *H. pylori* wt-infected mice. In mice infected with *H. pylori* ΔgGT, even less mice showed an antibody response against HpaA. Thus, antibodies against HpaA were induced by *H. pylori* wt and ΔgGT infection but did not correlate well with colonization status at one month post infection.

These results demonstrate that determination of CFU was the most sensitive and reliable method to monitor colonization status of *H. pylori* wt and ΔgGT.

3.2.1.3 Characterization of gGT-deficient *H. pylori* that were able to colonize

To check whether *H. pylori* ΔgGT that were able to colonize still contained the interrupting resistance cassette and were therefore not expressing gGT, stomach homogenates of mice inoculated with the gGT-deficient strain were always plated with and without kanamycin. Numbers of bacteria on both plates were comparable (no significant differences according to Wilcoxon matched pairs test) indicating that the kanamycin resistance was still present (Figure 43A). To further characterize *H. pylori* ΔgGT isolated from mice that were persistently infected, a subset of isolates were analyzed in more detail. Thus, gGT-specific PCR was performed on infection strains and isolates from stomachs of mice colonized with *H. pylori* ΔgGT to confirm that the kanamycin resistance cassette was still in place (Figure 43B). Furthermore, absence of gGT activity from *H. pylori* ΔgGT infection strain and isolated bacteria was confirmed using the gGT activity assay (Figure 43C). These data clearly demonstrate that some bacteria were able to colonize persistently despite lacking gGT-activity. However, it was unclear whether this was due to adaptations of the bacterium or differences encountered in the stomach of individual mice. To assess this, *H. pylori* ΔgGT reisolated at different days post infection and different colonization levels were used for infection experiments. Remarkably, all reisolates were able to persistently and stably colonize the gastric mucosa as *H. pylori* ΔgGT was recovered from all mice one month post infection (Figure 43D). This indicates that the colonizing gGT-deficient bacteria have adapted and acquired the ability to persistently infect mice in absence of gGT activity.

3.2.2 gGT-dependent differences in the adaptive immune response towards *H. pylori*

Mice persistently infected with *H. pylori* ΔgGT and colonized at the same level as with *H. pylori* wt represented an exceptional opportunity to study the immune response in presence and absence of gGT activity. Changes observed between the two groups could be attributed to gGT activity. The adaptive immune response towards *H. pylori* wt and ΔgGT was investigated in detail, as an immune regulatory role for *H. pylori* gGT during infection involving tolerogenic DCs and T-cells had been suggested [98, 163].

3.2.2.1 T-cell differentiation and cytokine profile in peripheral lymphoid organs after infection with H. pylori wt or ΔgGT

T-cell subsets and their cytokine profile were characterized in lymphoid organs of mice infected with *H. pylori* wt or ΔgGT for one month. Therefore, lymphocytes from peripheral immune organs linked to the gastrointestinal tract such as gastric lymph nodes (gLN), peyer's patches (PP), mesenteric lymph nodes (MLN), and spleen (SPL) as systemic control were isolated, restimulated, and subjected to flow cytometry. There was a trend towards increased infiltration of leucocytes into gLN and PP upon infection with *H. pylori* wt as well as ΔgGT (Figure 44A). However, the

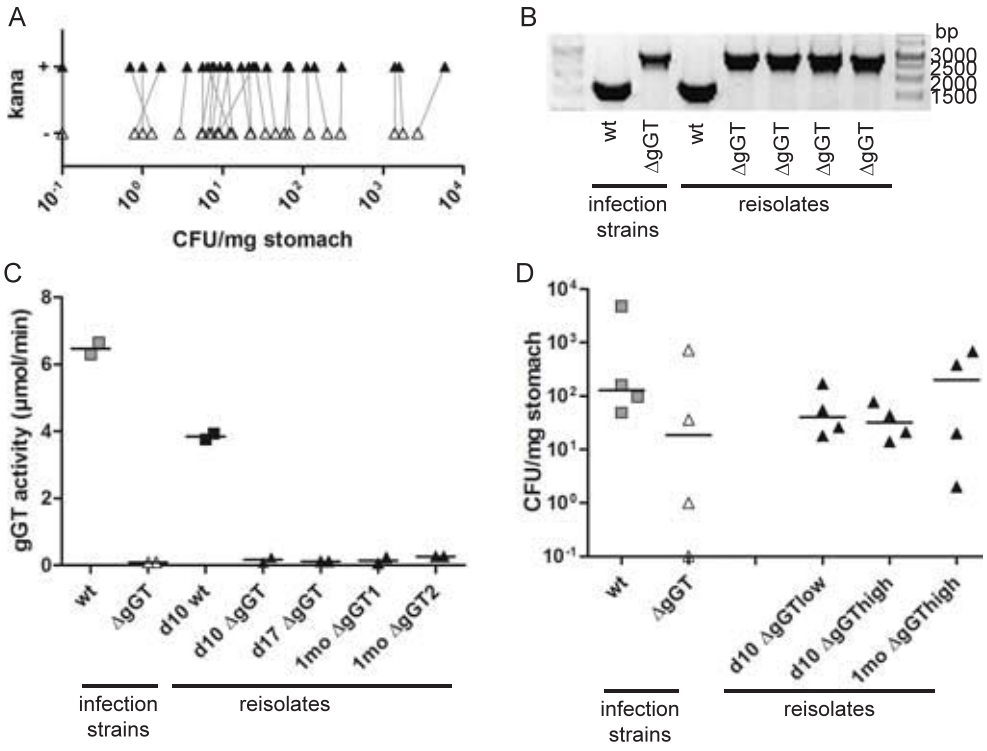

Figure 43: Adaptation of bacteria may allow persistent infection in mice colonized with *H. pylori* ΔgGT. *H. pylori* ΔgGT-infected stomach homogenates were plated in parallel on selective WC-dent special agar plates without (-) and with (+) kanamycin (kana). Data shown in this figure were pooled from nine independent experiments. (B) DNA was extracted from *H. pylori* infection strains and reisolates from stomachs of colonized mice and PCR analysis was performed. Bands increased in size show disruption of the gGT-gene due to a kana resistance cassette. (C) Infection strains and reisolated bacteria were resuspended in PBS and incubated for 6 h at 37 °C. Supernatant was subjected to the gGT activity assay performed in duplicates. (D) Colonization level of mice infected with bacterial isolates from mice that were colonized with *H. pylori* ΔgGT. Reisolates from different times of analysis (day 10 , one month) and different infection levels (low, high) were used. Colonization was assessed after one month of infection. Medians are indicated by horizontal lines; each symbol represents one mouse.

percentage of $CD3^+$ T-cells, $CD4^+$ T-cells or regulatory T-cells ($FoxP3^+/CD4^+$ cells) was not changed (Figure 44B). Surprisingly, an increased proportion of CD44-expressing CD4 cells was observed in PPs of mice inoculated with *H. pylori* ΔgGT (Figure 44C), which indicates that an increased proportion of cells had an antigen experienced phenotype. Stimulation with PMA/Iono of lymphocytes isolated from these immune organs did not show a differential cytokine profile for the Th1 cytokine, IFNγ, or the Th17 cytokine, IL-17A (Figure 44D). IL-17A-expressing $CD4^+$ cells were only detected in the PPs.

In peripheral immune organs, no significant changes in T-cell subtypes or cytokine profile were observed due to infection. Consequently, no differences between infection in presence or absence of gGT were detectable. However, cytokine restimulation was not *H. pylori*-specific; therefore, subtle changes might not have been detectable.

3.2.2.2 T-cell response in the gastric mucosa

Although hardly any signs of inflammation were observed in peripheral immune compartments, infiltration of immune cells and expression of cytokines were expected at the site of infection. Therefore, the adaptive immune response in the gastric mucosa of mice infected for at least one month was analyzed. As the role of gGT-activity in immunopathology can be assessed best when comparing mice persistently infected with *H. pylori* wt to those colonized with ΔgGT at similar levels, non-colonized mice inoculated with *H. pylori* ΔgGT are displayed in a separate group (noCFU ΔgGT).

Presence of *H. pylori* gGT induced T-cell infiltration, whereas PMNs were unaffected. Histopathological evaluation of gastric tissue revealed that *H. pylori* wt and colonizing ΔgGT caused a similar level of active gastritis characterized by infiltration of PMNs (Figure 45A/B). Overall the histopathology was rather mild with a median pathology of 2 and 2.5 (on a scale to 12) for *H. pylori* wt and ΔgGT infected mice, respectively. 35 % of the *H. pylori* wt-infected mice did not display histopathology at all like 29 % of mice colonized with *H. pylori* ΔgGT.

Infiltration of $CD3^+$ cells in mice colonized with *H. pylori* wt was only significantly different from uninfected controls (Figure 45A/B). Mice colonized with *H. pylori* ΔgGT also displayed infiltration of $CD3^+$ cells, albeit to a lesser extent than those colonized with *H. pylori* wt. Mice inoculated with *H. pylori* ΔgGT that did not show colonization did also not display any signs of pathology or lymphocyte infiltration in histological analysis, indicating that they were not colonized from the beginning. Only one mouse inoculated with *H. pylori* ΔgGT that was not colonized according to CFU assessment showed high gastritis scores and infiltration of T-cells in the αCD3 stain. It seems likely that this particular mouse had been colonized but that the infection was cleared.

From histological data, it can be concluded that attraction of T-cells partially depends on presence of gGT activity, whereas infiltration of PMNs depends on bacterial load in general.

gGT dependent infiltration of CD8 cells in the gastric mucosa of *H. pylori*-infected mice. In accordance with histopathology, an increased infiltration of $CD45^+$ leucocytes and in particular of $CD3^+$ T lymphocytes into the gastric mucosa upon infection with *H. pylori* wt was observed by flow cytometry (Figure 46A/B).

In mice colonized with *H. pylori* ΔgGT, the overall count of live $CD45^+$ leucocytes infiltrating into the gastric mucosa was lower than wt (Figure 46A/B). The proportion of $CD3^+$ cells was also increased in the stomachs of mice colonized with *H. pylori* ΔgGT, although not to the same extent as in presence of gGT. Non-colonized mice that were inoculated with *H. pylori* ΔgGT did not display infiltration of T-cells; with the exception of one mouse that had also displayed

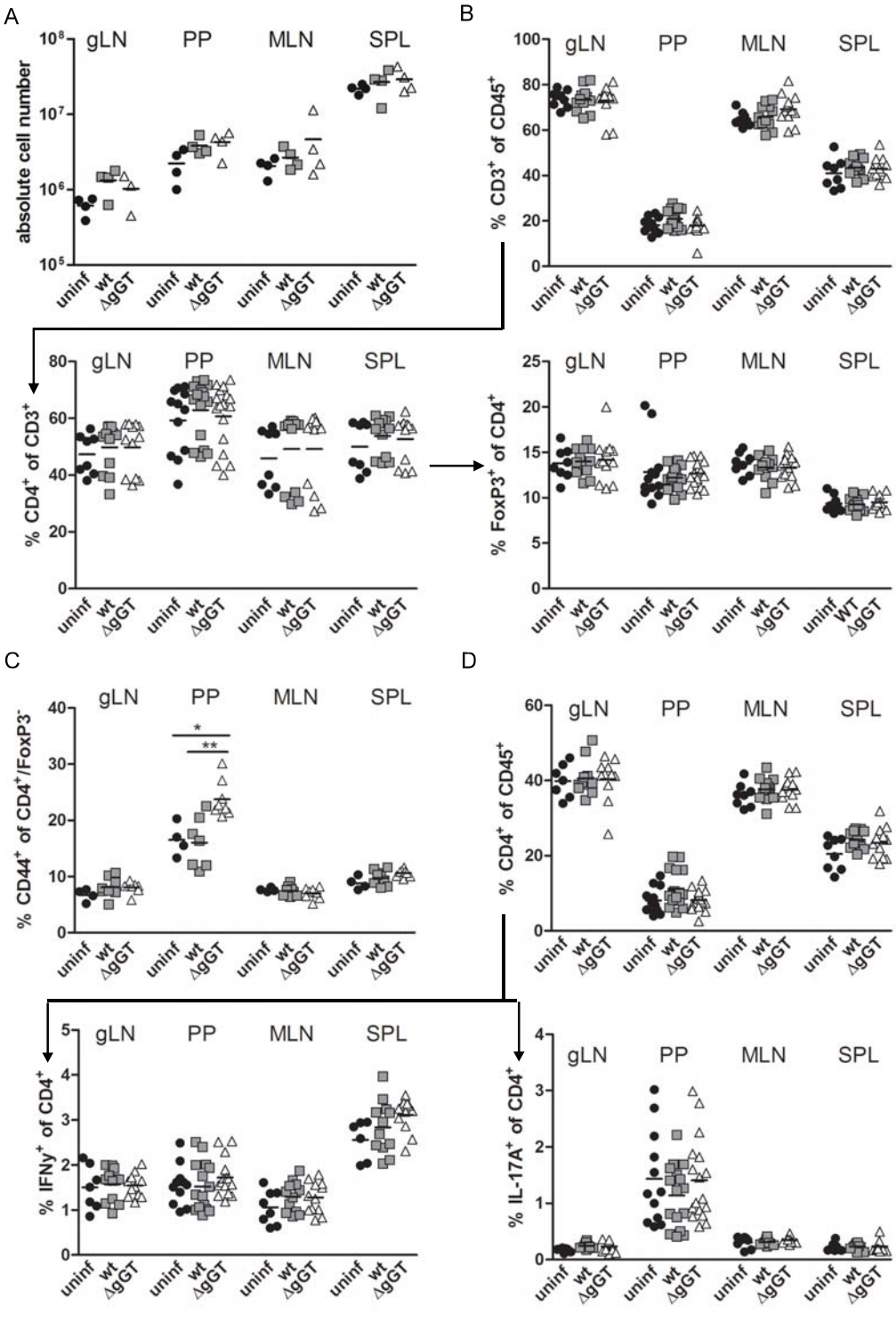

Figure 44: Characterization of Th-cell profile in peripheral immune organs induced by *H. pylori* wt and ΔgGT infection. Single cell suspensions of lymphocytes were prepared from gastric lymph nodes (gLN), peyer's patches (PP), mesenteric lymph nodes (MLN), and spleen (SPL) of *H. pylori* PMSS1 wt- or ΔgGT-infected C57Bl/6 mice one month post infection as well as uninfected control mice. (A) Absolute cell numbers of cells were determined by a hemocytometer after trypan blue exclusion stain (n=4). (B+D) Th-lymphocytes subsets were characterized by flow cytometry. Data for gLN, MLN, and SPL from 2 independent experiments and for PP from 3 independent experiments are shown. (B) Cells were directly stained *ex vivo* for CD45, CD3, CD4 and FoxP3. (C) For one experiment cells were additionally stained for CD44. (D) Cytokine profile was analyzed after stimulation of single cell suspensions with PMA/Ionomycin in presence of Brefeldin A for 3 h at 37 °C. Then cells were surface stained for CD45 and CD4 and intracellular cytokine staining for IL17A and IFNγ was performed.

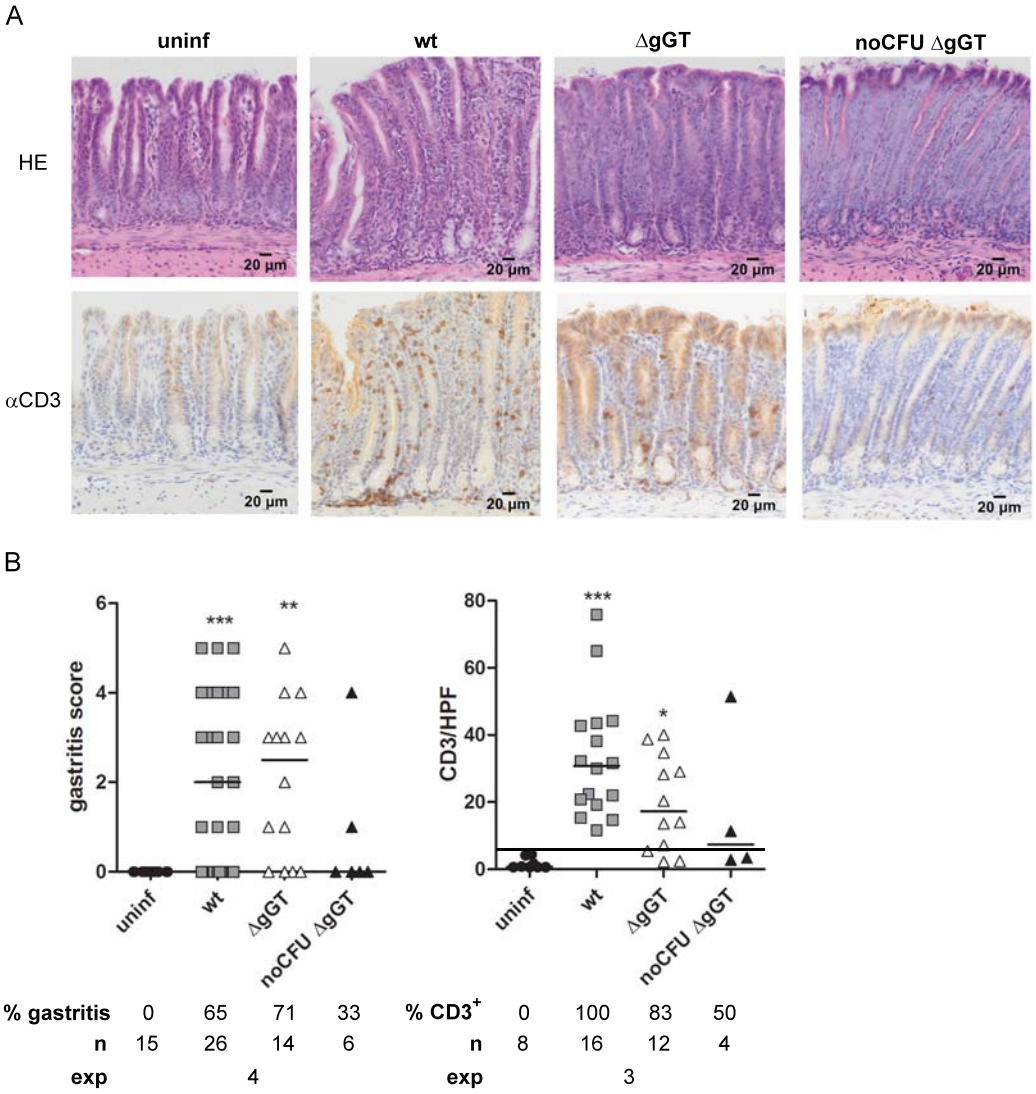

Figure 45: *H. pylori*-induced gastritis and T-cell infiltration in mice colonized with *H. pylori* wt or ΔgGT for one month. C57Bl/6 mice were infected with *H. pylori* wt or ΔgGT for one month before stomachs were subjected to histological analysis. (A) Representative H&E stain (upper panel) for histopathology and αCD3 stain (lower panel) for infiltrating T-lymphocytes from one mouse of each group. (B) Histological scores of gastritis and CD3 cell count/high power field at 20-fold magnification (CD3/HPF) were assessed after one month. Data in the figure is pooled from three to four independent experiments (exp) with groups of 4 to 8 mice (n). Horizontal lines represent median. Kruskal-Wallis test with Dunn's multiple comparison was used to establish statistical significance; ** $p < 0.01$, * $p < 0.05$. % gastritis defined as gastritis score > 0, % $CD3^+ > 5$ (highest score of uninf).

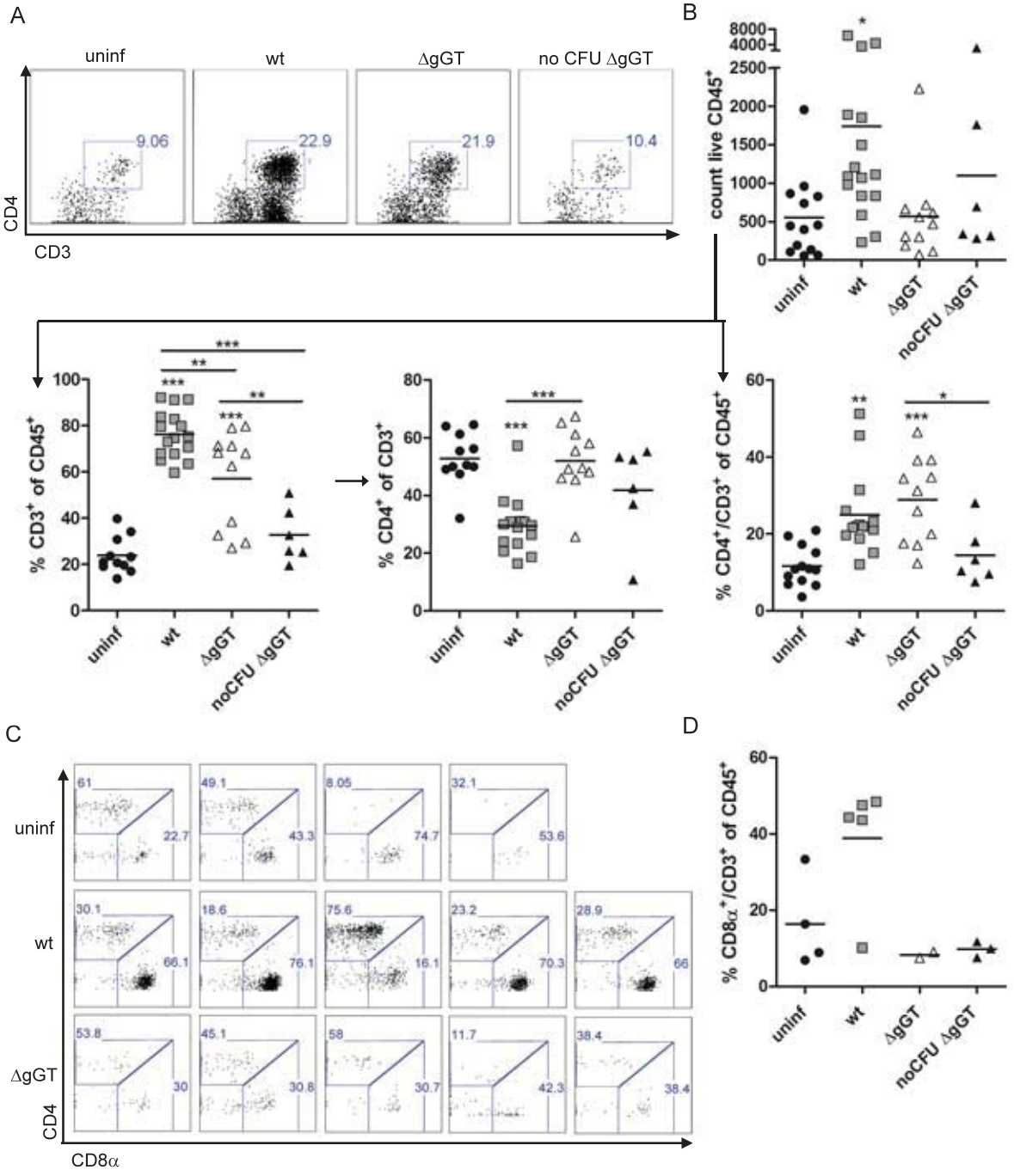

Figure 46: Immunophenotyping of T-cell subsets in stomachs infected with *H. pylori* wt and ΔgGT for one month. Collagenase/DNase digests of gastric tissue stained for CD45, CD3, CD4. (A) Scatter blot depicts the CD3/CD4 stain of live $CD45^+$ cells. A representative mouse from each group is shown. (B) Characterization of lymphocyte populations. Data in these figures were pooled from 3 independent experiments. (C/D) Additionally, CD4 T-cells were stained for CD8α in one experiment. (C) Scatter blot of live CD3/CD45 cells. (D) Proportion of infiltrating CD8α T-cells. Horizontal lines represent mean. *** $p < 0.001$, ** $p < 0.01$, * $p < 0.05$ (ANOVA).

immunopathology. This suggests that the infection had been cleared in this mouse, while other mice had not been colonized.

Strikingly, mice colonized with *H. pylori* ΔgGT displayed a similar proportion of $CD4^+$ T-cells regarding the leukocyte population as those infected with *H. pylori* wt (Figure 46A/B). However, the proportion of CD4 cells within the T-cell population was decreased in mice colonized with *H. pylori* wt compared to ΔgGT. Supposedly, this was due to an increase of another cell population. Indeed, when T-cells were stained for CD4 and CD8α, it could be shown that *H. pylori* wt induced much stronger infiltration of $CD8\alpha^+$ cells compared to *H. pylori* ΔgGT, while infiltration of $CD4^+$ cells was similar (Figure 46C/D).

After three month, lymphocytes infiltrating into the stomach of *H. pylori*-infected mice displayed a very similar pattern compared to one month infection. The strong T-cell infiltration upon infection was even less dependent on presence of gGT than after one month for those mice that were persistently colonized (Figure 47A/B). The shift towards a higher proportion of $CD8\alpha^+$ T-cells over $CD4^+$ T-cells infiltrating into stomachs infected with *H. pylori* wt was maintained (Figure 47A/B).

As regulatory T-cell responses may impact expansion of T helper (CD4) and cytotoxic (CD8) T-cells, CD4 cells in the gastric mucosa of infected mice were further characterized and stained for FoxP3 expression. An additional stain for CD44 showed that all $CD4^+$ cells infiltrating upon infections displayed a phenotype of antigen experience cells independent of whether the *H. pylori* strain contained gGT (Figure 48A). Infiltration of regulatory $FoxP3^+/CD4^+$ T-cells was slightly, yet not significantly, induced upon infection with *H. pylori* wt as well as ΔgGT (Figure 48B/C). Interestingly, the proportion of regulatory T-cells within the $CD4^+$ cell subpopulation correlated positively with the bacterial load irrespective of gGT status (Figure 48D). This indicates that regulatory T cell response is actively induced by *H. pylori* but that is independent of gGT activity. FoxP3-expressing $CD4^+$ T-cells were also positively correlated to colonization level after three month (Figure 48E), but due to different colonization levels, the proportion of FoxP3-expressing cells within the CD4 cell population was higher in mice infected with *H. pylori* wt and compared to ΔgGT.

gGT-deficient *H. pylori* induced a less pro-inflammatory chemokine and cytokine profile in the gastric tissue. To further characterize gGT-related differences in the immune response, expression of cytokines and chemokines in the gastric mucosa of mice colonized with *H. pylori* wt or ΔgGT were assessed.

First, expression of cytokines and chemokines that attract neutrophils and macrophages and drive differentiation of the T-cell response. They were analyzed in the gastric mucosa of mice infected for one month. These factors are mainly produced by innate immune and epithelial cells in chronically inflamed gastric tissues.

LIX (CXCL5), a neutrophil attracting chemokine that is expressed by epithelial cells and macrophages, and RANTES (CCL5), another potent chemoattractant for lymphocytes and monocytes, have been shown to be induced in the gastric mucosa upon *H. pylori* infection [239, 240]. Expression of LIX was induced 11.3-fold and expression of RANTES 9.8-fold upon colonization with *H. pylori* wt compared to uninfected and non-colonized mice, while colonization with *H. pylori* ΔgGT did not induce expression of these chemokines (Figure 49A). Since bacterial burden was similar, this induction can be attributed to presence of gGT. The murine IL-8 homologue, MIP-2, attracting neutrophils to the site of infection, and IL-1β, responsible for neutrophil and macrophage recruitment, showed a similar pattern of expression in stomachs one month post infection (Figure 49B). Expression levels of MIP-2 and IL-1β were 2.9- and 2.8-fold higher in *H. pylori* wt-infected mice than in non-infected mice. In mice colonized with gGT-deficient *H. pylori* strain, expression levels of MIP-2 and IL-1β were only slightly elevated, while non-colonized mice infected

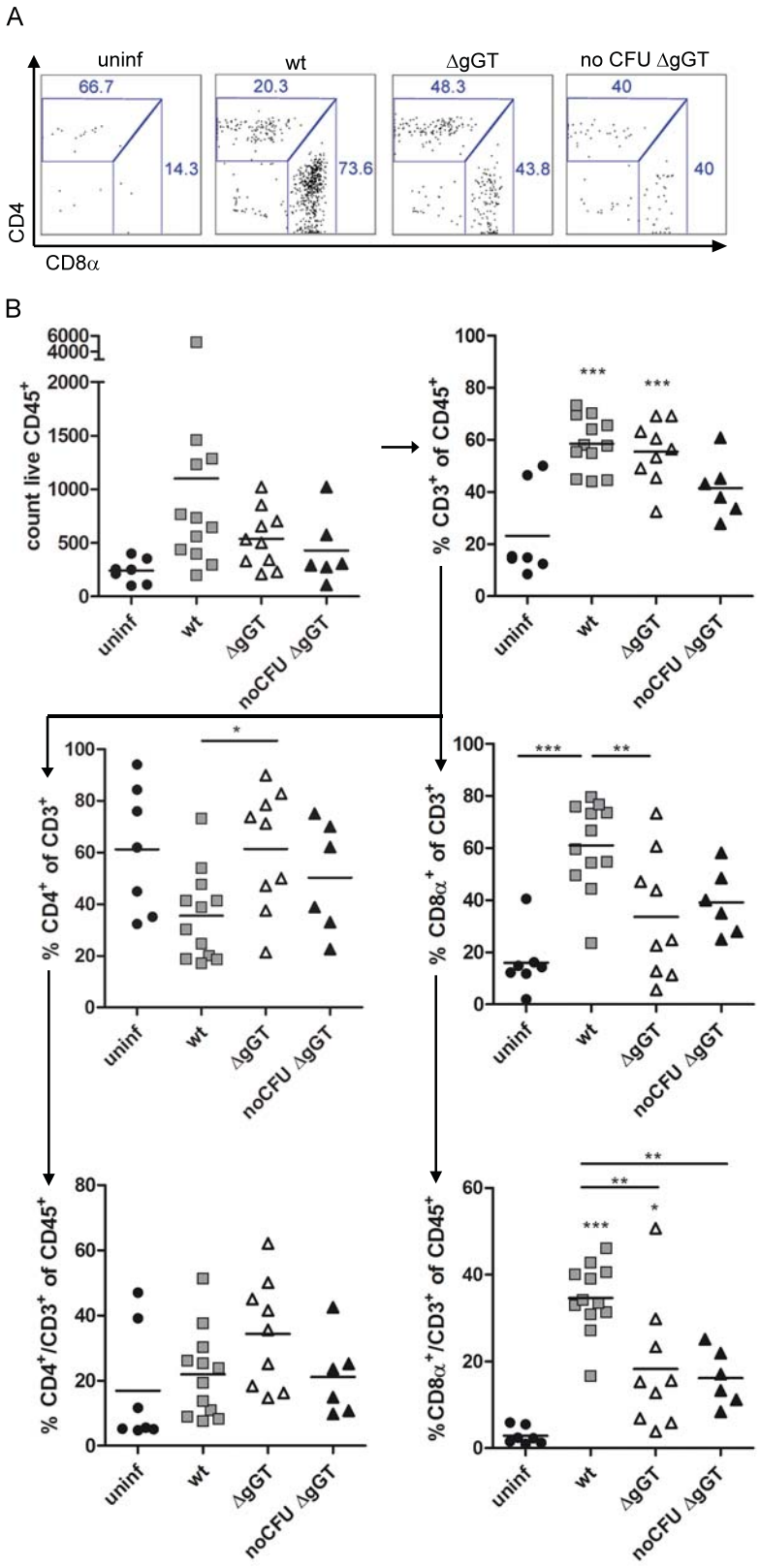

Figure 47: Immunophenotyping of T-cell subsets in stomachs infected with *H. pylori* wt and ΔgGT for three months Collagenase/DNase digests of gastric tissue stained for CD45, CD3, CD4, CD8α and FoxP3 were analyzed by flow cytometry. (A) CD4 and CD8α expression of live $CD3^+/CD45^+$ cells of one representative mouse from each group (B) Data in this figure were pooled from 2 independent experiments. Horizontal lines represent mean. *** $p < 0.001$, ** $p < 0.01$, * $p < 0.05$ (ANOVA)

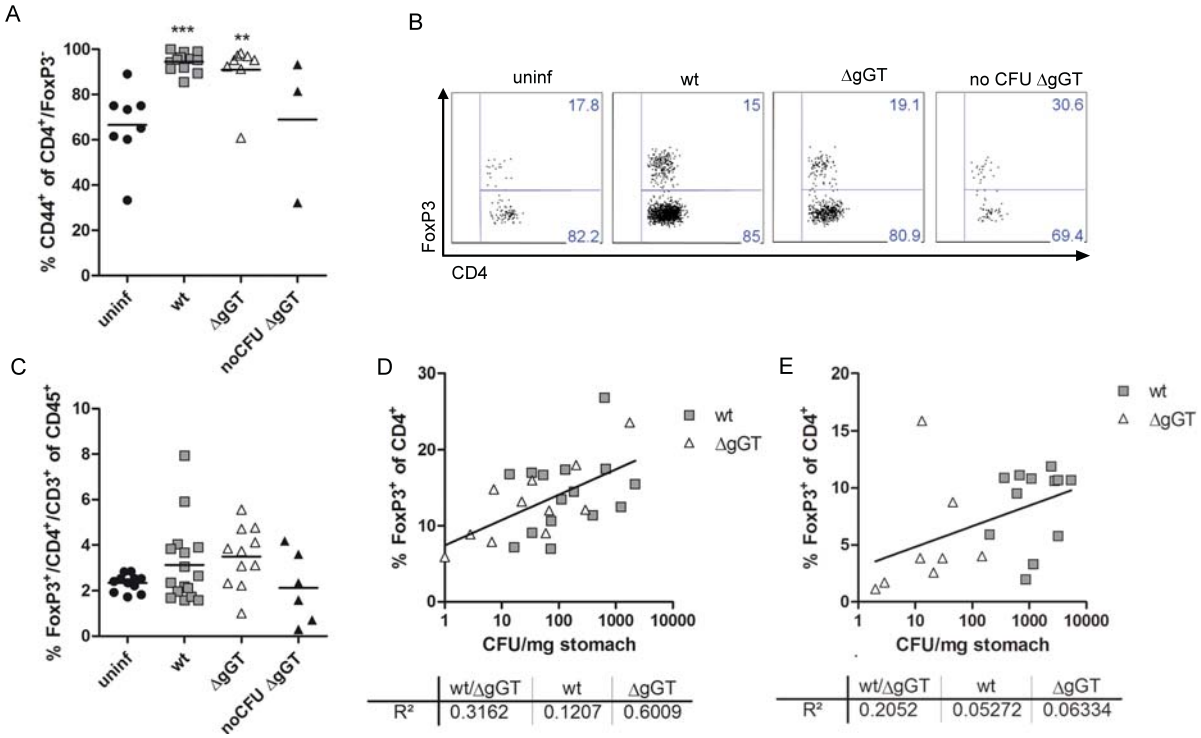

Figure 48: Characterization of CD4 T-cells infiltrating into gastric mucosa of mice infected with *H. pylori* wt and ΔgGT for one month. Collagenase/DNase digests of gastric tissue stained for CD45, CD3, CD4, CD44 and FoxP3 were analyzed by flow cytometry. (A) CD44 expression was analyzed in two experiments. Horizontal lines represent mean. *** $p < 0.001$, ** $p < 0.01$ (ANOVA). (B) Proportion of FoxP3-expressing $CD4^+$ cells within the $CD3^+$ cell population depicted from a representative mouse of each group. (C) Regulatory T-cells within leucocyte population. Nonlinear regression analysis was performed to describe the relationship between FoxP3-expressing T-helper cells and colonization level from cells isolated after 1 month (D) and 3 months (E). Data in figure C and D were pooled from 3 independent experiments and in figure E from 2 independent experiments.

with *H. pylori* ΔgGT were indistinguishable from uninfected mice. Thus, *H. pylori* ΔgGT triggered a much less pro-inflammatory environment in the gastric tissue than *H. pylori* wt at comparable colonization levels. As *H. pylori* infection is associated with cytokine expression inducing Th1 and Th17 differentiation, expression levels of IL-12 p40 and IL-23 p19 mRNA were analyzed. IL-12 p40 expression was induced (1.9-fold) by *H. pylori* wt infection, while colonization with ΔgGT strain did not induce expression of IL-12 (Figure 49C). IL-23 p19, required for maintenance of Th17 T-cells, was expressed at very low levels in the murine stomachs even after infection levels remained low and no differential expression was observed.

Second, mRNA expression of factors characterizing Th1, Th17, and Treg responses in the gastric mucosa was evaluated. As expected from increased level of IL-12 expression, infection with *H. pylori* wt strongly induced expression of the Th1-type cytokines IFNγ and TNFα 13.1- and 5.7-fold, respectively (Figure 50A). In mice inoculated with *H. pylori* ΔgGT expression of these cytokines were comparable to uninfected mice irrespective of colonization status (colonized vs. non-colonized). Taking a closer look revealed that IFNγ, but not TNFα, seemingly correlated negatively with bacterial load in *H. pylori* wt- as well as ΔgGT-infected stomachs, albeit at a different level (Figure 50B). Thus, the shift in IFNγ level was clearly gGT-dependent and might be caused by absence of an IFNγ-expressing cell type, such as CD8 cells, whereas a negative correlation of IFNγ with CFU might be due to suppression of IFNγ-producing cells by regulatory T-cells that correlate positively with bacterial load, as described earlier. Expression of IL-17A was increased 2.2-fold in mice infected with *H. pylori* wt compared to uninfected controls (Figure 50A). Induction of expression of the Th17 cytokine IL-17A in *H. pylori* wt-infected mice was less pronounced compared to Th1 cytokines. This is in line with low IL-23 expression observed in the stomach of *H. pylori*-infected mice. Expression of IL-17A was only slightly increased in mice colonized with *H. pylori* ΔgGT. Expression of factors determining a regulatory T-cell response, such as FoxP3, IL-10 and TGFβ was induced in *H. pylori* wt- as well as ΔgGT-infected mice (Figure 50C) indicating that a regulatory T-cell response was induced due to *H. pylori* colonization independently of gGT. This was in accordance with flow cytometry data. Thus, colonization with gGT-deficient *H. pylori* resulted in much lower effector cytokine expression but a similar expression of factors reflecting a regulatory T-cell response compared to infection with *H. pylori* wt.

Collectively, data from mice that were colonized with *H. pylori* ΔgGT compared to those infected with *H. pylori* wt demonstrate that, in presence of gGT, a stronger proinflammatory environment accompanied by a stronger adaptive immune response was evoked, whereas PMN infiltration did only depend on colonization. Colonization with *H. pylori* wt attracted leucocytes and in particular T-cells to the stomach mucosa. Remarkably, the proportion of infiltrating CD8α^+ T-cells was even higher than the proportion of infiltrating CD4$^+$ T-cells upon *H. pylori* wt infection. Thus, a CD8α^+ dominant T-cell phenotype was observed in the gastric mucosa. In *H. pylori* ΔgGT-infected mice a similar proportion of CD4 cells was infiltrating in the stomach mucosa, yet hardly any influx of CD8 cells was observed in contrast to *H. pylori* wt-infected mice. Concerning effector cytokines, colonizing *H. pylori* ΔgGT did not induce the typical expression patterns related to wt *H. pylori*-associated gastritis, characterized by a Th1/Th17-biased immune response, but a similar regulatory response compared to the *H. pylori* infection. Regarding to T-cell responses, mice inoculated with *H. pylori* ΔgGT that were not colonized were indistinguishable from uninfected mice.

3.2.3 Infection of lymphocyte-deficient Rag$^{-/-}$ mice with *H. pylori* wt and ΔgGT

To further dissect a role of gGT for the bacterial metabolism from an immunoregulatory role, colonization of lymphocyte-deficient Rag$^{-/-}$ mice with *H. pylori* wt and ΔgGT was analyzed. In-

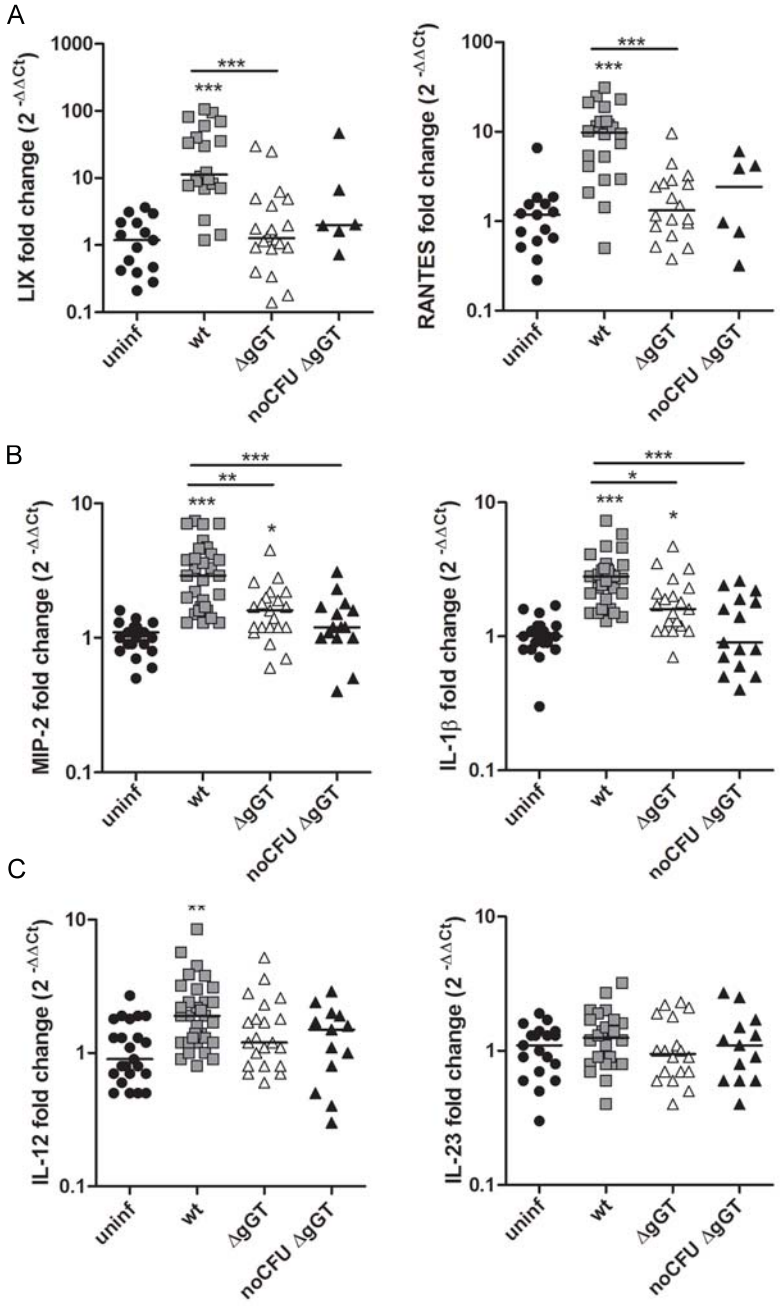

Figure 49: Expression of cytokines and chemokines driving inflammation and Th1/Th17 differentiation in stomach tissues. For RT-PCR analysis, total RNA was extracted from stomachs of *H. pylori* wt- and ΔgGT-infected mice one month post infection. Expression of proinflammatory chemokines and cytokines LIX and RANTES (A), MIP-2 and IL-1β (B), IL-12 and IL-23 (C). GAPDH served as house-keeping gene and uninfected controls were used to establish baseline. Data, expressed as fold change were calculated by ΔΔCt method; horizontal lines represent median. *** $p < 0.001$, ** $p < 0.01$, * $p < 0.05$ (Kruskal-Wallis). Each symbol represents one mouse. Data were summarized from 6 independent experiments for MIP-2, IL-1β, IL12, from 5 for IL23 and from 4 for LIX and RANTES.

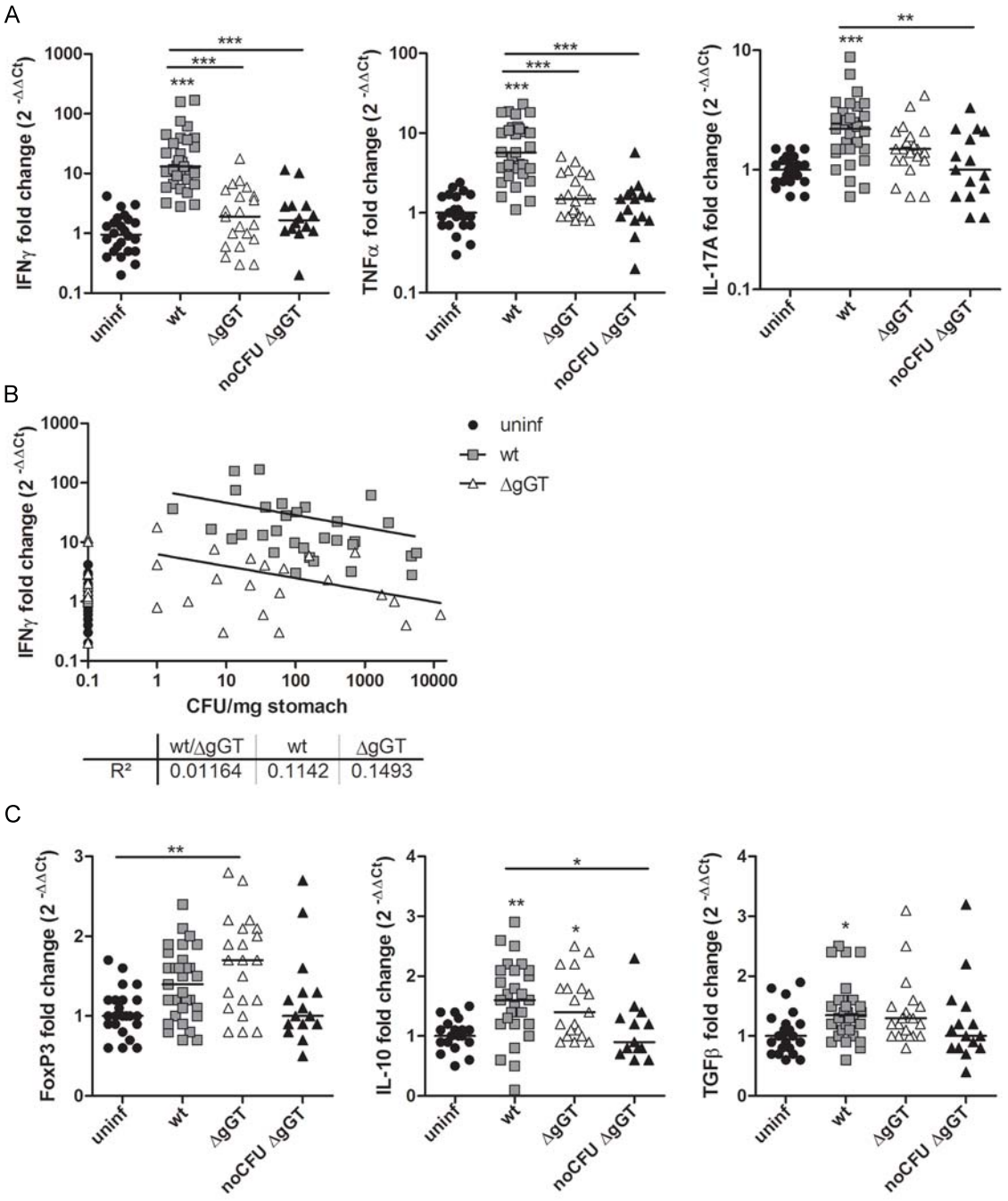

Figure 50: Expression of Th1/Th17 cytokines and of immunoregulatory factors in stomach tissues. Total RNA was extracted from stomachs of *H. pylori* wt- and ΔgGT-infected mice one month post infection. (A) Levels of IFNΓ, TNFα and IL-17A were detected by RT-PCR. (B) IFNΓ expression was correlated to the colonization level by regression analysis. (C) Levels of FoxP3, IL-10, and TGFβ expression assessed by RT-PCR. GAPDH served as house-keeping gene and uninfected controls were used to establish baseline. Data, expressed as fold change were calculated by ΔΔCt method. Horizontal lines represent median. *** $p < 0.001$, ** $p < 0.01$, * $p < 0.05$ (Kruskal-Wallis). Each symbol represents one mouse. Data were summarized from 6 independent experiments (except for IL-10: 5 experiments).

fection of Rag$^{-/-}$ mice with *H. pylori* wt resulted in a 120-fold and 49-fold increase of bacterial load compared to C57Bl/6 mice after one and three months of infection, respectively (Figure 51A and Figure 39A). Increased bacterial expansion together with absence of *Helicobacter*-induced gastritis had been observed in lymphocyte-deficient mice before [69, 116]. Therefore, it was interesting to explore how *H. pylori* ΔgGT would behave in absence of lymphocytes and a lack of post-infection gastritis. The colonization levels of Rag$^{-/-}$ mice inoculated with *H. pylori* ΔgGT, separated into two distinct groups at one as well as at three months post infection (Figure 51A). Like in C57Bl/6 mice, one group of mice inoculated with gGT-deficient *H. pylori* was not colonized. The other group represented lymphocyte-deficient mice infected with *H. pylori* ΔgGT that displayed very high bacterial burden with low variability (Figure 51A). Those gGT-deficient bacteria that managed to colonize Rag$^{-/-}$ mice did so at an about 100-fold higher level compared to those colonizing immunocompetent mice with much less variability. Nevertheless, colonizing *H. pylori* ΔgGT still displayed one log lower bacterial load than the *H. pylori* wt indicating that gGT activity confers some advantage to colonization irrespective of the adaptive immune response. Like in C57Bl/6 mice, the colonization rate of *H. pylori* ΔgGT in Rag$^{-/-}$ mice varied greatly from experiment to experiment in contrast to *H. pylori* wt (Figure 51B).

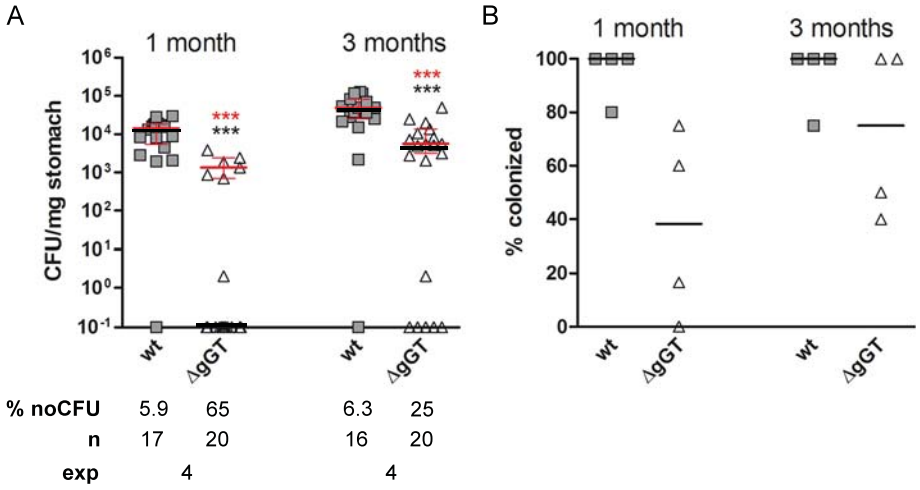

Figure 51: Colonization of lymphocyte-deficient mice with *H. pylori* ΔgGT. Rag$^{-/-}$ mice were orogastrically infected with 10^9 *H. pylori* PMSS1 wt or PMSS1 ΔgGT for the time indicated. (A) Colony forming units (CFU) /mg stomach are shown. Each symbol represents one mouse. Values on the base line are below the detection limit. Horizontal lines indicate the median for each group. Black median includes all mice, while red only includes those that were colonized at the time of analysis. For those mice also the interquartile range is depicted. Table below summarizes percentage of non-colonized mice (% noCFU), number of mice (n), and number of experiments with 4 to 7 mice in each group (exp). *** $p < 0.001$ (Mann-Whitney). (B) Colonization rates for independent experiments are shown. Each symbol represents the colonization rate of one inoculation. Horizontal lines indicate the median.

Collectively, these results suggest that, in absence of an adaptive immune response, gGT activity was required to overcome an initial hurdle or limitation before the bacteria could colonize the murine stomach. Once colonization was established, the gGT-deficient bacteria profited from the absence of an inflammatory response as they reached a very high level of colonization; although it was still lower than bacterial burden of *H. pylori* wt probably due to a defective bacterial metabolism.

3.2.4 CD4$^+$ T-cell reconstitution of *H. pylori* wt- or ΔgGT-infected Rag$^{-/-}$ mice

Several studies report that CD4$^+$ T-cells are responsible for *H. pylori*-induced gastric inflammation and suppression of bacterial burden [73, 116, 118, 137]. Since Rag$^{-/-}$ mice were colonized at high levels with *H. pylori* wt and ΔgGT, CD4$^+$ cells were transferred into infected Rag$^{-/-}$ to study the

effect on bacterial burden in dependence of gGT activity. Thus, $Rag^{-/-}$ mice were infected with *H. pylori* wt or ΔgGT and left untreated for one month to establish a stable infection To increase the probability that *H. pylori* ΔgGT would be able to colonize, *H. pylori* ΔgGT was inoculated together with 250 µg rgGT (comparable to Chapter 3.2.1.1). One month post infection, mice were reconstituted with $CD4^+$ cells (300 000 cells/mouse) isolated from spleen and lymph nodes of naïve mice.

The effect of transferred $CD4^+$ cells on colonization level of mice that had already been infected for one month was analyzed one month after transfer. Control mice were stably infected with *H. pylori* wt after two months (Figure 52A). The level of infection with *H. pylori* wt was comparable to mice infected for three months (Figure 51A). Interestingly, all *H. pylori* ΔgGT-infected mice were colonized at high levels (Figure 52A). Thus, oral treatment with rgGT had effectively complemented the gGT-deficiency during the early phase of infection. Colonizing *H. pylori* ΔgGT displayed the same bacterial load after two month of infection as after three months without rgGT treatment (Figure 52A and Figure 51A). These control groups indicate that all mice had been colonized when $CD4^+$ cells were transferred. Surprisingly, almost all mice infected with *H. pylori* wt had cleared the infection one month after CD4 cell transfer, while the colonization of mice infected with *H. pylori* ΔgGT was only slightly reduced. Therefore, transferred CD4 cells seemed to be more effective in controlling bacterial load of *H. pylori* wt than of *H. pylori* ΔgGT. To analyze whether a different level of gastric inflammation could be observed, histology for infiltrating immune cells was performed. Mice infected with *H. pylori* wt or ΔgGT developed similar levels of gastritis upon transfer of CD4 cells (Figure 52B), but the quality of the response differed at least in blood. Adopted CD4 cells from blood were characterized by flow cytometry. Reconstituted mice contained about 10 - 20 % $CD4^+/CD3^+$ cells in blood irrespective of *H. pylori* treatment one month after transfer (Figure 52C/D). This demonstrates that transferred cells had expanded well. Only three mice (1 wt, 2 ΔgGT) failed to adopt $CD4^+$ cell to the same extend and displayed a population of $CD4^+/CD3^+$ cells below 1 %. The three mice (1 wt, 2 ΔgGT) that had not adopted the $CD4^+$ cells were those with the highest bacterial load and displayed only a low level of gastritis (wt) or no gastritis at all (2 ΔgGT). The $CD4^+$ T-cells in *H. pylori* wt-infected mice had a more activated ($CD25^+/Foxp3^-$) and less regulatory phenotype ($Foxp3^+/CD25^+$) compared to mice inoculated with *H. pylori* ΔgGT (Figure 52C/D). Thus *H. pylori* ΔgGT seemed to elicit less inflammation and more regulatory $CD4^+$ cells in this setting, with the limitation that this data is derived from blood.

These data suggest that when the T-cell population is only comprised of CD4 cells, *H. pylori* ΔgGT might induce an inflammatory response, which might be characterized by a more regulatory phenotype and results in a less vigorous immune response that only reduces bacterial load, while *H. pylori* wt was cleared.

3.2.5 Adoptive transfer of $CD4^+/CD44^-$ cells in *H. pylori* wt- or ΔgGT-infected $Rag^{-/-}$ mice

In a further experiment, $CD4^+$ cells were depleted from $CD44^+$ cells before transfer. As $CD4^+/CD44^+$ cells do not only include antigen experienced cells, but also a high proportion of FoxP3-expressing regulatory T-cells, the sorted cells were enriched in effector T-cells (Figure 53A). $CD4^+/CD44^-$ cells isolated from spleen and lymph nodes of naïve mice were transferred into $Rag^{-/-}$mice (300 000 cells/mouse) that were infected with *H. pylori* wt or ΔgGT for 1.5 months and analyzed three month post infection. In this setting, not only mice inoculated with *H. pylori* wt but also with *H. pylori* ΔgGT cleared the infection after transfer of $CD4^+/CD44^-$ cells (Figure 53B). Stomachs were macroscopically swollen and a strong infiltration of CD45 cells into stomach mucosa was observed (Figure 53C). Almost 90 % of $CD45^+$ cells were $CD4^+$ T-cells in transferred mice containing

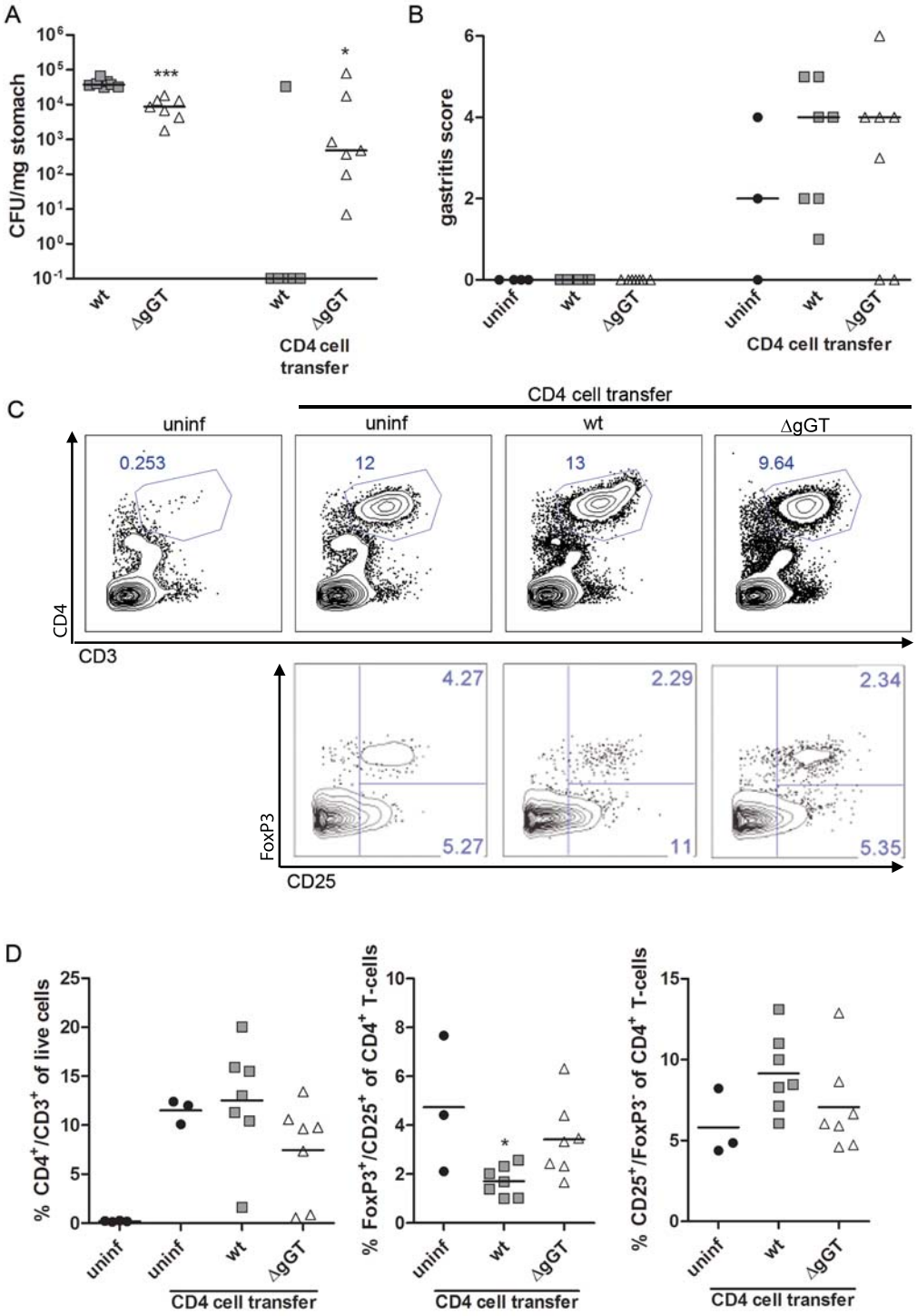

Figure 52: Transfer of CD4$^+$ cells in *H. pylori* wt- and ΔgGT-infected Rag$^{-/-}$ mice. Rag$^{-/-}$ mice were infected three times with *H. pylori* wt or ΔgGT. Mice inoculated with *H. pylori* ΔgGT were orally administered 250 µg rgGT at time of infection to support initial colonization. One month post infection, CD4$^+$ cells (300 000 i.p.) isolated from spleen and lymph nodes of naïve mice were transferred into Rag$^{-/-}$. Mice were analyzed one month after transfer. Data from one experiment are shown. (A) Colonization level of Rag$^{-/-}$ mice with and without transfer of CD4 cells is depicted. Horizontal lines represent median. * $p < 0.05$, *** $p < 0.001$ (Mann-Whitney). (B) Level of gastritis assessed by histology. Horizontal lines represent median. (C/D) Flow cytometry analysis from blood was performed after stain for CD3, CD4, CD25 and FoxP3 (C) Representative FACS blots from one mouse of each group are depicted. In the upper panel proportion of CD4$^+$/CD3$^+$ cells of live lymphocytes is displayed, while the lower panel shows CD25 and FoxP3 status of CD4/CD3 cells. (D) Adopted CD4/CD3 cells in blood: proportion of regulatory (FoxP3$^+$/CD25$^+$) cells and effector (CD25$^+$/FoxP3$^-$) cells. *$p < 0.05$ (ANOVA).

only a very low proportion of cells displaying Treg phenotype. Thus, the immune response elicited by transfer of $CD4^+/CD44^-$ cells against *H. pylori* wt and ΔgGT seemed to be the same with an identical outcome. These results suggest that stomach infiltrating CD4 cells that were partially depleted from Tregs were effectively clearing *H. pylori* irrespective of gGT in contrast to CD4 cell transfer, where only *H. pylori* wt was eradicated.

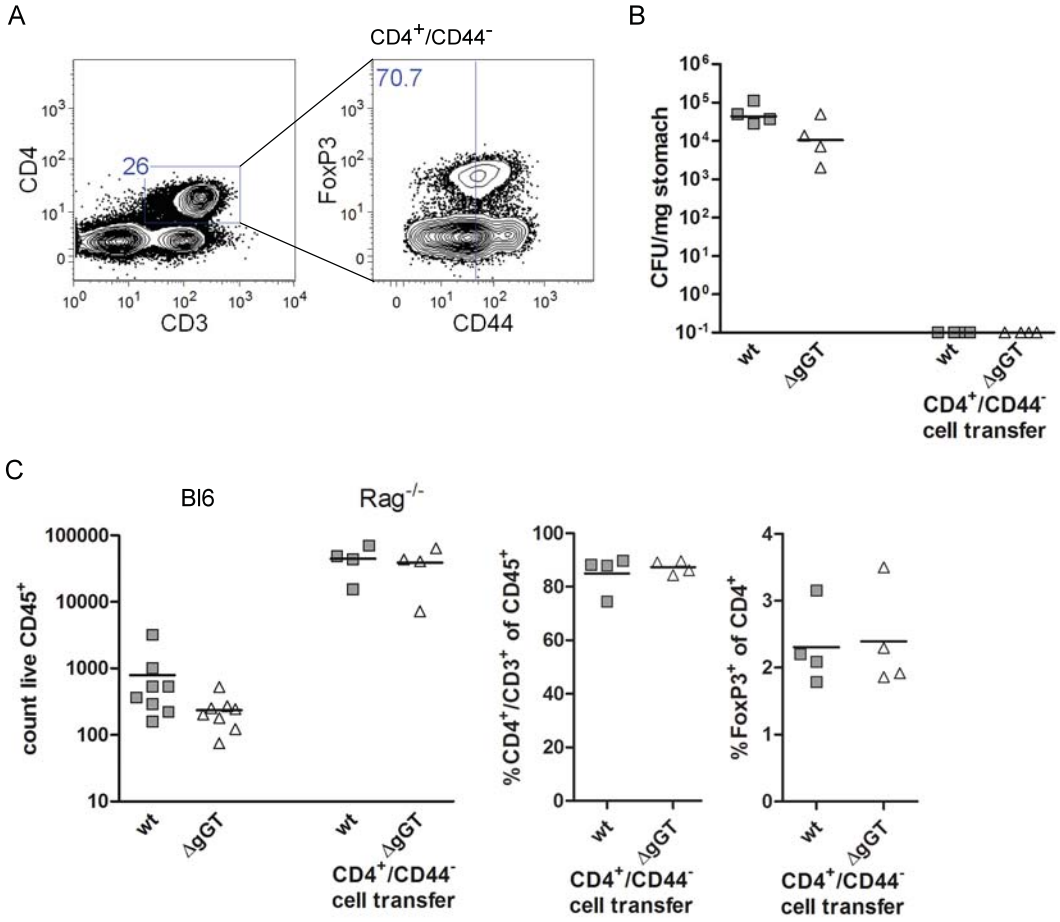

Figure 53: Transfer of $CD4^+/CD44^-$ cells in *H. pylori* wt- and ΔgGT-infected $Rag^{-/-}$ mice. $Rag^{-/-}$ mice were infected with *H. pylori* wt or ΔgGT. 1.5 months post infection, $CD4^+/CD44^-$ cells (300 000 i.p.) isolated from spleen and lymph nodes of naïve mice were transferred into these mice. Mice were analyzed after another 1.5 months after transfer. Data from one experiment are shown. (A) Splenocytes of a naïve mouse stained for CD3, CD4, CD44 and FoxP3 were analyzed by flow cytometry. (B) Colonization level of $Rag^{-/-}$ mice with and without transfer of $CD4^+/CD44^-$ cells is depicted. Horizontal lines represent median. (C) Stomach collagenase/DNase digests from infected C57Bl/6 wt and $Rag^{-/-}$ mice that received $CD4^+/CD44^-$ cells stained for CD45, CD3, CD4 and FoxP3 were analyzed by flow cytometry.

3.3 Effects of *H. pylori* gGT glutaminase activity during infection

H. pylori gGT exerts strong glutaminase activity; yet, it is not known whether this changes the gastric microenvironment and the overall glutamine concentration in the gastric mucosa during infection. To check whether glutamine was depleted from the gastric mucosa and associated immune cells, excessive glutamine was administered to counteract effects induced by gGT-dependent glutamine deprivation.

3.3.1 Glutamine level and transcriptional regulation during *H. pylori* infection

Preliminary data from stomach homogenates of mice infected with *H. pylori* wt or ΔgGT for one month suggested that glutamine and glutamate concentration were indeed inversely related in presence but not absence of gGT-activity (Figure 54A). However, the changes were only minor. Epithelial cell disruption due to tissue homogenization might mask local effects at the site of infection. Nevertheless, this suggested that glutaminase activity of *H. pylori* gGT contributes to a change in the microenvironment of the bacterium which might also affect the host cells.

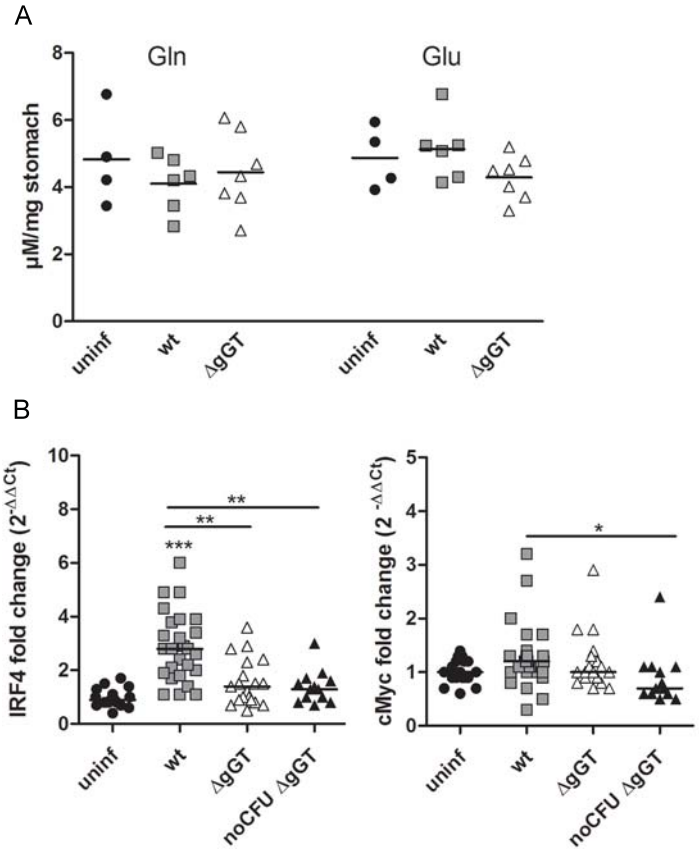

Figure 54: Glutamine level and expression of glutamine-dependent transcription factors in *H. pylori*-infected stomachs. (A) Glutamine and glutamate levels were determined by LC-MS homogenates of stomachs infected for one month with *H. pylori* wt, ΔgGT or uninfected controls. Data from one experiment are shown. (B) Expression of IRF4 and cMyc in murine stomach were analyzed by RT-PCR. Total RNA was extracted from stomachs of *H. pylori* wt- and ΔgGT- infected mice one month post infection. GAPDH served as house-keeping gene and uninfected controls were used to establish baseline. Data, expressed as fold change were calculated by ΔΔCt method. Data were summarized from 5 independent experiments. Each symbol represents one mouse. Horizontal bars show median. *** $p < 0.001$, ** $p < 0.01$, * $p < 0.05$ (Kruskal-Wallis)

Expression of transcription factors identified to be also sensitive to *H. pylori* gGT-induced glutamine deprivation in lymphocytes, IRF4 and cMyc, was investigated. IRF4 expression was found to be 2.8-fold induced upon *H. pylori* wt but not ΔgGT infection (Figure 54B). However, expression of these transcriptions factors in the stomach mucosa could not be directly linked to glutaminase activity of gGT during infection. The expression pattern of IRF4 was very similar to that of effector cytokines, in particular to IFNγ. This suggests that IRF4 is mainly expressed by infiltrating lymphocytes. $CD8^+$ T-cells which were more prominent in *H. pylori* wt-infected stomachs might be the main source. Expression of cMyc was only slightly induced in infected mice. One mouse in the non-colonizing ΔgGT group also displayed high IRF4 and cMyc expression.

This particular mouse had also highest gastritis score as well as strongest infiltration of CD3 and CD4/CD3 cells in histological analysis and FACS, respectively, as well as strongest expression of MIP-2, IL-1β, IL-23, IFNγ, TNFα, FoxP3, IL-10 in this group. In all of these parameters this exemplary mouse was more similar to *H. pylori* wt or ΔgGT mice that were colonized which indicated that the infection had been cleared in this mouse.

3.3.2 Supplementation of glutamate and glutamine during *H. pylori* infection

The next step to overcome gGT-induced effects during infection was to manipulate the extracellular glutamine and glutamate concentration in the stomach during *H. pylori* infection. Glutamate provided by glutaminase activity of gGT was reported to support the metabolism of the bacterium [175]. Thus, glutamate, derived from glutamine through gGT activity, might be needed as carbon source and for nitrogen metabolism facilitating survival of *H. pylori in vivo*. Instead of complementing the enzyme deaminating glutamine to produce glutamate and ammonia, supplementation of glutamate may be sufficient to support colonization of *H. pylori* ΔgGT. Addition of glutamate may circumvent the need of gGT activity. Conversely, supplementation of glutamine is known to support the epithelial cell integrity and immune cell function as well as replenishing intracellular glutathione [226, 241]. Therefore, provision of excessive glutamine may support the immune cells during infection with *H. pylori* wt and revert gGT-induced effects.

3.3.2.1 Glutamate supplementation in drinking water during initial colonization and persistent infection

10 % Glutamate was given orally via drinking water prior (pre) to inoculation of *H. pylori* wt or ΔgGT for a 4 day period and from inoculation until 3 days after (post) infection. Surprisingly, instead of supporting colonization of *H. pylori* ΔgGT, glutamate administration did almost completely clear *H. pylori* wt as well as ΔgGT infection (Figure 55A). To evaluate during which phase glutamate affects bacterial load, glutamate was administered either for 4 days before or for 3 days after inoculation of *H. pylori* wt. Glutamate administration affected colonization only when it was administered after inoculation. This suggested a direct effect of glutamate on the bacteria. Therefore, *H. pylori* wt and ΔgGT were incubated with increasing amounts of glutamate in brucella broth/ 10 % FCS for 5 h at 37 °C. Glutamate was tolerated well, as no decrease in number of viable bacteria was observed with up to 5 % glutamate (Figure 55B). At 10 % glutamate, a similar reduction in bacterial number was observed for *H. pylori* wt and ΔgGT. Therefore, a lower glutamate concentration (2.5 %) was given post inoculation and 10 % glutamate prior to inoculation. Under these conditions, *H. pylori* wt was able to colonize with reduced bacterial load (Figure 55A). However, in absence of gGT activity, bacteria were still not able to colonize at all. These results demonstrate that extracellular glutamate was not able to support *H. pylori* ΔgGT, but even prevents *H. pylori* wt from colonizing. Yet, these were only short term experiments monitoring the effect of glutamate during the initial phase of colonization. To analyze whether glutamate is able to inhibit and even clear a chronic infection, glutamate was administered either 3 days after inoculation or 3 days prior to analysis, which was performed after one month. Indeed, all mice even those persistently colonized were cured from infection (Figure 55C).

3.3.2.2 Dietary glutamate and glutamine supplementation during H. pylori infection.

Since compounds provided in food have a prolonged gastric retention time compared to liquid solutions, diets enriched with 10 % glutamate, 20 % glutamine or isonitrous control diet were fed to mice infected with *H. pylori* wt or ΔgGT.

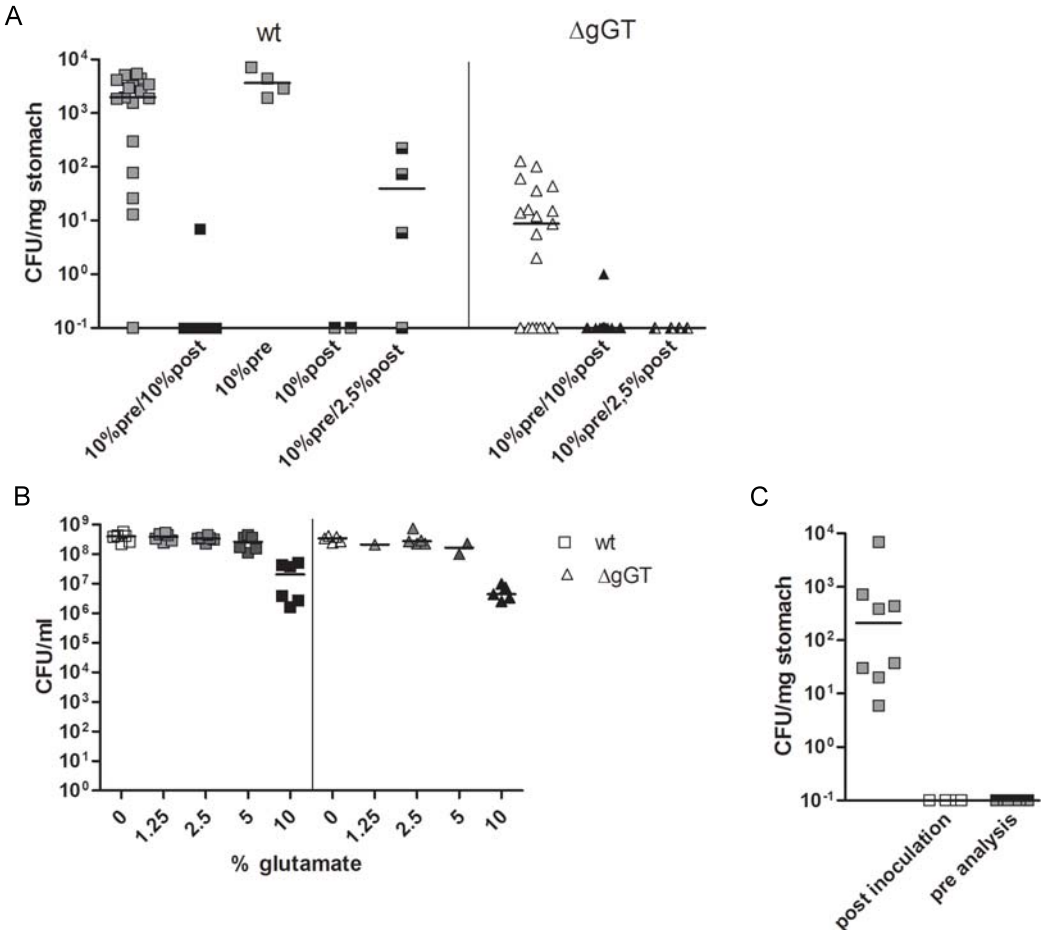

Figure 55: Effect of glutamate administration via drinking water on *H. pylori* colonization. (A+C) C57Bl/6 mice were inoculated with 10^9 CFU *H. pylori* wt or ΔgGT and subjected to different experimental schemes of glutamate-treatment. For glutamate administration, 10 or 2.5 % monosodium glutamate (MSG, neutral pH) was dissolved in deionized water and filter-sterilized. (A) Mice were given glutamate for either 4 days prior to infection (pre) and/or for 3 days after infection (post). Colonization levels were assessed 3 days after inoculation. (B) *H. pylori* PMSS1 was incubated in Brucella broth containing 10 % FCS with various concentrations of glutamate for 6 h at 37 °C. Thereafter, concentration of live bacteria was assessed by plating of serial dilutions. (C) Mice were given 10 % glutamate in drinking water for either 3 days after inoculation (post) or 4 days prior to analysis of colonization levels which were assessed one month after inoculation of *H. pylori* wt.

Colonization level of *H. pylori* wt-infected mice was not altered when fed a glutamine-enriched diet compared to mice fed the control diet (Figure 56A). Glutamate enrichment, however, strongly reduced bacterial load. This confirmed results from supplementation of glutamate with drinking water. Colonization of gGT-deficient *H. pylori* was completely inhibited by either of the two enriched diets, even though 60 % of mice receiving the control food were colonized. Histological scores were rather low and not all colonized mice displayed gastritis (Figure 56B). Therefore, analysis of infiltrates by flow cytometry was performed. Acute gastritis is characterized by infiltration of polymorphonuclear cells, such as neutrophils. For *H. pylori* wt, bacterial colonization was reflected by infiltration of $Ly6G^+/CD11b^+$ neutrophils. Thus, strong infiltration of neutrophils into gastric mucosa was observed with the glutamine-enriched and the control diet (Figure 56C). In addition to neutrophils, T-cells were infiltrating into the gastric mucosa. The proportion of $CD3^+$ cells was increased in mice inoculated with *H. pylori* wt irrespective of a specific diet (Figure 56D). Like in previous experiments, the majority of these infiltrating lymphocytes were $CD8\alpha^+$ and not $CD4^+$ (Figure 56D). Glutamine-enriched diet resulted in a lower level of $CD3^+$ and in particular $CD8\alpha^+$ cells compared to control diet in mice colonized with *H. pylori* wt indicating that gGT induced effects are counteracted. The stomach of some mice inoculated with *H. pylori* wt receiving glutamate-enriched diet was infiltrated with $CD8\alpha^+$ T-cells, which suggests that they may have been infected, since chronicity (T-cell infiltration) is longer present than activity (PMN infiltration) after the infection has been cleared. In contrast to *H. pylori* wt-infected mice, mice inoculated with gGT-deficient *H. pylori* did not display infiltration of T-cells irrespective of diet or colonization status.

Expression of chemokines attracting immune cells to the site of infection (LIX, MIP-2, KC, MCP-1, RANTES) and cytokines (TNFα, IFNγ) was induced upon *H. pylori* wt infection, while supplementation of glutamine attenuated expression of these proinflammatory factors (Figure 57A/B). Different diets and infections did not alter FoxP3 and IL-10 expression (Figure 57C). Thus, glutamine supplementation during *H. pylori* wt infection phenocopied *H. pylori* ΔgGT colonization, since stomach of mice were displaying much less proinflammatory cytokines and hardly any infiltration of $CD8^+$ cells.

When a persistent infection had already been established before feeding with glutamine- or glutamine-enriched diet started, *H. pylori* wt colonization density was not affected (Figure 58). Under these conditions *H. pylori* wt also tolerated glutamate from food. Colonization of *H. pylori* ΔgGT was reduced with glutamine-enriched diet and absent when a glutamate-enriched diet was administered. *H. pylori* ΔgGT did not profit from external glutamate but was even stronger affected by excessive glutamate than the wild-type bacteria.

Collectively, data on oral administration of the proposed *H. pylori* gGT substrate, glutamine, and its product, glutamate, during infection showed that release of glutamate does not seem to be limiting for colonization of *H. pylori* ΔgGT, whereas glutamine seems to be deprived from the stomach mucosa by *H. pylori* wt. Remarkably, glutamine supplementation reverted gGT-induced effects and attenuated gastric inflammation.

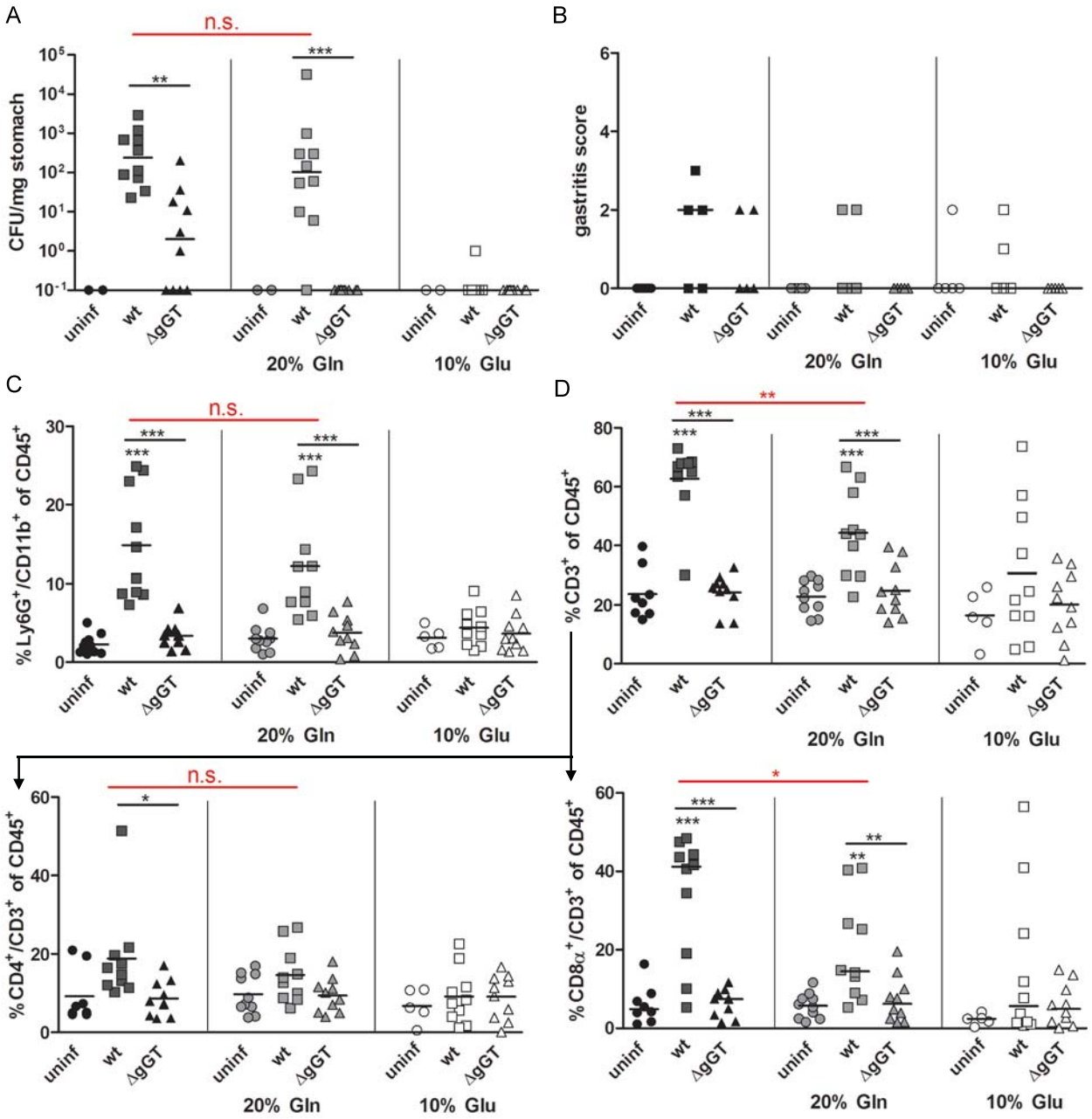

Figure 56: Effects of dietary glutamine and glutamate supplementation on colonization and gastric inflammation during *H. pylori* wt and ΔgGT infection of mice. C57Bl/6 mice were infected with 10^9 *H. pylori* PMSS1 wt or ΔgGT for one month and received a glutamine- (20 %) or a glutamate- (10 %) enriched diet for the infection period. (A) Gastric colonization was assessed by colony count. Horizontal lines represent median (Mann-Whitney). (B) Gastritis score determined from HE-stained slides of paraffin embedded stomach tissue. Horizontal lines represent median (Kruskal-Wallis). (C/D) Flow-cytometry of cells from digested stomach tissue. Horizontal lines represent mean (ANOVA). Data for CFU and FACS analysis is derived from two experiments and gastritis score from one experiment with 5 mice per group. Statistical analyzes indicated in red show differences between *H. pylori* wt-infected mice receiving a control versus a glutamine-enriched diet (Student's t-test). *** $p < 0.001$, ** $p < 0.01$, * $p < 0.05$

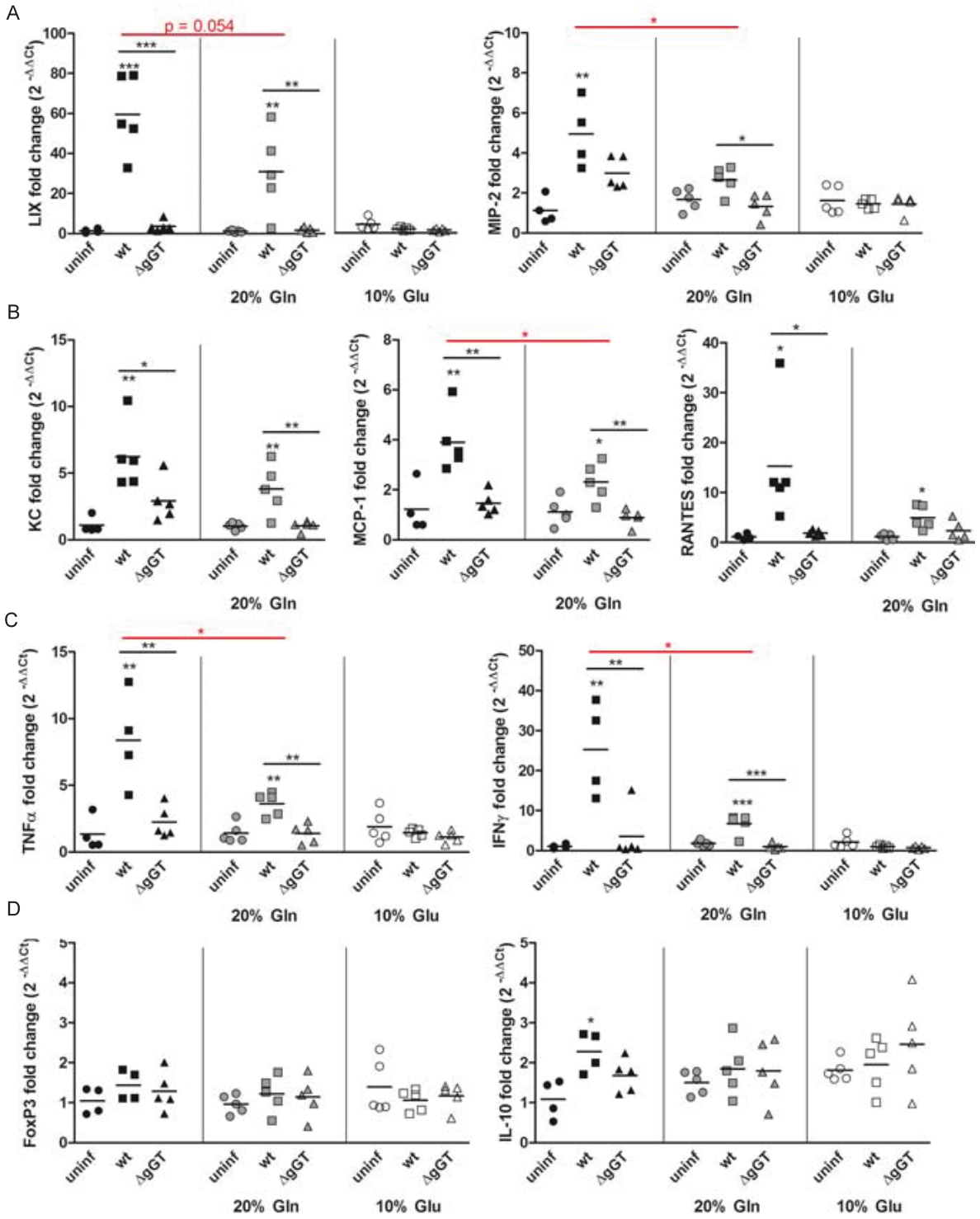

Figure 57: Transcriptional changes of cytokines and chemokines in the gastric mucosa of *H. pylori* wt- and ΔgGT-infected mice fed a glutamine- or glutamate-enriched diet. Total RNA was extracted from stomachs of *H. pylori* wt- and ΔgGT-infected mice one month post infection that received glutamine- (20 %) or glutamate- (10 %) enriched diets. RT-PCR analysis was performed for (A) LIX and MIP-2, (B) KC, MCP-1 and RANTES, (C) TNFα and IFNΓ, (D) FoxP3 and IL-10. GAPDH served as house-keeping gene and uninfected controls were used to establish baseline. Data, expressed as fold change were calculated by ΔΔCt method. Horizontal lines represent mean (ANOVA). Data from one experiment with 5 mice per group. Statistical analyzes indicated in red show differences between *H. pylori* wt-infected mice receiving a control versus a glutamine-enriched diet (Student's t-test). *** $p < 0.001$, ** $p < 0.01$, * $p < 0.05$.

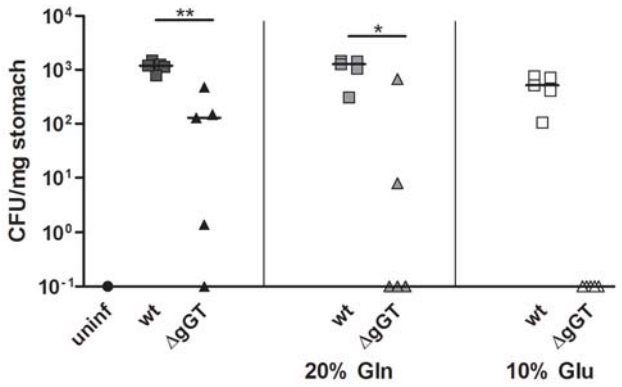

Figure 58: Administration of a glutamine- and glutamate-enriched diet to mice persistently infected with *H. pylori* wt and ΔgGT. C57Bl/6 mice were infected with 10^9 *H. pylori* PMSS1 wt or ΔgGT for one month when a glutamine- (20 %) or a glutamate- (10 %) enriched diet was administered for another month. Gastric colonization was assessed by colony count. Horizontal lines represent median. ** $p < 0.01$, * $p < 0.05$ (Mann-Whitney). Data from one experiment with 5 mice per group are shown.

Chapter 4

Discussion

Accumulating evidence suggests that *H. pylori* gGT is not only an essential virulence factor required by the bacterium for colonization of the gastric mucosa but that it also contributes to the induction of inflammation and shapes the host's immune response. An earlier study performed by our group demonstrated a direct inhibitory effect of *H. pylori* gGT on T-cells which suggested a role in immune evasion [163]. However, the molecular mechanisms mediating this effect and the contribution to persistent colonization were still unknown. Therefore, the main goal of this thesis was to establish in which way *H. pylori* gGT interferes with T-cell responses and how this may provide an advantage to the bacterium in the stomach mucosa.

4.1 Effect of *H. pylori* gGT-induced glutamine deprivation on T-cells

The results clearly demonstrate that the enzymatic activity of *H. pylori* gGT can lead to impaired T-cell function by depriving activated lymphocytes from glutamine. The microenvironment that might be created in the gastric mucosa by this enzyme was simulated through pretreatment of cell culture medium with *H. pylori* rgGT or whole bacterium producing gGT. Proliferation of activated T-lymphocytes was inhibited when they were incubated in preconditioned medium treated with gGT due to glutamine deprivation. Likewise, glutaminase activity of *E. coli* gGT inhibits lymphocyte proliferation and a consecutive immunosuppressive role has been been suggested [242].

4.1.1 *H. pylori* gGT acts on T-cells independently of glutathione degradation products

Besides glutamine, glutathione is another proven *H. pylori* gGT substrate, which is converted to glutamate and cysteinylglycine [175]. It has been proposed that not only glutamine deprivation but also oxidative products resulting from gGT-dependent glutathione degradation can harm host cells; intestinal epithelial cells in particular [191]. Yet, another study reported that supplementation of glutathione to AGS cells reduced IL-8 production indicating that it rather attenuates oxidative stress [188]. In line with this, viability and activation was not affected when T-cells were exposed to increasing amounts of glutathione in presence of *H. pylori* gGT activity. Conversely, glutathione supported proliferation when glutamine levels were inadequate due to active gGT. This might be due to the fact that reduced glutathione could provide these cells with cysteine, which promotes T-cell proliferation [243].

Nevertheless, glutamine and glutathione levels are tightly linked, since glutamine is an important precursor for glutathione, particularly in cells that cannot import glutamate as a substi-

tute [206, 219]. Thus, glutamine deprivation may subsequently result in decreased intracellular glutathione levels in lymphocytes [244]. Interestingly, decreased levels of glutathione have been measured in gastric mucosa of *H. pylori*-infected individuals [245]. Upon eradication of infection glutathione levels normalize [246].

4.1.2 T-cell functionality is affected by gGT-dependent changes in glutamine level

Inadequate glutamine supply has been shown to inhibit T-lymphocyte proliferation [200, 207, 219], impair expression of activation markers (CD25, CD45RO, CD71), and compromise secretion of inflammatory cytokines (IL-2 and IFNγ) [219, 247]. Results presented in this thesis demonstrate that IL-2, CD25, and effector cytokine expression correlated directly with the presence of active *H. pylori* gGT and glutamine availability. In this way, besides being advantageous to the bacteria, *H. pylori* gGT may suppress the T-helper lymphocyte response by turning over glutamine, which is conditionally essential for lymphocytes to become fully activated. The enzymatic activity of *H. pylori* gGT may by be sufficient to hinder the effector immune response towards the bacterium and contribute to its persistence.

4.1.3 *H. pylori* gGT manipulates expression of transcription factors required for metabolic reprogramming of activated T-cells

To get a better understanding on how *H. pylori* may interfere with T-cell functionality, the effect of *H. pylori* gGT on lymphocyte metabolism was analyzed. TCR-dependent stimulation imposes a great metabolic demand on T-lymphocytes which requires great enhancement of biosynthetic pathways as well as sufficient energy supply. Hypoxia-inducible factor 1α (HIF1α) and cMyc have been demonstrated to be important transcription factors in metabolic regulation of T-cells [197, 248]. While HIF1α mainly induces glycolysis, cMyc is responsible for expression of enzymes required for glutaminolysis and increased glutamine uptake in activated T-cells [197].

Upon T-cell stimulation, cMyc induction was severely compromised in presence of *H. pylori* gGT. It was found that cMyc expression in lymphocytes is highly sensitive to extracellular glutamine levels, as *H. pylori* gGT treatment impaired cMyc expression already two hours post TCR-stimulation. However, upstream events regulating cMyc expression remain unclear, since pathways that have been suggested to determine cMyc level in T-lymphocytes such as mTOR or MAPK were not changed at these early time points. Nevertheless, it was observed that *H. pylori* gGT reduced phosphorylation of the mTOR targets p70S6K and 4E-BP1 in a glutamine-dependent manner at later time points. Inhibition of mTOR has been reported to drive T-cells into a regulatory phenotype even in presence of co-stimulation [211, 249, 250, 251]. Thus it could can be speculated that inhibition of mTOR signaling by *H. pylori* gGT in T-cells may promote T-cell tolerance. Additionally, regulatory T-lymphocytes are much less dependent on glutamine and glucose supply compared to effector T-cells since they are able to perform β-oxidation of fatty acids [252].

To identify further pathways modified by *H. pylori* gGT in activated lymphocytes, expression patterns of proteins from TCR-dependently stimulated cells treated with active or inactive gGT were compared. Using a proteome analysis, the transcription factor IRF4 was found to be reduced in presence of active gGT. IRF4 expression was recently reported to require high-affinity TCR-stimulation, to be essential for differentiation and expansion of T-cells, and to sustain $CD8^+$ T-cells *in vivo* [209, 253]. The data presented here show that IRF4 expression in activated lymphocytes strongly depends on the extracellular glutamine level. Thus, it can be speculated that local glutamine deprivation by *H. pylori* gGT may suppress expression of IRF4 in T-lymphocytes during infection. Thus, IRF4 expression in T-lymphocytes infiltrating the gastric mucosa from *H. pylori*-

dependent and -independent gastritis was analyzed. Remarkably, IRF4 expression of T-cells was reduced in the gastric mucosa of *H. pylori*-infected subjects compared to T-cells in the control group. This indicates that *H. pylori* may also interfere with metabolic adaptation of T-cells during infection, even though it could not be demonstrated that this was due to gGT activity by this approach. By reducing glutamine levels in the stomach, *H. pylori* might induce changes in the expression levels of transcription factors important for T-cell metabolic reprogramming, such as cMyc or IRF4, and signaling cascades like mTOR. This would not only affect T-cell function but might also shape the type of immune response elicited.

In conclusion, the results presented here indicate that *H. pylori* gGT may induce changes in the extracellular milieu that can translate into glutamine limiting conditions for T-cells at the site of infection. *H. pylori* gGT-induced glutamine deprivation might be one of the molecular mechanisms important for bacterial immune evasion and persistence in the gastric mucosa. This hypothesis was further explored in a *H. pylori* infection model.

4.2 Role of *H. pylori* gGT during establishment of infection and effects on gastric immune response

Presence of gGT is a major advantage for *H. pylori* during infection [62, 98, 187]. This is stressed by the fact that it is present in all clinical isolates characterized so far. Yet, the main functional role of *H. pylori* gGT during infection remained to be established.

On the one hand, the bacteria itself may profit from gGT activity, which provides glutamate as nitrogen/carbon source and substrate for nitrogen assimilation as well as neutralizing the acidic environment through release of ammonia in the periplasm. On the other hand, gGT activity may induce changes in the stomach environment directly and indirectly affecting host cells. As T-cells are particularly sensitive to changes in the extracellular glutamine concentration and were shown to be affected by gGT activity *in vitro*, these cells were in the focus of the analysis. If results from the *in vitro* study were to be directly translated into the *in vivo* situation, one might expect that *H. pylori* lacking gGT activity might be able to colonize, but would be cleared over time due to a limited capability to restrict the adaptive immune response.

To study the physiological role of *H. pylori* gGT during infection, a gGT-deficient *H. pylori* strain was used. Upon inoculation of mice with the gGT-deficient *H. pylori* strain, mice could be grouped into two categories with respect to whether the bacterium was able to establish colonization or not. This outcome was advantageous for studying the role of gGT during infection, since mice where the gGT-deficient *H. pylori* was able to colonize could be compared to mice infected with the wild-type strain with regard to induction of inflammation. Additionally, multiple manipulations were employed such as complementation of recombinant gGT, co-infection of gGT-proficient and -deficient *H. pylori*, infection in absence of adaptive immune cells, or external provision of excessive amounts of the proposed gGT substrate (glutamine) or product (glutamate); thereby further establishing the mode of action of this enzyme during infection.

4.2.1 *H. pylori* gGT activity promotes ability to establish infection

H. pylori ΔgGT failed to establish an infection in about 50 % of the mice. These mice were indistinguishable from uninfected mice regarding signs of acute and chronic gastric inflammation. This indicates that most of the inoculated bacteria passage through the gastrointestinal tract without inducing an immune response. *H. pylori* ΔgGT seemed to face the same initial hurdle in $Rag^{-/-}$ mice resulting in a low colonization rate, which confirms that the failure to establish an infection is independent of the immune response.

The notion that *H. pylori* gGT is important for initial colonization is in accordance with previous studies that observed low infection rate with *H. pylori* lacking gGT from the very beginning [62, 187]. Even though gGT activity is not essential *in vitro*, it seems to be conditionally essential or at least strongly advantageous for *H. pylori* during initial establishment of infection. Yet, it is not clear how the absence of gGT activity is limiting the capacity of *H. pylori* to establish an infection.

In vitro studies of the bacterium suggest that *H. pylori* gGT is contributes to carbon and nitrogen metabolism as well as acid resistance. Shibayama *et al.* (2007) found that *H. pylori* gGT makes extracellular glutamine available for the bacterium, since it cannot be taken up directly [189]. *H. pylori* gGT converts glutamine to glutamate, which is subsequently transported into the bacterium where it is introduced into catabolic and biosynthetic pathways via glutamate deyhdrogenase or intracellular conversion to glutamine. This has been confirmed by Leduc *et al.* (2010), who demonstrated that glutamine can only be taken up when it is deaminated by gGT [165]. Using deletion mutants and radioactively labeled amino acids, they found that *gltS* encodes for the only glutamate transporter in *H. pylori* that could import the deaminated amino acid. Glutamate might required as a carbon and nitrogen source *in vivo* as *gltS*-deficient *H. pylori* failed to colonize Mongolian gerbils [254]. Furthermore, ammonium produced by deamination of glutamine contributes to maintain an acceptable periplasmic pH [179]. Therefore, absence of gGT might make *H. pylori* more susceptible to acid stress and limit bacterial expansion due to a defective metabolism.

Concerning the observations that *H. pylori* gGT seems to be dispensable *in vitro* and that some bacteria seem to adapt in a way that they can colonize even in absence of gGT activity, this indicates that gGT activity is not absolutely required for the energy, amino acid, and nitrogen metabolism but that its necessity depends also on environmental conditions. The observation that *H. pylori* ΔgGT has to overcome an initial hurdle before some bacteria are able to infect suggests that some kind of adaptation takes place, or that only those bacteria that reach a particular niche can survive. The hypothesis that the bacterium can adapt to compensate for lack of gGT activity is supported by the fact that reinfection of mice with isolates from mice that were colonized with gGT-deficient *H. pylori* resulted in colonization of all mice inoculated.

The finding of this thesis that reconstitution of gGT-deficient bacteria with an extracellular supply of rgGT during inoculation supports colonization indicates that the gGT acts on the external environment, which may allow the bacterium to penetrate the mucus layer, for example. There, it may find a more habitable environment where it can survive even in absence of gGT. Assuming that *H. pylori* gGT makes a major contribution to acid resistance due to production of ammonia in the periplasm, gGT-deficient *H. pylori* might be more sensitive to acidic pH in the lumen, but able to reside in the mucus close to epithelial cell layer where the pH is higher. This initial hurdle might be even higher in humans (lower pH compared to mice), as no clinical isolates lacking gGT activity have been found so far.

The fact that complementation of gGT by co-infection failed and that *H. pylori* wt outcompeted gGT-deficient bacteria indicates that the periplasmic gGT provides a strong advantage to the individual bacterium, which is stronger than the effect on the environment. This suggests that *H. pylori* ΔgGT has a more general defect. Additionally, bacteria may compete for other resources, such as urea or glutamate.

4.2.2 Supplementation of glutamate cannot support *H. pylori* ΔgGT

Even though glutamate can be produced from α-ketoglutarate through assimilation of ammonium by glutamate dehydrogenase, *H. pylori* depends on glutamate from external sources. Glutamate imported through the glutamate permease was found in several pathways of carbon and nitrogen metabolism [175]. Glutamate can act as a nitrogen donor via glutamate dehydrogenase or alanine-aminotransferase or can be used to assimilate ammonia via glutamine synthetase. Ammonia from

glutamate is used to convert ^{13}C-pyruvate to alanine to a similar extent as addition of urea [177]. If the main function of *H. pylori* gGT glutaminase activity were to provide glutamate as carbon and nitrogen source to *H. pylori*, additional glutamate would be expected to support the gGT-deficient *H. pylori* strain *in vivo*. However, instead of supporting colonization of *H. pylori* ΔgGT, oral supplementation of glutamate interfered with colonization of *H. pylori* wt as well as *H. pylori* ΔgGT. Glutamate concentration that still allowed colonization of *H. pylori* wt did not support *H. pylori* ΔgGT. On the contrary, *H. pylori* ΔgGT was even more sensitive to administration of glutamate. Glutamate exerted harmful effects on the bacteria when it was administered during and shortly after bacterial inoculation. Administration of glutamate on the established *H. pylori* wt infection was only effective when given by drinking water while persistent infection with *H. pylori* ΔgGT was also cleared by glutamate-enriched food.

Supplemented glutamate may make the gastric mucosa more resistant to colonization by increasing epithelial barrier function. Epithelial cells of the gastrointestinal tract rapidly metabolize glutamate. Chronic supplementation with 2.5 % glutamate promoted glutamine synthesis yet had little effect on physiological stomach functions in rats [255]. Luminal perfusion with glutamate protected duodenal mucosa from acid induced injury [256]. Furthermore, glutamate has been shown to increase mucus secretion [256], which may complicate colonization. But as glutamate given prior to infection had no effect, a direct adverse effect on the bacteria seems also likely. However, glutamate was tolerated well by *H. pylori* wt and ΔgGT when incubated in the inoculation medium (BB/10 % FCS) containing up to 10 % glutamate at neutral pH. At acidic pH, citrate is toxic in presence of urea due to depletion of α-ketoglutarate and intracellular accumulation of ammonia [257]. In a similar manner, increased glutamate may interfere with detoxification of intracellular ammonia accomplished by conversion of α-ketoglutarate and urease-dependently produced ammonia to glutamate via glutamate dehydrogenase. The alternative pathway for ammonia assimilation through glutaminase activity may require too much energy as it is ATP-dependent. Thus, excessive glutamate might have only toxic effects under acidic conditions encountered in the stomach, when intracellular ammonia concentration rises due to urease activity, but not at neutral pH.

4.2.3 *H. pylori* gGT contributes to a higher colonization density

Assuming that *H. pylori* gGT interferes with effector T-cell responses, one might expect that lymphocyte-deficient Rag$^{-/-}$ mice are colonized by gGT-deficient strain to a similar extent as mice infected with *H. pylori* wt. In those Rag$^{-/-}$ mice that were colonized with *H. pylori* ΔgGT a 100-fold higher bacterial load was detected, which indicated that *H. pylori* profits from absence of inflammation and is able to expand well irrespective of a lack of gGT activity. In accordance with previous studies, absence of inflammatory B- and T-cells allowed a higher level of colonization for *H. pylori* wt without any signs of gastritis or T-cell infiltration [118]. Nevertheless, the bacterial load was about 10-fold lower in Rag$^{-/-}$ mice colonized with *H. pylori* ΔgGT compared to mice colonized with *H. pylori* wt. As gastritis is absent in these mice, this difference in colonization density seems to be due to a metabolic deficiency of the *H. pylori* ΔgGT. Thus, the enzyme has an advantageous effect on the wild-type strain, equipping it with a higher colonization capacity irrespective of gastric inflammation.

Likewise, a substantial number of C57Bl/6 wild-type mice got infected with *H. pylori* deficient in gGT. Once it had successfully colonized, gGT-deficient *H. pylori* was able to establish a stable infection for up to six months. There was an overall trend towards lower colonization in particular at day three and three months, but similar levels at one and six months. These results are in line with the observation from McGovern *et al.* (2001) who found reduced colonization of gGT-deficient *H. pylori* KE26695 at day six but similar levels after 20 days compared to *H. pylori* wt control group in piglets [187]. Yet, Oertli *et al.* (2013) observed that the very same gGT-deficient *H. pylori*

stain as used in this thesis colonized all mice at one month but only a small fraction at two months [98]. They suggest that their observation is due to clearance of gGT-deficient *H. pylori* by the adaptive immune response. In contrast, no signs of inflammation were observed in mice that were inoculated with *H. pylori* ΔgGT but not colonized in this thesis.

Taken together, these data suggest that presence of gGT equips the bacterium with the capacity to establish a higher bacterial burden in absence of gastritis. In mice with a functional adaptive immune response, colonization density of wild-type bacteria might be controlled by an increased gastric inflammation, which results in a similar bacterial burden compared to gGT-deficient *H. pylori*. Conversely, *H. pylori* ΔgGT seem to have an intrinsic limitation to establish a higher bacterial load despite not eliciting such a strong adaptive immune response.

4.2.4 *H. pylori* with gGT activity induces stronger gastric inflammation

Mice colonized with *H. pylori* ΔgGT provided an exceptional tool to check for the influence of gGT on the adaptive immune response. As mice colonized with *H. pylori* wt or ΔgGT displayed a similar bacterial load after one month, this time point was chosen to evaluate gGT-dependent effects on the level and quality of immune parameters. Under these conditions, it is expected that other virulence factors shaping the immune response are present at similar levels. Histology, flow cytometry, and transcriptional analysis were used to the assess the inflammatory response in the stomach mucosa.

4.2.4.1 Less proinflammatory environment in the gastric mucosa in absence of gGT

H. pylori infection induces secretion of the proinflammatory chemokines, such as IL-8 and ENA-78, from gastric epithelial cells [239]. LIX, KC, and MIP-2 are the predominant (ENA-78-, IL-8-like) neutrophil activating factors in mice. The data presented suggest that *H. pylori* gGT is strongly involved in induction of LIX/CXCL5 expression and to a lesser extent in induction of KC and MIP-2. In contrast to mice colonized in *H. pylori* wt, LIX was hardly expressed in mice colonized with gGT-deficient *H. pylori*. The human CXCL5 homologue, ENA-78, is among the genes that are most strongly induced upon *H. pylori* infection in the gastric mucosa of humans [239]. ENA-78 is mainly produced by epithelial cells and to a lesser extent by monocytes as shown by immunofluorescence of antral biopsies from *H. pylori*-infected individuals [258]. Induction of ENA-78/CXCL5 expression was also observed in *H. pylori*-infected AGS cells [259]. During infection ENA-78 expression did not correlate with CagA status [258], in contrast to IL-8. Interestingly, induction of IL-8 in gastric epithelial cells has been suggested to be partially dependent on gGT-dependent glutaminase activity, as *H. pylori* ΔgGT or glutamine supplementation to *H. pylori* wt reduced IL-8 release [188]. Toxic effects due to production of ammonia were excluded as addition of glutamine resulted in higher levels of ammonia but still reduced IL-8 release. In this light, it would be interesting whether KC and MIP-2 expression in gastric epithelial cells would also respond to addition of glutamine and whether CXCL5 is responsive to glutamine in humans (ENA-78) and mice (LIX). This would support the hypothesis that *H. pylori* damages the epithelial cell layer due to glutamine deprivation.

Also, induction of other proinflammatory cytokines that are mainly produced by innate immune cells and create a proinflammatory environment recruiting lymphocytes to the site of infection, such as IL-1β, IL-12, and CCL5/RANTES, were associated with presence of gGT. Expression of IL-1β, IL-12, and RANTES were strongly induced upon *H. pylori* wt but not ΔgGT infection.

Even though expression of chemokines and cytokines related to epithelial cell damage and innate immune response were strongly decreased in absence of gGT, infiltration of polymorphonuclear cells were not affected by gGT activity as their level was increased in presence of colonization with either

H. pylori wt or ΔgGT. Still, other immune cells did infiltrate to a greater extent into the stomach mucosa infected with *H. pylori* wt compared to ΔgGT

4.2.4.2 Shift in influx of T-helper and cytotoxic T-cells in absence of gGT

Upon infection with *H. pylori* a strong influx of immune cells, in particular T-cells, into the gastric mucosa was observed. A significantly induced influx of $CD3^+$ cells was seen in mice colonized with *H. pylori* ΔgGT albeit to a lesser extent than in mice colonized with *H. pylori* wt. Besides an overall lower level of T-cell infiltration, a shift in the CD4/CD8 ratio was the main difference compared to control group when gGT was absent. *H. pylori* wt infection induced a stronger influx of cytotoxic (CD8) T-cells than influx of T-helper (CD4) cells. Infiltration of $CD8^+$ cells was much less prominent in mice colonized with *H. pylori* ΔgGT, yet, the proportion of CD4 cells with respect to all infiltrating immune cells ($CD45^+$) was similar.

H. pylori wt and ΔgGT, that had established an infection, induced comparable **T-helper cell** responses regarding proportion of CD4 cells and the recruitment of regulatory FoxP3-expressing CD4 cells. As differences in CD4 cell infiltration were not so profound, this indicated that other sources than CD4 cells contribute to strong increase of IFNγ and TNFα expression observed during *H. pylori* wt infection in contrast to colonization with *H. pylori* ΔgGT.

Expression of the TH17 cytokine IL-17A was induced in mice infected with *H. pylori* wt compared to uninfected mice. However, expression levels for IL-17A were very low and are thus not considered as major driver of the inflammatory response. C57Bl/6 mice are known for a lower production of IL-17 than Balb/c mice in general, and in the context of *Helicobacter* infection in particular [191]. Furthermore, CagA-expressing *H. pylori* PMSS1 strain selectively represses IL-17 in C57Bl/6 mice in contrast to the SS1 strain [260]. Therefore, Th17 cells may not play a major role in control of bacterial infection in this setting.

The effect of *H. pylori* gGT on regulatory T-cell response in an *in vivo* setting was of particular interest as it had been reported that *H. pylori* gGT drives a tolerogenic program in dendritic cells [98]. These tolerogenic dendritic cells induce a regulatory T-cell response *ex vivo* that is lower in absence of gGT activity [98]. However, results presented here show that the regulatory T-cell response in the gastric mucosa that was characterized by infiltration of $FoxP3^+$ CD4 cells and the expression of FoxP3, TGFβ, and IL-10 was induced by colonization with *H. pylori*, but was irrespective of gGT status. IL-10 expression was significantly increased with *H. pylori* wt and ΔgGT colonization, the same trend was observed for FoxP3 and TGFβ expression. This indicates that other bacterial factors play a more important role in inducing tolerance. This is supported by the fact that percentage of $FoxP3^+$ cells within the CD4 cell population increased with bacterial load. This may also explain differences to recently published data reporting a reduced proportion or $FoxP3^+$ cells of CD4 cells in mice colonized with *H. pylori* ΔgGT [98]. Yet, these mice were also colonized with *H. pylori* ΔgGT at a significantly lower level compared to those colonized with *H. pylori* wt, as seen here after three months. This makes it impossible to disentangle the effect of bacterial burden and gGT.

Collectively, the results presented here suggest that *H. pylori* ΔgGT induces a similar level of effector T-cells as well as Treg mediated tolerance compared to *H. pylori* wt.

Surprisingly, when CD4 cells were transferred into mice colonized with either *H. pylori* wt or ΔgGT, the infection with the gGT-deficient bacteria persisted while the wild-type bacteria were cleared. Infiltration of lymphocytes into the stomach mucosa was observed in all infected mice that effectively adopted the transferred cells. Yet, a higher proportion of effector T-cells and a lower proportion of Tregs was found in blood from mice colonized with gGT-proficient *H. pylori* compared to those colonized with gGT-deficient bacteria. This may suggest that gGT contributed to a stronger effector T-cell response. When $CD4^+$ cells that were enriched for effector

cells were transferred, a strong gastritis was induced effectively clearing all mice from *H. pylori* irrespective of the presence of gGT. This is in line with previous studies that demonstrated that during adoptive transfer of CD4 cells into *H. pylori*-infected immunodeficient mice proportion of effector and regulatory T-cells play an important role for the development of gastric inflammation and control of bacterial load [73, 118, 137]. The results obtained from infection of lymphocyte-deficient mice in this thesis indicate that gGT is involved in induction rather than repression of an effector T-cell response.

As mentioned before, infiltration of **cytotoxic T-cells (CD8α^+)** into gastric mucosa of *H. pylori*-infected mice was observed that was related to gGT activity.

Data on the CD4/CD8 cell ratio in the *H. pylori*-infected gastric mucosa are conflicting. The observation from this study, that CD8 T-cell infiltration is dominating over CD4 cell influx, is in accordance with data from Ruiz *et al.* (2012) who observed that accumulation of gastric $CD8^+$ lymphocytes in *H. pylori*-infected mice was more prominent than infiltration of $CD4^+$ cells [261]. In contrast, Algood *et al.* (2007) observed that the number of CD4 T-cells were strongly increasing in the gastric mucosa of *H. pylori*-infected mice, while number of CD8 lymphocytes remained low [237]. Yet, the significance of CD8 cell is stressed by the observation that CD8 cells dominate over CD4 lymphocytes in the stomachs of *H. pylori*- positive adults and children [131, 262].

Not much is known about the contribution of CD8 T-cells to gastric pathology and control of bacteria load. It has been shown that CD8 cells contribute to *H. pylori* associated gastritis, as mice lacking $CD4^+$ T-cells still develop severe gastritis dominated by CD8 T-cells [135]. This suggested that the regulatory T-cell response is also important for repressing CD8 cell responses. Another study showed that absence of either MHCII or MHCI, which resembles a defect in CD4 cell or CD8 cell response, respectively, result in an increase of bacterial load [134]. This indicates that CD8 and CD4 cells contribute to control of bacterial load during infection.

Remarkably, IFNγ is the major effector cytokine of cytotoxic T-cells. Therefore, the majority of IFNγ might be produced by CD8 cells rather than CD4 cells. This is supported by the fact that CD8 cells produce larger amounts of IFNγ than CD4 cells on a per cell basis. Also in humans it has been reported that the majority of IFNγ is produced by CD8 and not CD4 T-cells infiltrating the *H. pylori*-infected gastric mucosa [132, 133, 139].

One reason why T-helper cell responses had attracted so much attention, in contrast to cytotoxic T-cells, might be due to vaccination studies. In fact, the adjuvant cholera toxin may transiently deplete CD8 cells and select for *H. pylori* specific CD4 cells, which seem to be very effective in controlling bacterial load during challenge [263, 264]. IFNγ-deficient mice have been used to assess the role of IFNγ during *H. pylori* infection. The conclusions drawn from many of these studies have been based on the presumption that IFNγ is produced by CD4 cells. Thus, the contribution of CD4 cells to actively control of bacterial density might be overestimated during the natural infection.

Expression of IFNγ was much stronger induced during colonization with gGT-expressing strain compared to gGT-deficient *H. pylori*. This was accompanied by a greater influx of CD8 cells and similar levels of CD4 cells in *H. pylori* wt compared to ΔgGT-infected mice. Consequently, the increase of IFNγ expression reported here may rather reflect a cytotoxic CD8 T-cell response than a Th1 response. Therefore, IFNγ from non-CD4 T-cells seem to play an important role in the inflammatory response against *H. pylori* infection when gGT is present.

The immune response towards *H. pylori* is characterized by high levels of IFNγ, which is an important activator of macrophages and inducer of MHCII expression. Furthermore, it has been demonstrated that IFNγ induces MIP-2 expression in gastric epithelial cells [142]. During *H. pylori* infection, IFNγ has been shown to drive gastritis, as IFNγ-deficient mice do not develop gastric inflammation upon *Helicobacter* infection [73, 75, 76, 77, 115, 137, 141]. Additionally, presence of IFNγ has been related to lower bacterial load [75, 77, 141]. Correspondingly, results from this thesis indicate that IFNγ expression is inversely correlated to CFU. This suggests that either

H. pylori dose-dependently suppressed IFNγ expression or that increased IFNγ levels reduced bacterial burden. In mice colonized with *H. pylori* ΔgGT much less IFNγ expression was induced even though a similar correlation of IFNγ with CFU was detected. This indicates that gGT-activity induces IFNγ expression while there may be other bacteria derived factors that suppress IFNγ expression or recruitment of IFNγ-producing cells.

Collectively, the main effect of *H. pylori* gGT on host cells during experimental infection was an increased inflammation characterized by epithelial stress/damage and a CD8 T-cell-dominated gastritis; which was absent in mice colonized with *H. pylori* ΔgGT at a similar bacterial load. Overall T-cell responses were rather induced than repressed in presence of *H. pylori* gGT. This suggests that the gGT primarily harms epithelial cells which contributes to a proinflammatory environment while it subsequently affects immune cells migrating to the site of infection. The detrimental effect of *H. pylori* gGT on epithelial cells might be mediated through depletion of glutamine or production of toxic ammonia. Several studies have highlighted the toxic effects of ammonia produced by *H. pylori* on gastric epithelial cells [265, 266]. Yet, deprivation of glutamine might equally contribute to mediate gGT-induced effects.

4.2.5 Supplementation of glutamine suppresses gGT-induced gastric inflammation

H. pylori gGT may affect host cells due to glutamine-deprivation at site of infection; therefore, glutamine levels were manipulated. Indeed, glutamine supplementation reversed gGT-induced effects on gastric inflammation without affecting bacterial burden. In particular, administered glutamine reduced the expression of proinflammatory cytokines, influx of CD8 T-cells, and expression of IFNγ. Thus, glutamine depletion seems to be responsible for these changes during infection with *H. pylori*.

The results presented indicate that glutamine is the most important substrate of *H. pylori* gGT. Yet, it is not clear how much glutamine is available to the bacterium in the stomach lumen and at the gastric mucosa. Free amino acid concentration in gastric content might be limited. However, pepsin activity and acidic pH contribute to break-down of proteins and peptides from nutritional intake or from epithelial cells secretions. Even though the glutamine concentration in the stomach (0.9 mmol/kg) is similar to the rest of the gastrointestinal tract, the lower stomach has a very strong glutamine synthesizing capacity with high activity of glutamine synthetase that is hardly detectable in the rest of the gastrointestinal tract [267, 268, 269]. This indicates that glutamine in the stomach is derived from bio-synthesis rather than from uptake. Furthermore, glutamine synthesis contributes to detoxify ammonia. Glutamine is rapidly used or exported by gastric epithelial cells, which might be available to the bacterium. Additionally, once *H. pylori* has established the infection adjacent to the epithelial layer it may induce leakage of amino acids from apoptotic cells and the interstitial space towards the luminal side.

Results presented here suggest that gGT decreases the glutamine level in the *H. pylori* infected stomach tissue while it increases the glutamate level. Yet, the overall expression of IRF4 and cMyc, transcription factors that were shown to be glutamine sensitive in T-cells, was not reduced by gGT. On the contrary, IRF4 was induced in the stomach only upon *H. pylori* wt infection while its expression was low during colonization with *H. pylori* ΔgGT. As IRF4 is required for CD8 cells persistence [209], increased expression may reflect infiltration of CD8 cells as observed by flow cytometry. Even though IRF4 mRNA expression might be induced due to infiltrating T-lymphocytes in mice infected with *H. pylori* wt, IRF4 might be down-regulated in T-cells on a post transcriptional level at the site of infection, as observed in *H. pylori* associated gastritis in humans.

Glutaminase activity and low levels of plasma glutamine have been linked to immunosuppression under various conditions. Conversely, oral as well as parenteral supplementation of glutamine were

shown to attenuate detrimental consequences. On the one hand, decreased glutamine serum levels in response to severe injury and trauma, for example, are associated with increased susceptibility to infections [270]. Furthermore, asparaginase and glutaminase activity from *E. coli* asparaginase has been shown to deplete plasma glutamine levels and induce severe immunosuppression [271]. It has been found that asparaginase from *Vibrio succinogenes* can be used as a cytostaticum against acute lymphocytic leukemia [271]. In contrast to other bacterial asparaginases, *Vibrio succinogenes* asparaginase does not show glutaminase activity but is only depleting asparaginase, therefore not causing detrimental effects on the immune system [271]. On the other hand, glutamine supplementation for critically ill patients is general practice in intensive care units to support immune function [224, 272]. In mice, dietary glutamine supplementation enhances mitogenic responsiveness of T-lymphocytes promoting proliferation, activation and cytokine production [273].

In the context of *H. pylori* infection, *H. pylori* gGT activity may deprive epithelial as well as immune cells from glutamine at the site of infection. Therefore, glutamine was supplemented to mice infected with gGT-proficient *H. pylori* to counteract effects of glutamine deprivation. As glutamine may enhance immune function, a lower level of colonization might be expected. However, bacterial burden of mice colonized with *H. pylori* wt that were receiving a glutamine enriched diet was similar as in mice receiving the control diet. On the contrary, level of gastritis, infiltration of T-cells and expression of inflammatory cytokines was rather reduced in presence of glutamine. This might be due to the fact that glutamine augmented the barrier function of the gastric epithelium. It has been shown that glutamine supplementation preserves epithelial integrity, for example, by strengthening intestinal epithelial tight junction [274]. In non-*H. pylori* induced gastric ulcers, glutamine treatment had promising effects, curing epithelial injury and protect it from ulceration [275]. Therefore, the protective effect of glutamine on epithelial integrity may inhibit the inflammatory cascade at the very beginning.

Previous studies on glutamine supplementation during *H. pylori* infection in rodents performed to ameliorate the harmful effects of ammonia produced by urease, demonstrate enhanced immune function and reduced *H. pylori*-induced pathology [225, 226]. Even though an increase in inflammation due to glutamine-enriched diet was observed in one of these studies (at 6 weeks), that has been attributed to increased ammonia production due to *H. pylori* glutaminase activity. Yet, the results presented here indicate that the protective effects of glutamine were more pronounced than the toxicity of ammonia that may have been produced from additional glutamine.

Even though a glutamine-enriched diet did not affect the bacterial load of *H. pylori* wt, gGT-deficient *H. pylori* was unable establish an infection in presence of additional glutamine. *H. pylori* ΔgGT failed to colonize mice that received glutamine-enriched food in contrast to mice receiving control diet, where more than half of the mice were bearing bacteria. However, reduced bacterial burden was not associated to a higher inflammatory response. These results indicate that rather the host epithelial cells profit from dietary glutamine while no benefit to the bacterium could be observed.

Chapter 5

Conclusion

The results from this thesis demonstrate that the effect of *H. pylori* gGT on activation, cytokine expression, and proliferation of T-cells was glutamine-dependent. Furthermore, cMyc and IRF4 were identified as glutamine-regulated transcription factors involved in metabolic reprogramming of activated T-cells that were affected by *H. pylori* gGT. This is the first time that IRF4 is described to be controlled by extracellular glutamine levels and, more importantly, to be reduced in T-lymphocytes infiltrating the gastric mucosa of *H. pylori*-infected subjects. While results from the *in vitro* study support the hypothesis that *H. pylori* gGT constrains effector T-cell responses, results from murine infection experiments question a dominant effect of *H. pylori* gGT on T-cells in the stomach. Regarding the host response, the overall effect of *H. pylori* gGT was rather inducing than repressing the inflammatory response. *H. pylori* ΔgGT infection resulted in lower levels of neutrophil- and macrophage-attracting chemokines and less effector cytokines in the murine stomach. During infection *H. pylori* gGT induced a CD8-dominant inflammatory response together with high levels of IFNγ. Glutamine supplementation of mice attenuated *H. pylori* induced inflammation, which indicates that glutamine might be indeed locally depleted in the gastric mucosa.

- *H. pylori* gGT affects T-cells *in vitro* and *in vivo* due to their high sensitivity to extracellular glutamine.
- A dual role of *H. pylori* gGT was established: contribution to colonization capacity as well as to maintenance of high levels of bacterial density. *H. pylori* gGT seems to provide a metabolic advantage during establishment and persistence of infection at the expense of an increased inflammatory response.
- Glutamine had an important role in overcoming gGT-induced effects: *In vitro*, supplementation could restore metabolic adaptation, activation, and proliferation of T-cells; whereas the overall inflammatory response was dampened by a glutamine-enriched diet during infection.

Abbreviations

µ	micro
4F2hc	4F2 heavy chain
Ac-CoA	acetyl-CoA
ACT	ammonium chloride tris
amp	ampicilin
AMP	adenosine monophosphate
AMPK	AMP-activated protein kinase
APS	ammonium persulfate
AARE	amino acid response elements
ASCT2	alanine serine cysteine transporter 2
ATF4	activating transcription factor 4
ATP	adenosine triphosphate
BB	brucella broth
BSA	bovine serum albumin
C. jejuni	*Campylobacter jejuni*
CAE	chloroacetate esterase
CagA	Cytotoxin-associated gene A
CCL	C-C motive ligand
CD	cluster of differentiation
CEX	cation exchange
CFU	colony forming unit
cpm	counts per minute
CXCL	C-X-C motive ligand
d	day
DNA	deoxyribonucleic acid
DTT	dithiothreitol
ELISA	enzyme-linked immunosorbant assay
ENA-78	epithelial-derived neutrophil-activating peptide 78
ERK	extracellular-signal-regulated kinase
ETC	electron transport chain
exp	experiment
FCS	fetal calf serum
g	gram
GDH	glutamate dehydrogenase
gGpNA	L-γ-glutamyl-p-nitroanilide
gGT	γ-glutamyltransferase
Gln	glutamine
Glu	glutamate
GLUT1	glucose transporter type 1
GlyGly	glycyl-glycine
GSH	glutathione
h	hour
H. pylori	*Helicobacter pylori*
HIF1α	Hypoxia-inducible factor 1α
HpaA	*H. pylori* adhesin A
HPF	high power field
HRP	horse radish peroxidase
i.p.	intraperitoneal

IEL	intraepithelial lymphocytes
IFNγ	interferon gamma
IMAC	immobilized metal affinity chromatography
Iono	ionomycin
JNK	c-Jun N-terminal kinase
kana	kanamycin
kb	kilobases
KC	keratinocyte chemoattractant
kDa	kilo Dalton
l	liter
LAT1	L-amino acid transporter type 1
LC-MS	liquid chromatography–mass spectrometry
LDH	lactate dehydrogenase
LIX	lipopolysaccharide-induced CXC chemokine
m	mili
M	mol/l
MALDI	matrix-assisted laser desorption/ionization
MCP-1	monocyte chemoattractant protein-1
MCT1	monocarboxylate transporter 1
min	minute
MIP-2	macrophage inflammatory protein-2
mo	month
mRNA	messenger RNA
MS	mass spectrometry
mTOR	mammalian/mechanistic target of rapamycin
n	nano
NK cells	natural killer cells
nm	nanometer
OD	optical density
PAGE	polyacrylamide gel electrophoresis
PBMC	peripheral blood mononuclear cell
PBS	phosphate buffered saline
PI3K	phosphoinositide 3-kinase
PMN	polymorphonuclear cell
PMSS1	pre-mouse Sydney strain 1
PPP	pentose phosphate pathway
RNA	ribonucleic acid
rpm	rounds per minute
SD	standard deviation
SDS	sodium dodecyl sulfate
SEC	size exclusion chromatography
sec	second
SEM	standard error of mean
SLC	solute carrier
SNAT1	sodium-coupled neutral amino acid transporter type 1
TB	terrific broth
TCA	tricarboxylic acid
TEMED	tetramethylethylenediamine
TMB	tetrametylbenzidine
TNFα	tumor necrosis factor alpha
TOF	time-of-flight
uninf	uninfected
unstim	unstimulated
v_0	inital velocity
VacA	vacuolating toxin A
V_{max}	maximal velocity
WC	Wilkins Chalgren
wk	week
wt	wild-type
αKG	alpha-ketoglutarate

List of Figures

1 Bacterial factors facilitating the colonization of the gastric mucosa with *H. pylori* . . 2
2 Immune response towards *H. pylori* 6
3 Lymphoid structures associated with the gastrointestinal tract 7
4 Possible effects of *H. pylori* gGT during infection 25
5 Contribution of *H. pylori* gGT to energy metabolism, nitrogen assimilation, and acid stress resistance 26
6 Metabolism of activated T-cells is shifted towards glutaminolysis and glycolysis . . . 30
7 Amino acid sensing pathways in T-lymphocytes 32

8 Treatment of mice with acivicin during a short term *H. pylori* infection experiment . 40
9 Oral complementation of gGT-deficient *H. pylori* with recombinant gGT during experimental infection in mice 40
10 Adoptive transfer of CD4 cells into Rag-/- mice infected with *H. pylori* 41
11 Administration of glutamate in drinking water during infection with *H. pylori* wt and ΔgGT 42
12 Glutamine- and glutamate-enriched diet during *H. pylori* infection 42
13 Protein profile in a 2D gel derived from PBMC cell lysates 47

14 Purification of recombinant *H. pylori* gGT 52
15 *H. pylori* gGT-induced effects on activated human lymphocytes 53
16 Time dependency of *H. pylori* gGT-mediated effects on proliferation 54
17 Enzymatic activity of *H. pylori* gGT metabolizes glutamine and glutathione 56
18 Glutamine supplementation restores proliferation of gGT-treated lymphocytes 58
19 Glutamine supplementation restores proliferation impaired by *H. pylori* gGT only when enzymatic activity is abrogated 59
20 Enzymatic activity of gGT in preconditioned cell culture medium 60
21 Cyclin D3 expression restored by glutamine when gGT is inactivated 60
22 Aggregate size of activated PBMCs is decreased by *H. pylori* gGT activity 61
23 *H. pylori* wt impairs proliferation of T-cells by gGT-dependent glutamine deprivation 61
24 *H. pylori* gGT-induced glutamine deprivation impairs activation of $CD4^+$ T-cells . . 62
25 *H. pylori* gGT impairs upregulation of CD25, a prerequisite for proliferation 63
26 Supplementation of glutamine restores IL-2 secretion from PBMCs treated with *H. pylori* gGT preconditioned medium 63
27 rIL-2 cannot restore proliferation of *H. pylori* gGT-treated PBMCs 63
28 Supplementation of glutamine restores effector cytokine secretion from PBMCs treated with *H. pylori* gGT preconditioned medium 64
29 *H. pylori* gGT-induced glutamine deprivation impairs effector cytokine secretion of $CD4^+$ T-cells 65
30 Supplementation of reducing agents to PBMCs treated with *H. pylori* gGT 66

31 Supportive effect of glutathione only on *H. pylori* gGT-treated PBMCs supplemented with glutamine 67
32 Expression of mTOR up- and downstream targets in *H. pylori* gGT-treated PMBCs 68
33 Protein level of Cyclin D3 and cMyc in *H. pylori* gGT-treated PMBCs 70
34 Phosphorylation and expression of MAP kinases ERK and p38 71
35 Exemplary protein spots that were differentially regulated by active *H. pylori* gGT 71
36 IRF4 expression in stimulated PBMCs is altered by *H. pylori* gGT activity 72
37 Down-regulation of IRF4 by *H. pylori* gGT is reversed by glutamine supplementation 72
38 IRF4 and CD3 expression in the gastric mucosa of *H. pylori*-infected individuals . . 73
39 Influence of *H. pylori* gGT on gastric colonization during the course of infection . . . 75
40 Gastric inflammation and infiltration of immune cells in stomach mucosa or related lymphoid tissue after three days of *H. pylori* infection 77
41 Colonization of mice upon manipulation of *H. pylori* gGT by inhibition and complementation 78
42 Determination and confirmation of gastric colonization status 79
43 Adaptation of bacteria may allow persistent infection in mice colonized with *H. pylori* ΔgGT 81
44 Characterization of Th-cell profile in peripheral immune organs induced by *H. pylori* wt and ΔgGT infection 83
45 *H. pylori*-induced gastritis and T-cell infiltration in mice colonized with *H. pylori* wt or ΔgGT for one month 84
46 Immunophenotyping of T-cell subsets in stomachs infected with *H. pylori* wt and ΔgGT for one month 85
47 Immunophenotyping of T-cell subsets in stomachs infected with *H. pylori* wt and ΔgGT for three months 87
48 Characterization of CD4 T-cells infiltrating into gastric mucosa of mice infected with *H. pylori* wt and ΔgGT for one month 88
49 Expression of cytokines and chemokines driving inflammation and Th1/Th17 differentiation in stomach tissues 90
50 Expression of Th1/Th17 cytokines and of immunoregulatory factors in stomach tissues 91
51 Colonization of lymphocyte-deficient mice with *H. pylori* ΔgGT 92
52 Transfer of $CD4^+$ cells in *H. pylori* wt- and ΔgGT-infected $Rag^{-/-}$ mice 94
53 Transfer of $CD4^+/CD44^-$ cells in *H. pylori* wt- and ΔgGT-infected $Rag^{-/-}$ mice . . . 95
54 Glutamine level and expression of glutamine-dependent transcription factors in *H. pylori*-infected stomachs 96
55 Effect of glutamate administration via drinking water on *H. pylori* colonization . . . 98
56 Effects of dietary glutamine and glutamate supplementation on colonization and gastric inflammation during *H. pylori* wt and ΔgGT infection of mice 100
57 Transcriptional changes of cytokines and chemokines in the gastric mucosa of *H. pylori* wt- and ΔgGT-infected mice fed a glutamine- or glutamate-enriched diet . . . 101
58 Administration of a glutamine- and glutamate-enriched diet to mice persistently infected with *H. pylori* wt and ΔgGT 102

List of Tables

1 *Helicobacter* infection of mice deficient in B- and T-cell responses 10
2 *Helicobacter* infection and immunization of mice deficient in humoral and Th2 cell responses 11
3 *Helicobacter* infection and immunization of mice deficient in T-cell responses 13
4 Functional studies on Th1-cell responses in mice upon *H. pylori* infection and immunization 15
5 Functional studies on Th17-cell responses in mice upon *H. pylori* infection and immunization 19
6 Functional studies on Th1/Th17-cell responses in mice upon *H. pylori* infection and immunization 21
7 Functional studies on regulatory T-cell responses in mice upon *H. pylori* infection . 23

8 Oligonucleotides for RT-PCR 49

9 *H. pylori* gGT regulates protein expression in activated PBMCs 69

Bibliography

[1] Krienitz, W. (1906) Über das Auftreten von Spirochaeten verschiedener Form im Magenihalt bei Carcinoma ventriculi. *Deutsche medizinische Wochenschrift*, p. 872.

[2] Doenges, J. L. (1938) Spirochaetes in the gastric glands of Macacus rhesus and humans without definite hist ory of related diseases. *Proceedings of the Society for Experimental Medicine and Biology*, pp. 536–538.

[3] Marshall, B. J., Armstrong, J. A., McGechie, D. B., and Glancy, R. J. (1985) Attempt to fulfil Koch's postulates for pyloric Campylobacter. *The Medical journal of Australia*, **142**, 436–439.

[4] Goodwin, C. S., Armstrong, J. A., Chilvers, T., Peters, M., Collins, M. D., Sly, L., McConnell, W., and Harper, W. E. S. (1989) Transfer of Campylobacter pylori and Campylobacter mustelae to Helicobacter gen. nov. as Helicobacter pylori comb. nov. and Helicobacter mustelae comb. nov., Respectively. *International Journal of Systematic Bacteriology*, **39**, 397–405.

[5] Solnick, J. V., O'Rourke, J. L., Vandamme, P., and Lee, A. (2006) The Genus Helicobacter. Dworkin, M., Falkow, S., Rosenberg, E., Schleifer, K.-H., and Stackebrandt, E. (eds.), *The Prokaryotes*, pp. 139–177, Springer New York.

[6] Ge, Z., Feng, Y., Muthupalani, S., Eurell, L. L., Taylor, N. S., Whary, M. T., and Fox, J. G. (2011) Coinfection with Enterohepatic Helicobacter species can ameliorate or promote Helicobacter pylori-induced gastric pathology in C57BL/6 mice. *Infection and immunity*, **79**, 3861–3871.

[7] Haesebrouck, F., Pasmans, F., Flahou, B., Smet, A., Vandamme, P., and Ducatelle, R. (2011) Non-Helicobacter pylori Helicobacter species in the human gastric mucosa: a proposal to introduce the terms H. heilmannii sensu lato and sensu stricto. *Helicobacter*, **16**, 339–340.

[8] Solnick, J. V. and Schauer, D. B. (2001) Emergence of diverse Helicobacter species in the pathogenesis of gastric and enterohepatic diseases. *Clinical microbiology reviews*, **14**, 59–97.

[9] Kusters, J. G., van Vliet, Arnoud H. M., and Kuipers, E. J. (2006) Pathogenesis of Helicobacter pylori infection. *Clinical microbiology reviews*, **19**, 449–490.

[10] Lavelle, J. P., Landas, S., Mitros, F. A., and Conklin, J. L. (1994) Acute gastritis associated with spiral organisms from cats. *Digestive diseases and sciences*, **39**, 744–750.

[11] Mohammadi, M., Czinn, S., Redline, R., and Nedrud, J. (1996) Helicobacter-specific cell-mediated immune responses display a predominant Th1 phenotype and promote a delayed-type hypersensitivity response in the stomachs of mice. *Journal of Immunology*, **156**, 4729–4738.

[12] Mobley, Harry L. T., Mendz, G. L., and Hazell, S. L. (2001) *Helicobacter pylori: Physiology and genetics*. NCBI Bookshelf, ASM Press.

[13] Wunder, C., Churin, Y., Winau, F., Warnecke, D., Vieth, M., Lindner, B., Zähringer, U., Mollenkopf, H.-J., Heinz, E., and Meyer, T. F. (2006) Cholesterol glucosylation promotes immune evasion by Helicobacter pylori. *Nature medicine*, **12**, 1030–1038.

[14] Tomb, J. F., et al. (1997) The complete genome sequence of the gastric pathogen Helicobacter pylori. *Nature*, **388**, 539–547.

[15] Bik, E. M., Eckburg, P. B., Gill, S. R., Nelson, K. E., Purdom, E. A., Francois, F., Perez-Perez, G., Blaser, M. J., and Relman, D. A. (2006) Molecular analysis of the bacterial microbiota in the human stomach. *Proceedings of the National Academy of Sciences of the United States of America*, **103**, 732–737.

[16] Sachs, G., Weeks, D. L., Wen, Y., Marcus, E. A., Scott, D. R., and Melchers, K. (2005) Acid acclimation by Helicobacter pylori. *Physiology*, **20**, 429–438.

[17] Rektorschek, M., Buhmann, A., Weeks, D., Schwan, D., Bensch, K. W., Eskandari, S., Scott, D., Sachs, G., and Melchers, K. (2000) Acid resistance of Helicobacter pylori depends on the UreI membrane protein and an inner membrane proton barrier. *Molecular microbiology*, **36**, 141–152.

[18] Sycuro, L. K., Pincus, Z., Gutierrez, K. D., Biboy, J., Stern, C. A., Vollmer, W., and Salama, N. R. (2010) Peptidoglycan crosslinking relaxation promotes Helicobacter pylori's helical shape and stomach colonization. *Cell*, **141**, 822–833.

[19] Ottemann, K. M. and Lowenthal, A. C. (2002) Helicobacter pylori uses motility for initial colonization and to attain robust infection. *Infection and immunity*, **70**, 1984–1990.

[20] Schreiber, S., Konradt, M., Groll, C., Scheid, P., Hanauer, G., Werling, H.-O., Josenhans, C., and Suerbaum, S. (2004) The spatial orientation of Helicobacter pylori in the gastric mucus. *Proceedings of the National Academy of Sciences of the United States of America*, **101**, 5024–5029.

[21] Necchi, V., Candusso, M. E., Tava, F., Luinetti, O., Ventura, U., Fiocca, R., Ricci, V., and Solcia, E. (2007) Intracellular, intercellular, and stromal invasion of gastric mucosa, preneoplastic lesions, and cancer by Helicobacter pylori. *Gastroenterology*, **132**, 1009–1023.

[22] Amieva, M. R., Vogelmann, R., Covacci, A., Tompkins, L. S., Nelson, W. J., and Falkow, S. (2003) Disruption of the epithelial apical-junctional complex by Helicobacter pylori CagA. *Science*, **300**, 1430–1434.

[23] Murata-Kamiya, N., et al. (2007) Helicobacter pylori CagA interacts with E-cadherin and deregulates the beta-catenin signal that promotes intestinal transdifferentiation in gastric epithelial cells. *Oncogene*, **26**, 4617–4626.

[24] Wroblewski, L. E., Le Shen, Ogden, S., Romero-Gallo, J., Lapierre, L. A., Israel, D. A., Turner, J. R., and Peek, R. M. (2009) Helicobacter pylori dysregulation of gastric epithelial tight junctions by urease-mediated myosin II activation. *Gastroenterology*, **136**, 236–246.

[25] Hoy, B., et al. (2010) Helicobacter pylori HtrA is a new secreted virulence factor that cleaves E-cadherin to disrupt intercellular adhesion. *EMBO reports*, **11**, 798–804.

[26] van Amsterdam, K. and van der Ende, Arie (2004) Nutrients released by gastric epithelial cells enhance Helicobacter pylori growth. *Helicobacter*, **9**, 614–621.

[27] Schilling, C. H., Covert, M. W., Famili, I., Church, G. M., Edwards, J. S., and Palsson, B. O. (2002) Genome-scale metabolic model of Helicobacter pylori 26695. *Journal of bacteriology*, **184**, 4582–4593.

[28] Hunt, R. H., et al. (2011) Helicobacter pylori in developing countries. World Gastroenterology Organisation Global Guideline. *Journal of gastrointestinal and liver diseases : JGLD*, **20**, 299–304.

[29] Rowland, M. (2000) Transmission of Helicobacter pylori: is it all child's play? *Lancet*, **355**, 332–333.

[30] Kivi, M. and Tindberg, Y. (2006) Helicobacter pylori occurrence and transmission: a family affair? *Scandinavian journal of infectious diseases*, **38**, 407–417.

[31] Ferguson, D. A., Li, C., Patel, N. R., Mayberry, W. R., Chi, D. S., and Thomas, E. (1993) Isolation of Helicobacter pylori from saliva. *Journal of clinical microbiology*, **31**, 2802–2804.

[32] Parsonnet, J., Shmuely, H., and Haggerty, T. (1999) Fecal and oral shedding of Helicobacter pylori from healthy infected adults. *JAMA : the journal of the American Medical Association*, **282**, 2240–2245.

[33] Allaker, R. P., Young, K. A., Hardie, J. M., Domizio, P., and Meadows, N. J. (2002) Prevalence of helicobacter pylori at oral and gastrointestinal sites in children: evidence for possible oral-to-oral transmission. *Journal of medical microbiology*, **51**, 312–317.

[34] Eslick, G. D., Lim, L. L., Byles, J. E., Xia, H. H., and Talley, N. J. (1999) Association of Helicobacter pylori infection with gastric carcinoma: a meta-analysis. *The American journal of gastroenterology*, **94**, 2373–2379.

[35] Uemura, N., Okamoto, S., Yamamoto, S., Matsumura, N., Yamaguchi, S., Yamakido, M., Taniyama, K., Sasaki, N., and Schlemper, R. J. (2001) Helicobacter pylori infection and the development of gastric cancer. *The New England journal of medicine*, **345**, 784–789.

[36] IARC (1994) Infection with Helicobacter pylori. *IARC monographs on the evaluation of carcinogenic risks to humans / World Health Organization, International Agency for Research on Cancer*, **61**, 177–240.

[37] Ferlay, J., Shin, H.-R., Bray, F., Forman, D., Mathers, C., and Parkin, D. M. (2010) Estimates of worldwide burden of cancer in 2008: GLOBOCAN 2008. *International journal of cancer. Journal international du cancer*, **127**, 2893–2917.

[38] Atherton, J. C., Tham, K. T., Peek, R. M., Cover, T. L., and Blaser, M. J. (1996) Density of Helicobacter pylori infection in vivo as assessed by quantitative culture and histology. *The Journal of infectious diseases*, **174**, 552–556.

[39] Vieth, M. and Stolte, M. (2006) Elevated risk for gastric adenocarcinoma can be predicted from histomorphology. *World journal of gastroenterology : WJG*, **12**, 6109–6114.

[40] Wolfe, M. M. and Nompleggi, D. J. (1992) Cytokine inhibition of gastric acid secretion–a little goes a long way. *Gastroenterology*, **102**, 2177–2178.

[41] El-Omar, E. M., et al. (2000) Interleukin-1 polymorphisms associated with increased risk of gastric cancer. *Nature*, **404**, 398–402.

[42] Wroblewski, L. E., Peek, R. M., and Wilson, K. T. (2010) Helicobacter pylori and gastric cancer: factors that modulate disease risk. *Clinical microbiology reviews*, **23**, 713–739.

[43] Nguyen, L. T., Uchida, T., Murakami, K., Fujioka, T., and Moriyama, M. (2008) Helicobacter pylori virulence and the diversity of gastric cancer in Asia. *Journal of medical microbiology*, **57**, 1445–1453.

[44] Naylor, G. M., Gotoda, T., Dixon, M., Shimoda, T., Gatta, L., Owen, R., Tompkins, D., and Axon, A. (2006) Why does Japan have a high incidence of gastric cancer? Comparison of gastritis between UK and Japanese patients. *Gut*, **55**, 1545–1552.

[45] Rieder, G., Merchant, J. L., and Haas, R. (2005) Helicobacter pylori cag-type IV secretion system facilitates corpus colonization to induce precancerous conditions in Mongolian gerbils. *Gastroenterology*, **128**, 1229–1242.

[46] Polk, D. B. and Peek, R. M. (2010) Helicobacter pylori: gastric cancer and beyond. *Nature reviews. Cancer*, **10**, 403–414.

[47] Yamaoka, Y. (2010) Mechanisms of disease: Helicobacter pylori virulence factors. *Nature reviews*, **7**, 629–641.

[48] Kuck, D., Kolmerer, B., Iking-Konert, C., Krammer, P. H., Stremmel, W., and Rudi, J. (2001) Vacuolating cytotoxin of Helicobacter pylori induces apoptosis in the human gastric epithelial cell line AGS. *Infection and immunity*, **69**, 5080–5087.

[49] Gunn, M. C., Stephens, J. C., Stewart, J. A., Rathbone, B. J., and West, K. P. (1998) The significance of cagA and vacA subtypes of Helicobacter pylori in the pathogenesis of inflammation and peptic ulceration. *Journal of clinical pathology*, **51**, 761–764.

[50] Kato, I., et al. (2004) Environmental factors in Helicobacter pylori-related gastric precancerous lesions in Venezuela. *Cancer epidemiology, biomarkers & prevention : a publication of the American Association for Cancer Research*, **13**, 468–476.

[51] Malfertheiner, P., et al. (2012) Management of Helicobacter pylori infection–the Maastricht IV/ Florence Consensus Report. *Gut*, **61**, 646–664.

[52] Formichella, L., et al. (2013) A novel line immunoassay based on recombinant virulence factors enables highly specific and sensitive serologic diagnosis of Helicobacter pylori infection. *Clinical and vaccine immunology : CVI*, **20**, 1703–1710.

[53] Dubois, A., Fiala, N., Heman-Ackah, L. M., Drazek, E. S., Tarnawski, A., Fishbein, W. N., Perez-Perez, G. I., and Blaser, M. J. (1994) Natural gastric infection with Helicobacter pylori in monkeys: a model for spiral bacteria infection in humans. *Gastroenterology*, **106**, 1405–1417.

[54] Euler, A. R., Zurenko, G. E., Moe, J. B., Ulrich, R. G., and Yagi, Y. (1990) Evaluation of two monkey species (Macaca mulatta and Macaca fascicularis) as possible models for human Helicobacter pylori disease. *Journal of clinical microbiology*, **28**, 2285–2290.

[55] Krakowka, S., Morgan, D. R., Kraft, W. G., and Leunk, R. D. (1987) Establishment of gastric Campylobacter pylori infection in the neonatal gnotobiotic piglet. *Infection and immunity*, **55**, 2789–2796.

[56] Sjunnesson, H., Sturegård, E., Grubb, A., Willén, R., and Wadström, T. (2001) Comparative study of Helicobacter pylori infection in guinea pigs and mice - elevation of acute-phase protein C3 in infected guinea pigs. *FEMS immunology and medical microbiology*, **30**, 167–172.

[57] Matsumoto, S., Washizuka, Y., Matsumoto, Y., Tawara, S., Ikeda, F., Yokota, Y., and Karita, M. (1997) Induction of ulceration and severe gastritis in Mongolian gerbil by Helicobacter pylori infection. *Journal of medical microbiology*, **46**, 391–397.

[58] Watanabe, T., Tada, M., Nagai, H., Sasaki, S., and Nakao, M. (1998) Helicobacter pylori infection induces gastric cancer in mongolian gerbils. *Gastroenterology*, **115**, 642–648.

[59] Franco, A. T., Johnston, E., Krishna, U., Yamaoka, Y., Israel, D. A., Nagy, T. A., Wroblewski, L. E., Piazuelo, M. B., Correa, P., and Peek, R. M. (2008) Regulation of gastric carcinogenesis by Helicobacter pylori virulence factors. *Cancer research*, **68**, 379–387.

[60] Ferrero, R. L., Thiberge, J. M., Huerre, M., and Labigne, A. (1998) Immune responses of specific-pathogen-free mice to chronic Helicobacter pylori (strain SS1) infection. *Infection and immunity*, **66**, 1349–1355.

[61] Lee, A., O'Rourke, J., Ungria, M. C. de, Robertson, B., Daskalopoulos, G., and Dixon, M. F. (1997) A standardized mouse model of Helicobacter pylori infection: introducing the Sydney strain. *Gastroenterology*, **112**, 1386–1397.

[62] Chevalier, C., Thiberge, J. M., Ferrero, R. L., and Labigne, A. (1999) Essential role of Helicobacter pylori gamma-glutamyltranspeptidase for the colonization of the gastric mucosa of mice. *Molecular microbiology*, **31**, 1359–1372.

[63] Crabtree, J. E., Ferrero, R. L., and Kusters, J. G. (2002) The mouse colonizing Helicobacter pylori strain SS1 may lack a functional cag pathogenicity island. *Helicobacter*, **7**, 139–40; author reply 140–1.

[64] Ding, H., Nedrud, J. G., Blanchard, T. G., Zagorski, B. M., Li, G., Shiu, J., Xu, J., and Czinn, S. J. (2013) Th1-mediated immunity against Helicobacter pylori can compensate for lack of Th17 cells and can protect mice in the absence of immunization. *PloS one*, **8**, e69384.

[65] Arnold, I. C., Dehzad, N., Reuter, S., Martin, H., Becher, B., Taube, C., and Muller, A. (2011) Helicobacter pylori infection prevents allergic asthma in mouse models through the induction of regulatory T cells. *The Journal of clinical investigation*, **121**, 3088–3093.

[66] Kazi, J. I., Sinniah, R., Jaffrey, N. A., Alam, S. M., Zaman, V., Zuberi, S. J., and Kazi, A. M. (1989) Cellular and humoral immune responses in Campylobacter pylori-associated chronic gastritis. *The Journal of pathology*, **159**, 231–237.

[67] Suzuki, T., Kato, K., Ohara, S., Noguchi, K., Sekine, H., Nagura, H., and Shimosegawa, T. (2002) Localization of antigen-presenting cells in Helicobacter pylori-infected gastric mucosa. *Pathology international*, **52**, 265–271.

[68] Dixon, M. F., Genta, R. M., Yardley, J. H., and Correa, P. (1996) Classification and grading of gastritis. The updated Sydney System. International Workshop on the Histopathology of Gastritis, Houston 1994. *The American journal of surgical pathology*, **20**, 1161–1181.

[69] Roth, K. A., Kapadia, S. B., Martin, S. M., and Lorenz, R. G. (1999) Cellular immune responses are essential for the development of Helicobacter felis-associated gastric pathology. *Journal of immunology*, **163**, 1490–1497.

[70] Gorrell, R. J., Wijburg, Odilia L. C., Pedersen, J. S., Walduck, A. K., Kwok, T., Strugnell, R. A., and Robins-Browne, R. M. (2013) Contribution of secretory antibodies to intestinal mucosal immunity against Helicobacter pylori. *Infection and immunity*, **81**, 3880–3893.

[71] Linz, B., et al. (2007) An African origin for the intimate association between humans and Helicobacter pylori. *Nature*, **445**, 915–918.

[72] Marchetti, M., Aricò, B., Burroni, D., Figura, N., Rappuoli, R., and Ghiara, P. (1995) Development of a mouse model of Helicobacter pylori infection that mimics human disease. *Science*, **267**, 1655–1658.

[73] Sayi, A., Kohler, E., Hitzler, I., Arnold, I., Schwendener, R., Rehrauer, H., and Muller, A. (2009) The CD4+ T cell-mediated IFN-gamma response to Helicobacter infection is essential for clearance and determines gastric cancer risk. *Journal of immunology*, **182**, 7085–7101.

[74] DeLyria, E. S., Nedrud, J. G., Ernst, P. B., Alam, M. S., Redline, R. W., Ding, H., Czinn, S. J., Xu, J., and Blanchard, T. G. (2011) Vaccine-induced immunity against Helicobacter pylori in the absence of IL-17A. *Helicobacter*, **16**, 169–178.

[75] Sawai, N., Kita, M., Kodama, T., Tanahashi, T., Yamaoka, Y., Tagawa, Y., Iwakura, Y., and Imanishi, J. (1999) Role of gamma interferon in Helicobacter pylori-induced gastric inflammatory responses in a mouse model. *Infection and immunity*, **67**, 279–285.

[76] Akhiani, A. A., Pappo, J., Kabok, Z., Schon, K., Gao, W., Franzen, L. E., and Lycke, N. (2002) Protection against Helicobacter pylori infection following immunization is IL-12-dependent and mediated by Th1 cells. *Journal of immunology*, **169**, 6977–6984.

[77] Garhart, C. A., Heinzel, F. P., Czinn, S. J., and Nedrud, J. G. (2003) Vaccine-induced reduction of Helicobacter pylori colonization in mice is interleukin-12 dependent but gamma interferon and inducible nitric oxide synthase independent. *Infection and immunity*, **71**, 910–921.

[78] Necchi, V., Manca, R., Ricci, V., and Solcia, E. (2009) Evidence for transepithelial dendritic cells in human H. pylori active gastritis. *Helicobacter*, **14**, 208–222.

[79] Janeway, C. A. and Medzhitov, R. (2002) Innate immune recognition. *Annual review of immunology*, **20**, 197–216.

[80] Peek, Richard M. JR, Fiske, C., and Wilson, K. T. (2010) Role of innate immunity in Helicobacter pylori-induced gastric malignancy. *Physiological reviews*, **90**, 831–858.

[81] Bergman, M. P., Engering, A., Smits, H. H., van Vliet, Sandra J., van Bodegraven, Ad A., Wirth, H.-P., Kapsenberg, M. L., Vandenbroucke-Grauls, Christina M. J. E., van Kooyk, Y., and Appelmelk, B. J. (2004) Helicobacter pylori modulates the T helper cell 1/T helper cell 2 balance through phase-variable interaction between lipopolysaccharide and DC-SIGN. *The Journal of experimental medicine*, **200**, 979–990.

[82] Gewirtz, A. T., Yu, Y., Krishna, U. S., Israel, D. A., Lyons, S. L., and Peek, R. M. (2004) Helicobacter pylori flagellin evades toll-like receptor 5-mediated innate immunity. *The Journal of infectious diseases*, **189**, 1914–1920.

[83] Rad, R., et al. (2006) CD25+/Foxp3+ T cells regulate gastric inflammation and Helicobacter pylori colonization in vivo. *Gastroenterology*, **131**, 525–537.

[84] Sun, X., Zhang, M., El-Zataari, M., Owyang, S. Y., Eaton, K. A., Liu, M., Chang, Y.-M., Zou, W., and Kao, J. Y. (2013) TLR2 mediates Helicobacter pylori-induced tolerogenic immune response in mice. *PloS one*, **8**, e74595.

[85] Viala, J., et al. (2004) Nod1 responds to peptidoglycan delivered by the Helicobacter pylori cag pathogenicity island. *Nature immunology*, **5**, 1166–1174.

[86] Kao, J. Y., et al. (2010) Helicobacter pylori immune escape is mediated by dendritic cell-induced Treg skewing and Th17 suppression in mice. *Gastroenterology*, **138**, 1046–1054.

[87] Keates, S., Hitti, Y. S., Upton, M., and Kelly, C. P. (1997) Helicobacter pylori infection activates NF-kappa B in gastric epithelial cells. *Gastroenterology*, **113**, 1099–1109.

[88] Bäckhed, F., Torstensson, E., Seguin, D., Richter-Dahlfors, A., and Rokbi, B. (2003) Helicobacter pylori infection induces interleukin-8 receptor expression in the human gastric epithelium. *Infection and immunity*, **71**, 3357–3360.

[89] Crabtree, J. E., Covacci, A., Farmery, S. M., Xiang, Z., Tompkins, D. S., Perry, S., Lindley, I. J., and Rappuoli, R. (1995) Helicobacter pylori induced interleukin-8 expression in gastric epithelial cells is associated with CagA positive phenotype. *Journal of clinical pathology*, **48**, 41–45.

[90] Graham, D. Y., Opekun, A. R., Osato, M. S., El-Zimaity, H. M. T., Lee, C. K., Yamaoka, Y., Qureshi, W. A., Cadoz, M., and Monath, T. P. (2004) Challenge model for Helicobacter pylori infection in human volunteers. *Gut*, **53**, 1235–1243.

[91] Crabtree, J. E. and Lindley, I. J. (1994) Mucosal interleukin-8 and Helicobacter pylori-associated gastroduodenal disease. *European journal of gastroenterology & hepatology*, **6 Suppl 1**, S33–8.

[92] Ye, G., Barrera, C., Fan, X., Gourley, W. K., Crowe, S. E., Ernst, P. B., and Reyes, V. E. (1997) Expression of B7-1 and B7-2 costimulatory molecules by human gastric epithelial cells: potential role in CD4+ T cell activation during Helicobacter pylori infection. *The Journal of clinical investigation*, **99**, 1628–1636.

[93] Fan, X., Crowe, S. E., Behar, S., Gunasena, H., Ye, G., Haeberle, H., van Houten, N., Gourley, W. K., Ernst, P. B., and Reyes, V. E. (1998) The effect of class II major histocompatibility complex expression on adherence of Helicobacter pylori and induction of apoptosis in gastric epithelial cells: a mechanism for T helper cell type 1-mediated damage. *The Journal of experimental medicine*, **187**, 1659–1669.

[94] Thelemann, C., et al. (2014) Interferon-γ induces expression of MHC class II on intestinal epithelial cells and protects mice from colitis. *PloS one*, **9**, e86844.

[95] Shiu, J. and Blanchard, T. G. (2013) Dendritic cell function in the host response to Helicobacter pylori infection of the gastric mucosa. *Pathogens and disease*, **67**, 46–53.

[96] Hafsi, N., Voland, P., Schwendy, S., Rad, R., Reindl, W., Gerhard, M., and Prinz, C. (2004) Human dendritic cells respond to Helicobacter pylori, promoting NK cell and Th1-effector responses in vitro. *Journal of immunology*, **173**, 1249–1257.

[97] Khamri, W., Walker, M. M., Clark, P., Atherton, J. C., Thursz, M. R., Bamford, K. B., Lechler, R. I., and Lombardi, G. (2010) Helicobacter pylori stimulates dendritic cells to induce interleukin-17 expression from CD4+ T lymphocytes. *Infection and immunity*, **78**, 845–853.

[98] Oertli, M., Noben, M., Engler, D. B., Semper, R. P., Reuter, S., Maxeiner, J., Gerhard, M., Taube, C., and Muller, A. (2013) Helicobacter pylori gamma-glutamyl transpeptidase and vacuolating cytotoxin promote gastric persistence and immune tolerance. *Proceedings of the National Academy of Sciences of the United States of America*, **110**, 3047–3052.

[99] Watanabe, N., Kiriya, K., and Chiba, T. (2008) Small intestine Peyer's patches are major induction sites of the Helicobacter-induced host immune responses. *Gastroenterology*, **134**, 642–643.

[100] Terrés, A. M. and Pajares, J. M. (1998) An increased number of follicles containing activated CD69+ helper T cells and proliferating CD71+ B cells are found in H. pylori-infected gastric mucosa. *The American journal of gastroenterology*, **93**, 579–583.

[101] Mai, U. E., Perez-Perez, G. I., Allen, J. B., Wahl, S. M., Blaser, M. J., and Smith, P. D. (1992) Surface proteins from Helicobacter pylori exhibit chemotactic activity for human leukocytes and are present in gastric mucosa. *The Journal of experimental medicine*, **175**, 517–525.

[102] Harris, P. R., Ernst, P. B., Kawabata, S., Kiyono, H., Graham, M. F., and Smith, P. D. (1998) Recombinant Helicobacter pylori urease activates primary mucosal macrophages. *The Journal of infectious diseases*, **178**, 1516–1520.

[103] Ramarao, N. and Meyer, T. F. (2001) Helicobacter pylori resists phagocytosis by macrophages: quantitative assessment by confocal microscopy and fluorescence-activated cell sorting. *Infection and immunity*, **69**, 2604–2611.

[104] Amedei, A., et al. (2006) The neutrophil-activating protein of Helicobacter pylori promotes Th1 immune responses. *The Journal of clinical investigation*, **116**, 1092–1101.

[105] Ramarao, N., Gray-Owen, S. D., and Meyer, T. F. (2000) Helicobacter pylori induces but survives the extracellular release of oxygen radicals from professional phagocytes using its catalase activity. *Molecular microbiology*, **38**, 103–113.

[106] Gobert, A. P., McGee, D. J., Akhtar, M., Mendz, G. L., Newton, J. C., Cheng, Y., Mobley, H. L., and Wilson, K. T. (2001) Helicobacter pylori arginase inhibits nitric oxide production by eukaryotic cells: a strategy for bacterial survival. *Proceedings of the National Academy of Sciences of the United States of America*, **98**, 13844–13849.

[107] Hayday, A., Theodoridis, E., Ramsburg, E., and Shires, J. (2001) Intraepithelial lymphocytes: exploring the Third Way in immunology. *Nature immunology*, **2**, 997–1003.

[108] Hatz, R. A., Meimarakis, G., Bayerdorffer, E., Stolte, M., Kirchner, T., and Enders, G. (1996) Characterization of lymphocytic infiltrates in Helicobacter pylori-associated gastritis. *Scandinavian journal of gastroenterology*, **31**, 222–228.

[109] Han, S.-H., Joo, M., and Kim, K.-M. (2013) High proportion of granzyme B+ intraepithelial lymphocytes contributes to epithelial apoptosis in Helicobacter pylori-associated lymphocytic gastritis. *Helicobacter*, **18**, 290–298.

[110] Crabtree, J. E., Shallcross, T. M., Heatley, R. V., and Wyatt, J. I. (1991) Mucosal tumour necrosis factor alpha and interleukin-6 in patients with Helicobacter pylori associated gastritis. *Gut*, **32**, 1473–1477.

[111] Lindholm, C., Quiding-Järbrink, M., Lönroth, H., Hamlet, A., and Svennerholm, A. M. (1998) Local cytokine response in Helicobacter pylori-infected subjects. *Infection and immunity*, **66**, 5964–5971.

[112] Luzza, F., Parrello, T., Monteleone, G., Sebkova, L., Romano, M., Zarrilli, R., Imeneo, M., and Pallone, F. (2000) Up-regulation of IL-17 is associated with bioactive IL-8 expression in Helicobacter pylori-infected human gastric mucosa. *Journal of immunology*, **165**, 5332–5337.

[113] Mizuno, T., et al. (2005) Interleukin-17 levels in Helicobacter pylori-infected gastric mucosa and pathologic sequelae of colonization. *World journal of gastroenterology : WJG*, **11**, 6305–6311.

[114] Goll, R., Gruber, F., Olsen, T., Cui, G., Raschpichler, G., Buset, M., Asfeldt, A. M., Husebekk, A., and Florholmen, J. (2007) Helicobacter pylori stimulates a mixed adaptive immune response with a strong T-regulatory component in human gastric mucosa. *Helicobacter*, **12**, 185–192.

[115] Smythies, L. E., Waites, K. B., Lindsey, J. R., Harris, P. R., Ghiara, P., and Smith, P. D. (2000) Helicobacter pylori-induced mucosal inflammation is Th1 mediated and exacerbated in IL-4, but not IFN-gamma, gene-deficient mice. *Journal of immunology*, **165**, 1022–1029.

[116] Eaton, K. A., Mefford, M., and Thevenot, T. (2001) The role of T cell subsets and cytokines in the pathogenesis of Helicobacter pylori gastritis in mice. *Journal of immunology*, **166**, 7456–7461.

[117] Raghavan, S., Fredriksson, M., Svennerholm, A.-M., Holmgren, J., and Suri-Payer, E. (2003) Absence of CD4+CD25+ regulatory T cells is associated with a loss of regulation leading to increased pathology in Helicobacter pylori-infected mice. *Clinical and experimental immunology*, **132**, 393–400.

[118] Lee, C.-W., Rao, V. P., Rogers, A. B., Ge, Z., Erdman, S. E., Whary, M. T., and Fox, J. G. (2007) Wild-type and interleukin-10-deficient regulatory T cells reduce effector T-cell-mediated gastroduodenitis in Rag2-/- mice, but only wild-type regulatory T cells suppress Helicobacter pylori gastritis. *Infection and immunity*, **75**, 2699–2707.

[119] Eaton, K. A. and Mefford, M. E. (2001) Cure of Helicobacter pylori infection and resolution of gastritis by adoptive transfer of splenocytes in mice. *Infection and immunity*, **69**, 1025–1031.

[120] Macpherson, A. J. and Slack, E. (2007) The functional interactions of commensal bacteria with intestinal secretory IgA. *Current opinion in gastroenterology*, **23**, 673–678.

[121] Rathbone, B. J., Wyatt, J. I., Worsley, B. W., Shires, S. E., Trejdosiewicz, L. K., Heatley, R. V., and Losowsky, M. S. (1986) Systemic and local antibody responses to gastric Campylobacter pyloridis in non-ulcer dyspepsia. *Gut*, **27**, 642–647.

[122] Birkholz, S., Schneider, T., Knipp, U., Stallmach, A., and Zeitz, M. (1998) Decreased Helicobacter pylori-specific gastric secretory IgA antibodies in infected patients. *Digestion*, **59**, 638–645.

[123] Ermak, T. H., Giannasca, P. J., Nichols, R., Myers, G. A., Nedrud, J., Weltzin, R., Lee, C. K., Kleanthous, H., and Monath, T. P. (1998) Immunization of mice with urease vaccine affords protection against Helicobacter pylori infection in the absence of antibodies and is mediated by MHC class II-restricted responses. *The Journal of experimental medicine*, **188**, 2277–2288.

[124] Blanchard, T. G., Czinn, S. J., Redline, R. W., Sigmund, N., Harriman, G., and Nedrud, J. G. (1999) Antibody-independent protective mucosal immunity to gastric helicobacter infection in mice. *Cellular immunology*, **191**, 74–80.

[125] Garhart, C. A., Nedrud, J. G., Heinzel, F. P., Sigmund, N. E., and Czinn, S. J. (2003) Vaccine-induced protection against Helicobacter pylori in mice lacking both antibodies and interleukin-4. *Infection and immunity*, **71**, 3628–3633.

[126] Nedrud, J. G., Czinn, S. J., Ding, H., Zagorski, B. M., Redline, R. W., Twaddell, W., and Blanchard, T. G. (2012) Lack of genetic influence on the innate inflammatory response to helicobacter infection of the gastric mucosa. *Frontiers in immunology*, **3**, 181.

[127] Bontems, P., Robert, F., van Gossum, A., Cadranel, S., and Mascart, F. (2003) Helicobacter pylori modulation of gastric and duodenal mucosal T cell cytokine secretions in children compared with adults. *Helicobacter*, **8**, 216–226.

[128] Nurgalieva, Z. Z., Conner, M. E., Opekun, A. R., Zheng, C. Q., Elliott, S. N., Ernst, P. B., Osato, M., Estes, M. K., and Graham, D. Y. (2005) B-cell and T-cell immune responses to experimental Helicobacter pylori infection in humans. *Infection and immunity*, **73**, 2999–3006.

[129] Strömberg, E., Lundgren, A., Edebo, A., Lundin, S., Svennerholm, A.-M., and Lindholm, C. (2003) Increased frequency of activated T-cells in the Helicobacter pylori-infected antrum and duodenum. *FEMS immunology and medical microbiology*, **36**, 159–168.

[130] Hitzler, I., Kohler, E., Engler, D. B., Yazgan, A. S., and Muller, A. (2012) The role of Th cell subsets in the control of Helicobacter infections and in T cell-driven gastric immunopathology. *Frontiers in immunology*, **3**, 142.

[131] Fan, X. J., Chua, A., Shahi, C. N., McDevitt, J., Keeling, P. W., and Kelleher, D. (1994) Gastric T lymphocyte responses to Helicobacter pylori in patients with H pylori colonisation. *Gut*, **35**, 1379–1384.

[132] Bamford, K. B., Fan, X., Crowe, S. E., Leary, J. F., Gourley, W. K., Luthra, G. K., Brooks, E. G., Graham, D. Y., Reyes, V. E., and Ernst, P. B. (1998) Lymphocytes in the human gastric mucosa during Helicobacter pylori have a T helper cell 1 phenotype. *Gastroenterology*, **114**, 482–492.

[133] Quiding-Järbrink, M., Lundin, B. S., Lönroth, H., and Svennerholm, A. M. (2001) CD4+ and CD8+ T cell responses in Helicobacter pylori-infected individuals. *Clinical and experimental immunology*, **123**, 81–87.

[134] Pappo, J., Torrey, D., Castriotta, L., Savinainen, A., Kabok, Z., and Ibraghimov, A. (1999) Helicobacter pylori infection in immunized mice lacking major histocompatibility complex class I and class II functions. *Infection and immunity*, **67**, 337–341.

[135] Tan, M. P., Pedersen, J., Zhan, Y., Lew, A. M., Pearse, M. J., Wijburg, Odilia L C, and Strugnell, R. A. (2008) CD8+ T cells are associated with severe gastritis in Helicobacter pylori-infected mice in the absence of CD4+ T cells. *Infection and immunity*, **76**, 1289–1297.

[136] Flach, C.-F., Östberg, A. K., Nilsson, A.-T., Malefyt, Rene De Waal, and Raghavan, S. (2011) Proinflammatory cytokine gene expression in the stomach correlates with vaccine-induced protection against Helicobacter pylori infection in mice: an important role for interleukin-17 during the effector phase. *Infection and immunity*, **79**, 879–886.

[137] Gray, B. M., Fontaine, C. A., Poe, S. A., and Eaton, K. A. (2013) Complex T cell interactions contribute to Helicobacter pylori gastritis in mice. *Infection and immunity*, **81**, 740–752.

[138] Karttunen, R., Karttunen, T., Ekre, H. P., and MacDonald, T. T. (1995) Interferon gamma and interleukin 4 secreting cells in the gastric antrum in Helicobacter pylori positive and negative gastritis. *Gut*, **36**, 341–345.

[139] Sommer, F., Faller, G., Konturek, P., Kirchner, T., Hahn, E. G., Zeus, J., Rollinghoff, M., and Lohoff, M. (1998) Antrum- and corpus mucosa-infiltrating CD4(+) lymphocytes in Helicobacter pylori gastritis display a Th1 phenotype. *Infection and immunity*, **66**, 5543–5546.

[140] D'Elios, M. M., Manghetti, M., Carli, M. d., Costa, F., Baldari, C. T., Burroni, D., Telford, J. L., Romagnani, S., and Del Prete, G. (1997) T helper 1 effector cells specific for Helicobacter pylori in the gastric antrum of patients with peptic ulcer disease. *Journal of immunology*, **158**, 962–967.

[141] Yamamoto, T., Kita, M., Ohno, T., Iwakura, Y., Sekikawa, K., and Imanishi, J. (2004) Role of tumor necrosis factor-alpha and interferon-gamma in Helicobacter pylori infection. *Microbiology and immunology*, **48**, 647–654.

[142] Obonyo, M., Guiney, D. G., Harwood, J., Fierer, J., and Cole, S. P. (2002) Role of gamma interferon in Helicobacter pylori induction of inflammatory mediators during murine infection. *Infection and immunity*, **70**, 3295–3299.

[143] Eaton, K. A., Benson, L. H., Haeger, J., and Gray, B. M. (2006) Role of transcription factor T-bet expression by CD4+ cells in gastritis due to Helicobacter pylori in mice. *Infection and immunity*, **74**, 4673–4684.

[144] Korn, T., Bettelli, E., Oukka, M., and Kuchroo, V. K. (2009) IL-17 and Th17 Cells. *Annual review of immunology*, **27**, 485–517.

[145] Mills, Kingston H. G. (2008) Induction, function and regulation of IL-17-producing T cells. *European journal of immunology*, **38**, 2636–2649.

[146] Serrano, C., Wright, S. W., Bimczok, D., Shaffer, C. L., Cover, T. L., Venegas, A., Salazar, M. G., Smythies, L. E., Harris, P. R., and Smith, P. D. (2013) Downregulated Th17 responses are associated with reduced gastritis in Helicobacter pylori-infected children. *Mucosal immunology*, **6**, 950–959.

[147] Freire de Melo, Fabricio, et al. (2012) A regulatory instead of an IL-17 T response predominates in Helicobacter pylori-associated gastritis in children. *Microbes and infection / Institut Pasteur*, **14**, 341–347.

[148] Shiomi, S., et al. (2008) IL-17 is involved in Helicobacter pylori-induced gastric inflammatory responses in a mouse model. *Helicobacter*, **13**, 518–524.

[149] Shi, Y., et al. (2010) Helicobacter pylori-induced Th17 responses modulate Th1 cell responses, benefit bacterial growth, and contribute to pathology in mice. *Journal of immunology*, **184**, 5121–5129.

[150] Velin, D., Favre, L., Bernasconi, E., Bachmann, D., Pythoud, C., Saiji, E., Bouzourene, H., and Michetti, P. (2009) Interleukin-17 is a critical mediator of vaccine-induced reduction of Helicobacter infection in the mouse model. *Gastroenterology*, **136**, 2237–2246.e1.

[151] DeLyria, E. S., Redline, R. W., and Blanchard, T. G. (2009) Vaccination of mice against H pylori induces a strong Th-17 response and immunity that is neutrophil dependent. *Gastroenterology*, **136**, 247–256.

[152] Harris, P. R., et al. (2008) Helicobacter pylori gastritis in children is associated with a regulatory T-cell response. *Gastroenterology*, **134**, 491–499.

[153] Lundgren, A., et al. (2005) Mucosal FOXP3-expressing CD4+ CD25high regulatory T cells in Helicobacter pylori-infected patients. *Infection and immunity*, **73**, 523–531.

[154] Kandulski, A., Wex, T., Kuester, D., Peitz, U., Gebert, I., Roessner, A., and Malfertheiner, P. (2008) Naturally occurring regulatory T cells (CD4+, CD25high, FOXP3+) in the antrum and cardia are associated with higher H. pylori colonization and increased gene expression of TGF-beta1. *Helicobacter*, **13**, 295–303.

[155] Wu, Y.-Y., Chen, J.-H., Kao, J.-T., Liu, K.-C., Lai, C.-H., Wang, Y.-M., Hsieh, C.-T., Tzen, Jason T. C., and Hsu, P.-N. (2011) Expression of CD25(high) regulatory T cells and PD-1 in gastric infiltrating CD4(+) T lymphocytes in patients with Helicobacter pylori infection. *Clinical and vaccine immunology : CVI*, **18**, 1198–1201.

[156] Zhang, M., Liu, M., Luther, J., and Kao, J. Y. (2010) Helicobacter pylori directs tolerogenic programming of dendritic cells. *Gut microbes*, **1**, 325–329.

[157] Chen, W., Shu, D., and Chadwick, V. S. (2001) Helicobacter pylori infection: mechanism of colonization and functional dyspepsia Reduced colonization of gastric mucosa by Helicobacter pylori in mice deficient in interleukin-10. *Journal of gastroenterology and hepatology*, **16**, 377–383.

[158] Ismail, H. F., Fick, P., Zhang, J., Lynch, R. G., and Berg, D. J. (2003) Depletion of neutrophils in IL-10(-/-) mice delays clearance of gastric Helicobacter infection and decreases the Th1 immune response to Helicobacter. *Journal of immunology*, **170**, 3782–3789.

[159] Matsumoto, Y., Blanchard, T. G., Drakes, M. L., Basu, M., Redline, R. W., Levine, A. D., and Czinn, S. J. (2005) Eradication of Helicobacter pylori and resolution of gastritis in the gastric mucosa of IL-10-deficient mice. *Helicobacter*, **10**, 407–415.

[160] Boncristiano, M., Paccani, S. R., Barone, S., Ulivieri, C., Patrussi, L., Ilver, D., Amedei, A., D'Elios, M. M., Telford, J. L., and Baldari, C. T. (2003) The Helicobacter pylori vacuolating toxin inhibits T cell activation by two independent mechanisms. *The Journal of experimental medicine*, **198**, 1887–1897.

[161] Gebert, B., Fischer, W., Weiss, E., Hoffmann, R., and Haas, R. (2003) Helicobacter pylori vacuolating cytotoxin inhibits T lymphocyte activation. *Science*, **301**, 1099–1102.

[162] Sundrud, M. S., Torres, V. J., Unutmaz, D., and Cover, T. L. (2004) Inhibition of primary human T cell proliferation by Helicobacter pylori vacuolating toxin (VacA) is independent of VacA effects on IL-2 secretion. *Proceedings of the National Academy of Sciences of the United States of America*, **101**, 7727–7732.

[163] Schmees, C., Prinz, C., Treptau, T., Rad, R., Hengst, L., Voland, P., Bauer, S., Brenner, L., Schmid, R. M., and Gerhard, M. (2007) Inhibition of T-cell proliferation by Helicobacter pylori gamma-glutamyl transpeptidase. *Gastroenterology*, **132**, 1820–1833.

[164] Gerhard, M., et al. (2005) A secreted low-molecular-weight protein from Helicobacter pylori induces cell-cycle arrest of T cells. *Gastroenterology*, **128**, 1327–1339.

[165] Leduc, D., Gallaud, J., Stingl, K., and Reuse, H. d. (2010) Coupled amino acid deamidase-transport systems essential for Helicobacter pylori colonization. *Infection and immunity*, **78**, 2782–2792.

[166] Megraud, F., Bonnet, F., Garnier, M., and Lamouliatte, H. (1985) Characterization of "Campylobacter pyloridis" by culture, enzymatic profile, and protein content. *Journal of clinical microbiology*, **22**, 1007–1010.

[167] Wachino, J.-I., Shibayama, K., Suzuki, S., Yamane, K., Mori, S., and Arakawa, Y. (2010) Profile of Expression of Helicobacter pylori gamma-glutamyltranspeptidase. *Helicobacter*, **15**, 184–192.

[168] Backert, S., Kwok, T., Schmid, M., Selbach, M., Moese, S., Peek, R. M., König, W., Meyer, T. F., and Jungblut, P. R. (2005) Subproteomes of soluble and structure-bound Helicobacter pylori proteins analyzed by two-dimensional gel electrophoresis and mass spectrometry. *Proteomics*, **5**, 1331–1345.

[169] Boanca, G., Sand, A., and Barycki, J. J. (2006) Uncoupling the enzymatic and autoprocessing activities of Helicobacter pylori gamma-glutamyltranspeptidase. *The Journal of biological chemistry*, **281**, 19029–19037.

[170] Morrow, A. L., Williams, K., Sand, A., Boanca, G., and Barycki, J. J. (2007) Characterization of Helicobacter pylori gamma-glutamyltranspeptidase reveals the molecular basis for substrate specificity and a critical role for the tyrosine 433-containing loop in catalysis. *Biochemistry*, **46**, 13407–13414.

[171] Gong, M., Ling, Samantha Shi Min, Lui, S. Y., Yeoh, K. G., and Ho, B. (2010) Helicobacter pylori gamma-glutamyl transpeptidase is a pathogenic factor in the development of peptic ulcer disease. *Gastroenterology*, **139**, 564–573.

[172] Rossi, M., Bolz, C., Revez, J., Javed, S., El-Najjar, N., Anderl, F., Hyytiainen, H., Vuorela, P., Gerhard, M., and Hanninen, M.-L. (2012) Evidence for conserved function of gamma-glutamyltranspeptidase in Helicobacter genus. *PloS one*, **7**, e30543.

[173] Tate, S. S. and Meister, A. (1981) gamma-Glutamyl transpeptidase: catalytic, structural and functional aspects. *Molecular and cellular biochemistry*, **39**, 357–368.

[174] Stark, R. M., Suleiman, M. S., Hassan, I. J., Greenman, J., and Millar, M. R. (1997) Amino acid utilisation and deamination of glutamine and asparagine by Helicobacter pylori. *Journal of medical microbiology*, **46**, 793–800.

[175] Shibayama, K., Wachino, J.-I., Arakawa, Y., Saidijam, M., Rutherford, N. G., and Henderson, Peter J. F. (2007) Metabolism of glutamine and glutathione via gamma-glutamyltranspeptidase and glutamate transport in Helicobacter pylori: possible significance in the pathophysiology of the organism. *Molecular microbiology*, **64**, 396–406.

[176] Mendz, G. L. and Hazell, S. L. (1995) Aminoacid utilization by Helicobacter pylori. *The international journal of biochemistry & cell biology*, **27**, 1085–1093.

[177] Chalk, P. A., Roberts, A. D., and Blows, W. M. (1994) Metabolism of pyruvate and glucose by intact cells of Helicobacter pylori studied by 13C NMR spectroscopy. *Microbiology (Reading, England)*, **140 (Pt 8)**, 2085–2092.

[178] Garner, R. M., Fulkerson, J. JR, and Mobley, H. L. (1998) Helicobacter pylori glutamine synthetase lacks features associated with transcriptional and posttranslational regulation. *Infection and immunity*, **66**, 1839–1847.

[179] Miller, E. F. and Maier, R. J. (2014) Ammonium metabolism enzymes aid Helicobacter pylori acid resistance. *Journal of bacteriology*, **196**, 3074–3081.

[180] Williams, C. L., Preston, T., Hossack, M., Slater, C., and McColl, K. E. (1996) Helicobacter pylori utilises urea for amino acid synthesis. *FEMS immunology and medical microbiology*, **13**, 87–94.

[181] Bauerfeind, P., Garner, R., Dunn, B. E., and Mobley, H. L. (1997) Synthesis and activity of Helicobacter pylori urease and catalase at low pH. *Gut*, **40**, 25–30.

[182] McConnell, E. L., Basit, A. W., and Murdan, S. (2008) Measurements of rat and mouse gastrointestinal pH, fluid and lymphoid tissue, and implications for in-vivo experiments. *The Journal of pharmacy and pharmacology*, **60**, 63–70.

[183] Rektorschek, M., Weeks, D., Sachs, G., and Melchers, K. (1998) Influence of pH on metabolism and urease activity of Helicobacter pylori. *Gastroenterology*, **115**, 628–641.

[184] Scott, D. R., Marcus, E. A., Weeks, D. L., Lee, A., Melchers, K., and Sachs, G. (2000) Expression of the Helicobacter pylori ureI gene is required for acidic pH activation of cytoplasmic urease. *Infection and immunity*, **68**, 470–477.

[185] Bury-Moné, S., Skouloubris, S., Labigne, A., and Reuse, H. d. (2001) The Helicobacter pylori UreI protein: role in adaptation to acidity and identification of residues essential for its activity and for acid activation. *Molecular microbiology*, **42**, 1021–1034.

[186] Neithercut, W. D., Milne, A., Chittajallu, R. S., el Nujumi, A M, and McColl, K. E. (1991) Detection of Helicobacter pylori infection of the gastric mucosa by measurement of gastric aspirate ammonium and urea concentrations. *Gut*, **32**, 973–976.

[187] McGovern, K. J., Blanchard, T. G., Gutierrez, J. A., Czinn, S. J., Krakowka, S., and Youngman, P. (2001) gamma-Glutamyltransferase is a Helicobacter pylori virulence factor but is not essential for colonization. *Infection and immunity*, **69**, 4168–4173.

[188] Rimbara, E., Mori, S., Kim, H., and Shibayama, K. (2013) Role of gamma-glutamyltranspeptidase in the pathogenesis of Helicobacter pylori infection. *Microbiology and immunology*, **57**, 665–673.

[189] Shibayama, K., et al. (2003) A novel apoptosis-inducing protein from Helicobacter pylori. *Molecular microbiology*, **47**, 443–451.

[190] Kim, K.-M., Lee, S.-G., Park, M.-G., Song, J.-Y., Kang, H.-L., Lee, W.-K., Cho, M.-J., Rhee, K.-H., Youn, H.-S., and Baik, S.-C. (2007) Gamma-glutamyltranspeptidase of Helicobacter pylori induces mitochondria-mediated apoptosis in AGS cells. *Biochemical and biophysical research communications*, **355**, 562–567.

[191] Flahou, B., et al. (2011) Gastric epithelial cell death caused by Helicobacter suis and Helicobacter pylori gamma-glutamyl transpeptidase is mainly glutathione degradation-dependent. *Cellular microbiology*, **13**, 1933–1955.

[192] Valenzuela, M., Bravo, D., Canales, J., Sanhueza, C., Díaz, N., Almarza, O., Toledo, H., and Quest, Andrew F. G. (2013) Helicobacter pylori-induced loss of survivin and gastric cell viability is attributable to secreted bacterial gamma-glutamyl transpeptidase activity. *The Journal of infectious diseases*, **208**, 1131–1141.

[193] Busiello, I., Acquaviva, R., Di Popolo, A., Blanchard, T. G., Ricci, V., Romano, M., and Zarrilli, R. (2004) Helicobacter pylori gamma-glutamyltranspeptidase upregulates COX-2 and EGF-related peptide expression in human gastric cells. *Cellular microbiology*, **6**, 255–267.

[194] Gong, M. and Ho, B. (2004) Prominent role of gamma-glutamyl-transpeptidase on the growth of Helicobacter pylori. *World journal of gastroenterology : WJG*, **10**, 2994–2996.

[195] Schwartz, R. H. (1990) A cell culture model for T lymphocyte clonal anergy. *Science*, **248**, 1349–1356.

[196] Lenschow, D. J., Walunas, T. L., and Bluestone, J. A. (1996) CD28/B7 system of T cell costimulation. *Annual review of immunology*, **14**, 233–258.

[197] Wang, R., et al. (2011) The transcription factor Myc controls metabolic reprogramming upon T lymphocyte activation. *Immunity*, **35**, 871–882.

[198] Greiner, E. F., Guppy, M., and Brand, K. (1994) Glucose is essential for proliferation and the glycolytic enzyme induction that provokes a transition to glycolytic energy production. *The Journal of biological chemistry*, **269**, 31484–31490.

[199] Pfeiffer, T., Schuster, S., and Bonhoeffer, S. (2001) Cooperation and competition in the evolution of ATP-producing pathways. *Science*, **292**, 504–507.

[200] Ardawi, M. S. and Newsholme, E. A. (1983) Glutamine metabolism in lymphocytes of the rat. *The Biochemical journal*, **212**, 835–842.

[201] Ardawi, M. S. (1988) Glutamine and glucose metabolism in human peripheral lymphocytes. *Metabolism: clinical and experimental*, **37**, 99–103.

[202] Calder, P. C. (1995) Fuel utilization by cells of the immune system. *The Proceedings of the Nutrition Society*, **54**, 65–82.

[203] Newsholme, P., Procopio, J., Lima, Manuela Maria Ramos, Pithon-Curi, T. C., and Curi, R. (2003) Glutamine and glutamate–their central role in cell metabolism and function. *Cell biochemistry and function*, **21**, 1–9.

[204] Newsholme, P., Curi, R., Pithon Curi, T. C., Murphy, C. J., Garcia, C., and Pires de Melo, M. (1999) Glutamine metabolism by lymphocytes, macrophages, and neutrophils: its importance in health and disease. *The Journal of nutritional biochemistry*, **10**, 316–324.

[205] Newsholme, E. A., Crabtree, B., and Ardawi, M. S. (1985) Glutamine metabolism in lymphocytes: its biochemical, physiological and clinical importance. *Quarterly journal of experimental physiology*, **70**, 473–489.

[206] Chang, W.-K., Yang, K. D., Chuang, H., Jan, J.-T., and Shaio, M.-F. (2002) Glutamine protects activated human T cells from apoptosis by up-regulating glutathione and Bcl-2 levels. *Clinical immunology (Orlando, Fla*, **104**, 151–160.

[207] Yaqoob, P. and Calder, P. C. (1997) Glutamine requirement of proliferating T lymphocytes. *Nutrition*, **13**, 646–651.

[208] Heikkila, R., Schwab, G., Wickstrom, E., Loke, S. L., Pluznik, D. H., Watt, R., and Neckers, L. M. (1987) A c-myc antisense oligodeoxynucleotide inhibits entry into S phase but not progress from G0 to G1. *Nature*, **328**, 445–449.

[209] Man, K., et al. (2013) The transcription factor IRF4 is essential for TCR affinity-mediated metabolic programming and clonal expansion of T cells. *Nature immunology*, **14**, 1155–1165.

[210] Beugnet, A., Tee, A. R., Taylor, P. M., and Proud, C. G. (2003) Regulation of targets of mTOR (mammalian target of rapamycin) signalling by intracellular amino acid availability. *The Biochemical journal*, **372**, 555–566.

[211] Delgoffe, G. M., Kole, T. P., Zheng, Y., Zarek, P. E., Matthews, K. L., Xiao, B., Worley, P. F., Kozma, S. C., and Powell, J. D. (2009) The mTOR kinase differentially regulates effector and regulatory T cell lineage commitment. *Immunity*, **30**, 832–844.

[212] Nicklin, P., et al. (2009) Bidirectional transport of amino acids regulates mTOR and autophagy. *Cell*, **136**, 521–534.

[213] Tamás, P., Hawley, S. A., Clarke, R. G., Mustard, K. J., Green, K., Hardie, D. G., and Cantrell, D. A. (2006) Regulation of the energy sensor AMP-activated protein kinase by antigen receptor and Ca2+ in T lymphocytes. *The Journal of experimental medicine*, **203**, 1665–1670.

[214] Jacobs, S. R., Herman, C. E., MacIver, N. J., Wofford, J. A., Wieman, H. L., Hammen, J. J., and Rathmell, J. C. (2008) Glucose uptake is limiting in T cell activation and requires CD28-mediated Akt-dependent and independent pathways. *Journal of immunology*, **180**, 4476–4486.

[215] Peter, C., Waldmann, H., and Cobbold, S. P. (2010) mTOR signalling and metabolic regulation of T cell differentiation. *Current opinion in immunology*, **22**, 655–661.

[216] Zaborske, J. M., Wu, X., Wek, R. C., and Pan, T. (2010) Selective control of amino acid metabolism by the GCN2 eIF2 kinase pathway in Saccharomyces cerevisiae. *BMC biochemistry*, **11**, 29.

[217] Kilberg, M. S., Pan, Y.-X., Chen, H., and Leung-Pineda, V. (2005) Nutritional control of gene expression: how mammalian cells respond to amino acid limitation. *Annual review of nutrition*, **25**, 59–85.

[218] Hundal, H. S. and Taylor, P. M. (2009) Amino acid transceptors: gate keepers of nutrient exchange and regulators of nutrient signaling. *American journal of physiology*, **296**, E603–13.

[219] Carr, E. L., Kelman, A., Wu, G. S., Gopaul, R., Senkevitch, E., Aghvanyan, A., Turay, A. M., and Frauwirth, K. A. (2010) Glutamine uptake and metabolism are coordinately regulated by ERK/MAPK during T lymphocyte activation. *Journal of immunology*, **185**, 1037–1044.

[220] Szondy, Z. and Newsholme, E. A. (1990) The effect of various concentrations of nucleobases, nucleosides or glutamine on the incorporation of [3H]thymidine into DNA in rat mesenteric-lymph-node lymphocytes stimulated by phytohaemagglutinin. *The Biochemical journal*, **270**, 437–440.

[221] Nakaya, M., Xiao, Y., Zhou, X., Chang, J.-H., Chang, M., Cheng, X., Blonska, M., Lin, X., and Sun, S.-C. (2014) Inflammatory T Cell Responses Rely on Amino Acid Transporter ASCT2 Facilitation of Glutamine Uptake and mTORC1 Kinase Activation. *Immunity*.

[222] Franchi-Gazzola, R., Visigalli, R., Bussolati, O., Dall'Asta, V., and Gazzola, G. C. (1999) Adaptive increase of amino acid transport system A requires ERK1/2 activation. *The Journal of biological chemistry*, **274**, 28922–28928.

[223] Bungard, C. I. and McGivan, J. D. (2004) Glutamine availability up-regulates expression of the amino acid transporter protein ASCT2 in HepG2 cells and stimulates the ASCT2 promoter. *The Biochemical journal*, **382**, 27–32.

[224] Wischmeyer, P. E., Dhaliwal, R., McCall, M., Ziegler, T. R., and Heyland, D. K. (2014) Parenteral glutamine supplementation in critical illness: a systematic review. *Critical care (London, England)*, **18**, R76.

[225] Amagase, K., Nakamura, E., Endo, T., Hayashi, S., Hasumura, M., Uneyama, H., Torii, K., and Takeuchi, K. (2010) New frontiers in gut nutrient sensor research: prophylactic effect of glutamine against Helicobacter pylori-induced gastric diseases in Mongolian gerbils. *Journal of pharmacological sciences*, **112**, 25–32.

[226] Hagen, S. J., Ohtani, M., Zhou, J.-R., Taylor, N. S., Rickman, B. H., Blackburn, G. L., and Fox, J. G. (2009) Inflammation and foveolar hyperplasia are reduced by supplemental dietary glutamine during Helicobacter pylori infection in mice. *The Journal of nutrition*, **139**, 912–918.

[227] Dent, J. C. and McNulty, C. A. (1988) Evaluation of a new selective medium for Campylobacter pylori. *European journal of clinical microbiology & infectious diseases : official publication of the European Society of Clinical Microbiology*, **7**, 555–558.

[228] Wickham, S., West, M. B., Cook, P. F., and Hanigan, M. H. (2011) Gamma-glutamyl compounds: substrate specificity of gamma-glutamyl transpeptidase enzymes. *Analytical biochemistry*, **414**, 208–214.

[229] Schneider, U., Schwenk, H. U., and Bornkamm, G. (1977) Characterization of EBV-genome negative "null" and "T" cell lines derived from children with acute lymphoblastic leukemia and leukemic transformed non-Hodgkin lymphoma. *International journal of cancer. Journal international du cancer*, **19**, 621–626.

[230] Livak, K. J. and Schmittgen, T. D. (2001) Analysis of relative gene expression data using real-time quantitative PCR and the 2(-Delta Delta C(T)) Method. *Methods*, **25**, 402–408.

[231] Zhang, G., Ducatelle, R., Pasmans, F., D'Herde, K., Huang, L., Smet, A., Haesebrouck, F., and Flahou, B. (2013) Effects of Helicobacter suis gamma-glutamyl transpeptidase on lymphocytes: modulation by glutamine and glutathione supplementation and outer membrane vesicles as a putative delivery route of the enzyme. *PloS one*, **8**, e77966.

[232] Wise, D. R., et al. (2008) Myc regulates a transcriptional program that stimulates mitochondrial glutaminolysis and leads to glutamine addiction. *Proceedings of the National Academy of Sciences of the United States of America*, **105**, 18782–18787.

[233] Liu, X., Lin, C.-Y., Lei, M., Yan, S., Zhou, T., and Erikson, R. L. (2005) CCT chaperonin complex is required for the biogenesis of functional Plk1. *Molecular and cellular biology*, **25**, 4993–5010.

[234] Won, K. A., Schumacher, R. J., Farr, G. W., Horwich, A. L., and Reed, S. I. (1998) Maturation of human cyclin E requires the function of eukaryotic chaperonin CCT. *Molecular and cellular biology*, **18**, 7584–7589.

[235] Yuryev, A. and Wennogle, L. P. (2003) Novel raf kinase protein-protein interactions found by an exhaustive yeast two-hybrid analysis. *Genomics*, **81**, 112–125.

[236] Koch, H. B., Zhang, R., Verdoodt, B., Bailey, A., Zhang, C.-D., Yates, J. R., Menssen, A., and Hermeking, H. (2007) Large-scale identification of c-MYC-associated proteins using a combined TAP/MudPIT approach. *Cell cycle*, **6**, 205–217.

[237] Algood, Holly M. Scott, Gallo-Romero, J., Wilson, K. T., Peek, Richard M. JR, and Cover, T. L. (2007) Host response to Helicobacter pylori infection before initiation of the adaptive immune response. *FEMS immunology and medical microbiology*, **51**, 577–586.

[238] Rokbi, B., Seguin, D., Guy, B., Mazarin, V., Vidor, E., Mion, F., Cadoz, M., and Quentin-Millet, M. J. (2001) Assessment of Helicobacter pylori gene expression within mouse and human gastric mucosae by real-time reverse transcriptase PCR. *Infection and immunity*, **69**, 4759–4766.

[239] Wen, S., Felley, C. P., Bouzourene, H., Reimers, M., Michetti, P., and Pan-Hammarström, Q. (2004) Inflammatory gene profiles in gastric mucosa during Helicobacter pylori infection in humans. *Journal of immunology*, **172**, 2595–2606.

[240] Hellmig, S., Mascheretti, S., Fölsch, U., and Schreiber, S. (2005) Functional promotor polymorphism in RANTES gene does not influence the clinical course of Helicobacter pylori infection. *Journal of gastroenterology and hepatology*, **20**, 405–408.

[241] Manhart, N., Vierlinger, K., Spittler, A., Bergmeister, H., Sautner, T., and Roth, E. (2001) Oral feeding with glutamine prevents lymphocyte and glutathione depletion of Peyer's patches in endotoxemic mice. *Annals of surgery*, **234**, 92–97.

[242] Hersh, E. M. (1971) L-glutaminase: suppression of lymphocyte blastogenic responses in vitro. *Science (New York, N.Y.)*, **172**, 736–738.

[243] Levring, T. B., Hansen, A. K., Nielsen, B. L., Kongsbak, M., Essen, Marina Rode von, Woetmann, A., Odum, N., Bonefeld, C. M., and Geisler, C. (2012) Activated human CD4+ T cells express transporters for both cysteine and cystine. *Scientific reports*, **2**, 266.

[244] Chang, W. K., Yang, K. D., and Shaio, M. F. (1999) Lymphocyte proliferation modulated by glutamine: involved in the endogenous redox reaction. *Clinical and experimental immunology*, **117**, 482–488.

[245] Shirin, H., Pinto, J. T., Liu, L. U., Merzianu, M., Sordillo, E. M., and Moss, S. F. (2001) Helicobacter pylori decreases gastric mucosal glutathione. *Cancer letters*, **164**, 127–133.

[246] Oijen, A. H., Verhulst, M. L., Roelofs, H. M., Peters, W. H., Boer, W. A. de, and Jansen, J. B. (2001) Eradication of Helicobacter pylori restores glutathione S-transferase activity and glutathione levels in antral mucosa. *Japanese journal of cancer research : Gann*, **92**, 1329–1334.

[247] Horig, H., Spagnoli, G. C., Filgueira, L., Babst, R., Gallati, H., Harder, F., Juretic, A., and Heberer, M. (1993) Exogenous glutamine requirement is confined to late events of T cell activation. *Journal of cellular biochemistry*, **53**, 343–351.

[248] McNamee, E. N., Korns Johnson, D., Homann, D., and Clambey, E. T. (2013) Hypoxia and hypoxia-inducible factors as regulators of T cell development, differentiation, and function. *Immunologic research*, **55**, 58–70.

[249] Powell, J. D., Lerner, C. G., and Schwartz, R. H. (1999) Inhibition of cell cycle progression by rapamycin induces T cell clonal anergy even in the presence of costimulation. *Journal of immunology*, **162**, 2775–2784.

[250] Zheng, Y., Collins, S. L., Lutz, M. A., Allen, A. N., Kole, T. P., Zarek, P. E., and Powell, J. D. (2007) A role for mammalian target of rapamycin in regulating T cell activation versus anergy. *Journal of immunology*, **178**, 2163–2170.

[251] Kopf, H., La Rosa, Gonzalo M. de, Howard, O. M. Zack, and Chen, X. (2007) Rapamycin inhibits differentiation of Th17 cells and promotes generation of FoxP3+ T regulatory cells. *International immunopharmacology*, **7**, 1819–1824.

[252] Waickman, A. T. and Powell, J. D. (2012) mTOR, metabolism, and the regulation of T-cell differentiation and function. *Immunological reviews*, **249**, 43–58.

[253] Yao, S., Buzo, B. F., Pham, D., Jiang, L., Taparowsky, E. J., Kaplan, M. H., and Sun, J. (2013) Interferon regulatory factor 4 sustains CD8(+) T cell expansion and effector differentiation. *Immunity*, **39**, 833–845.

[254] Kavermann, H., Burns, B. P., Angermuller, K., Odenbreit, S., Fischer, W., Melchers, K., and Haas, R. (2003) Identification and characterization of Helicobacter pylori genes essential for gastric colonization. *The Journal of experimental medicine*, **197**, 813–822.

[255] Boutry, C., Bos, C., Matsumoto, H., Even, P., Azzout-Marniche, D., Tome, D., and Blachier, F. (2011) Effects of monosodium glutamate supplementation on glutamine metabolism in adult rats. *Frontiers in bioscience (Elite edition)*, **3**, 279–290.

[256] Akiba, Y., Watanabe, C., Mizumori, M., and Kaunitz, J. D. (2009) Luminal L-glutamate enhances duodenal mucosal defense mechanisms via multiple glutamate receptors in rats. *American journal of physiology. Gastrointestinal and liver physiology*, **297**, G781–91.

[257] Neithercut, W. D., Greig, M. A., Hossack, M., and McColl, K. E. (1991) Suicidal destruction of Helicobacter pylori: metabolic consequence of intracellular accumulation of ammonia. *Journal of clinical pathology*, **44**, 380–384.

[258] Rieder, G., Einsiedl, W., Hatz, R. A., Stolte, M., Enders, G. A., and Walz, A. (2001) Comparison of CXC chemokines ENA-78 and interleukin-8 expression in Helicobacter pylori-associated gastritis. *Infection and immunity*, **69**, 81–88.

[259] Mustapha, P., et al. (2014) Chemokines and antimicrobial peptides have a cag-dependent early response to Helicobacter pylori infection in primary human gastric epithelial cells. *Infection and immunity*, **82**, 2881–2889.

[260] Lina, T. T., Pinchuk, I. V., House, J., Yamaoka, Y., Graham, D. Y., Beswick, E. J., and Reyes, V. E. (2013) CagA-dependent downregulation of B7-H2 expression on gastric mucosa and inhibition of Th17 responses during Helicobacter pylori infection. *Journal of immunology*, **191**, 3838–3846.

[261] Ruiz, V. E., Sachdev, M., Zhang, S., Wen, S., and Moss, S. F. (2012) Isolating, immunophenotyping and ex vivo stimulation of CD4+ and CD8+ gastric lymphocytes during murine Helicobacter pylori infection. *Journal of immunological methods*, **384**, 157–163.

[262] Krauss-Etschmann, S., Gruber, R., Plikat, K., Antoni, I., Demmelmair, H., Reinhardt, D., and Koletzko, S. (2005) Increase of antigen-presenting cells in the gastric mucosa of Helicobacter pylori-infected children. *Helicobacter*, **10**, 214–222.

[263] Flach, C.-F., Lange, S., Jennische, E., Lönnroth, I., and Holmgren, J. (2005) Cholera toxin induces a transient depletion of CD8+ intraepithelial lymphocytes in the rat small intestine as detected by microarray and immunohistochemistry. *Infection and immunity*, **73**, 5595–5602.

[264] Elson, C. O., Holland, S. P., Dertzbaugh, M. T., Cuff, C. F., and Anderson, A. O. (1995) Morphologic and functional alterations of mucosal T cells by cholera toxin and its B subunit. *Journal of immunology*, **154**, 1032–1040.

[265] Ricci, V., Sommi, P., Fiocca, R., Cova, E., Figura, N., Romano, M., lvey, K. J., Solcia, E., and Ventura, U. (1993) Cytotoxicity of Helicobacter pylori on human gastric epithelial cells in vitro: role of cytotoxin(s) and ammonia. *European Journal of Gastroenterology & Hepatology*, **5**.

[266] Igarashi, M., Kitada, Y., Yoshiyama, H., Takagi, A., Miwa, T., and Koga, Y. (2001) Ammonia as an accelerator of tumor necrosis factor alpha-induced apoptosis of gastric epithelial cells in Helicobacter pylori infection. *Infection and immunity*, **69**, 816–821.

[267] James, L. A., Lunn, P. G., Middleton, S., and Elia, M. (1998) Distribution of glutaminase and glutamine synthetase activities in the human gastrointestinal tract. *Clinical science*, **94**, 313–319.

[268] James, L. A., Lunn, P. G., and Elia, M. (1998) Glutamine metabolism in the gastrointestinal tract of the rat assess by the relative activities of glutaminase (EC 3.5.1.2) and glutamine synthetase (EC 6.3.1.2). *The British journal of nutrition*, **79**, 365–372.

[269] van Straaten, Henny W. M., He, Y., van Duist, Marjan M., Labruyère, W. T., Vermeulen, Jacqueline L. M., van Dijk, Paul J., Ruijter, J. M., Lamers, W. H., and Hakvoort, Theodorus B. M. (2006) Cellular concentrations of glutamine synthetase in murine organs. *Biochemistry and cell biology = Biochimie et biologie cellulaire*, **84**, 215–231.

[270] Houdijk, A. P., et al. (1998) Randomised trial of glutamine-enriched enteral nutrition on infectious morbidity in patients with multiple trauma. *Lancet*, **352**, 772–776.

[271] Kafkewitz, D. and Bendich, A. (1983) Enzyme-induced asparagine and glutamine depletion and immune system function. *The American journal of clinical nutrition*, **37**, 1025–1030.

[272] Andrews, F. J. and Griffiths, R. D. (2002) Glutamine: essential for immune nutrition in the critically ill. *The British journal of nutrition*, **87 Suppl 1**, S3–8.

[273] Kew, S., Wells, S. M., Yaqoob, P., Wallace, F. A., Miles, E. A., and Calder, P. C. (1999) Dietary glutamine enhances murine T-lymphocyte responsiveness. *The Journal of nutrition*, **129**, 1524–1531.

[274] Rao, R. and Samak, G. (2012) Role of Glutamine in Protection of Intestinal Epithelial Tight Junctions. *Journal of epithelial biology & pharmacology*, **5**, 47–54.

[275] Okabe, S., Takeuchi, K., Takata, Y., Naganuma, T., and Takagi, K. (1976) Effects of L-glutamine on various gastric lesions in rats and guinea pigs. *Digestion*, **14**, 325–331.

Acknowledgements

Foremost, I would like to express my special appreciation and thanks to my advisor Professor Dr. Markus Gerhard for his continuous support and valuable input, who put a lot of trust in me allowing me to grow as a research scientist.

My thanks also go to Professor Dr. Dirk Haller for pointing out interesting research questions and for constructive discussions.

My deepest gratitude is to Dr. Raquel Mejías-Luque, who always had a word of encouragement at the right time. I have greatly benefited from her focused mind and her exceptional ideas how to approach tricky hypotheses. Her great gift as a "Storyteller" creating a well-structured frame work combined with excellent skills to communicate research inspired me a lot.

Furthermore, I thank Dr. Florian Anderl for long in-depth discussions on immunological questions. This thesis would not be possible without his skills and experience with preclinical studies. I am very grateful that he was always there helping me to sort out the technical details.

Special thanks also go to Dr. Christian Bolz and Tobias Kruse for providing proteins and assisting with protein expression and assay setup, to Dr. Eva Rath who kindly introduced me to 2DGE, and to Max Koch, who carefully established the LC-MS analysis for glutamine and glutamate.

I am very thankful for the incredibly valuable support of our technicians Anke Bettenbrock, Sarah Franke, Jeanny Probst, Jeanette Koch and Ina Sebald.

Gladly, I have been blessed with wonderful labmates. The inspiration, practical advice, support, and friendship of a number of wonderful individuals greatly contributed to this thesis: Raphaela, Martina, Romy, Zohra, Luca, Behnam, Anahita, Christina and Hanni. It was a great pleasure to work with you!

Of course, I would like to especially thank my family for their loving support. In particular, I owe my loving thanks to my husband Ludwig who was very encouraging and supportive throughout the years. I would like to offer my special thanks to my mother for taking excellent care of Felicia. So I did not had to worry a minute about her well-being.

Lastly, I offer my regards and blessings to all of those who supported me in any respect during the completion of this thesis.